PB89-190375

Development of Sampling Methods for Source PM10 Emissions

Southern Research Inst., Birmingham, AL

Prepared for:

Environmental Protection Agency, Research Triangle Park, NC

Apr 89

U.S. Department of Commerce
National Technical Information Service
NTIS

PB89-190375

EPA/600/3-88/056
April 1989

DEVELOPMENT OF SAMPLING METHODS FOR SOURCE PM_{10} EMISSIONS

by

Ashley D. Williamson
W. E. Farthing
Sherry S. Dawes
Joseph D. McCain
Randal S. Martin
James W. Ragland
Southern Research Institute
Birmingham, AL 35255-5305

Cooperative Agreement No. CR-812274

Project Officer

Thomas E. Ward
Quality Assurance Division
Atmospheric Research and Exposure Assessment Laboratory

ATMOSPHERIC RESEARCH AND EXPOSURE ASSESSMENT LABORATORY
OFFICE OF RESEARCH AND DEVELOPMENT
U.S. ENVIRONMENTAL PROTECTION AGENCY
RESEARCH TRIANGLE PARK, NC 27711

REPRODUCED BY
U.S. DEPARTMENT OF COMMERCE
NATIONAL TECHNICAL INFORMATION SERVICE
SPRINGFIELD, VA. 22161

TECHNICAL REPORT DATA
(Please read Instructions on the reverse before completing)

1. REPORT NO. EPA/600/3-88/056

2.

3. RECIPIENT'S ACCESSION NO. PB89 190375/AS

4. TITLE AND SUBTITLE
Development of Sampling Methods for Source PM-10 Emissions

5. REPORT DATE April 1989

6. PERFORMING ORGANIZATION CODE

7. AUTHOR(S) Ashley D. Williamson, W.E. Farthing, S.S. Dawes, J.D. McCain, R.S. Martin, and J.W. Ragland

8. PERFORMING ORGANIZATION REPORT NO.

9. PERFORMING ORGANIZATION NAME AND ADDRESS
Southern Research Institute
Birmingham, AL 35255-5305

10. PROGRAM ELEMENT NO.

11. CONTRACT/GRANT NO. CR-812274

12. SPONSORING AGENCY NAME AND ADDRESS
Atmospheric Research and Exposure Assessment Laboratory
Office of Research and Development
U.S. Environmental Protection Agency
Research Triangle Park, NC 27711

13. TYPE OF REPORT AND PERIOD COVERED Final

14. SPONSORING AGENCY CODE EPA/600/09

15. SUPPLEMENTARY NOTES

16. ABSTRACT

This report describes an investigation of the needs and available techniques for in-stack PM-10 sampling. Discussion includes the conceptualization, development, documentation, and testing of two candidate methods. The first method, Constant Sampling Rate (CSR), is a procedural approach which adds particle size separation to sampling hardware that has been widely used in EPA Methods 5 and 17 but modifies the sampling protocol to accomplish the PM-10 objectives. The second method, Exhaust Gas Recycle (EGR), is an equipment approach which accomplishes the PM-10 objectives by using a modified sampling train to implement the concept of exhaust gas recirculation.

Six field studies indicated that these techniques were practical and compared well with one another and with more labor-intensive approaches. Laboratory investigations with monodisperse aerosols indicated that commonly used geometries for sampling nozzles could cause a decrease in the particle size out of a closely coupled inertial sizing device. Nozzle geometries were also found which eliminated the observed shifts in particle size cut.

17. KEY WORDS AND DOCUMENT ANALYSIS

a. DESCRIPTORS	b. IDENTIFIERS/OPEN ENDED TERMS	c. COSATI Field/Group

18. DISTRIBUTION STATEMENT Release to Public

19. SECURITY CLASS *(This Report)* Unclassified

20. SECURITY CLASS *(This page)* Unclassified

21. NO. OF PAGES 192

22. PRICE

EPA Form 2220-1 (Rev. 4-77) PREVIOUS EDITION IS OBSOLETE

DISCLAIMER AND PEER REVIEW NOTICE

The information in this document has been funded wholly or in part by the United States Environmental Protection Agency under Cooperative Agreement CR-812274 to Southern Research Institute. It has been subjected to the Agency's peer review and administrative review, and it has been approved for publication as an EPA document. Mention of trade names or commercial products does not constitute endorsement or recommendation for use.

FOREWORD

Measurement and monitoring research efforts are designed to anticipate environmental problems, to support regulatory actions by developing an in-depth understanding of the nature and processes that impact health and the ecology, to provide innovative means of monitoring compliance with regulations, and to evaluate the effectiveness of health and environmental protection efforts through the monitoring of long-term trends. The Atmospheric Research and Exposure Assessment Laboratory, Research Triangle Park, NC, has responsibility for: assessment of environmental monitoring technology and systems for air, implementation of agency-wide quality assurance programs for air pollution measurement systems, and supplying technical support to other groups in the Agency including the Office of Air and Radiation, the Office of Toxic Substances, and the Office of Solid Waste.

The environmental effects of PM_{10} particulate matter are of concern to the Agency. Acceptable measurement methodology is critical for proper assessment of the impact on the environment of these emissions from stationary sources. Development and validation of measurement methods are key components for producing an acceptable method. Laboratory and field studies were performed for development and validation of methodology for the measurement of PM_{10} emissions from stationary sources.

Gary J. Foley
Acting Director
Atmospheric Research and Exposure Assessment Laboratory
Research Triangle Park, North Carolina 27711

ABSTRACT

The body of this report describes a study of the needs and available techniques for PM_{10} sampling, which led to the conceptualization, development, documentation, and testing of two candidate methods. The first, the Constant Sampling Rate (CSR) technique, involves modified sampling methodology and the addition of particle size separation to sampling hardware that has been widely used in EPA Methods 5 or 17. The second method uses a new sampling train based on the concept of Exhaust Gas Recycle (EGR). This train has been characterized in over four years of laboratory and field study and has evolved into a mature design. Six field studies have been performed to develop and characterize the methods. As measured by a modified dual probe technique, the precision of each method is better than ±5%, comparable to that of EPA Method 17 at the same location. Comparability of the two techniques is within 16% at all sites tested. The EGR measured lower PM_{10} concentrations than CSR and other reference samplers at two sites, and higher than both at a third. Laboratory studies in this program indicate that decreases in particle size cut can occur in inertial sizing devices in which the sampling nozzle has small inlet diameter and is closely coupled with the inertial separation stage. Such shifts were observed to occur in the current PM_{10} sizing device (Cyclone I) with several of the current nozzles, including, in particular, the three EGR nozzles and those nonrecycle nozzles which had an abrupt expansion within a short distance from the cyclone body. It is projected that this nozzle effect occurs in other commercially available inertial samplers. Limited attempts to optimize sampling nozzles for Cyclone I indicate that the shifts in cyclone collection efficiency can be eliminated by lengthening the expansion zone in the nozzle. However, this lengthening increases the error caused by particle deposition in the nozzle, so the potential for some residual error remains. Particle deposition, averaged over particle sizes of 4 to 10 μm, range from about 1% at low velocity, to 13% at medium velocity, to 20% at high velocity. In view of these conclusions, the highest priority for further research is a more thorough design and characterization to optimise the nozzles to be ultimately used in a PM_{10} sampling method, in particular the EGR nozzles. While both EGR and CSR are usable in their present form with no modifications, the current methods appear likely to show a negative bias in measured PM_{10} which increases with duct velocity. Detailed specifications on nozzle geometry and/or performance specifications, as described in the application guide for CSR and EGR, will assure standardization of PM_{10} emission measurements.

CONTENTS

Page

Disclaimer ii
Foreword iii
Abstract iv
Figures vi
Tables x

1. Introduction 1
2. Conclusions and Recommendations 2
3. Background 4
    - General considerations: size fractionation 5
    - General considerations: representative sampling 6
    - Possible approaches 8
    - Evaluation of sampling errors 10
    - Summary: methods selected for development 19
4. Formulation of PM_{10} Methods 20
    - Selection of PM_{10} sizing device 20
    - Development of Constant Sampling Rate method 23
    - Development of Exhaust Gas Recycle method 27
5. PM_{10} Field Studies 45
    - Overview of field studies 45
    - Summary description of field tests 50
    - Conclusions from field test series 62
6. Laboratory Characterization of Cyclone I and Nozzles 69
    - Background summary 69
    - Experimental equipment and procedures 69
    - Basic performance results 79
    - Results of varying stream velocity 82
    - Conclusions relative to laboratory data 114

References 123

Appendices

A. Determination of emissions from stationary sources (using a single-stage PM_{10} cyclone, Constant Sample Rate, and in-stack filtration) 126
B. Determination of source emission PM_{10} particulate matter using Emission Gas Recycle (EGR) sampling procedures and a single-stage PM_{10} cyclone 152

FIGURES

Number Page

3-1 Ninety-five percent tolerance region vs. number of traverse points 11

3-2 Aspiration coefficient versus velocity ratio 15

4-1 Cyclone dimensions 22

4-2 Velocity ratio, R, versus duct velocity to give aspiration coefficient of 1.2 and 0.8 for 10-μm particles 25

4-3 Gas flow in exhaust gas recycle train 31

4-4 Schematic of the emission gas recycle train 32

4-5 Cross-sectional detail of the EGR mixing nozzles 34

4-6 First-generation EGR control console (front view) 35

4-7 First-generation EGR control console (rear view) 36

4-8 EGR sampling system control module (front view) 37

4-9 EGR sampling system control module (rear view) 38

4-10 EGR sampling system control module (rear view) showing internal components 39

4-11 EGR sampling system control module (right side) 40

4-12 EGR sampling system control module (left side) with 4-cfm pump .. 41

4-13 EGR PM_{10} cyclone sampling device (front view) 42

4-14 EGR PM_{10} cyclone sampling device (front view) 43

5-1 Collocated cascade impactor and Method 17 filter (used in test 2) 48

5-2 Three collocated cascade impactors (as used in test 2) 48

5-3 Multiple probe sampling arrangement used in test 6 49

6-1 VOAG calibration system with isokinetic velocities at inlet to sampler nozzle 71

6-2 Velocity profiles in flow stream at inlet of Cyclone I nozzles .. 72

FIGURES (Continued)

Number Page

6-3 Geometry of Cyclone I nozzles.................................. 74

6-4 Equipment setup for nozzle velocity profile measurements........ 77

6-5 Pitot coefficient (Cp) for hypodermic pitot versus pressure drop (Δp), measured with a standard pitot....................... 78

6-6 Collection efficiency of Cyclone I versus aerodynamic diameter.. 78

6-7 Collection efficiency of Cyclone I and 1/2-in. nozzle at 0.45 acfm and 27 °C... 80

6-8 Cyclone I D_{50} versus flow rate at several temperatures.......... 81

6-9 Cyclone I $\sqrt{STK_{50}}$ versus Re... 83

6-10 Collection efficiencies of Cyclone I with tapered nonrecycle nozzles and reference nozzle (1/2 in.).......................... 84

6-11 Collection efficiencies of tapered nonrecycle nozzles in Cyclone I.. 85

6-12 Velocity profiles at exit of tapered nonrecycle nozzles and reference nozzle (1/2 in.)...................................... 86

6-13 Collection efficiencies of Cyclone I with nozzles having large expansion angles and reference nozzle (1/2 in.)........... 88

6-14 Collection efficiencies of nozzles having large expansion angles... 89

6-15 Velocity profiles at exit of nozzles having large expansion angles and reference nozzle (1/2 in.).......................... 90

6-16 Collection efficiency of Cyclone I with 1/4-in. EGR nozzle at three recycle rates and reference nozzle (1/2 in.)........... 92

6-17 Velocity profiles at exit of 1/4-in. EGR nozzles at four recycle rates and reference nozzle (1/2-in.).................... 93

6-18 Collection efficiencies of Cyclone I with 3/16-in. EGR nozzle at three recycle rates and reference nozzle (1/2 in.).... 94

6-19 Velocity profiles at exit of 3/16-in. EGR nozzle at four recycle rates and reference nozzle (1/2 in.)................... 95

FIGURES (Continued)

Number Page

6-20 Collection efficiencies of Cyclone I with 1/8-in. EGR nozzle at three recycle rates and reference nozzle (1/2 in.)........... 96

6-21 Collection efficiencies of 1/8-in. EGR nozzle at three recycle rates.. 97

6-22 Velocity profiles at exit of 1/8-in. EGR nozzle at four recycle rates and reference nozzle (1/2 in.).................... 98

6-23 Collection efficiencies of Cyclone I with EGR nozzles at 0% recycle rate and reference nozzle (1/2 in.)..................... 99

6-24 Collection efficiencies of EGR nozzles at 0% recycle rate.......100

6-25 Velocity profiles at exit of EGR nozzles at 0% recycle rate and reference nozzle (1/2 in.).................................101

6-26 Collection efficiencies of Cyclone I with EGR nozzles at 75% recycle rate and reference nozzle (1/2 in.).....................102

6-27 Collection efficiencies of EGR nozzles at 75% recycle rate......103

6-28 Velocity profiles at exit of EGR nozzles at 75% recycle rate and reference nozzle (1/2 in.).................................104

6-29 Geometries of 1/8-in. nozzles with large expansion angles and varying lengths...106

6-30 Comparison of geometries of nozzles with small or large expansion angle...107

6-31 Geometries of recycle nozzles with and without extensions.......108

6-32 EGR shear nozzle...108

6-33 Collection efficiencies of Cyclone I with 1/8-in. nozzles having large expansion angles and different lengths and with reference nozzle (1/2 in.)....................................109

6-34 Collection efficiencies of 1/8-in. nozzles having large expansion angles and different lengths.........................111

6-35 Velocity profiles at exit of 1/8-in. nozzles having large expansion angles and different lengths.........................112

FIGURES (Continued)

Number Page

6-36 Collection efficiencies of Cyclone I with nozzles having large or small expansion angle and reference nozzle (1/2 in.)...113

6-37 Collection efficiencies of nozzles having large or small expansion angle...115

6-38 Velocity profiles at exit of nozzles having large or small expansion angle and reference nozzle (1/2 in.)..................116

6-39 Collection efficiencies of Cyclone I with EGR nozzles of different lengths and reference nozzle (1/2 in.)................117

6-40 Collection efficiencies of EGR nozzles of different lengths.....118

6-41 Velocity profiles at exit of EGR nozzles of different lengths and reference nozzle (1/2 in.).................................119

6-42 Summary of nozzle losses..121

TABLES

Number		Page
3-1	Particulate Mass Rate Errors from Three Types of Distributions in Circular Stacks	12
3-2	Anisokinetic Error Coefficient Particles versus Velocity for Aerosol Size Distributions Measured at Four Sampling Locations	16
3-3	Anisokinetic Error Coefficient for Total Particulate Concentration versus Velocity for Aerosol Size Distributions Measured at Four Sampling Locations	17
3-4	Errors in PM_{10} Concentrations (%) Resulting from Varying the Flow Rate through the PM_{10} Sizing Device to Maintain Isokinetic Sampling Conditions	19
4-1	CSR Setup Forms	28
4-2	Results of Parallel Tests Using Dual Cyclone Trains with EGR Nozzle and with Standard Nonrecycle Configuration	44
5-1	Averages and Confidence Limits of Total Mass Concentration for Field Test 1	52
5-2	Comparison of Size Distribution Data Obtained Under Subtest B of Field Test 1	53
5-3	Field Test 2, Subtest A: Simultaneous CSR Impactor and Method 17 Traverses	53
5-4	Results of Field Test 2, Impactor Subtest B, Corrected for Anisokinetic Sampling	54
5-5	Comparison of Particulate Concentrations Measured with a CSR Impactor and Single Point Isokinetic Impactors for Field Test 2	55
5-6	Comparison of Particulate Concentrations Measured by Impactors, CSR, and EGR for Field Test 3	56
5-7	Field Test 4: Comparison of PM_{10} Concentrations at the Inlet	58
5-8	Field Test 4: Comparison of Total Particulate Concentrations at the Inlet	58
5-9	Field Test 4: Comparison of PM_{10} Fractions at the Inlet	59
5-10	Field Test 4: Comparison of Particulate Concentrations Measured at the Outlet by Impactors and by Method 17	59

TABLES (Continued)

Number Page

5-11 Field Test 5 Statistical Results........ 61

5-12 Field Test 6 Statistical Results........ 63

5-13 Percentage Differences in Particulate Concentrations Measured During Test Series........ 66

6-1 Dimensions of Cyclone I Nozzles Tested........ 75

6-2 Dimensions of Modified Nozzles Tested........ 110

SECTION 1

INTRODUCTION

A size-specific PM_{10} ambient-air particulate standard has been promulgated by EPA. The introduction of size into the definition of suspended particulate matter in the ambient air suggests the need for measurement of size-specific emissions from stationary sources. Technology related to such measurements has been developed in connection with evaluation of control devices on process streams. Inertial impactors and cyclones can separate or classify aerosol particles in situ but are more complex to operate than total particulate mass trains. Furthermore, operation of these devices for typical engineering evaluation purposes does not require the documented accuracy and reproducibility desired for emissions inventory development or compliance purposes.

The Quality Assurance Division of the Atmospheric Research and Exposure Assessment Laboratory has initiated a research program to develop source measurement techniques to support the proposed PM_{10} standard. The extensive particle size sampling technology developed as a result of research efforts associated with Inhalable Particulate matter from stationary sources and particulate control devices provided valuable background information for the PM_{10} efforts. The development phases of the PM_{10} program were conducted under contract by Southern Research Institute (SRI). This work has focused on two promising techniques for source PM_{10} measurement. The first involves a new sampling train design which incorporates exhaust gas recycle (EGR) to avoid isokinetic sampling bias. The second, the Constant Sampling Rate (CSR) approach, uses existing sampling hardware with an altered traversing protocol to minimize this bias. In former related documents these techniques were named Emmission Gas Recycle and Simulated Method 5 (SIM-5) or Constant Flow Rate (CFR).

This document is a summary program report of the source PM_{10} method development work performed at SRI. This report covers the period from February, 1983 - August, 1986, and summarizes research performed under EPA contracts 68-02-3118 and 68-02-3696 and EPA Cooperative Agreement CR-812274. Much of this material is described more fully in several project reports (Farthing, 1983; Farthing et al. 1986, 1988; Martin, et al. 1988) and presentations (Williamson et al. 1984, 1985, 1986; Farthing et al. 1985; Ward et al. 1985). Section 2 presents conclusions and recommendations based on all work performed to date. Section 3 presents technical background relevant to the problem of obtaining size-specific particulate samples. Initial development and description of the EGR and CSR methods are described in Section 4. Section 5 contains a summary of six field characterization trials of the two candidate methods, and Section 6 describes laboratory characterization and optimization of the inertial sizing device and sampling nozzles. Detailed documentation of both methods is contained in two appendices.

SECTION 2

CONCLUSIONS AND RECOMMENDATIONS

The body of this report describes a study of the needs and available techniques for PM_{10} sampling, which led to the conceptualization, development, documentation, and testing of two candidate methods. The first, the Constant Sampling Rate (CSR) technique, involves a modified sampling methodology but uses equipment that has been commercially available from vendors for several years and that is thus presumedly well-characterized. The second method uses a new sampling train based on the concept of exhaust gas recycle. This train has been characterized in laboratory and field study and has evolved into a mature design. More detailed conclusions are given at the end of Sections 5 and 6.

Six field studies were performed to develop and characterize the methods. As measured by a modified dual probe technique, the precision of each method was within ±5%, comparable to that of EPA Method 17 at the same location. Comparability of the two methods was within 16% at all sites tested. The EGR method measured lower PM_{10} concentrations than CSR and other reference samplers at two sites, and higher concentrations than both at a third. All differences were significant at the 95% confidence level.

Laboratory studies in this program indicate that decreases in particle size cut can occur in inertial sizing devices in which the sampling nozzle has small inlet diameter and is closely coupled with the inertial separation stage. Such shifts were observed to occur in the current PM_{10} sizing device (Cyclone I) with several of the current nozzles, including in particular the three EGR nozzles and those nonrecycle nozzles which had an abrupt expansion within a short distance from the cyclone body. It is projected that this nozzle effect probably occurs in other commercially available inertial samplers.

Limited optimization studies for sampling nozzles for Cyclone I indicate that the shifts in cyclone collection efficiency can be eliminated by lengthening the expansion zone in the nozzle. However, this lengthening increases particle deposition in the nozzle. Nozzle losses averaged over particle sizes of 4 to 10 μm were observed to range from 1% at low velocity, to 13% at medium velocity, to 30% at high velocity. It is anticipated that further optimization studies would produce other nozzle designs which have smaller losses.

In view of these conclusions, the highest priority for further research is a more thorough design and characterization to optimize the nozzles, in particular the EGR nozzles. While both EGR and CSR are usable in their present form with no modifications other than simple extensions of the smallest nozzles, the current methods appear likely to show a slight negative bias in measured PM_{10} which increases with duct velocity. Nozzle optimization and detailed specifications on nozzle design will probably be useful for measurement of PM_{10} at very high duct velocities.

Recommendations for further research of somewhat lower priority can also be made. Reduction of approximate setup calculations for both methods to forms suitable for programmable calculators should be attempted. Extension of performance data of the PM_{10} sampling procedures to source conditions beyond the range currently studied are recommended. Further field studies are suggested to test any new nozzles from the recommended design study. Finally, extensive field studies are recommended to extend the number of source types tested by these methods.

SECTION 3

BACKGROUND

In the 1970s the U.S. Environmental Protection Agency began plans to set air pollution standards for ambient air particles on a particle-size-specific basis. This new (or revised) standard was to be based on health effects and was to consider primarily those particles which could penetrate to the lower respiratory tract and lungs. Initially, the term used for such particles was "inhalable particulate (IP)"; and the definition, based on studies of particle deposition in the human airways, considered those particles smaller than 15 μm on an aerodynamic basis to fall in the IP classification. At that time it was recognized that should a size-specific ambient air standard be promulgated, source characterization would also be needed; and perhaps source emission regulations based on particle size might be required as well. The particle size range to be included in the new standard was reduced to those smaller than 10 μm on an aerodynamic basis as work on the proposed regulation progressed. Because the upper limit of 15 μm had become so intimately associated with the term "inhalable particulate," the term "PM_{10}," for particulate matter smaller than 10 μm, was used to explicitly designate the revised range.

Adequate particle size characterization of emissions from a source requires measurement of stack or fugitive emissions from the source, as well as measurements of background levels of ambient particles in the case of fugitive emissions. The concentration and particle size distribution of the suspended particulate matter and, in some instances, its chemical composition and biological properties must be measured. To assist the EPA in planning research on the sampling and analysis problem, a workshop was held at Research Triangle Park in late 1978 (Smith et al. 1982a). Although at that time the upper limit to the size range of interest was 15 μm rather than the current 10 μm, most of the conclusions reached at the workshop are also valid for PM_{10}. Since the IP workshop represented the state of the art in particle sizing at emissions sources, and since the current source PM_{10} measurement program built on their findings, the workshop perspective provides the basis for the descriptions in this section.

In the following subsections we first summarize two general considerations of the problem of accurate sampling of size-specific (IP or PM_{10}) particulate emissions. The first step is the extraction of particles from the gas stream in a representative fashion. The second step then is to carry out the required size fractionation of the sample. The next subsection considers possible approaches to solving the difficulties presented when size fractionation must be combined with representative sampling. The fourth subsection presents a semi-quantitative assessment of the errors associated with the three major variables in potential sampling approaches. The final subsection summarizes the approaches actually chosen for development in this program.

GENERAL CONSIDERATIONS: SIZE FRACTIONATION

Examining the problem of size fractionation first, we find that prior to the time of the IP workshop the major emphasis in research regarding particle sizing methods for source characterization had been related to control device evaluation. Because control devices of all types tended to be very efficient in the removal of large particles, this effort had focused on the measurement of concentration by particle size for particles smaller than 3 to 5 µm. The latter range of particle sizes is the most troublesome to collect and consequently represented the range in which the greatest potential gains in control technology might be made. A number of techniques had been developed for measuring emissions by particle size in this fine-particle size range based on several mechanisms, among which were electrical mobility, diffusion, light scattering, and inertial (aerodynamic) sizing. Inertial, or aerodynamic, sizing was the most highly developed and widely used of these techniques. Data obtained by inertial sizing methods were often reported extending to sizes in the nominal range of 10 to 20 µm, but caveats regarding its accuracy, especially for the larger particle sizes, were necessary. As is still the case, no reference methods for particle sizing were available by which accuracy could be tested.

The inertial sizing devices in use were cascade impactors and cyclones, the impaction devices being the more highly developed of the two types. Cyclones held three significant operational advantages over impactors: no effect from particle bounce, no interferences from reactions with substrates or substrate coatings, and, for practical purposes, no overload problem. However, impactor behavior was much more thoroughly understood on a theoretical basis. Consequently, changes in performance resulting from changes in operating conditions could be predicted much more satisfactorily for impactors than for cyclones. Thus, in general, impactor stages could be designed with confidence based on calculations from theory, while cyclone design was largely cut and try. Predictions of changes in the performance of a cyclone with changes in operating conditions then required extensive calibrations over the expected range of conditions to be encountered. No cyclones for source testing applications had been designed to produce size cuts in the 10- to 15-µm range at the time the IP program started. Even with impactors, problems were known to exist with respect to deviations in performance from theoretical predictions, especially for the coarser particle sizing at the device inlet. This effectively meant that no satisfactory aerodynamic classifier existed for the IP program. Again, although the IP program required a 15-µm rather than a 10-µm size cut, a similar lack of a 10-µm sizing device also existed at that time.

Two approaches to meeting the size fractionation requirement for the measurement of IP emissions were suggested as a result of the workshop. The first, to be applied when detailed size distribution data were needed in addition to the IP emission rate, was to use cascade impactors to obtain the data. The impactors were to be operated either so that one of the stages provided the size cut required for IP purposes (preferably), or so that the IP concentration could be found by interpolation between stages which straddled the required cut. If no reliable size cut at or above the designed value could be obtained, the IP concentration would be estimated by extrapolation of size distribution information from impactor stages which provided size cuts below that needed for IP purposes. The second approach to meeting the IP size fractionation requirement was to develop a cyclone sampler, or samplers, which would provide the needed size cut directly. The latter approach would be the simplest and most effective when only the IP concentration was needed. The use of a single-stage cyclone sampler eliminates potential errors due to particle bounce, stage overloading, and substrate interferences, which plague impactor measurements. Further, with only one stage to contend with, the labor and time required for setup, sample recovery, and analysis are reduced considerably. Similar conclusions were reached with respect to PM_{10} when the transition was made from the initial 15-μm IP size cut for development of a revised ambient particulate standard to the 10-μm size cut, and a single-stage PM_{10} cyclone classifier was developed under the present program.

GENERAL CONSIDERATIONS: REPRESENTATIVE SAMPLING

Obtaining a representative sample of particulate emissions from a source involves three key factors: appropriate temporal averaging, nonbiasing of the sample with respect to particle size, and appropriate spatial averaging. The first of these governs the selection of the time period over which the sampling should be carried out. The second results in the necessity for the sampling to be done at or near isokinetic conditions. The third governs the location and number of sampling points needed to adequately represent the particulate flux through a given sampling plane. The need for representative sampling applies to total particulate emissions sampling at least as much as to size-specific sampling. In this subsection, we show how the procedures of Method 5 cannot be applied to size-specific sampling methods without compromise of accuracy in particle size fractionation.

Temporal Variations

First, the emissions from most sources are not constant in time with respect to either particulate concentration or size distribution. Thus the time period over which the sampling takes place must be rationally selected on the basis of some knowledge of the process which produces the emissions. Representative measurement of emissions from a batch process will usually require sampling throughout the process. Sampling of cyclic processes should be set up so that the samples cover integral numbers of process cycles to avoid undue weighting of periods of minimum or maximum emissions. It is worth noting that cyclic variations can be present in emissions from nominally steady-state processes. For instance, soot blowing, rapping of plates in electrostatic precipitators (ESPs), and bag cleaning in fabric filters all result in time-dependent emissions from coal-fired boilers which would otherwise have relatively steady emission rates.

Temporal variations are addressed in Method 5 by specifications on consideration of sampling period with process cycles. The same considerations can be used for size-specific sampling, although the more limited range of acceptable particulate catches with cascade impactors can complicate the sampling process. Appropriate consideration of temporal variations in emissions was called for in the IP sampling protocols, and such consideration has been retained in the PM_{10} protocols developed under this program.

Isokinetic Sampling

In order to obtain a sample which is unbiased with respect to particle size, one must sample isokinetically. That is, the gas velocity of the sample stream entering the sampling intake nozzle must match the local gas velocity in the duct from which the sample is being withdrawn. If the gas velocity in the nozzle is greater than the local duct velocity, the flux of small particles through the nozzle cross-section will be greater than that for the free stream in the duct, and the apparent concentration of large particles will be less than the true concentration in the duct. In this case the sample will be biased toward an apparently smaller mean particle size or an apparently greater percentage of small particles than actually exists in the free stream. Conversely, if the gas velocity in the nozzle is lower than the local duct velocity, the flux of small particles through the nozzle cross-section will be less than that of the free stream, and the apparent concentration of large particles will be greater than the true concentration. In this case, the apparent size distribution will be biased toward a larger mean particle size or an apparently greater percentage of large particles than is actually the case in the free stream. The apparent concentration of very small particles in the sample remains unchanged from that in the duct in either case. The apparent concentration of very large particles in the sample approaches the ratio of the duct velocity to the nozzle velocity. Meeting the requirement for velocity matching in order to eliminate bias with respect to particle size while traversing a sampling plane causes no great difficulty in sampling for total emissions by Methods 5 and 17. In that type of sampling, a nozzle size is selected so that the velocity matching can be accomplished by changing the sampling flow rate as needed to obtain the required nozzle velocity.

Unfortunately, this approach cannot easily be applied when making measurements with an aerodynamic particle size classifier such as an impactor or cyclone. The effective cutoff particle diameter provided by an inertial particle size classifier such as an impaction stage or a cyclone is set by the properties of the gas stream being sampled (gas density and viscosity), the geometry of the separator, and the gas flow rate through the separator. When using any particular sampler in any given sampling situation, only the sampling flow rate can be set by the user; the hardware and the duct conditions set the other parameters. Thus the separation diameter is set by the selection of the sampling flow rate. If a specified size cut (10 or 15 μm) is required, some degree of anisokinetic sampling is inevitable unless the required flow rate fortuitously produces the isokinetic velocity with an available nozzle. If interpolation between size cuts is allowed with a multistage sampler, isokinetic conditions can be satisfied for a given duct velocity. Unfortunately, isokinetic sampling cannot be maintained when the local duct velocity changes. Changing the sampler flow rate after sampling has begun will change the cut diameter(s) provided by the device. Consequently, maintaining fixed size fractionation diameters requires operation at fixed flow rates whereas maintaining isokinetic sampling conditions requires variable flow rates. These conflicting requirements must then be jointly satisfied if representative results are to be obtained.

Spatial Averaging

Spatial variations in particulate fluxes across sampling planes make it necessary to use traverse sampling techniques rather than simple single point sampling. Stratified or nonuniform particulate concentrations are often found in ducts and stacks. The Method 5 traverse performs spatial averaging by dividing the total sample into a specified number of subsamples representing equal area zones of the duct. The number of zones is determined according to the expected degree of stratification of emissions (Method 1), and the isokinetic sampling criterion guarantees appropriate weighing of the subsamples. Since the sample volume flow rate is proportional to the duct velocity (and thus the volume flow rate through the traverse zone), the total sample will properly represent the total emissions flux.

Unfortunately, the constant flow rate requirements of inertial size classifiers force unwelcome compromises in size-specific sampling. Since gas velocities vary over the cross section of a duct, isokinetic sampling conditions cannot be maintained over a multipoint traverse. Nor will constant flow sampling for fixed dwell times across a traverse properly average the emissions over the traverse. On the other hand, while a single-point inertial sampler may be operated under approximately isokinetic conditions, a single-point sample is unlikely to provide an accurate measure of the average emissions across the duct.

POSSIBLE APPROACHES

Different approaches to resolving the dilemma posed by the conflicting requirements for fixed cut diameters and isokinetic sampling have been taken in the past. Approaches frequently used in the control device evaluation programs mentioned previously were to make a nominal effort to sample isokinetically while traversing a duct by setting the flow rate to be isokinetic at the average duct velocity or individual sampling points at near-isokinetic velocity. Since the concentrations of the fine particles, which were the particles of greatest interest, could be measured correctly without sampling isokinetically, this mode of operation was acceptable for the purpose. In fact, in some cases, deliberate sampling at highly nonisokinetic conditions was performed to bias against sampling large particles. This was done to avoid overloading the stages which collected the large particle end of the size spectrum before sufficient quantities of fine particles could be collected for analysis. On the other hand, sampling in such fashions did not permit any real accuracy to be obtained in the measurement of overall size distributions.

In the IP program, where accuracy in the measurement of the concentrations of larger particles was needed, a set of interim guidelines was developed to deal with the problem pending the development of advanced hardware and techniques as final solutions. The interim approach, which was suggested as a means of generating a reasonably reliable emission factor data base, was to perform a "synthesized" traverse at near-isokinetic conditions. The sampling plane was to be divided into quadrants, and a single-point sample taken at the centroid of each quadrant was to be obtained. These samples were to be taken at the flow rate required to obtain a 15-μm

D_{50} for the first stage of the size fractionation device (a cyclone) by using a nozzle size which would result in a nozzle velocity within 20% of the duct velocity. This interim approach was labor-intensive, as it required four individual sampling runs in order to obtain one traverse.

A number of approaches to the ultimate resolution of the problem were suggested during the course of the IP development work. These are discussed by Smith et al. (1982a) and include the following:

1) Synthesizing a traverse from a multiplicity of single-point samples (one sampler per traverse point), as in the interim approach.

2) Permitting some deviation from isokinetic sampling rates and changing nozzle sizes as needed during a traverse to hold the isokinetic error within the permitted limits.

3) Using sampling nozzles for which the inlet cross-sectional area could be changed while sampling to maintain isokinetic conditions.

4) Using a split stream probe to permit isokinetic sampling at a rate greater than that needed by the sizing device, with the excess flow being dumped upstream of the device.

5) Using a two-stream probe in which the isokinetic sampling rate is always less than that needed by the sizing device and augmenting the sample flow with filtered flue gas to make up the difference.

6) Using a two-stream probe in which the isokinetic sampling rate is always less than that needed by the sizing device and augmenting the sample flow by recycling a portion of the spent sample stream to make up the difference.

7) Using a shrouded probe (or probe within a probe) to provide a slipstream with a high fixed volume flow taken through a very large bore nozzle with a secondary isokinetic sample being taken from the slipstream for the sizing device. Errors in measured particle concentrations and fluxes could be held to acceptable levels for particles smaller than 30 μm by this means.

These approaches became the starting points for the selection of candidates for PM_{10} methods development. The first two approaches involve modifications in traversing protocol. The last five involve modified sampling hardware.

Two other approaches were considered which were not mentioned at the IP workshop. The first is a combination of measurements using data obtained with a particle sizing device together with measurements with a total particulate reference method. The problem posed by stratification would not be difficult to solve if the relative concentrations of particles of all sizes were uniform across the sampling plane and only the overall concentrations varied (uniform particle size distribution on a cumulative percentage basis). In the latter case, a single point isokinetic sample for particle size could be used to define the relative size distribution, and a full traverse using conventional total particulate sampling methods (e.g., Method 5 or 17) could be used to obtain the total emission rate. The PM_{10} emissions could then be found by multiplying the total emission rate by the fraction of particles smaller than 10 μm found from the size distribution measurement. Unfortunately, the mechanisms which lead to stratification in particulate concentrations also tend to result in variations in the relative concentrations of particles of different sizes. For instance, settling in long runs of horizontal ducting, inertial separation in bends, and rapping puffs from dry ESPs are all mechanisms which produce zones of relatively higher total particulate concentration as a result of relative local enrichment in the concentrations of larger particles. Therefore, except in rare and fortuitous instances, the size distribution measured at a single point in the sampling plane will not be representative of the emissions as a whole; hence, the above technique is not valid in general. For these reasons this technique, which has been proposed for IP measurements, was not considered for further development under the PM_{10} program.

A final possible technique is to use an inertial sizing device, but operate it at a variable flow rate to maintain isokinetic sampling. Under this approach, the sampler nozzle size selected would produce a mean flow rate to equal as closely as possible to that required for the specified size cut. This approach, while not satisfying because of the undefined sizing inaccuracy, does solve the problems of spatial averaging and isokinetic sampling. This approach, which was not developed in this program, is discussed in the next subsection.

EVALUATION OF SAMPLING ERRORS

In order to make rational selections of candidate PM_{10} measurement methods, estimates are needed of the uncertainties or errors which might be introduced into the results as consequences of the problems described previously.

In this subsection we are primarily concerned with the approaches which involve conventional sampling hardware and modified traversing protocols. For these approaches, the important factors are relative errors (and effort) involved in restriction of the number of traverse points, in anisokinetic sampling, and in use of other than the proper flow rate for the desired size cut.

Each of the candidate approaches which involve modified sampling trains has the potential of accuracy comparable to Method 5 total particulate sampling. Rather than using the considerations described in this subsection, evaluations of these approaches must be based on feasibility of design, fabrication, and maintenance. Finally, acceptability of any such concept will depend on actual tests on the new hardware to verify that the concept does indeed provide satisfactory size segregation and representative particulate extraction from the source duct.

Most of the following material is summarized from an analysis of sampling errors and PM_{10} strategies performed under this program (Farthing 1983). The full report of this analysis contains considerably more detail than can be presented here.

Uncertainty Versus the Number of Points Sampled

Extensive analyses have been previously performed of the uncertainty in measurements of total particulate emission caused by spatial variation in process streams. Figure 3-1 illustrates a summary of such results by

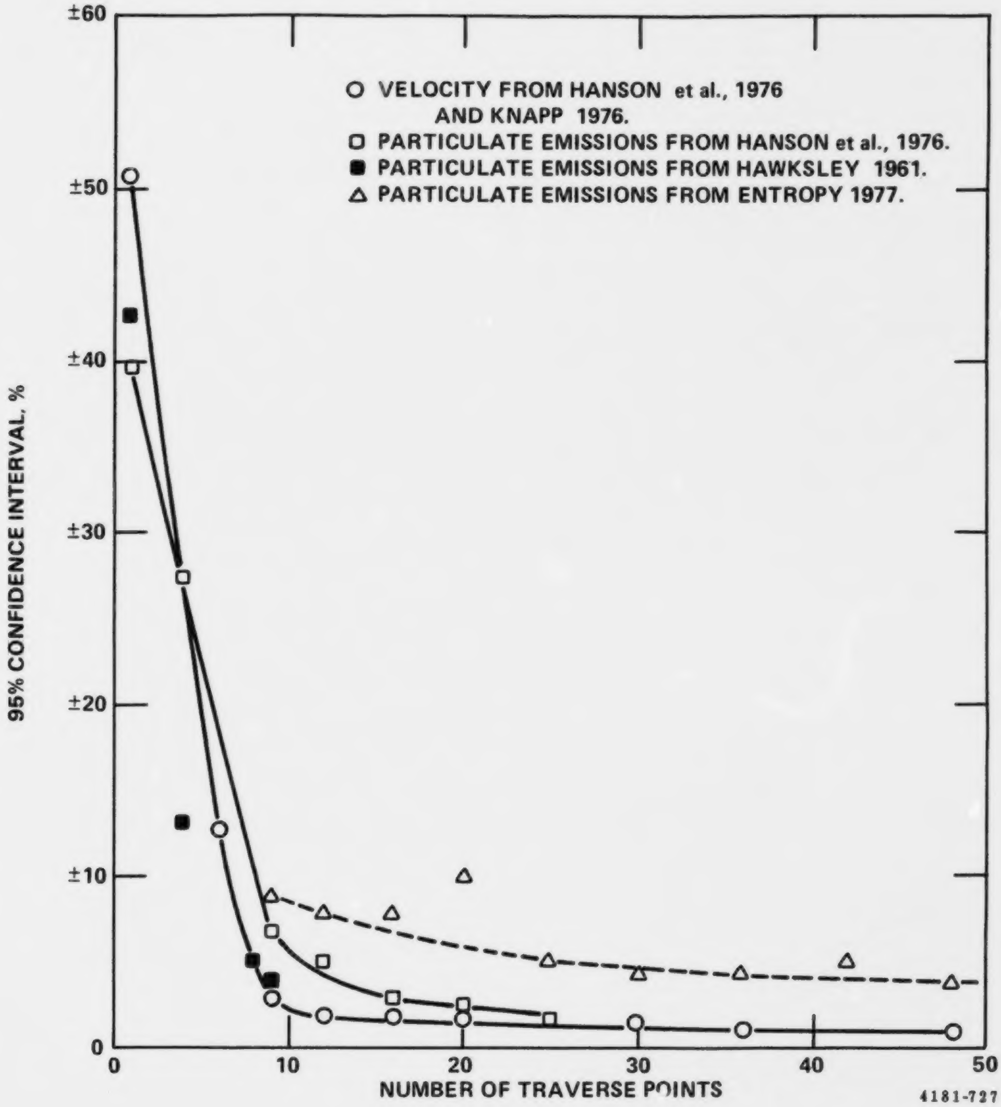

Figure 3-1. Ninety-five percent tollerance region vs. number of traverse points (after Shigehara 1982).

Shigehara (1982); the 95% confidence interval, in terms of percent of the mean emission rate for a source, is plotted as a function of the number of points sampled in a duct cross section. These data are based upon emission rate profiles measured with high resolution (>24 points). From each profile, measurements were simulated for several numbers of traverse points and the error was calculated for each simulated measurement. The 95% confidence interval for each number of traverse points was then calculated from the resulting set of error values obtained from all available profiles for the specified number of traverse points. Figure 3-1 suggests that using 8 to 12 traverse points provides a large reduction in error from one point, while additional points provide little additional decrease. This behavior is believed to be a fundamental characteristic of the scale of variations which exist in process streams and the strategy employed for choosing sampling points: the sample plane of the duct is resolved into N equal area zones, where N is the number of traverse points, and the centroid of each zone is sampled.

Shigehara (1982) also reports emission rate errors from a theoretical investigation for circular ducts. Three emission rate profiles were assumed, V-shaped, skewed, and parabolic. Sampling errors were calculated as a function of the number of points. These results are given in Table 3-1. Note that errors are always small with 4 or more points for the V-shaped and parabolic profiles, while for the skewed profile, error drops and remains below 5% for 12 or more points. These results, along with Figure 3-1, suggest that the magnitude of error varies substantially from source to source (or profile to profile) for less than 8 to 12 points and is consistently low for more than 8 to 12 points.

TABLE 3-1. PARTICULATE MASS RATE ERRORS FROM THREE TYPES OF DISTRIBUTIONS IN CIRCULAR STACKS*

No. of traverse points on a line+	Percentage error		
	U-shaped	Skewed	Parabolic
2 (4)	±0.4	+18.0	-0.8
4 (8)	±0.4	+37.8	+0.4
6 (12)	-0.4	+ 3.6	+0.4
8 (16)	+0.4	0	+0.4
10 (20)	0	+ 0.9	0
12 (24)	+0.4	+ 4.5	0

*After Shigehara (1982).

+The number of points in a complete traverse are given in parentheses.

When compared to random sampling, the strategy of selecting sampling points from equal-area zones is effective at reducing error with a relatively small number of sample points. The strategy in essence divides the emission rate population of the sample plane into subpopulations from which the centroid value for each is selected. Then the amount of error depends on two factors, the magnitude of variation and the scale of spatial variations. If the scale of variations is much smaller than the zone size, then the chances are low that any particular centroid value will be representative of the average for the zone. When the zone size is smaller than the scale of variations, then additional sampling points or zones does not reduce error. The greatest error reduction occurs when the zone size is smaller than but approaching the scale of variations. This type behavior is that depicted in Figure 3-1 and more or less repeated in other test data reviewed by Farthing (1983). Twelve sampling points consistently reduced the magnitude of error to less than 10%, including examples of severe stratification, while error for fewer points varies greatly from emission source to source.

It is expected that in general PM_{10} is less stratified than total particulate emissions. Reentrained particles from an ESP tend to be larger. The lower inertia of PM_{10} would cause less deviation from gas flow in bends and faster damping from turbulent diffusion once stratification is produced. However, the degree to which the above-given sampling errors should be reduced to describe PM_{10} cannot be stated except in those instances where PM_{10} profiles can be deduced. Limited data was cited by Farthing (1983) in reaching the conservative conclusion to use the error estimates in Figure 3-1 for PM_{10} as well as total particulate. The goal of traversing strategy should be to reduce errors due to spatial variation so that it is not the dominant source of error but is comparable to or less than other sources of error.

Anisokinetic Sampling Errors

Belyaev and Levin (1974) developed a semi-empirical relationship for aspiration coefficient, A, in terms of the particle Stokes number, K, and the ratio of stream velocity, v, to nozzle velocity, u, where

$$A = 1 + (R - 1)\frac{B}{B + 1} \qquad (3\text{-}1)$$

where A = measured concentration/actual concentration,
R = velocity ratio v/u,
$B = (2 + 0.617/R)K$,
K = particle Stokes number with respect to the nozzle, $\tau v/d$,
τ = particle relaxation time $CD^2/18\mu$ (seconds),
C = Cunningham slip factor,
D = particle aerodynamic diameter,
μ = gas viscosity (poise), and
d = nozzle diameter.

The laboratory data of Iinoya (1979) and Durham (1978) support this expression for aspiration coefficient. Note that sampling error expressed by the second term in Equation (3-1) depends on Stokes number, K, as well as the velocity ratio R. In the limit of large K, the relative sampling bias $|A - 1|$ approaches the relative velocity mismatch $|R - 1|$. For finite K, $|A - 1|$ is always smaller than $|R - 1|$. Thus, sampling error is smaller for smaller particle sizes, lower stream velocities, larger nozzle diameters, and larger gas viscosities. In sampling for PM_{10} emissions $|R - 1|$ could be larger than the 0.1 limit stated for total emissions in Methods 5 and 17 and still retain equivalent accuracy.

To consider anisokinetic sampling error more quantitatively, the entire size distribution may be considered. The aspiration coefficient of particulate mass less than size D' is defined by

$$A(<D') \equiv 1 + (R - 1)b \qquad (3\text{-}2)$$

where

$$b \equiv \frac{\int_0^{D'} m(D) \frac{B}{B + 1} dD}{\int_0^{D'} m(D) dD} \qquad (3\text{-}3)$$

and m(D) describes the aerosol size distribution; it is the derivative of cumulative mass versus particle size for the aerosol of interest. The dependence of the aspiration coefficient for PM_{10}, A(<10), upon velocity ratio R is illustrated in Figure 3-2. A(<10) was calculated from the size distribution measured in this investigation at the outlet of an ESP on a coal-fired power boiler where the mass median diameter (MMD) was 9.4 μm and the geometric standard deviation, σ_g, was 2.5. A typical gas viscosity (220×10^{-6} poise) was assumed. The sampler flow rate was 17 actual liters per min (alpm), appropriate at this viscosity for a 10-μm size cut with Cyclone I, one of several cyclone separators designed for operations of this type (Smith et al., 1979, 1982a,b). A (<10) is given as a function of R for each of five different nozzle sizes; that is nozzle velocity is constant and stream velocity ($v = uR$) is actually the independent variable. The sampling error is readily obtained from each curve for sampling at stream velocities ranging from 0.7 u to 1.3 u. When u = 28 m/s, sampling error would range from -13% to 14% as v ranged from 20 to 37 m/s and lower errors would be experienced at lower stream velocities and with larger nozzle sizes.

Note that the slope of each curve in Figure 3-2 is essentially constant; that is, b in Equation 3-2 is a slowly varying function of v when u is held constant. Thus b is a useful parameter for summarizing anisokinetic sampling error; it is referred to here as the "anisokinetic error coefficient." The sampling error is equal to b times the relative velocity mismatch, (R - 1). This coefficient was calculated for several nozzle velocities and size distributions measured in field tests in this program and reported by Farthing et al. (1988) assuming the same flow rate and viscosity as in Figure 3-2. The results are given in Table 3-2. The anisokinetic error coefficient varies somewhat from site to site because of changes of the size distribution for sizes less than 10 μm. In general, b(<10) increases as the MMD approaches 10 μm and as σ_g decreases. The smallest value of σ_g for any mode in the PM_{10} size range observed by the

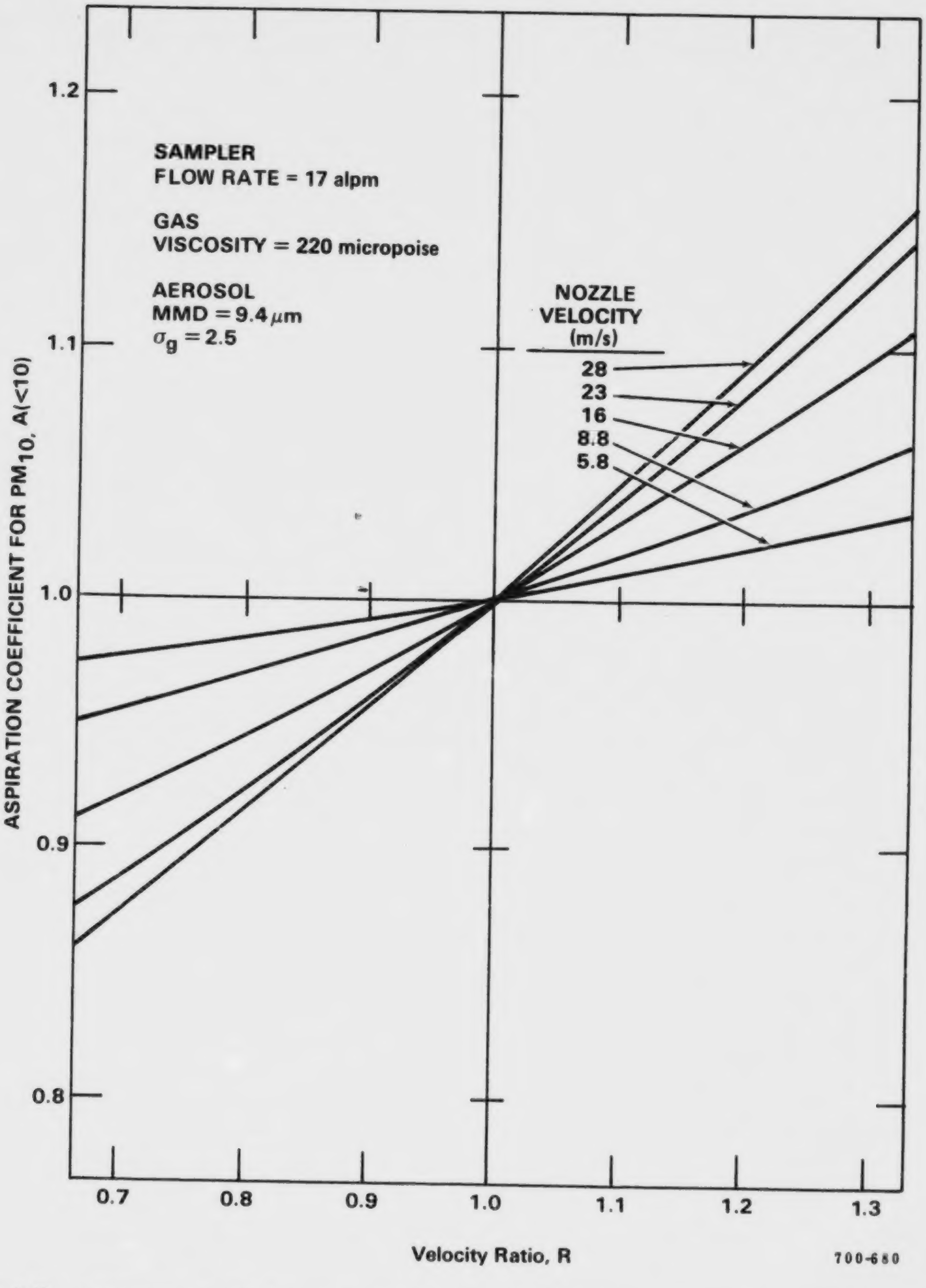

Figure 3-2. Aspiration coefficient versus velocity ratio. A(<10) calculated from the aerosol size distribution measured downstream of control device of a coal-fired power boiler. MMD = mass median diameter; σ_g = geometric standard deviation, alpm = actual liters per minute.

TABLE 3-2. ANISOKINETIC ERROR COEFFICIENT PARTICLES VERSUS VELOCITY FOR AEROSOL SIZE DISTRIBUTIONS MEASURED AT FOUR SAMPLING LOCATIONS[*]

		Anisokinetic error coefficient for PM_{10}					
				Site 3			
Nozzle diameter (in.)	Nozzle velocity (ft/s)	Site 1 MMD=20μm σ_g=2.3	Site 2 MMD=9.4μm σ_g =2.5	Inlet MMD=32μm σ_g=3.6	Outlet MMD=23μm σ_g=2.3	MMD=10μm σ_g=1.8	MMD=10μm σ_g=1.0 b(10)[+]
0.141	93	0.52	0.45	0.41	0.54	0.66	0.84
0.156	75	0.46	0.39	0.36	0.49	0.60	0.79
0.188	52	0.35	0.29[‡]	0.28[‡]	0.38[‡]	0.47	0.69
0.219	38	0.27	0.22	0.21	0.29	0.37	0.58
0.250	29	0.21[‡]	0.17	0.16	0.23	0.29	0.48
0.313	19	0.13	0.09	0.10	0.14	0.18	0.32

[*] Sample flow rate = 0.6 acfm; gas viscosity = 220 x 10^{-6} poise.

[+] Anisokinetic error coefficient for 10-μm particles is the largest value possible for the error coefficient.

[‡] Indicates the values for the actual velocities encountered at each sampling location.

authors at numerous industrial exhaust streams was 1.8. Values of the error coefficient for an assumed lognormal size distribution with σ_g = 1.8 and MMD = 10 μm are also given in Table 3-2. The highest possible value of the anisokinetic error coefficient for PM_{10} is also given for reference purposes; this is for a monodisperse aerosol with σ_g = 1.0 and MMD = 10 μm. Of course, monodisperse aerosols are not encountered in industrial exhaust streams, and a σ_g < 2 is rare.

The anisokinetic error coefficient for PM_{10} decreases substantially as velocity decreases. The sampling error for PM_{10} is always less than the relative velocity mismatch, and is usually much lower. For most sampling locations b(<10) is less than 0.5 and is also less than half of the corresponding coefficient for a monodisperse aerosol of 10-μm particles.

For reference purposes, values of anisokinetic error coefficient for total particulate concentration, b(tot), are given in Table 3-3. As one might expect, the values of b(tot) are substantially higher than corresponding values of b(<10) in Table 3-2, because the larger the particle size the greater the error due to anisokinetic sampling. Note also that b(<10) decreases by 75% as velocity decreases from 28 to 5.8 m/s while b(tot) decreases by less than 50%.

TABLE 3-3. ANISOKINETIC ERROR COEFFICIENT FOR TOTAL PARTICULATE CONCENTRATION VERSUS VELOCITY FOR AEROSOL SIZE DISTRIBUTIONS MEASURED AT FOUR SAMPLING LOCATIONS*

Nozzle diameter (in.)	Nozzle velocity, (ft/s)	Site 1 MMD=20μm σ_g=2.3	Site 2 MMD=9.4μm σ_g=2.5	Site 3 Inlet MMD=32μm σ_g=3.6	Site 3 Outlet MMD=23μm σ_g=2.3
0.141	93	0.86	0.73	0.90	0.89
0.156	75	0.83	0.69	0.89	0.87
0.188	52	0.78	0.62$^+$	0.85$^+$	0 83$^+$
0.219	38	0.72	0.55	0.82	0.78
0.250	29	0.66$^+$	0.49	0.78	0.73
0.313	19	0.55	0.38	0.71	0.63

*Sample flow rate = 0.6 acfm; gas viscosity = 220 X 10^{-6} poise.
$^+$Indicates the values for the actual velocities encountered at each sampling location.

If the PM_{10} probe samples at multiple points in one run with one nozzle size (constant nozzle velocity), the net anisokinetic error is the velocity weighted average of the errors incurred at each of the sample points. The relative error, $\overline{A} - 1$, can be expressed as

$$\overline{A} - 1 = \frac{\sum v_i A_i}{\sum v_i} - 1 = b(\overline{R}-1 + \frac{S^2}{\overline{R}}) \qquad (3\text{-}4)$$

where the index i covers all the sample points, and S^2 is the variance of R for the run. The velocity-weighted average of A_i is appropriate because emission rate is the parameter sought. Equation 3-4 is based on the approximation that stream velocity does not correlate with concentration. Contributions from this type of correlation are ignored because calculations at eight sites for which point-by-point data are available have shown them to be insignificant (Farthing 1983; Hanson et al. 1976; Farthing et al. 1985). Thus the net anisokinetic error is determined by the average and the variance of R.

To limit the error due to the variance of R, the values of R at individual points sampled during a run must be limited. This requirement impacts upon the number of different nozzle sizes which the operator must use to sample all of the points for a complete traverse of the duct. The choice of the limits on individual values of R, R_{min} and R_{max}, is important because small limits would mean small error, but the required effort may be high because some sites may require multiple nozzle sizes for a complete traverse.

The highest possible anisokinetic sampling error would occur in the hypothetical situation in which all of the stream velocities at points to be sampled were either high or low or both compared to the nozzle velocity. This would mean that all of the individual values of R for the run would be either R_{min} or R_{max} or both. With such a distribution $|\overline{R} - 1|$ and S, which determine error in Equation (3-4), are related. If all or most of the R-values were at R_{max} or R_{min} then $|\overline{R} - 1|$ would be high and S would be small. If about the same number of points had low R-values as high R-values then $|\overline{R} - 1|$ would be small and S would be large. Analysis of a PM_{10} traverse in a sample plane with this extreme distribution of stream velocities subject to the limits given in Section 4, $b(10)|R' - 1|<0.2$, shows that the highest possible error would be ±20% for 10-μm particles and any $\overline{R}$ which could occur within those limits. This maximum error would occur when all of the sample points would have R-values of R_{min} or R_{max}, where $b(10)|\overline{R} - 1| = 0.2$. If $|\overline{R} - 1|$ were 0.2 or 0.1, the maximum possible error for 10-μm particles would be ±18% or ±12%, respectively. At most sources, where $b(<10) < 0.5$, the maximum possible error which could occur would be 12% for any $\overline{R}$, 11% for $|\overline{R} - 1| = 0.2$, and 7% for $|\overline{R} - 1| = 0.1$.

Errors Resulting from Changing the Flow Rate Through the Size Separator

As discussed in the previous paragraphs, we find that error due to anisokinetic sampling in the PM_{10} measurement can be held to reasonable values while the sampling velocity is held constant and traversing with one run (at most sources). Whether the latter, fixed-flow-rate approach produces lower errors than those which would be introduced by altering the flow rate to hold isokinetic conditions must now be examined. Although withdrawing the sample from the duct isokinetically ensures that the sample is unbiased with respect to particle size, errors would be introduced because of the concomitant changes which would take place in the diameter at which size fractionation takes place. This question will be examined here.

The effective cutoff diameters for impactor stages and for Cyclone I both vary roughly as the inverse square root of the flow rate through the separator. Values of the errors in apparent PM_{10} concentrations as compared to the true values were calculated for several aerosols which had lognormal size distributions in the range typically found in industrial source sampling. The mass median diameters used were in the range of 10 to 50 μm, and geometric standard deviations of 2 and 3 were used. Errors were calculated for test cases in which the actual flow rates were 20 and 40% off the flow rate required to produce a 10-μm size cut. That is, the flow rates needed to produce isokinetic conditions were taken to be 60, 80, 120, and 140% of the correct flow for a 10 μm cut. The results of these calculations are given in Table 3-4. As can be seen, the errors resulting from the shift in the separation diameter from 10 μm can easily exceed those from anisokinetic sampling for comparable velocity (flow rate) mismatches. Therefore, the option of varying the flow rate through the sizing device to permit isokinetic sampling appears to be inferior to maintaining the correct flow rate at the cost of anisokinetic sampling.

TABLE 3-4. ERRORS IN PM_{10} CONCENTRATIONS (%) RESULTING FROM VARYING THE FLOW RATE THROUGH THE PM_{10} SIZING DEVICE TO MAINTAIN ISOKINETIC SAMPLING CONDITIONS

Aerosol MMD, μm	20% Flow Change		40% Flow Change	
	$\sigma_g = 2$	$\sigma_g = 3$	$\sigma_g = 2$	$\sigma_g = 3$
10	12	6	30	20
12.5	15	8	34	23
16.7	18	10	44	26
20	23	12	47	28
25	26	13	55	30
33	29	14	71	34

SUMMARY: METHODS SELECTED FOR DEVELOPMENT

Considering the factors involved in the preceding subsection, one can quickly note undesirable extremes in traversing protocols for PM_{10} measurement. Single point sampling protocols can minimize anisokinetic errors but are subject to unacceptable uncertainty due to spatial variation of emissions. Syntheses of multiple single-point runs (the interim IP protocol) reduce this uncertainty due to spatial variation but multiply the cost of measurements considerably. Full, unrestricted traverses at fixed flow rate (the common practice in particle sizing measurements) are subject to anisokinetic errors of unknown magnitude, as well as inaccurate weighting in the spatial averaging of emissions. The traversing protocol chosen for development involves restricted traverses within defined velocity limits. This technique, the Constant Sampling Rate technique, has the advantage of clearly defining the expected limits of sampling error. In addition, a technique was selected for development which involves modified sampling hardware to combine isokinetic sampling with fixed-flow-rate operation of an inertial sizing device. This technique, designated exhaust gas recycle, is based on sampling isokinetically at a lower flow rate than that required by the sizing device and making up the difference by recycling a portion of the spent sample gas. The latter approach has the advantage of permitting constant separation diameters to be maintained while simultaneously holding isokinetic sampling conditions. However, it requires more complex sampling equipment, and the possibility of successful development was not as certain as was the case for the CSR technique. CSR could, in principle, be applied with any inertial particle sizing device without the necessity of additional hardware and could confidently be counted upon to perform satisfactorily. Development and characterization of both of these methods are described in the following sections.

SECTION 4

FORMULATION OF PM_{10} METHODS

SELECTION OF PM_{10} SIZING DEVICE

Obviously, in order to construct a PM_{10} sampling method, a suitable device to segregate particles on the basis of aerodynamic size is required. The two classes of inertial particle sizing devices commonly used for in-stack measurements are cascade impactors and small sampling cyclones. Devices of either type can in principle be used for source PM_{10} sampling, and both devices were in fact used in the course of our methods development program.

Of the two classes, cascade impactors are more familiar, more widely accessible, and have a longer history of field use. Impactor stage D_{50} values can be predicted with some confidence over the typical range of stack gas conditions and sampler flow rate. Because of particle bounce and reentrainment, impactors have limited capacity and must generally be operated as multistage devices rather than single-cut classifiers. Multistage cascade impactors provide moderately high resolution particle size distribution data from which PM_{10} concentrations may be inferred by interpolation. These data are obtained at the expense of more complicated preparation, sample recovery, and data reduction procedures, thus placing greater demands on the training, experience, and insight of the operating team. Likewise, more complicated procedures and greater demands on the sampling crew are required to recognize, prevent, or correct for other nonideal effects such as gas-substrate interactions.

Cyclones, on the other hand, are essentially free from problems of bounce, reentrainment, and overloading. They have no substrates and are simple in operation and sample recovery. Cyclones are therefore suitable for single-stage sizing devices. The principal disadvantages of cyclones are not operational, but consist of the more limited understanding of cyclone behavior. Unlike impactors, the D_{50} of a cyclone cannot be adequately predicted from geometric considerations. The variation of the D_{50}'s of typical sampling cyclones with stack gas density, viscosity, and flow rate does follow a similar functional form, but laboratory calibrations of each cyclone design must be performed to develop predictive equations for the D_{50} of that cyclone over a range of gas conditions. These equations, moreover, cannot easily be extrapolated to other cyclones or to conditions beyond the range of the calibration data. Therefore, much more extensive calibration data must be obtained for the development and validation of a PM_{10} cyclone than for a PM_{10} impactor sampler.

In summary, cascade impactors can be useful for PM_{10} sizing, especially when detailed particle size information is also necessary. However, the added time and material costs, the greater skill and training requirements for the sampling team, and the higher probability of unrecognized errors make impactors less attractive for a general method. Since a single-stage PM_{10} sampler is best suited to the needs of a PM_{10} method, the decision was made to develop a cyclone sampler for a PM_{10} sizing device, even though considerably more laboratory characterization of the device would be required as compared to impactors.

Two existing cyclone designs were obvious candidates for PM_{10} use. Both were designed by Southern Research Institute and had been used at several classes of emissions sources. Dimensions of both cyclones are shown in Figure 4-1. On the basis of limited laboratory characterization, it was apparent that each was capable of operation with a 10-μm size cut. The first, Cyclone IX, was designed and used as part of the IP program (Smith et al. 1982a,b). It was designed to be a 15-μm cyclone precollector for cascade impactors, but the characterization data which had been performed indicated proper gas flow rates to obtain 10-μm cuts as well for three temperatures. At 150 °C, Cyclone IX flowrates on the order of 28 L/min (1 acfm) are required for a 10-μm D_{50}. The second choice was Cyclone I of the Southern Research Institute five-stage cyclone train (Smith et al. 1979). Although characterization of this cyclone for 10-μm particles was less extensive, the gas flow rate for a 10-μm cut was predicted to be 18-20 L/min (0.65 - 0.7 acfm) at 150 °C.

While both cyclones appeared adequate in performance, Cyclone I was chosen on the basis of several secondary considerations. First, Cyclone I was smaller and could be used with 4-in. sampling ports commonly found on stationary emissions sources, whereas 5- or 6-in. ports were required for Cyclone IX. Second, Cyclone I was more readily available, since it had been commercialized, and several vendors of sampling equipment sold versions having the same interior dimensions as the original SRI prototype designs. The only vendor who sold a version of Cyclone IX had made significant design changes to the inlet so that it could no longer be considered functionally equivalent to the original prototypes.

A third difference existed between the two cyclones, the effect of which could not be evaluated as a clear advantage for either unit. As is shown in Figure 4-1, Cyclone IX has a typical geometry with the gas exit tube located at the top of the cyclone, adjacent to the sample inlet. Cyclone I, on the other hand, uses an internal "turnaround cup" to redirect the gas flow into a longer outlet tube passing through the body and collection cup of the cyclone. This design allows the cyclone to access traverse points up to 2.5 cm (1 in.) from the far wall of a duct, whereas the nozzle of Cyclone IX can be placed no closer than 10.9 cm (4.1 in.) from the far wall. This difference is significant primarily when sampling from circular ducts, since Cyclone IX cannot reach the far traverse point of even a minimal (16 point) traverse line for ducts smaller than 2.4 m (93 in.) diameter. A possible additional advantage of the bottom exit cyclone configuration is that the nozzle may experience less perturbation near the outboard end of the probe because of the downstream obstruction caused by the cyclone body. The effect of the bottom exit is not a clear benefit, however. The relatively long gas outlet tube in Cyclone I collects a significant amount of particulate matter on both inside and outside surfaces. Particles collected on the outside surface of the outlet tube may be reentrained if the cyclone is jarred during sampling and may erroneously be counted as PM_{10}. Particles on the inside of the collection tube are considered to have left the cyclone

CYCLONE DIMENSIONS

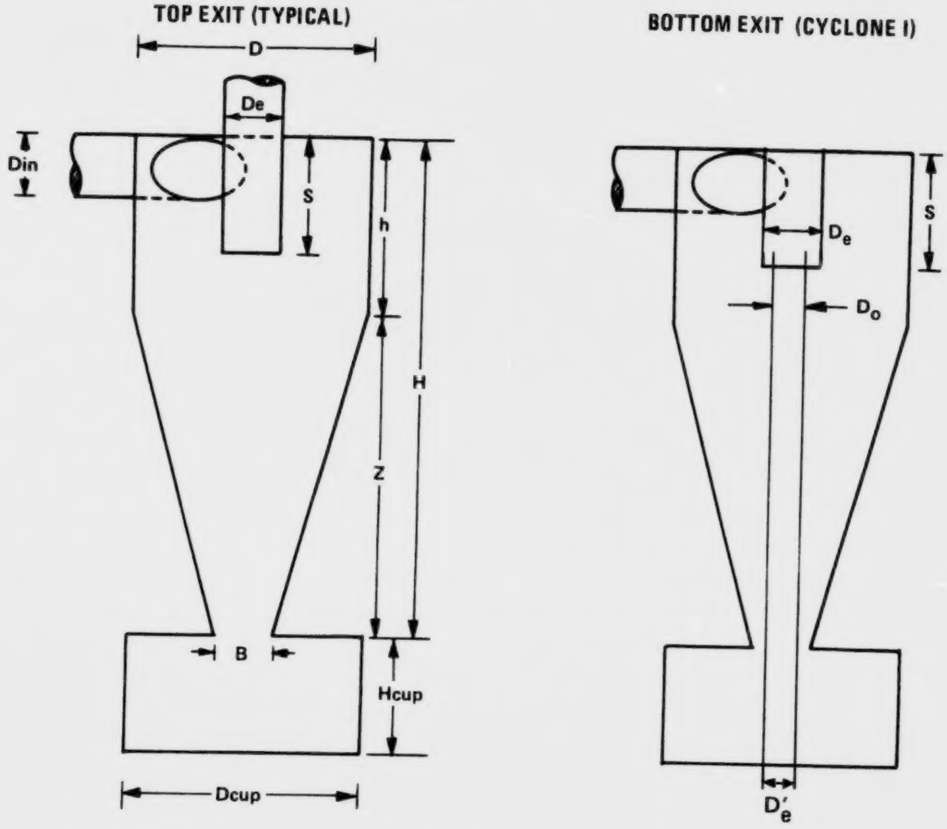
TOP EXIT (TYPICAL)
D
De
Din
S
h
H
Z
B
Hcup
Dcup
BOTTOM EXIT (CYCLONE I)
S
D_e
D_o
D'_e

CYCLONE	DIMENSIONS, cm											
	Din	D	De	B	H	h	Z	S	Hcup	Dcup	D'_e	D_o
I	1.27	4.47	1.50	1.88	6.95	2.24	4.71	1.57	2.25	4.45	1.02	1.24
IX	1.53	5.12	1.81	2.43	7.06	2.35	4.71	2.00	2.26	5.12	—	—

5595-71

Figure 4-1. Cyclone dimensions.

and are counted as PM_{10}, but they may not be recovered efficiently when a very light particulate loading is collected.

In the experimental work described in this report, Cyclone I was the primary PM_{10} sizing device used. Cyclone I has been the only sizing device used in the EGR train, although designs for EGR nozzles adapted for other sizing devices have been formulated. Most of the CSR field sampling described in Section 5 also used Cyclone I. In one test of CSR, cascade impactors (University of Washington Mark V) equipped with external, right-angle-geometry precollector (Southern Research design manufactured by Andersen Samplers, Inc.) were used as the inertial sizing device. The same impactors, operated isokinetically at single points, were used in other tests as reference samplers to provide full particle size distributions, as well as PM_{10} and total particulate mass concentrations.

DEVELOPMENT OF CONSTANT SAMPLING RATE METHOD

Basic Objectives of CSR Sampling Strategy

The CSR sampling protocol was developed as a result of the detailed analysis by Farthing (1983) of errors in particulate sampling. Several specific objectives shaped the details of the method. First, the technique was designed to use existing sampling equipment (as of 1983) in order to avoid lengthy hardware development. Second, the details of the traversing strategy were selected to limit errors from all controllable sources to the level of other more intrinsic errors (such as fluctuations in source emissions or basic measurement inaccuracy). Finally, the measurements should give an appropriate weighted spatial average in order to be representative of true PM_{10} emission rates.

The operating principle chosen for the CSR technique was to obtain a multipoint sample over a restricted traverse determined by duct velocity. Stack gas is sampled at the fixed flow rate calculated to give a 10-µm cut point. Anisokinetic errors are restricted at each sampling point by limits on the allowable isokinetic ratio R. If the range of duct velocities would cause these limits to be exceeded by a full traverse, the traverse is broken into two or more subtraverses with different sampling nozzle sizes to remain within the calculated anisokinetic sampling limits. The number of traverse points is selected to reduce errors due to spatial variation of emissions to acceptable levels while allowing sufficient time for necessary operator decisions between sampling points. In order to provide proper averaging of emissions, the dwell time at each traverse point is proportional to the local duct velocity. Current specifications were designed to limit worst-case anisokinetic sampling errors for PM_{10} to less than 20%, with the knowledge that in essentially all sampling situations, cancellation of sampling errors will limit overall anisokinetic sampling error to much less than this value. The following subsection explains the steps involved in CSR sampling. The full recommended protocol, documented in Federal Register format, is contained in Appendix A.

Outline of CSR Protocol

Determination of Anisokinetic Sampling Limits--

Management of anisokinetic sampling error requires setting limits as point-by-point values of the isokinetic ratio R. These are determined by the requirement that anisokinetic error be limited to ±20%, that is, $|A - 1| < 0.2$. From Equation 3-2 it is seen that this condition occurs when R is limited so that $b(10)|R - 1| < 0.2$, where R, b(10), and A are defined as in Section 3. In other words, R must be regulated to remain between R_{min} and R_{max}, where $R_{min} = 1 - [0.2/b(10)]$ and $R_{max} = 1 + [0.2/b(10)]$. Choosing the highest possible values of b, those for a monodisperse 10 μm aerosol, b(10), ensures sampling within the desired error limits. Corresponding limits on R can be obtained by substituting $d = (4QR'/v\pi)^{1/2}$ and D = 10 μm into Equation 3-1 and solving for stream velocity:

$$v^{3/2} = \frac{36(A-1)\mu Q^{1/2}(R')^{3/2}}{\pi^{1/2}(R'-A)(2R'+0.617)(10\mu m)^2} \qquad (4\text{-}1)$$

where A = 0.8 for $R' = R_{min}$ and A = 1.2 for $R' = R_{max}$.

The value of $\mu Q^{1/2}$ depends upon the sampler and the temperature and composition of the gas. If a single-stage PM_{10} sampler is used, then Q should be the flow rate which provides a 10-μm size cut. With a cascade impactor, the flow rate is somewhat adjustable, but should be selected to produce at least one size cut above or very near 10 μm.

While closed-form solutions to the two forms of equation 4-1 can be calculated, a nomograph has been constructed which provides a graphical solution for the limiting values of R or v. Values for R' were calculated from Equation 4-1 for various assumed values of $\mu Q^{1/2}$ which are in the expected range for stationary sources and available sampling equipment. The results are shown graphically in Figure 4-2 with the upper and lower curves representing, respectively, R' versus v obtained by setting A = 1.2 and 0.8 in Equation 4-1. The function R = v/u with u, a constant, is represented in Figure 4-2 as the curve designated R(v,u) and running in a nearly vertical line. On a logarithmic plot such as Figure 4-2, this function has exactly the same shape and slope no matter where it is centered on the "R = 1" line. It is needed in reading the appropriate limits, R_{min} and R_{max}, or the corresponding v_{min} and v_{max}, determined by the value of u. This vertical curve is shifted left or right so that its center (at R = 1) matches the nozzle velocity. The limits, R_{min} and R_{max} or v_{min} and v_{max}, are the values where the vertical curve intersects the limit curves appropriate for the $\mu Q^{1/2}$ value. Typically, $\mu Q^{1/2}$ is in the range of 750 to 1310 for combustion sources and commercial samplers.

The limits depicted in Figure 4-2 are broad enough so that the velocities in a point-by-point traverse at most sources will fall within the specified limits. However, in some ducts, velocities at some traverse points will be outside of these limits for one nozzle. In that circumstance, additional nozzles, having limits which include the other velocities, should be used, and the traverse must be divided into two or more subtraverses with different nozzle diameters.

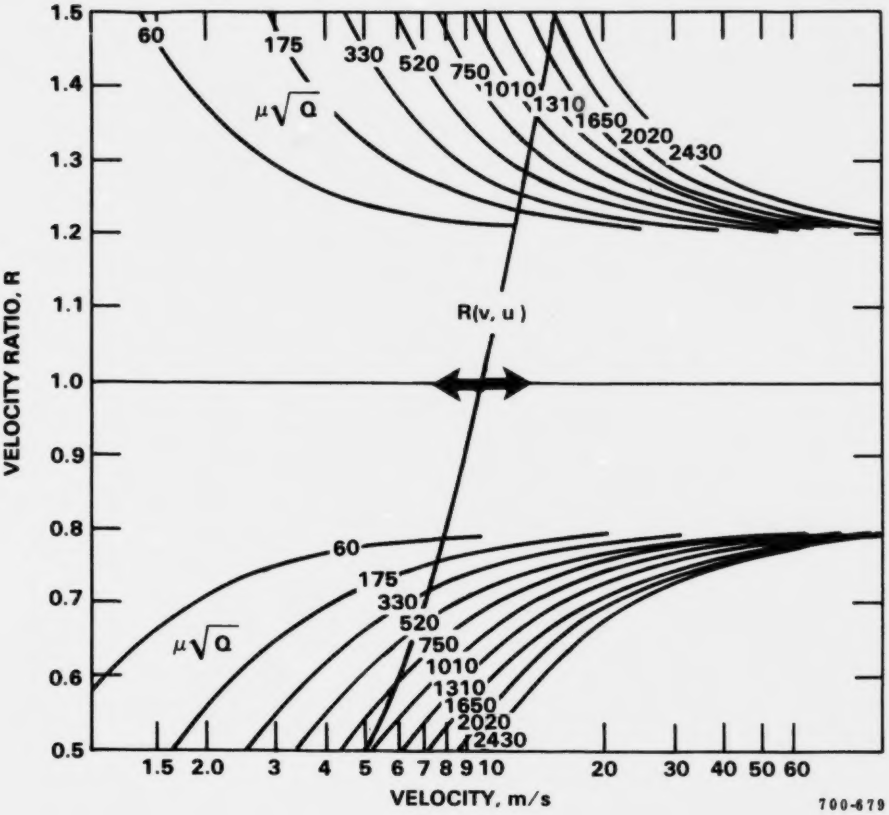

Figure 4-2. Velocity ratio, R, versus duct velocity to give aspiration coefficient of 1.2 (upper curves) and 0.8 (lower curves) for 10-µm particles.

The frequency of tests in which one nozzle size is not sufficient for the complete traverse is related to the increments of nozzle sizes available. Performance of a velocity traverse before the sampling run permits selection of the optimum nozzle size available. Small increments for the nozzle sizes increase the likelihood that a nozzle size will be available to give a nozzle velocity near the mean stream velocity. In this case, $|\overline{R} - 1|$ is at its lowest possible value; moreover, the likelihood is then less that stream velocities will exceed the limits for the chosen nozzle. Thus using smaller nozzle increments simplifies the measurements as well as improves the accuracy. The current set of 10 nozzles used for Cyclone I has a mean area ratio between adjacent sizes of approximately 1.25, and spans a duct velocity of about 10.4 with allowances for $|\overline{R} - 1| < 0.2$ for the largest and smallest nozzle. A set of nozzles spaced exactly 1.2 apart would span a duct velocity range of 8.9, approximately 8 to 72 ft/s for typical Cyclone I flow rates. In principle, with this nozzle set, $|\overline{R} - 1|$ could be limited to 0.1, further increasing the accuracy of the CSR technique. However, temporal variation of many processes make this limit on $|\overline{R} - 1|$ difficult to achieve. The average stream velocity sometimes varies between the time of initial measurement of it for choosing the nozzle size and the time at which the sample is obtained. Therefore, no limit is imposed upon $|\overline{R} - 1|$ by the current CSR protocol when the point-by-point limits are satisfied and the optimum nozzle size is chosen from the previous velocity data.

Dwell Time and Traverse Points--

Another important difference in CSR protocol and Methods 5 and 17 is the dwell time. In these EPA methods the dwell time is the same for all traverse points. The measured concentration is a velocity-weighted average for all points, as it should be for determination of emission rate, because the sampling rate is varied at each point to be proportional to point velocity. Since flow rate cannot be adjusted from point to point with a PM_{10} sampler, the dwell time at each point must be proportional to the point velocity to obtain a velocity-weighted sample.

The number of traverse points in CSR was determined on basis of restricting costs and effort in field sampling, as well as the consideration of sampling errors described in Section 3. Analysis of error due to spatial variation of total particulate emissions versus number of traverse points (Shigehara 1982) indicates that 95% confidence intervals drop rapidly from ±50% for one sample point to less than ±10% at eight more traverse points. Further analysis by Farthing (1983) indicates that particles smaller than 10 μm are less stratified than total particulate matter, but one site was found in which 12 traverse points were necessary to reduce this type of error to less than 10%. It is concluded that this type of error would be limited to acceptable levels (less than 10%) if the number of traverse points is 8 or 9 when the location of the sample plane is 8 duct diameters downstream and 2 duct diameters upstream from the nearest disturbance as specified by Method 1. Otherwise, 12 traverse points are necessary. Two benefits arise from sampling sampling a maximum of 12 points rather than 24 or 25, as might be required by Method 5. First, with a lower number of points, the dwell time at each point is kept high enough to allow the operator to make the additional on-the-spot calculations and decisions necessary for CSR. Second, when sampling is conducted in circular ducts, the points eliminated are the ones nearest the duct walls which would be more likely to have velocities low enough to require a nozzle change.

To more clearly illustrate CSR protocol, a setup form and instructions are presented as Table 4-1. This form can be used after a velocity traverse has been performed and measurement of various parameters indicated which are normally obtained in stack sampling. The handwritten values were those obtained for a traverse performed in this investigation. The term "CSR Nomograph" refers to Figure 4-2.

DEVELOPMENT OF EXHAUST GAS RECYCLE METHOD

Several alternate sampling train design approaches have been considered that allow isokinetic sampling over a full duct traverse while maintaining a constant flow rate through an inertial sizing device (Smith et al. 1982a). These include such concepts as variable area nozzles, split stream sampling probes, probe shroud extractive sampling, and gas recycle concepts. Several of these concepts, including exhaust gas recycle, were proposed as modifications to the EPA Source Assessment Sampling System (SASS) to allow isokinetic sampling traverses with this fixed-flow-rate sampling train (Blake 1978).

The EGR concept was subsequently developed into a prototype sampling train (Harris and Beddingfield 1981), and some testing was performed both at the EPA facilities at Research Triangle Park and under contract by Southern Research Institute. The sampling train design allowed a variable fraction of conditioned and filtered exhaust gas to be added to the sample between the sample nozzle and the inertial sampler. This allowed a preselected, constant flow rate through the inertial sampler while the gas flow rate into the sampling nozzle was adjusted to remain isokinetic with the local duct velocity.

In this section we explain the emission gas recycle principle of operation, describe the sampling train, and present the results of preliminary laboratory testing in a wind tunnel source simulator.

Principle of Operation

The principle of operation of the EGR train is illustrated in Figure 4-3. Stack gas is extracted isokinetically at volumetric flow rate Q_s. If the stack moisture fraction is B_{ws}, the sample flow consists of $B_{ws} \cdot Q_s$ moisture and $Q_s(1-B_{ws})$ dry gas flow. At the mixing point a flow, Q_r, of dry recycle gas is added to the sample stream to bring the total flow rate to the predetermined constant level, Q_t. In the impingers or condenser, the moisture content $B_{ws} \cdot Q_s$ is removed. After the pump and total flow metering element, the recycle flow Q_r is diverted by means of an adjustable valve. By mass balance, in a leak-free system, the remaining flow which passes the dry gas meter and orifice will simply be $Q_s(1 - B_{ws})$, exactly as would occur in an isokinetic sampling train without gas recycle.

There are several practical requirements for a functional EGR sampling system. The operator must be able to monitor and control accurately two flow rates rather than one. Setup and operation of the train must be

Table 4-1. CSR SETUP FORMS

A. CSR SETUP WITH CYCLONE I (PM_{10} SIZE CUT)

1. $Q = 3.35\text{x}10^{-6}\,\mu^{2.228} = 3.35\text{x}10^{-6}\,(\underline{222})^{2.228} = \boxed{0.5659}$ (acfm) with μ in micropoise

2. $\mu\sqrt{Q} = (\underline{222})\sqrt{(0.5659)\text{x}28.32} = \underline{889}$, Round UP to the nearest value in CSR Nomograph, 1010

Nozzle velocity, $u = 3.056\,Q/d^2 = 3.056\,(0.5659)/d^2 = \boxed{1.729\ /d^2}$ (ft/s) with d in inches

Nozzle ID =	2-1	2-3	2-2	
d =	0.3653	0.1857	0.2533	(inches)
u =	12.96	50.15	26.95	(ft/s)
Minimum Velocity, $V_{\ell\ell}$ =	—	32.8	—	(ft/s)
Maximum Velocity, $V_{u\ell}$ =	—	64.0	37.7	(ft/s)

3. Pitot $\Delta P = 1.368\text{x}10^{-4}\,\frac{P_{stk}}{T_{stk}}\,M_w\,\frac{1}{C_p^2}\,v^2 = 1.368\text{x}10^{-4}\,\frac{(24.61)(29.60)}{(743)(0.844)^2}\,v^2 = \underset{\text{with v in ft/s}}{\underline{1.883\times10^{-4}}}\,v^2$ (H_2O")

$\Delta P_{\ell\ell}$ =	—	0.203	—	(H_2O")
$\Delta P_{u\ell}$ =	—	0.771	0.268	(H_2O")

4. Choose Nozzle(s) from $\Delta P_{\ell\ell}$ and $\Delta P_{u\ell}$ and Expected Pitot ΔPs (From Last Traverse) $(C_p/C_p')^2 = 1.0095$

	Port A		Port B		Port C		Port D	
Point #	ΔP	Noz. ID	ΔP	Noz. ID	ΔP	Noz. ID	ΔP	Noz. ID
1	0.56	2-3	0.58	2-3	0.56	2-3	0.54	2-3
2	0.52	2-3	0.50	2-3	0.50	2-3	0.49	2-3
3								
4								

Note: During a traverse, if ΔP of a point is found to be out of range for the current nozzle, skip it and come back with an appropriate nozzle.

5. $\Delta H = Q^2\,\frac{T_{dgm}}{T_{stk}^2}\,\frac{P_{stk}^2}{P_o}\,(1\text{-}f_{H_2O})^2\,M_d\,K_{cal} = (0.5659)^2\,\frac{T_{dgm}}{(743)^2}\,\frac{(24.61)^2}{(24.65)}\,(1\text{-}0.\underline{0617})^2\,(\underline{29.60})\,K_{cal}$

$= \underline{3.714\times10^{-4}}\,T_{dgm}\,K_{cal} = \underline{3.714\times10^{-4}}\,(\underline{525})\,(\underline{7.23}) = \boxed{1.41}$ H_2O"

DWELL TIMES

6. $t_1 = \frac{\sqrt{\Delta P_1}}{\sqrt{\overline{\Delta P}}}\,\frac{\text{Total run time}}{\text{No. points}} = \frac{(0.742)}{(0.726)}\,(60) = \underline{61.25};\ t_n = \frac{t_1}{\sqrt{\Delta P_1}}\,\sqrt{\Delta P_n} = \frac{(61.25)}{\sqrt{(0.55)}}\sqrt{\Delta P_n} = \underline{82.59}\,\sqrt{\Delta P_n}$

DWELL TIMES AND ΔP

	Port A		Port B		Port C		Port D	
Point #	ΔP	t	ΔP	t	ΔP	t	ΔP	t
1	0.56	61 (t)	0.59	63	0.56	62	0.59	63
2	0.51	59	0.51	59	0.51	59	0.54	61
3								
4								

Traverse # ______ Setup by ______ Operator ______

Table 4-1. (Continued).

B. INSTRUCTIONS FOR CSR SETUP WITH CYCLONE I (PM_{10} SIZE CUT).
(STEPS 1 THROUGH 3)

1. Flow rate, Q, for PM_{10} Size Cut Determined from Gas Viscosity, μ.

   Viscosity is given by

$$\mu = C_1 + C_2T_{stk} + C_3T_{stk}^2 + C_4f_{H_2O} + C_5f_{O_2}$$

$$\mu = 51.05+0.207(743)+3.24\times10^{-5}(743)^2 - 74.1(0.0617)+53.1(0.070)$$

$$= \boxed{222} \text{ micropoise}$$

   where T_{stk} is gas temperature in °R and f_{H_2O} and f_{O_2} are the mole or volume fractions of water and O_2, respectively. Calculate Q and put the value on the setup form.

2. Lower and Upper Limits ($v_{\ell\ell}$ and $v_{u\ell}$) for Stream Velocity.

   $\mu\sqrt{Q}$ and nozzle velocity, u, are necessary to read $v_{\ell\ell}$ and $v_{u\ell}$ from the CSR nomograph. List IDs and diameters (in.) of prospective nozzles, and calculate u for each nozzle. Read $v_{\ell\ell}$ and $v_{u\ell}$ from the CSR nomograph by overlaying the R=v/u curve so that its center (R=1) matches the nomograph at R=1 and v=u. Then $v_{\ell\ell}$ ($v_{u\ell}$) is the velocity, v, at which the R=v/u curve intersects the appropriate $u\sqrt{Q}$ curve toward the bottom (top) of the nomograph. Find at list these values for each nozzle. (Note that velocities in the current nomograph are in m/s; the conversion to ft/s is x 3.28).

3. Conversion of $v_{\ell\ell}$ and $v_{u\ell}$ to Corresponding Pitot, $\Delta P_{\ell\ell}$ and $\Delta P_{u\ell}$.

   The Pitot equation is given where:

   P_{stk} = the duct absolute pressure = $P_{BAR} + \Delta P_{stk}$ = 24.61 Hg",
   T_{stk} = gas temperature = 743 °R, 28(0.80) + 32(0.07) + 44(0.13)
   M_d = dry molecular weight of the gas = $28\ f_{N_2} + 32\ f_{O_2} + 44\ f_{CO_2}$ = 30.36,
   M_w = wet molecular weight of the gas = $M_d\ [1-f_{H_2O}]+18\ f_{H_2O}$ = 29.60, and
   C_p = Pitot coefficient for CSR probe = 0.844.
   The coefficient of v^2 can be expected to remain constant during constant load. List $\Delta P_{\ell\ell}$ and $\Delta P_{u\ell}$ for each prospective nozzle. During a sampling run, the Pitot reading for each point must be within the specified limits for the nozzle used at the point.

Table 4-1. (Continued).

C. INSTRUCTIONS FOR CSR SETUP WITH A CYCLONE (PM_{10} SIZE CUT).

(Steps 4 through 6)

4. Choosing the Appropriate Nozzle(s).

List previously measured Pitot ΔPs for the points to be traversed. Note that if these were obtained with a different Pitot, conversion to equivalent values for the Pitot on the CSR probe is advised. The conversion is $x(Cp/Cp')^2$, where Cp' is the coefficient for the Pitot used in the previous traverse. Choose the nozzle for which $\Delta P_{\ell\ell}$ and $\Delta P_{u\ell}$ bracket the measured values. If more than one nozzle is acceptable, choose the one giving the greatest symmetry. Encircle the nozzle chosen. Note that if the expected Pitot ΔP for one or more points is near a limit for the chosen nozzle, then it may be outside the limits at the time of the run, so the potential requirement for an additional nozzle should be anticipated. During a traverse, if the Pitot ΔP of a point is found to be out of range for the current nozzle, skip it and come back to sample at it later with an appropriate nozzle. If more than one nozzle may or will be required, put the appropriate nozzle identification beside the Pitot. The CSR nomograph has limits broad enough so that multiple nozzles seldom will be necessary. However, the temporal and/or spatial variation of stream velocity is sufficient in some ducts at some sources to require more than one nozzle.

5. Calculate Pressure Drop (ΔH) for Setting Sampler Flow Rate.

The orifice equation is given where ΔH is in H_2O",
T_{DGM} = temperature of dry gas meter in °R
P_o = absolute pressure at the orifice entrance in Hg"
$= P_{BAR} + \frac{\Delta H}{13.6} \approx$ 24.75 for (ΔH = 1.41)
K_{cal} = orifice calibration constant = 7.23

At a particular source under constant load these parameters are expected to be constant from traverse to traverse, except T_{DGM} may vary with weather. Iteration must be used since ΔH enters into P_o. First calculate ΔH assuming $P_o = P_{BAR}$, and enter it above with a final estimate of P_o.

6. Dwell Times.

The dwell time at each point of a run should be proportional to the velocity at the point. The dwell time for the first sample point is calculated prior to starting the run as the average dwell time per point multiplied by the ratio of $\sqrt{\Delta P_1}/\sqrt{\Delta P}$ using ΔPs from the previous traverse. Of course, any traverse point can be sampled first. Write t, at its appropriate location in the dwell time-ΔP matrix. Then each succeeding dwell time, t_n (n>1), is calculated during the run using ΔPs from the same run. After positioning the nozzle at the nth point, the operator records the ΔP_n and calculates the time to sample at that point as $(t_1/\sqrt{\Delta P_1})\sqrt{\Delta P_n}$ rounded to the nearest 1/4 min. This is expedited by calculating the coefficient $t_1/\sqrt{\Delta P_1}$ immediately after measuring ΔP_1 (at the first point).

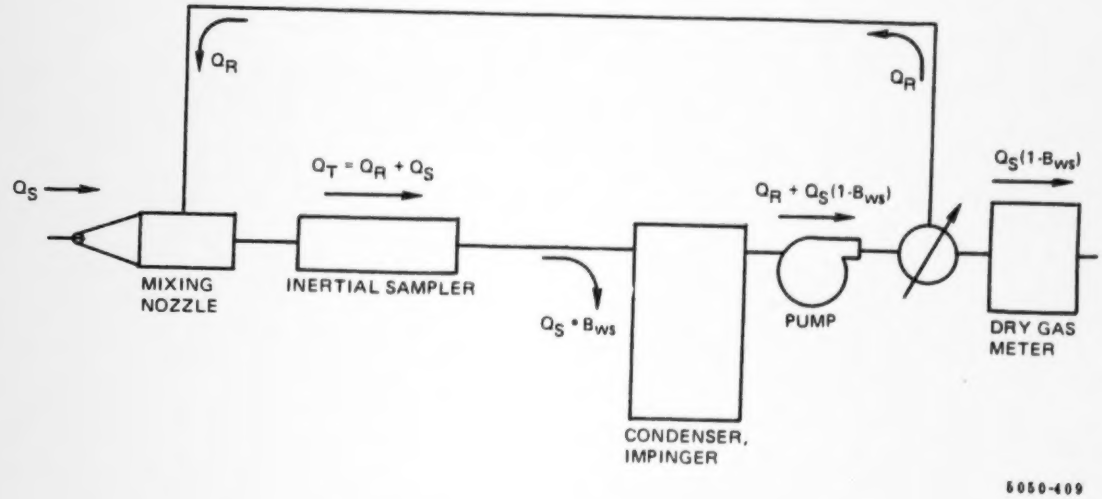

Figure 4-3. Gas flow in exhaust gas recycle train.

simple, and the train must function reliably in normal field sampling environments. The recycle gas mixing must not cause significant particle deposition, must not perturb the cut points of the inertial sizing device, and must not introduce artifact particulate matter.

In order to meet these constraints, the prototype train was constructed by modifications to the control module and sampling hardware of a commercially available Method 5 sampling train. Laminar flow elements (LFEs) were used to monitor the recycle and total flow rates. In order to minimize particulate losses, the recycle gas was introduced coaxially in an annulus around the sample gas.

Prototype and Second-Generation EGR Trains

A block diagram of the prototype field EGR train is shown in Figure 4-4. Stack gas is isokinetically extracted through the sample portion of the EGR mixing nozzle, mixed with the conditioned recycle gas, and then passed into Cyclone SRI-I, the initial sizing component of the sample train. After passing the inertial sizing device and in-stack sample filter, the sample gas passes through the probe and condenser or impinger train and into the EGR flow control module. As in conventional Method 5 control modules, the flow rate of the gas entering the control module is controlled by coarse and fine control valves (V_1 and V_2, respectively) at the entrance of the sealed pump. At the exit of the pump and absolute filter, the total flow is measured with an LFE (Meriam Model 50MJ10-1/2 Type 10). The gas stream is then split into the recycle and sample flow lines. The sample flow is monitored in the normal manner with a dry gas meter and a calibrated orifice. The recycle gas flow rate is measured with a second LFE (Meriam Model 50MJ10-1/2 Type 11). The partitioning between sample and recycle gas is controlled by a valve (V_3) located downstream of the LFE. Valve V_4 was added to the system to extend the range of control to higher recycle percentages by adding back pressure to the sample flow line.

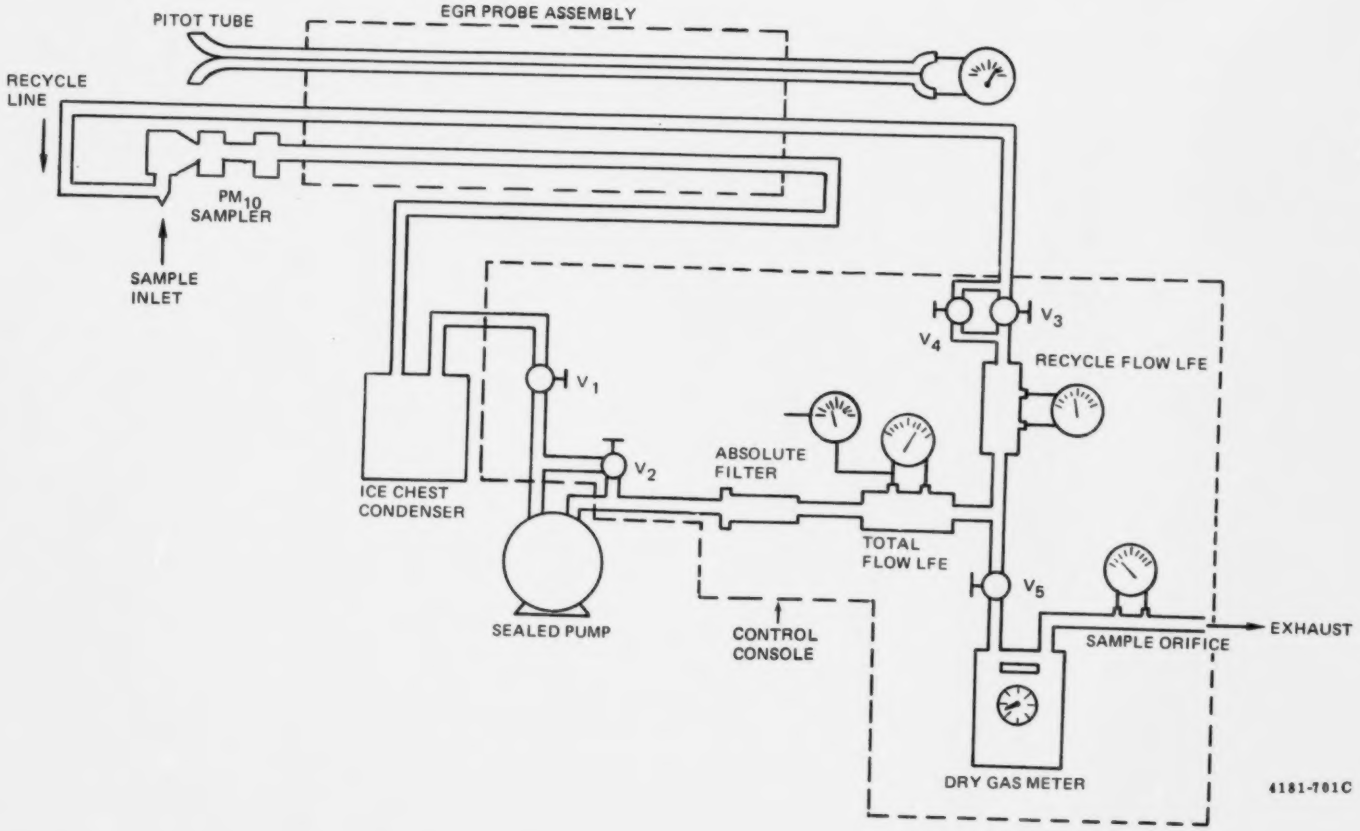
PITOT TUBE
EGR PROBE ASSEMBLY
RECYCLE LINE
PM_{10} SAMPLER
SAMPLE INLET
ICE CHEST CONDENSER
V_1
V_2
SEALED PUMP
ABSOLUTE FILTER
TOTAL FLOW LFE
CONTROL CONSOLE
V_4
V_3
RECYCLE FLOW LFE
V_5
SAMPLE ORIFICE
EXHAUST
DRY GAS METER
4181-701C

Figure 4-4. Schematic of the exhaust gas recycle train.

Figure 4-5 shows an annular mixing nozzle designed for recycle use with Cyclone SRI-I. The dimensions of this nozzle allow the sampler to be inserted into a 4-in. sampling port. Figures 4-6 and 4-7 show the prototype EGR control console.

Figures 4-8 through 4-12 show the control module for the second-generation EGR system designed during this program. As can be seen, the appearance of the module is similar to that of a standard Method 5 sampling box, with the exception of the total, inlet, and recycle Magnehelic® gauges, the recycle and sample (back pressure) control valves, and the recycle gas outlet. The PM_{10} size-fractioning cyclone used in conjunction with the EGR system is shown in Figures 4-13 and 4-14. The cyclone chosen as the PM_{10} sizing device was the commercially available version of the SRI/EPA Cyclone I (of the five-stage series cyclone). The particular cyclone used was of the Flow Sensor type, currently marketed by Andersen Samplers, Inc. It should be noted that in the interest of clarity the side view of the EGR PM_{10} cyclone sampling device (Figure 4-14) is shown with the recirculating nozzle pointing 180°from the operation position. As shown, the device would not fit through a typical 4-in. sampling port.

Wind Tunnel Tests of the EGR Prototype Train

In order to assess the performance of the prototype EGR train, simultaneous parallel tests were conducted at the wind tunnel facility at Southern Research Institute. A dual sampling probe with a single pitot allowed the EGR train and a second isokinetic sampling train to operate side by side in the same test port of the wind tunnel. A dual cyclone train consisting of Cyclones I and IV of the EPA/SRI five stage cyclone sampler was used with each train. Both trains were operated isokinetically with identical cyclone flow rates. Run conditions were varied to test comparability of the two trains at different EGR recycle fractions. For all runs, the 3/16-in. EGR mixing nozzle was used in the EGR train. Three different nozzles with nominal diameters of 5, 6, and 7 mm were used in the nonrecycle train. As both trains sampled isokinetically from points having the same duct velocity, recycle fractions of 9, 36, and 52%, respectively, were added to the emission gas recycle sample flow in order to obtain equal cyclone flow rates in both trains. Several runs were made for each recycle fraction. In all but the last run, the wind tunnel velocity was adjusted so that the cyclone flow rate in both trains was approximately 0.6 ft^3/min (17 L/min).

The results of the cyclone tests are contained in Table 4-2. As indicated by the mean percent difference and standard deviation values shown in Table 4-2 the mass concentrations measured with the paired recycle and nonrecycle trains agree within the expected experimental error. The ratio of the concentrations measured with the EGR train to those measured with the nonrecycle train shows no obvious dependence on recycle fraction. The particulate fractions collected by the initial cyclones in the parallel trains are likewise comparable in magnitude. There is a possible bias toward lower collection efficiency in the exhaust gas recycle cyclone, but this difference appears to be on the order of a few percent in all but one run.

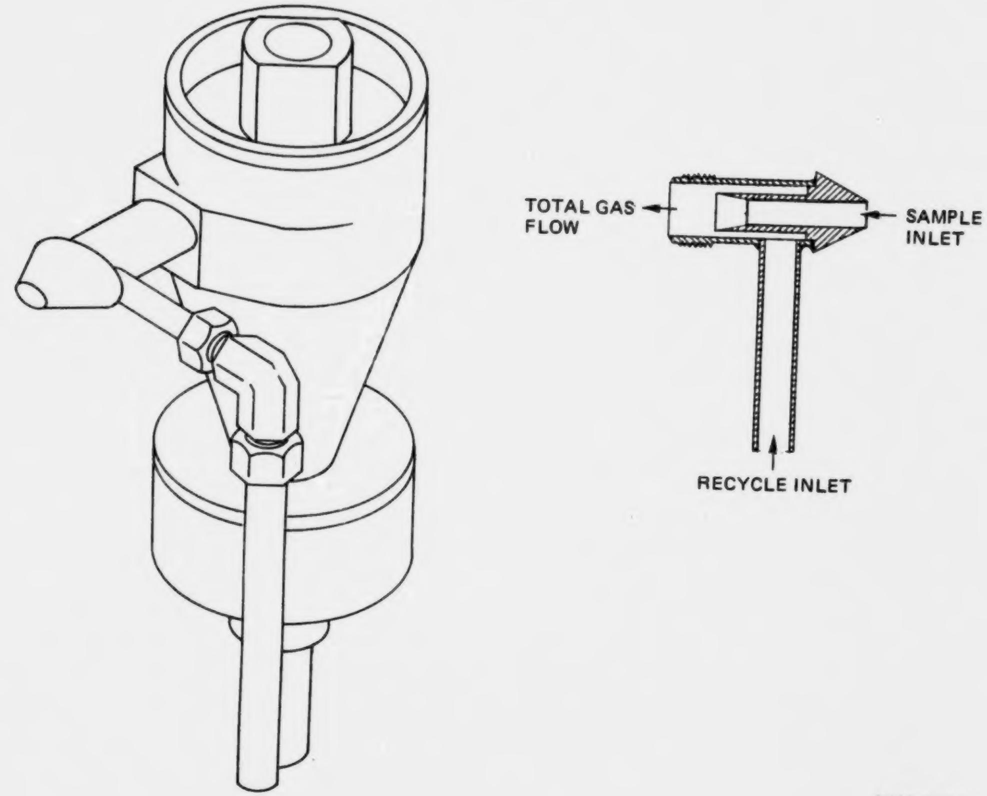
TOTAL GAS FLOW
SAMPLE INLET
RECYCLE INLET
5050-407A

Figure 4-5. Cross-sectional detail of the EGR mixing nozzles.
Mixing nozzle for PM$_{10}$ cyclone in prototype EGR train.

Reproduced from
best available copy.

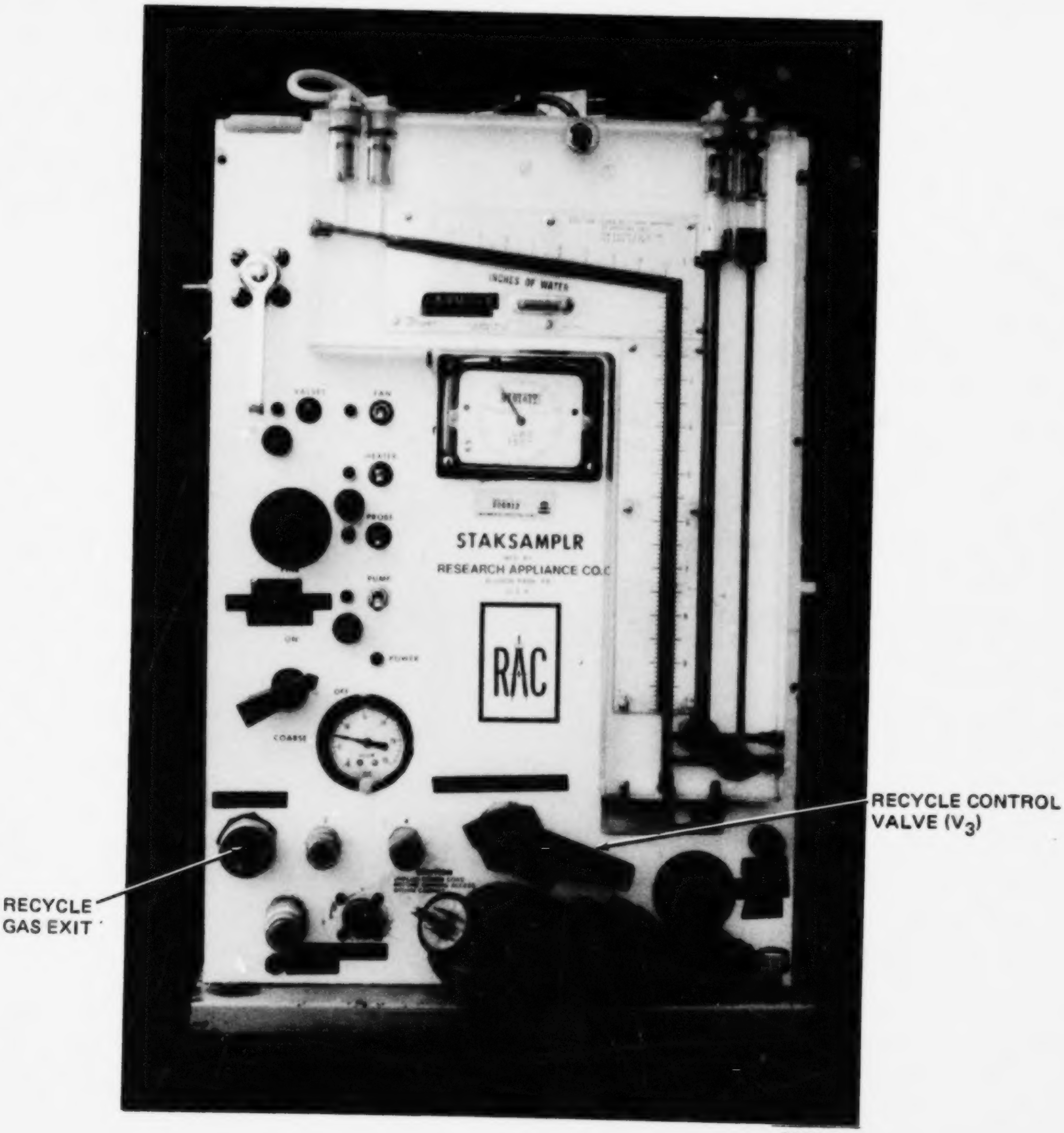
INCHES OF WATER
VALVE
FAN
HEATER
PROBE
PUMP
ON
POWER
OFF
COARSE
STAKSAMPLR
RESEARCH APPLIANCE CO.
RAC
RECYCLE CONTROL VALVE (V_3)
RECYCLE GAS EXIT

5050-414

Figure 4-6. First-generation EGR control console (front view).

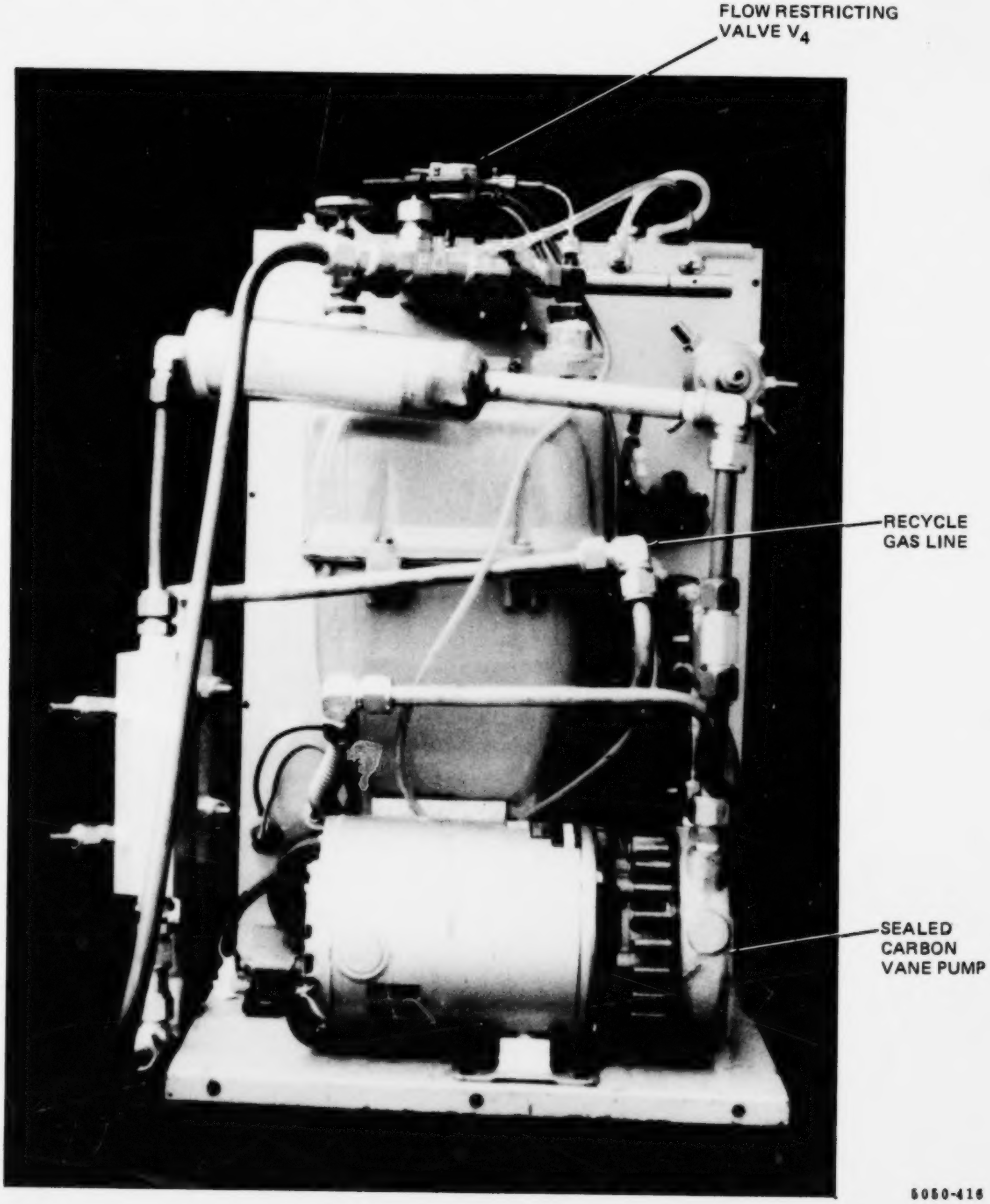
FLOW RESTRICTING VALVE V_4
RECYCLE GAS LINE
SEALED CARBON VANE PUMP
5050-416

Figure 4-7. First-generation EGR control console (rear view).

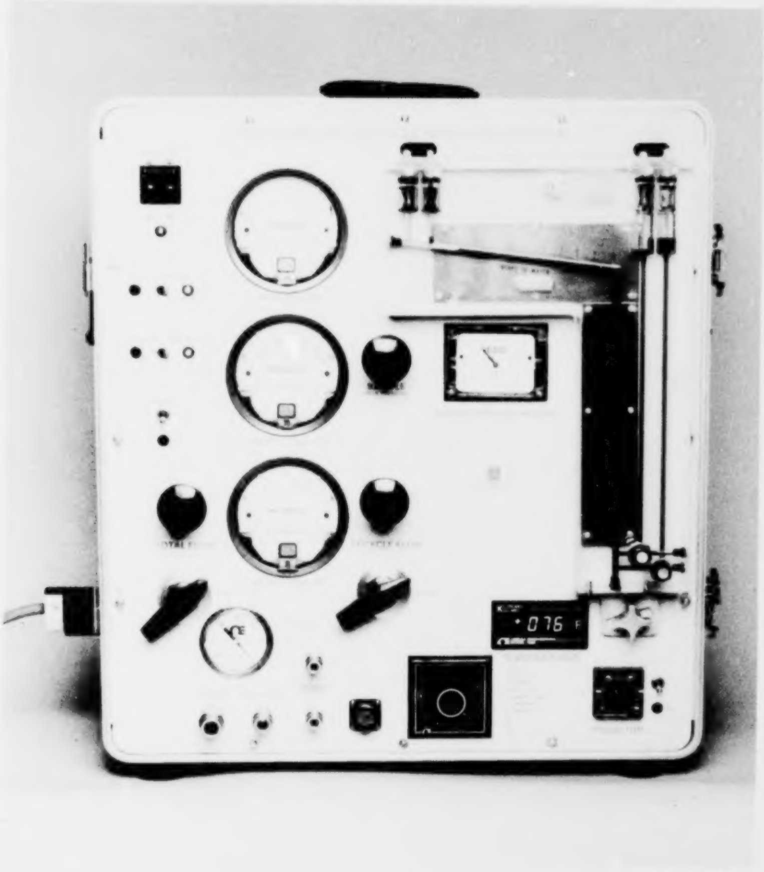

5598-30

Figure 4-8. EGR sampling system control module (front view).

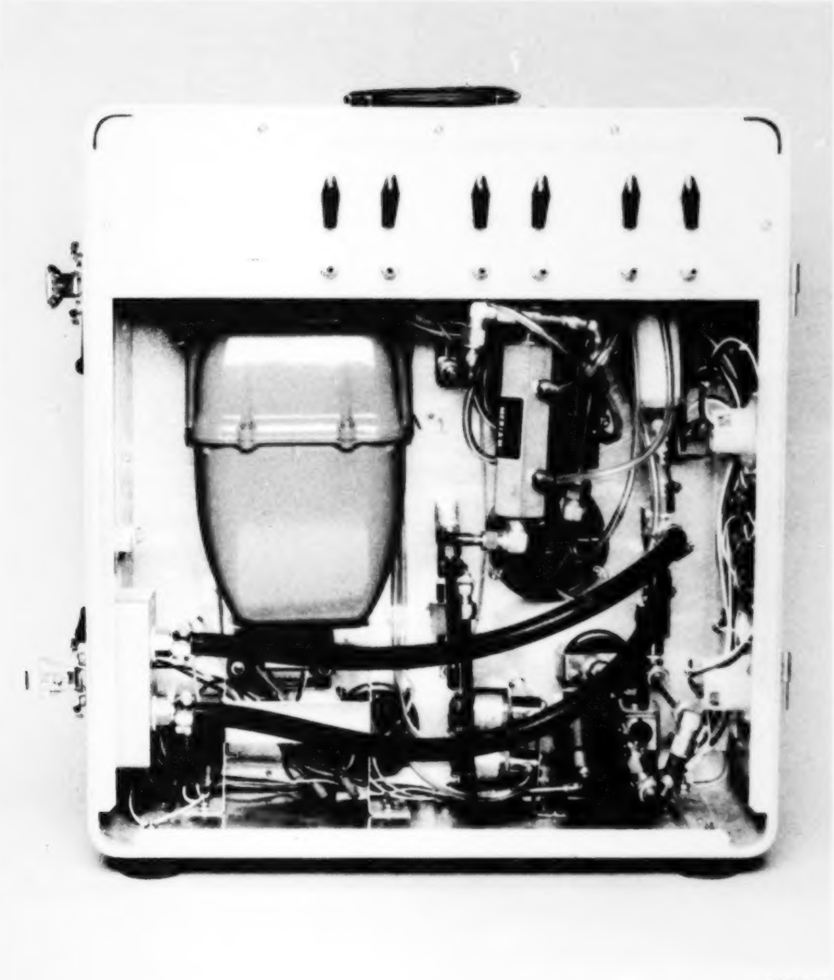

5598-31

Figure 4-9. EGR sampling system control module (rear view).

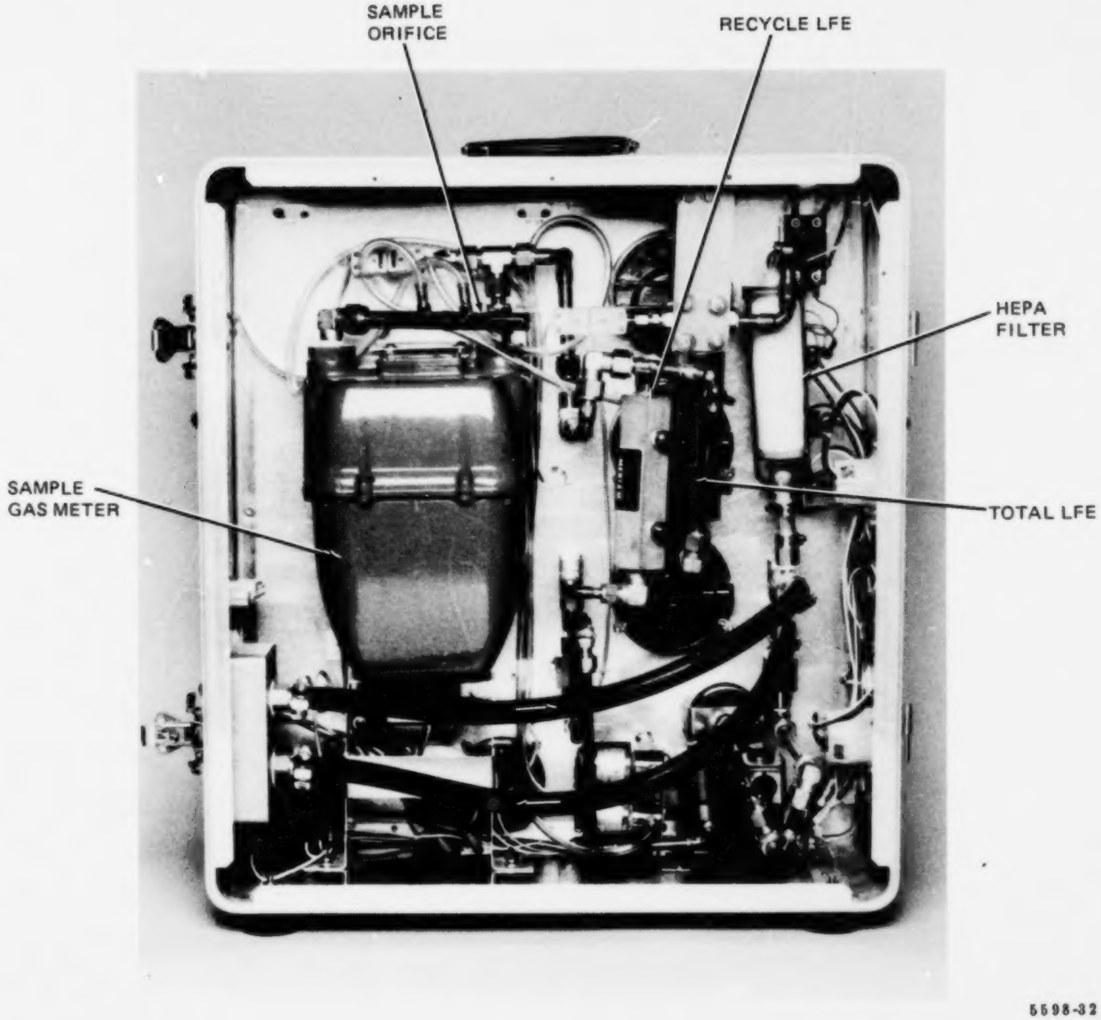
SAMPLE ORIFICE
RECYCLE LFE
HEPA FILTER
SAMPLE GAS METER
TOTAL LFE
5598-32

Figure 4-10. EGR sampling system control module (rear view) showing internal components.

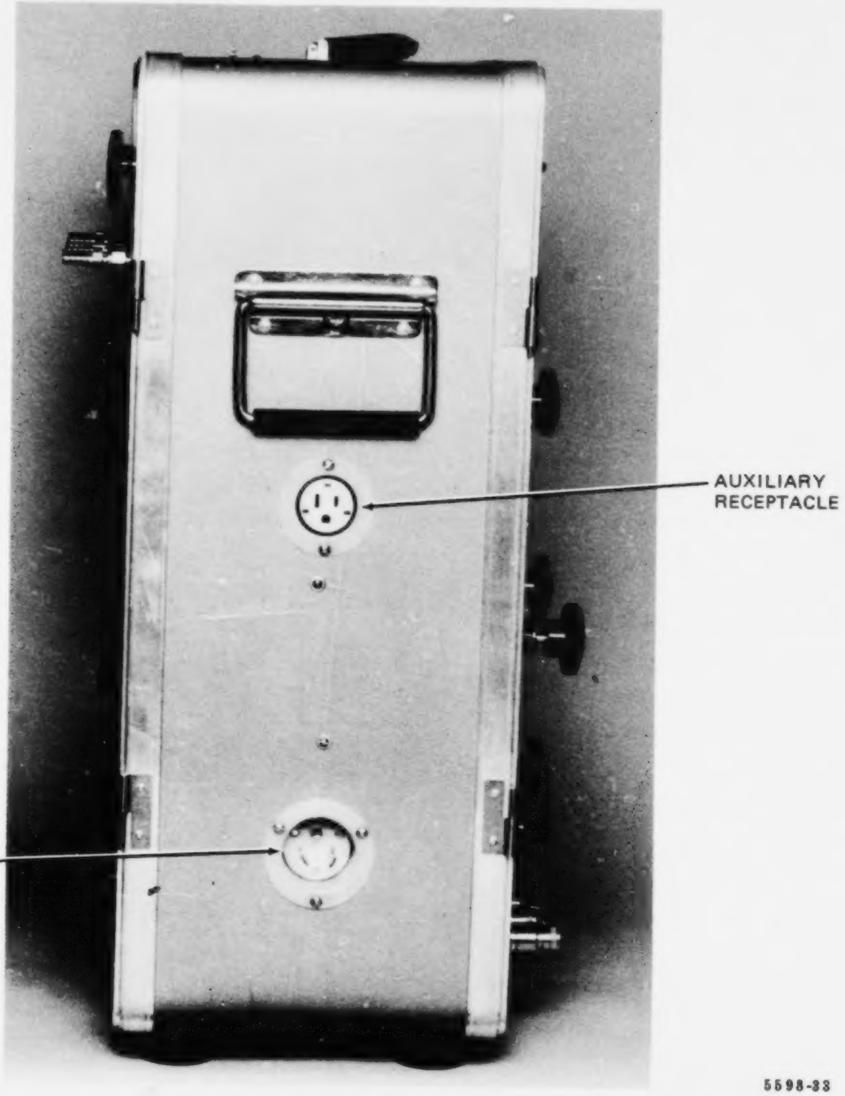
AUXILIARY RECEPTACLE
MAIN POWER INPUT
5598-33

Figure 4-11. EGR sampling system control module (right side).

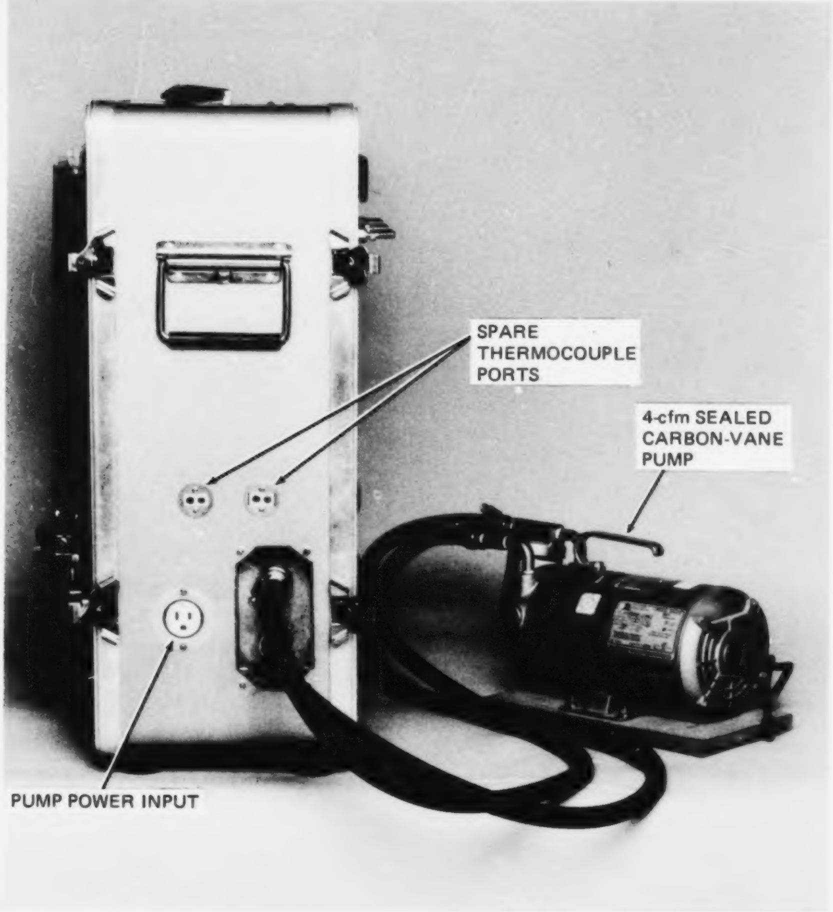
SPARE THERMOCOUPLE PORTS
4-cfm SEALED CARBON-VANE PUMP
PUMP POWER INPUT
5598-34

Figure 4-12. EGR sampling system control module (left side) with 4-cfm pump.

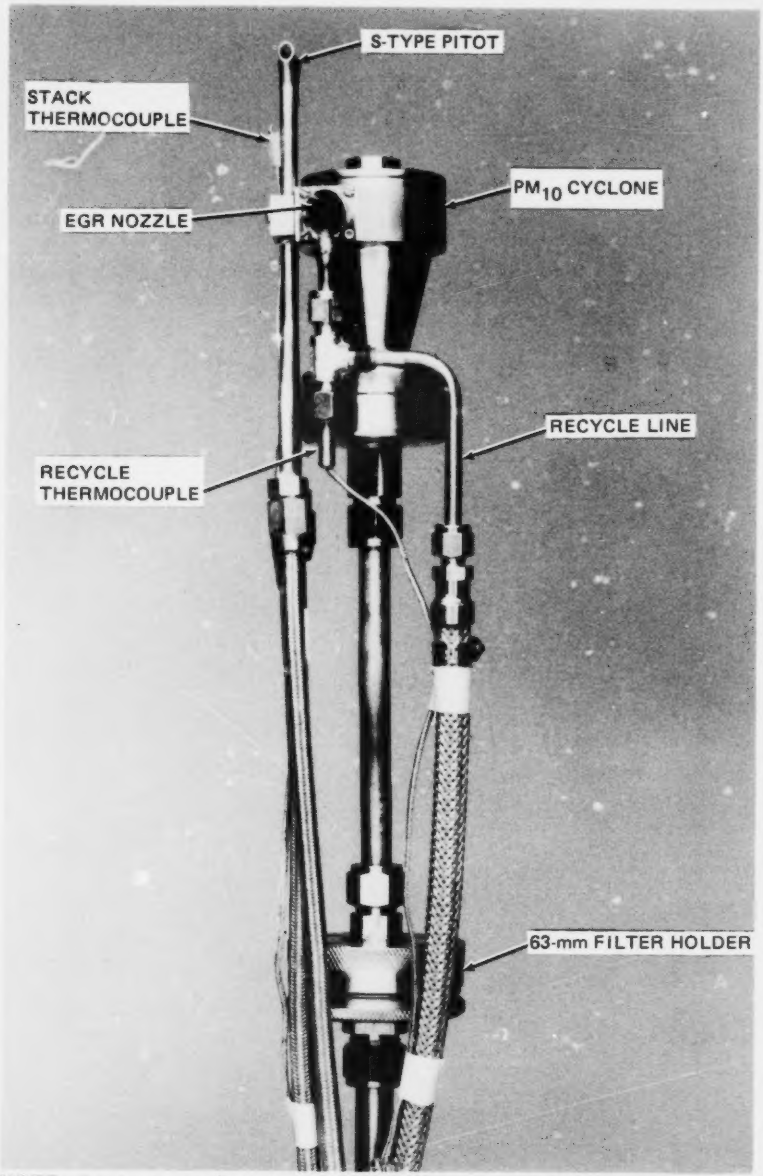
S-TYPE PITOT
STACK THERMOCOUPLE
PM_{10} CYCLONE
EGR NOZZLE
RECYCLE LINE
RECYCLE THERMOCOUPLE
63-mm FILTER HOLDER

NOTE: See text regarding pitot tube location.

5598-35

Figure 4-13. EGR PM_{10} cyclone sampling device (front view).

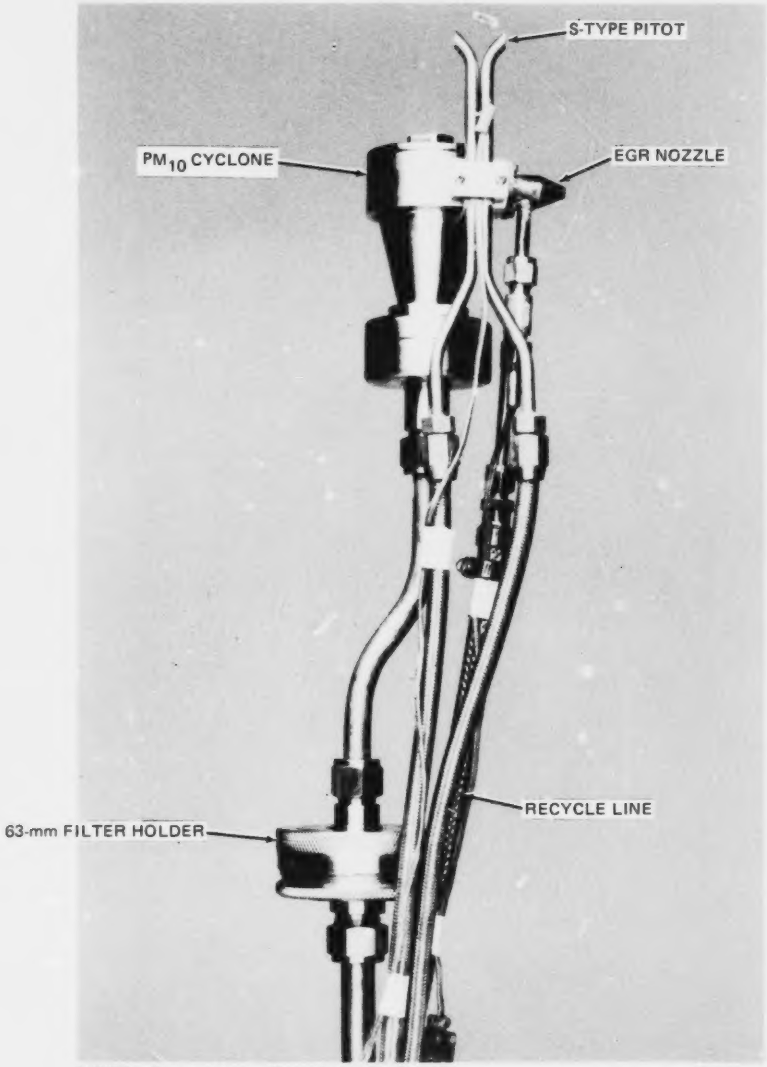
S-TYPE PITOT
PM_{10} CYCLONE
EGR NOZZLE
RECYCLE LINE
63-mm FILTER HOLDER

NOTE: See text regarding pitot tube location.

5598-36

Figure 4-14. EGR PM_{10} cyclone sampling device (side view).

TABLE 4-2. RESULTS OF PARALLEL TESTS USING DUAL CYCLONE TRAINS (CYCLONES I and IV) WITH EGR NOZZLE AND WITH STANDARD (STD) NONRECYCLE CONFIGURATION

Sample Train	Sample Flow (acfm)	Percent Recycle Flow	Percent Isokinetic	Mass Loading (mg/dsm^3)	Difference, Percent	Cyclone I Catch, Percent
EGR	0.5157	9.3	95.8	219.0	-0.3	66.9
STD	0.6020	-	101.8	219.5		68.9
EGR	0.5246	9.2	96.6	275.3	5.5	67.7
STD	0.6187	-	103.6	261.0		70.5
EGR	0.5302	9.1	97.1	277.1	4.3	61.9
STD	0.6168	-	102.8	265.8		70.4
EGR	0.3733	35.7	98.8	337.3	-8.9	63.6
STD	0.6150	-	102.9	370.3		67.5
EGR	0.3782	35.3	99.5	345.4	-0.4	64.2
STD	0.6219	-	103.4	346.7		70.5
EGR	0.2806	51.5	102.3	502.1	6.2	49.2
STD	0.5903	-	99.9	472.7		68.3
EGR	0.2692	52.0	99.3	1591.5	-1.5	80.8
STD	0.5949	-	101.9	1615.1		82.9
EGR	0.2763	52.2	101.9	638.0	-11.0	88.1
STD	0.5970	-	102.3	716.7		88.2
EGR	0.2771	52.9	99.2	882.8	-2.4	75.2
STD	0.6199	-	103.0	904.4		78.8
EGR	0.4455	51.4	97.5	772.9	-3.8	87.4
STD	1.0365	-	105.3	803.1		88.7
			Mean percent difference		-1.2	
			Standard deviation		5.7	

SECTION 5

PM_{10} FIELD STUDIES

As a key part of the PM_{10} development program, six field studies were conducted at four emissions sources. In the course of these field tests, the two candidate methods were refined and tested, and PM_{10} measurements were performed at a range of source conditions. This section contains an overview of the objectives, methodology, and key findings of the entire test series. More detailed discussion of the tests are contained in two EPA reports (Farthing et al., 1986, 1988).

OVERVIEW OF FIELD STUDIES

Test Objectives

The field studies in this program were designed with several objectives in view. Since both PM_{10} methods have hardware or procedural elements which are quite different from other source sampling methods, the field studies were used as means of obtaining basic data about these new procedures as well as development, refinement, and validation of the overall methods.

The first objective of the field studies was to test and refine the procedures and sampling hardware of both PM_{10} methods. The EGR concept at the beginning of this program had not been incorporated into a sampling train suitable for field use with particle sizing equipment. The procedures involved lengthy setup calculations and atypical protocols for operation and sample recovery. Both equipment and procedures needed testing in a field environment to discover weak points in hardware design and undesirable elements in operating protocols. As a result, several modifications to the EGR train and procedures were made during the test series and incorporated into the two second generation trains constructed for use in field tests 5 and 6 described in this section.

Like the EGR method, the CSR procedure involved significant departure from typical source sampling operation. In particular, the protocol requires on-the-spot decisions by the sampling team at each traverse point, as well as at other key times in the course of each sampling run. Several approaches to this decision-making process had to be evaluated in the field. Moreover, background data were needed on the technical assumptions behind the CSR protocol. As a result of the early field tests, the CSR operating procedure was streamlined considerably, and some key uncertainties were resolved.

One further element in the testing and refinement of both candidate methods was the inertial sizing device itself. While the candidate PM_{10} cyclone had been used for several years in other applications, it had not been characterized either in the laboratory or field under conditions typical of PM_{10} operation. The versions of the cyclone which are commercially available have different exterior dimensions and nozzle designs from the SRI-owned prototypes which were used on the initial studies. These differences prevented design of a single EGR nozzle system suitable for both versions of the cyclone. Several adaptations in both versions were necessary for use as a PM_{10} precollector for a single- or dual-stage sizing train. It was also not clear how well a 10-µm cut could be predicted over a range of stack gas conditions with the cyclone either in a gas recycle or a conventional nozzle configuration. During the test series, several of these potential difficulties were clarified or resolved.

A second objective of the test series was to obtain comparison measurements of PM_{10} and total particulate concentration by each method and by the best available reference measurements. An obvious difficulty in test design is that no absolute reference measurement method exists for particulate concentration (total or size-specific) which can serve as an accuracy test for the candidate methods. Other potential measurement methods suffer from the same sources of error as the two PM_{10} methods under evaluation. Thus, if an independent "reference" method shows a significant deviation from a candidate PM_{10} method, it is difficult to apportion the inaccuracy between the method under evaluation and the "reference." Moreover, if the errors in both measurements arise from a common mechanism, the agreement between the two measurements may obscure a common systematic inaccuracy. In view of these pitfalls, the field tests were designed to obtain the best possible comparison between the PM_{10} measurements and independent measurements using well characterized hardware. Specific aspects of test design are described in the following subsection.

A third objective of the test series was to measure the precision of each PM_{10} method at a common source and compare these precision measurements to like measurements by using Method 17. Tests 5 and 6 were designed to meet this objective by using collocated multiple train sampling test designs.

Test Design

In order to meet the objectives described above, careful attention to test design was required. While the detailed design of each test varied according to the primary objective in focus and according to specifics of each test site, certain elements are common to several tests. These common elements, discussed in this section, include use of independent measurements as the best available reference on the accuracy of each technique; control of external variables by maximum feasible use of collocated and simultaneous sample protocols; site selection for significant challenge of the methods over a range of source conditions.

As mentioned above, in the absence of a true reference for size-specific particle concentrations, measurements using independent techniques were selected in order to identify systematic biases of either PM_{10} method. First, in several tests, the two methods were compared with each other. Since CSR and EGR measurements of PM_{10} concentration should, in principle, agree perfectly when averaged over a large sample set and within 20% at all points, comparisons of the two types of measurement should demonstrate comparability within this range.

In addition, attempts were made to compare each method to reference measurements with similar sizing devices which would be expected to eliminate one or more sources of error. Thus, both EGR and CSR sampling runs were compared to samples taken with an isokinetic sampling train with the same inertial sizing device. In order to accomplish this comparison, restricted sample traverses or single-point sampling was necessary.

Field-test designs also specified independent comparison measurements with different sampling hardware. For example, in several tests PM_{10} measurements using cyclones were compared with particle size distribution measurements using cascade impactors. These comparisons provide several cross-checks. First, cyclones and impactors are subject to somewhat different sampling artifacts, so comparison measurements may be used to identify, or place limits on, errors due to anomalous collection or size misclassification artifacts in either device. Second, since stage D_{50} values are somewhat better defined for impactors, and since cascade impactors give continuous size distribution data, impactor data may be used to identify shifts in the D_{50} of the cyclones. Finally, since impactors may be used in some PM_{10} applications, it is useful to have measurements of the comparability of the samplers.

Likewise, total mass concentration measurements using both PM_{10} were compared to Method 17 measurements as an independent reference (Method 17 was chosen as more appropriate than Method 5 because both PM_{10} sampling systems operate with in stack sizing devices and filters). While total particulate mass concentration measurements are not the primary goal of either PM_{10} method, these measurements are useful "worst-case" diagnostics of sampling errors which would be reflected in PM_{10} measurements as well.

In order to obtain the most reliable comparison data between methods, external source-related variables were controlled by the maximum feasible use of collocated or simultaneous sample protocols. Collocated samples in principle eliminate the effects of source temporal variation and stratification of emissions within the sampling duct (spatial variations). Where possible, collocated samples were obtained by a modified dual-probe technique; that is, the probes of two samplers were physically attached. An example of this type of probe, shown in Figure 5-1, is a collocated cascade impactor (for CSR measurements) and Method 17 filter. This train was used in test 2. A similar dual train consisting of a Method 17 and an EGR/cyclone sampler was used in test 1. This train required installation of a 6 in. sampling port. Where it was not feasible to physically attach probes of the collocated sampler, individual probes were inserted to the same point in the sampling duct and aligned by observation from outside the duct. An example was the collocated three-impactor arrangement shown in Figure 5-2. This arrangement required simultaneous access to the same duct location through a 6-in. and a 4-in. sampling port. Other such arrangements were used where possible. The most ambitious collocation scheme, used in test 6, is shown in Figure 5-3. This arrangement involves location of dual Method 17 samplers, dual CSR cyclones, and an EGR cyclone sampler within a 6-in. diameter zone in the center of a duct.

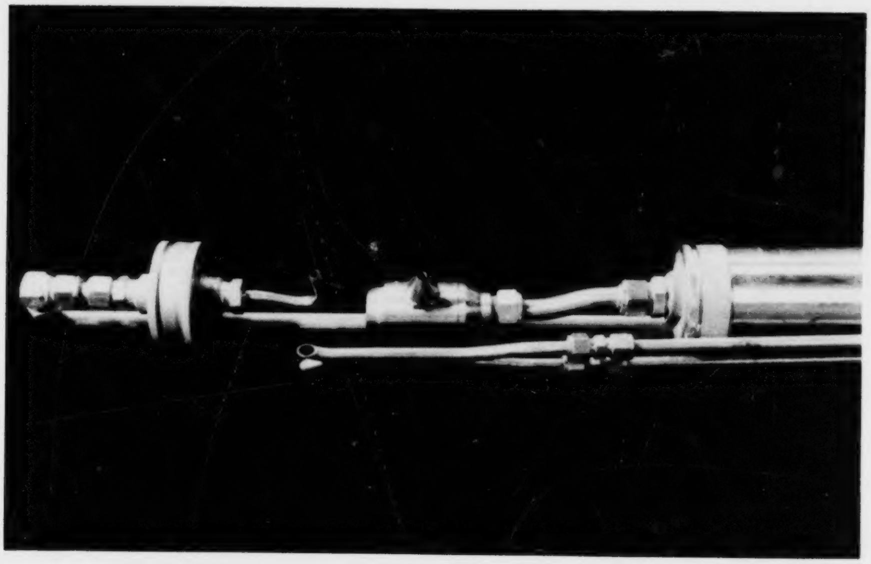

5050-449

Figure 5-1. Collocated cascade impactor and Method 17 filter (used in test 2).

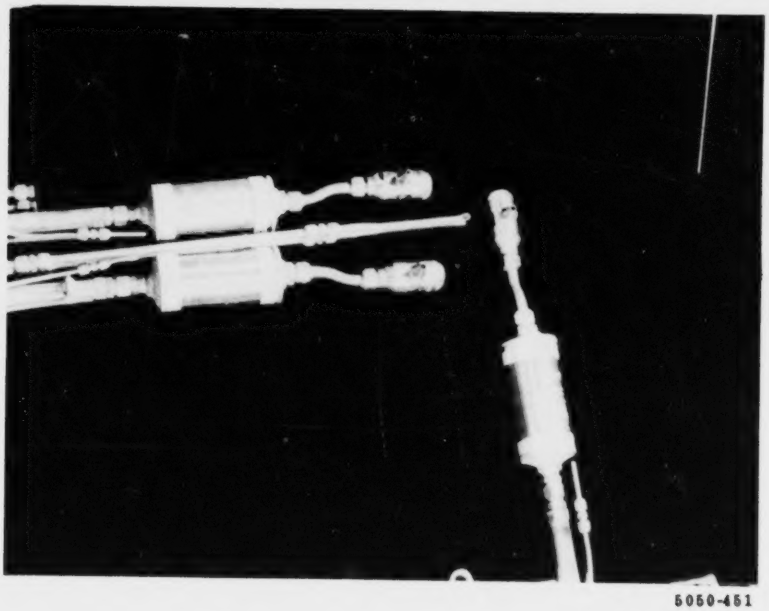

5050-451

Figure 5-2. Three collocated cascade impactors (as used in test 2).

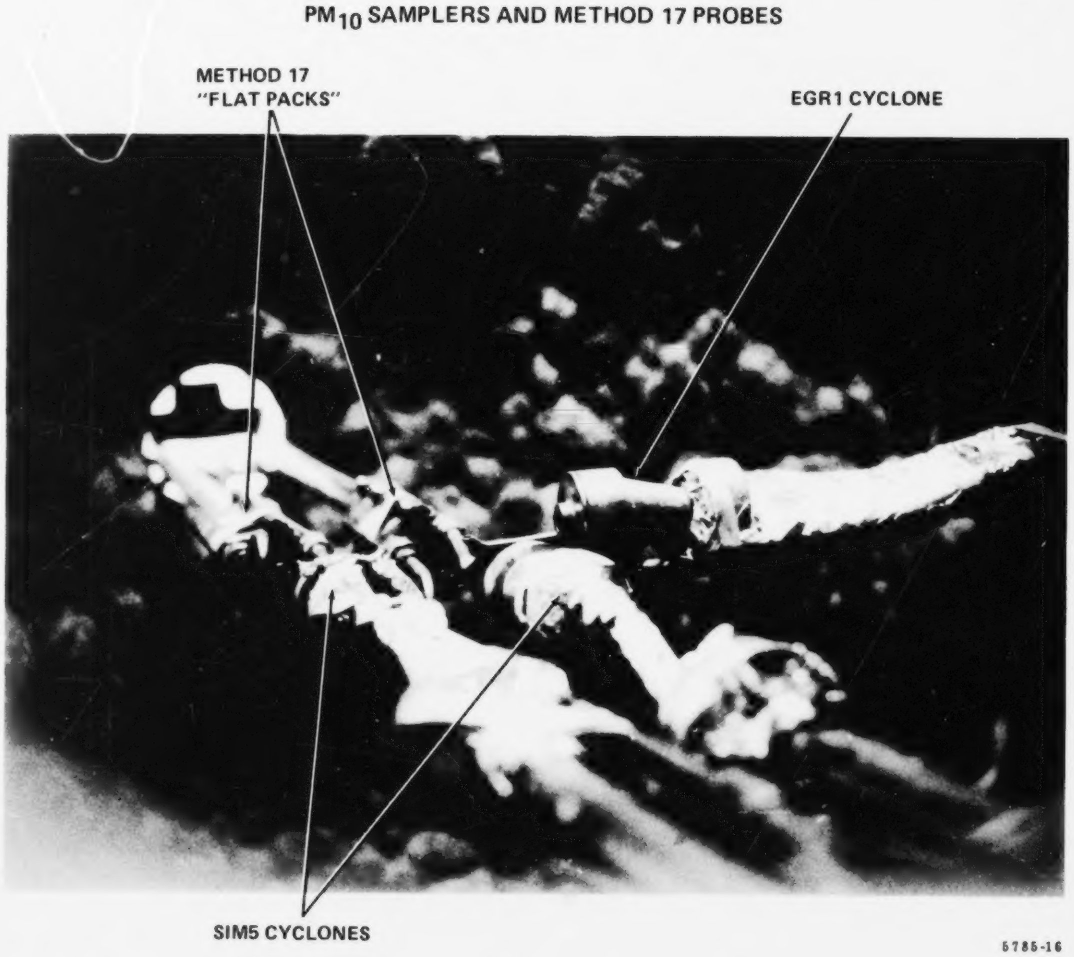
PM$_{10}$ SAMPLERS AND METHOD 17 PROBES
METHOD 17
"FLAT PACKS"
EGR1 CYCLONE
SIM5 CYCLONES
5785-16

Figure 5-3. Multiple probe sampling arrangement used in test 6.

Needless to say, arrangements of sampling trains such as were discussed above require unusual duct access and artificially restricted traverses. For more general sampling traverses, collocated samplers are not feasible, and a simultaneous independent traverse protocol was used. In this sampling arrangement, two or more comparison samplers are started simultaneously at different points in the duct and are operated for essentially the same sampling period. The samplers traverse the same points, but in different order. In rectangular ducts, the probes are typically inserted in adjacent ports to keep the samplers in the same general region of the duct. This arrangement was used in EGR-CSR comparison runs in tests 3 and 4. In this simultaneous independent traverse arrangement, spatial and temporal source variations are controlled to some degree, although source fluctuations will probably not cancel completely.

A final aspect of test design was site selection to provide a significant challenge of the methods over a range of source conditions. At all sites selected, significant fractions of the particulate emissions were greater than 10 µm aerodynamic size. At no site was the velocity constant over the traverse plane. In fact, two sites were selected specifically to provide skewed duct velocity distributions. Beyond these common specifications, the sites chosen reflect a range of particulate concentrations, stack gas compositions, and temperatures. Emissions were sampled at outlets of three different types of particulate control device and at one duct site upstream of the particulate control device. Of course, site selection was somewhat constrained by the port access requirements of the tests, which required collocated samplers.

SUMMARY DESCRIPTION OF FIELD TESTS

Field Test 1: Initial EGR Test

The first field test of the EGR system took place at one of two 56 MW coal-fired boilers in a utility generating station. The combustion gas exhausted from each unit was directed through two electrostatic precipitators in series. The outlet duct of the first ESP was chosen as the sampling location.

The flow area of the duct was approximately 132 ft^2. The velocity in the duct with the boiler at half load averaged 22.0 ft/s with a range of 16.3 to 27.2 ft/s. Ten 4-in. ports provided access to the duct interior. To allow collocated sampling and accommodate the large diameter of a dual-probe configuration, three 6-in. ports were installed in the duct at 90° to the pre-existing ports.

The test plan for field test 1 consisted of two subtests. Subtest A involved the comparison of traverses performed with the EGR train and a standard Method 17 train. To eliminate spatial and temporal bias, a dual probe configuration was used. Three traverse points were selected which represented the maximum point-to-point velocity change accessible through one of the 6-in. ports. The recycle rate of the EGR train was adjusted to achieve isokinetic sampling at each point while maintaining the chosen constant flow rate through the inertial sizing device. The flow rate through the Method 17 filter was adjusted at each point to sample isokinetically.

In subtest B, the dual probe previously described was collocated with a nonrecycle cyclone. Sampling was confined to a single point. The nozzle for the nonrecycle cyclone was chosen to provide a 10-μm cut at the isokinetic sample flow rate. A smaller nozzle was attached to the EGR cyclone so that recycle gas was required to achieve a 10-μm cut in this cyclone as well. The gas flow rate in the Method 17 sampler was adjusted in the usual manner to maintain isokinetic sampling.

Table 5-1 shows the comparisons of total mass loadings obtained under both subtests. As is shown, most of subtest A was performed with the boiler at full load (56 MW); however, one run (run 3) was performed at an intermediate boiler load of 34-MW. At full load, the Method 17 mass train indicated an average concentration of 2120.5 mg/dncm with a 95% confidence interval of 30.1%. The collocated EGR cyclone train collected an average concentration of 1904.3 mg/dnm^3 with a 95% confidence interval of ±10.1%. At the intermediate boiler load the mass train and the EGR cyclones showed concentrations of 585.5 and 542.6 mg/dnm^3, respectively. In subtest B the total mass concentrations obtained with Method 17, EGR, and nonrecycle cyclone averaged 74, 64, and 58 mg/dnm^3 with 95% confidence intervals of 27, 37, and 21, respectively. In both subtest A and subtest B, run-to-run differences due to process variation and random measurement error obscure or are substantially larger than differences or biases in the sampling techniques.

Table 5-2 compares the cumulative loadings for the EGR cyclones, nonrecycle cyclones, and University of Washington impactors. These cascade impactors were run independently of the subtests previously described as another means of determining the particle size distribution. In the table, D_{50} refers to the aerodynamic particle diameter of the 50% cut point for the given sampler. The impactor data were reduced with a microcomputer version of a data reduction system for cascade impactors (Johnson et al. 1978).

Field Test 2: Initial CSR Test

The first field test of the CSR sampling protocol took place at the same site as that used for field test 1. This series of tests was performed with the boiler at a constant load of 28 MW.

The test plan consisted of three subtests. In all subtests the CSR sizing devices were modified University of Washington Mark V cascade impactors. In subtest A, a Method 17 in-stack filter and cascade impactor were used in a 12-point traverse of the duct area using the CSR sampling protocol. The impactor was operated at a constant flow rate, while the flow rate through the 63-mm filter was changed so as to be isokinetic at each of the traverse points.

For subtest B, three identical impactors sampled simultaneously at the same point. To quantify the magnitude of error in PM_{10} determinations

TABLE 5-1. AVERAGES AND CONFIDENCE LIMITS OF TOTAL MASS CONCENTRATION FOR FIELD TEST 1

	Average Loading (mg/dncm)	Standard Deviation	95% Confidence Interval (Range)	95% Confidence Interval (Percent)
SUBTEST A 56-MW Boiler Load				
Method 17 Train (Runs 4, 5, 6)	2120.5	257.2 (12.1%)	1481.5-2759.5	±30.1
EGR Cyclones (Runs 2, 4, 5, 6)	1904.3	120.4 (6.3%)	1712.7-2095.9	±10.1
34-MW Boiler Load				
Method 17 Train (Run 3 only)	585.5	----	----	--
EGR Cyclones (Run 3 only)	542.6	----	----	--
SUBTEST B* 28-MW BOILER LOAD				
Method 17 Train (Runs 7, 8, 9, 10)	74.0	12.4 (16.8%)	54.3-93.7	±26.7
EGR Cyclones (Runs 7, 8, 9, 10)	64.2	15.2 (23.4%)	40.8-89.2	±37.2
Nonrecycle Cyclones (Runs 7, 8, 9, 10)	57.8	7.5 (13.2%)	45.1-68.9	±20.9

---

*Not traversed--sampled at single point only.

resulting from anisokinetic sampling error, one impactor sampled isokinetically while the remaining two operated at the upper and lower limits of acceptability according to the CSR protocol.

Subtest C involved three identical impactors sampling simultaneously and isokinetically at three points in the sample plane with widely differing velocities. A fourth impactor traversed the same points as prescribed by CSR sampling procedures.

TABLE 5-2. SUMMARY OF SIZE DISTRIBUTION DATA OBTAINED UNDER SUBTEST B OF FIELD TEST 1 WITH CUMULATIVE LOADING LESS THAN CYCLONE D_{50}

	D_{50} (µm)	(mg/dncm)	Standard Deviation	95% Confidence Interval (Range)	(Percent)	Cumulative Percent
Impactors* (Runs UW3, 5, 6)	8.85	28.6	3.2 (11%)	20.6-36.6	±27.8	41.0
EGR Cyclones (Runs 7, 8, 9, 10)	8.8	22.0	4.2 (19.1%)	15.3-28.7	±30.4	33.8
STD Cyclones (Runs 7, 8, 9, 10)	8.9	23.9	4.7 (19.7%)	16.4-31.4	±31.3	41.9

*Impactor data interpolated from spline curve fit of actual data.

Table 5-3 summarizes the results of subtest A. While the variability of the source was high, paired run analysis of collocated measurements indicates that the 13% lower CSR measurements of total mass is significant at the 95% confidence level.

TABLE 5-3. FIELD TEST 2, SUBTEST A: SIMULTANEOUS CSR IMPACTOR AND METHOD 17 TRAVERSES

Method	Replications	Total Concentration mg/dncm	PM_{10} (mg/dncm)	95% Confidence Intervals (mg/dncm)
CSR Impactor	3	310		±302
CSR Impactor	3		84	± 33
Collocated Method 17	3	356		±295
Differences Collocated M17/CSR	3	46(13%)		± 42

Table 5-4 presents the results of impactor runs under subtest B. As one might expect, the measured concentrations increased as the percent isokinetic decreased, more so for total concentration than for PM_{10}. However, the correlation is not ideal, indicating the presence of other factors. To more clearly view the importance of the other factors, the

TABLE 5-4. RESULTS OF FIELD TEST 2, IMPACTOR SUBTEST B, CORRECTED FOR ANISOKINETIC SAMPLING

Impactor Run	Concn (mg/dncm) Measured		Concn (mg/dncm) Corrected		COV* Measured (%)		COV Corrected (%)	
	PM_{10}	Total	PM_{10}	Total	PM_{10}	Total	PM_{10}	Total
2-1	98.7	267	105	316				
2-2	94.6	305	95.0	310	6.2	30.8	11.8	6.0
2-3	87.3	468	82.8	346				
2-4	81.8	210	85.4	241				
2-5	83.3	283	82.8	277	6.8	20.4	11.3	9.4
2-6	73.3	318	68.8	233				
2-7	81.7	215	86.1	257				
2-8	77.1	222	77.2	224	8.8	42.4	5.8	15.9
2-9	91.5	431	84.8	307				
2-10	112	409	118	488				
2-11	124	594	123	573	9.7	20.0	4.1	12.5
2-12	136	593	128	450				

*COV = coefficient of variation.

measured size distributions were corrected for errors due to anisokinetic sampling by calculating aspiration coefficient of 20 size increments by the equation of Belyaev and Levin (1974). Corrected PM_{10} and total concentrations are also given in Table 5-4. Also, coefficients of variation (COVs) of the sets of runs are given for measured and corrected results. It is seen the COV of total concentration is greatly reduced (from about 30 to 10%) when the variation due to anisokinetic sampling is removed. However, the COV of PM_{10} is not greatly affected by correcting for anisokinetic sampling; COV was increased in two sets and decreased in two sets. These results suggest that while anisokinetic sample error is quite important relative to other sources of uncertainty for total concentration, anisokinetic sampling error is obscured by other factors PM_{10} is measured.

Table 5-5 summarizes the results of subtest C. The observed difference between the CSR impactor and the reference measurements with single-point impactors was insignificant for PM_{10}. The CSR impactors gave a higher PM_{10} fraction, 28% compared to 21%. Although this difference is not statistically significant at the 95% confidence level, one might expect the difference to be in this direction because the CSR impactor flow rate was overisokinetic on the average, causing proportionately less of the large particles to be sampled. This mechanism, however, had insignificant effect on PM_{10}. Although the difference in total concentration between the CSR impactor and

Table 5-5. COMPARISON OF PARTICULATE CONCENTRATIONS MEASURED WITH A CSR IMPACTOR AND SINGLE POINT ISOKINETIC IMPACTORS FOR FIELD TEST 2

	Number of Observations	Average	95% Confidence Limits
PM_{10}			
Single-Point Impactors	4	107	±36
CSR Impactor	4	105	±53
Single-Point - CSR Impactor			
Pm_{10} Fraction			
Single-Point Impactor	4	21%	±13%
CSR Impactor	4	28%	±23%
Single-Point - CSR Impactor			
Total Mass			
Single-Point Impactors	4	593	±461
CSR Impactor	4	514	±599
Single-Point - CSR Impactor	4	79(14%)	±353(65%)

single-point impactors was not statistically significant at the 95% confidence level, it is also likely to be due to the overisokinetic sampling by the CSR impactor. However, the reader is cautioned that, in general, total measured concentration may not always depend only on the average anisokinetic ratio, especially if spatial variation is severe and by chance the concentration is high when sampling is overisokinetic and low when sampling is underisokinetic.

Field Test 3: EGR/CSR Comparison Test

The site chosen for field test 3 was a 500-MW coal-fired power plant. This site was selected because it offered access to a flowstream with velocities near 60 ft/s, substantial velocity spread, and aerosol mass median diameter in the 7-14-μm range. The plant had two 250-MW units with each unit controlled by two cold side electrostatic precipitators. At the outlet of each ESP, the gas stream was ducted to an induced draft fan and then through a common duct to the base of the stack. The sampling site was the duct directly downstream of of one ID fan with access to the duct interior through eight 4-in. ports.

Table 5-5. COMPARISON OF PARTICULATE CONCENTRATIONS MEASURED WITH A CSR IMPACTOR AND SINGLE POINT ISOKINETIC IMPACTORS FOR FIELD TEST 2

	Number of Observations	Average	95% Confidence Limits
PM_{10}			
Single-Point Impactors	4	107	±36
CSR Impactor	4	105	±53
Single-Point - CSR Impactor			
Pm_{10} Fraction			
Single-Point Impactor	4	21%	±13%
CSR Impactor	4	28%	±23%
Single-Point - CSR Impactor			
Total Mass			
Single-Point Impactors	4	593	±461
CSR Impactor	4	514	±599
Single-Point - CSR Impactor	4	79(14%)	±353(65%)

single-point impactors was not statistically significant at the 95% confidence level, it is also likely to be due to the overisokinetic sampling by the CSR impactor. However, the reader is cautioned that, in general, total measured concentration may not always depend only on the average anisokinetic ratio, especially if spatial variation is severe and by chance the concentration is high when sampling is overisokinetic and low when sampling is underisokinetic.

Field Test 3: EGR/CSR Comparison Test

The site chosen for field test 3 was a 500-MW coal-fired power plant. This site was selected because it offered access to a flowstream with velocities near 60 ft/s, substantial velocity spread, and aerosol mass median diameter in the 7-14-μm range. The plant had two 250-MW units with each unit controlled by two cold side electrostatic precipitators. At the outlet of each ESP, the gas stream was ducted to an induced draft fan and then through a common duct to the base of the stack. The sampling site was the duct directly downstream of of one ID fan with access to the duct interior through eight 4-in. ports.

The test consisted of two major subtests. For subtest A, a simultaneous three-point traverse of the duct was performed with both the CSR and EGR samplers. Both of these PM_{10} sampling trains used Cyclones I and IV of the SRI/EPA five-stage cyclone set followed by a 47-mm filter. The flow rate through both trains was set to produce a 10-μm aerodynamic D_{50} for the first cyclone. Three traverse points were chosen with velocities that were low, medium, and high relative to the nozzle velocity of the CSR sampler. Both sample train traverses were performed simultaneously, but the probes could not be collocated in the 4-in. ports. Therefore, each train sampled the points in a different order.

For subtest B, three University of Washington Mark V impactors were run simultaneously, as near in time as practical to each set of subtest A. Each impactor was operated isokinetically at one of the three traverse points used for subtest A.

The differences of impactor results from each of the CSR and EGR results are given in Table 5-6, along with 95% confidence limits. Confidence limits for the average from each technique are also given. No significant differences can be distinguished between EGR and single-point impactors or between CSR and single point impactors with 95% confidence for either PM_{10} or total particulate concentration. The impactor measurements could not be performed simultaneously with the CSR and EGR measurements. It appears that temporal variations obscure the relatively small differences in techniques.

Table 5-6. COMPARISON OF PARTICULATE CONCENTRATIONS MEASURED BY IMPACTORS, CSR, AND EGR FOR FIELD TEST 3

	No. of Observations	Average*	95% Confidence Limits*
PM_{10}			
Impactor	6	103	±22
CSR	7	107	±20
EGR	6	92	±26
Impactor CSR	5	-3.8	±25
Impactor EGR	5	-11	±31
Total Mass			
Impactor	6	193	±49
CSR	7	221	±51
EGR	5	196	±72
Impactor CSR	5	-28	±62
Impactor EGR	5	-2.6	±73

*All concentrations are given in mg/dncm.

Field Test 4: EGR-CSR Comparison Test

The site for field test 4 was a 221 MW pulverized coal-fired utility boiler. The test plan was designed to evaluate the control device, as well as the EGR and CSR protocols, in high and low mass concentrations.

The high-concentration tests were performed in each of the dual inlets of the control device. In each instance the site chosen was a 9 ft x 16 ft rectangular duct with 144 ft^2 of flow area. Eight 4-in. ports provided access to the duct interior. Stream velocities averaged 51 ft/s at side A and 53 ft/s at side B. Gas stream temperatures ranged from 250 to 290 °F.

Sampling was also done at the outlet on the stack. Eight 4-in. ports 230 ft from the base of the stack at a stack diameter of 20 ft served as the sampling site. Stream velocities in the sample plane ranged from 46 to 53 ft/s with an average of 50 ft/s.

This test consisted of five subtests. Subtest A involved a simultaneous 12-point traverse of the duct with the EGR and CSR samplers. Each 12-point traverse involved sampling at three points in four of the eight ports. Both sampling trains used Cyclones I and IV followed by a 47-mm filter, as in field test 3. The flow rate in each train was set to give a 10-μm aerodynamic D_{50} in Cyclone I. Subtest B provided reference particle size distributions using University of Washington Mark V impactors. The cascade impactors were operated over the same 12-point traverse used for subtest A. The traverse was subdivided into four subtraverses, each subtraverse corresponding to a different port. Each subtraverse was sampled with a different impactor by using CSR protocol, with the flow rate fixed so that the nozzle velocity equaled the mean measured velocity of the three points. The four impactors in a set were run in series, 15-min for each, over a 1.5 h period. Subtest C consisted of Method 17 mass train samples at the inlet of the control device. These samples were taken at both side A and B. Subtest D involved simultaneous impactor traverses in the exhaust stack at the outlet of the control device. For the first four repetitions of this subtest, two impactors traversed the stack simultaneously, each sampling at eight points. The impactor nozzle velocity was set at the average of the velocities at the eight points and kept constant throughout the traverse. Two additional repetitions were performed with four impactors in the stack simultaneously, one in each port. Each impactor traversed the two sampling points within the assigned port. The nozzle velocity was set at the average of the stream velocities at the two sampling points and held constant. For subtest E, Method 17 mass train samples were taken at the outlet sampling site. Each run consisted of a three-point traverse of each port. The nozzle velocity was adjusted at each point to maintain isokinetic sampling.

The results of this field test are given in Tables 5-7 through 5-10. Averages and 95% confidence limits of each technique are given in each table. Differences in techniques are also shown. EGR and CSR measurements were analyzed as paired samples; that is, confidence limits given for the CSR-EGR difference were calculated from differences between runs in individual pairs. Confidence limits given for other combinations of techniques were obtained by assuming independent samples.

TABLE 5-7. FIELD TEST 4: COMPARISON OF PM_{10} CONCENTRATIONS AT THE INLET

	No. of Observations	Average*	95% Confidence Limits*
Impactor	5	613	±102
CSR	6	716	±69
EGR	6	803	±90
CSR/EGR Difference	6	- 87(-11%)	±74(±9%)
Impactor CSR Difference		-103(-16%)	±105(±16%)
Impactor EGR Difference		-190(-27%)	±116(±16%)

---

*Averages and confidence limits are in mg/dncm unless otherwise shown.

TABLE 5-8. FIELD TEST 4: COMPARISON OF TOTAL PARTICULATE CONCENTRATIONS AT THE INLET

	No. of Observations	Average*	95% Confidence Limits*
Impactor	5	4022	±444
CSR	6	3590	±444
EGR	6	3648	±547
Method 17	11	3077	±702
CSR/EGR Difference	6	-58(-1%)	±722(±21%)
Impactor/CSR Difference		432(11%)	±533(±14%)
Impactor/EGR Difference		374(10%)	±602(±16%)
Method 17/Impactor Difference		-945(-27%)	±758(±21%)
Method 17/CSR Difference		-513(-15%)	±766(±23%)
Method 17/EGR Difference		-571(-17%)	±810(±24%)

---

*Averages and confidence limits are in mg/dncm unless otherwise shown.

TABLE 5-9. FIELD TEST 4: COMPARISON OF PM_{10} FRACTIONS AT THE INLET

	No. of Observations	Average	95% Confidence Limits
Impactor	5	15%	±1.7%
CSR	6	20%	±2.7%
EGR[a]	5	21%	±1.4%
CSR/EGR[a] Difference	5	-0.5%	±1.7%
Impactor/CSR[a] Difference	5	-5%	±2.8%
Impactor/EGR[a] Difference	4	-6%	±1.9%

---

[a] Outlier analysis (Grubbs and Beck 1972) indicates that the EGR value in test set 3, 27.3%, should be excluded at the 95% confidence level. When this value was included, the EGR result was 22.2% ± 6.9%, the CSR-EGR difference was -2.1% ± 5%, and the impactor-EGR difference was -7% ± 2.9%.

TABLE 5-10. FIELD TEST 4: COMPARISON OF PARTICULATE CONCENTRATIONS MEASURED AT THE OUTLET BY IMPACTORS AND BY METHOD 17

	No. of Observations	Average*	95% Confidence Limits*
PM_{10}			
CSR Impactor	10	2.9	±0.28(±10%)
Total Mass			
CSR Impactor	10	14.5	±0.9(±6%)
Method 17	7	15.6	±3.6(±23%)
CSR Impactor/Method 17 Difference	7	-1.1(-7%)	±3.3(±22%)
PM_{10} Fraction			
Impactor	10	19.9%	±2.2%

---

*Averages and confidence limits are in mg/dncm unless otherwise shown.

Field Test 5: EGR Precision Test

A Portland cement plant was chosen as the site for field test 5. The test was conducted at the outlet of a Rexnord gravel bed filter system, which was used to control the emissions from the clinker coolers of two 500-T/day cement kilns. The sampling area was located on the exhaust stack at the outlet of the gravel bed filter. The circular stack with an inside diameter of 1.93 m was accessible through three 6-in. ports located around the stack in 90° increments A 3-in. port was located beside each of the 6-in. ports.

Both kilns were operating at full load during the test. The temperature at the sample location averaged 266 °F with a range of 224 to 378 °F. The gas flow rate ranged from 57,000 to 94,000 acfm.

The test plan for field test 5 was designed with two objectives: first, evaluation of the precision of the EGR system; second, determination of the accuracy of EGR in measuring total emissions. To satisfy both objectives, two identical EGR trains sampled simultaneously with two Method 17 trains at approximately the same point (within 5-in.). The EGR trains were operated as described by Martin et al. (1988) and the Method 17 trains were operated as specified by EPA Reference Method 17. The EGR sampler consisted of Cyclone I and a 63-mm filter. The Method 17 trains used "flat pack" filter holders.

To remove possible bias due to particulate stratification across the small region around the collocated nozzles, probe positions were switched wherever practical. To exclude variations associated with velocity measurement in the evaluation of the precision of the EGR technique, the same pitot was used for both trains. Four sets of runs were performed utilizing a six-point traverse of the sampling plane by all four probes. Three sets of runs were performed with the probes sampling only at the center of the stack.

The statistical results of this test are shown in Table 5-11. The "paired run" values relate to the precision of the techniques. For the EGR the percent difference between collocated simultaneous runs averaged -2.4 in PM_{10} and -0.9 in total mass; standard deviations were 4.6 and 4.1, respectively. Confidence intervals (at 95% level) are also given for these measurements of percent differences (biases) and standard deviations. The apparent small percent biases between the two EGR trains are not significant at the 95% level.

The average percent difference between the Method 17 trains was -5.1 with a standard deviation of 7.7. This small apparent bias is not significant for a 95% confidence interval of ±7.1%. Further analysis on the differences between Method 17 trains in the first run of this test indicated that it should be excluded. Then the percent difference averaged -2.7 with standard deviation of 4.8. The standard deviations for paired runs in this test indicate the precision of EGR and Method 17. The observed percent standard deviations with the EGR trains were the same or smaller than those

TABLE 5-11. FIELD TEST 5 STATISTICAL RESULTS

	Paired Runs			EGR-M17 Average total mass
	EGR		M17	
	<10 μm	Total mass	Total mass	
Average error (%)	-2.4	-0.9	-5.1 (-2.7)*	-12.6 (-12.9)*
Std. deviation (%)	4.6	4.1	7.7 (4.8)*	6.0 (5.7)*
95% CI for average (%)	±4.9	±4.3	±7.1 (±4.0)*	±3.6 (±3.6)*
95% CI for std. dev. (%)	2.9→11.3	2.6→10.0	5.0→15.5 (3.0→11.9)*	5.1→11.0 (4.0→9.7)

*Number in parenthese are determined with the first run eliminated by Dixon (1953) outlier analysis.

of Method 17. Thus the results indicate that the precision of the EGR technique in measurement of both PM_{10} and total particulate emissions is equivalent to the precision of Method 17. The rightmost column of the table gives the percent error of the EGR results for total mass using the average results for each set of runs as the reference. Excluding the first Method 17 run changed the EGR-M17 comparison only slightly. In this test the EGR trains had a significant bias of -13% (collected less) relative to the Method 17 trains.

Field Test 6: CSR Precision Test

Field test 6 took place on the same site as field test 5. The plant was operating as described under field test 5 for the first three sets of runs for this test. A power outage and subsequent inability to reestablish proper operation forced the shutdown of one kiln for the remainder of the test. With only one kiln on-line, the gas stream temperature in the sampling plane averaged 182 °F with a range of 130 to 240 °F. The gas flow rate in the stack ranged from 55,000 to 68,000 acfm.

The test plan for this field test was designed to evaluate the precision of the CSR technique and the comparability of this protocol with EGR. To satisfy these objectives, two CSR trains and one EGR train were operated simultaneously. Although the CSR technique is not intended for the measurement of total emissions, it was deemed important to continue the Method 17 sampling begun during field test 5. The Method 17 probes were run simultaneously with the CSR and EGR trains. All probes sampled at approximately the same point (within 6-in.). The sampling hardware mounted on the EGR and Method 17 probes were the same as described for field test 5. The PM_{10} sampler used on the CSR probes was the same as that for EGR with the exception of a nonrecycle nozzle.

Although the probes did not physically traverse the stack, a 12-point traverse was simulated by dividing the run into 12 time segments. It was expected that substantial stack velocity variation would then be introduced over the course of each run by changing the setting of the damper at the I.D. fan at the base of the stack. However, the loss of one kiln early in the week made this plan unworkable. Thus, only the first two sets of runs had the anticipated variation of gas velocity, while the remaining seven runs did not.

Table 5-12 gives statistical results for this test. The precision of the CSR technique was found to be 6.6 ± 3.8%. Most of this difference was probably due to running one train, CSR at a higher flow rate, causing a slightly lower cut point. The precision of the CSR trains for total particulate matter is given as a point of interest, 1.2 ± 5.4%. Although the CSR technique is not intended for measurement of total mass, one would expect that the two trains would give the same results when the percent isokinetic were close.

The difference between CSR and EGR techniques (for PM_{10} measurements) was 15.8 ± 7.8% with CSR results being higher. A significant portion of this difference can be attributed to differences in flow rate of the cyclones, causing a difference in collection efficiencies, since such uncertainty in setting flow rate can be expected in field sampling.

CONCLUSIONS FROM FIELD TEST SERIES

As described in this section, the EGR and CSR techniques were tested at five sampling locations at three coal-fired utility boilers and at one cement plant. The sites were selected to provide a range of particulate concentrations (15-4000 mg/dncm) and duct velocities (15-100 ft/s), significant fractions of particulate matter larger than 10 μm (50-80%), and substantial velocity nonuniformity. At each site the EGR and CSR measurements were compared with reference measurements of PM_{10} and/or total particulate concentrations, at three sites the EGR and CSR measurements were run simultaneously and compared to each other, and at one site collocated identical PM_{10} trains were operated to measure precision of each method.

In accord with the test objectives stated at the beginning of this section, several specific results and conclusions from the field test series can be noted concerning development of the methods, comparison of independent measurements, and precision measurements of the two methods.

Development of EGR and CSR Methods

The tests in this series represent the first field trials of each PM_{10} technique. Thus, it is not surprising that some modifications and improvements to each technique were made as a result of field experience. Likewise, other difficulties became apparent which could not be adequately addressed in this project. Some of these are summarized below.

TABLE 5-12. FIELD TEST 6 STATISTICAL RESULTS

	Paired Runs				Total loading (relative to M17)	
	CSR		M17	PM10 loading		
	<10 µm	Total mass	Total mass	(avg. CSR-EGR)	avg. CSR	EGR
Average error (%)	6.6	1.2	1.1	15.8	0.4	-4.0 (-4.8)*
Std. deviation (%)	5.0	7.0	7.3	10.1	8.2	8.9 (2.0)*
95% CI for average (%)	±3.8	±5.4	±5.2	±7.8	±6.3	±6.9 (±1.7)*
95% CI for std. dev. (%)	3.3→10.1	4.6→14.3	5.0→13.3	6.8→19.3	5.5→15.7	6.0→17.0 (1.29→4.4)

*EGR/M17 comparison from CP5-3 and CP5-8 eliminated by Dixon (1953) outlier analysis.

Equipment Changes to EGR Train--

Several hardware components of the EGR train were upgraded during the course of the field tests.

- The prototype EGR control module had a thin wall, flexible stainless steel tubing between the recycle control valve (V_3 in Figure 4-4) and the recycle gas exit. This tubing developed a leak in test 1 and was replaced.
- Arrangement of the EGR recycle lines, nozzle, and pitot lines on the in-stack end of the probe was a frequent source of difficulty in EGR Tests 1 and 2. The primary source of the problem was the difficulty of aligning these extra lines to allow easy fit through typical 4-in. sampling ports. Before test 4 the in-stack lines were replaced with flexible tubing. This change helped the mounting and alignment problems while allowing flexibility in the choice of samplers. When a sampling train with specified in-stack hardware is constructed for routine use, a more rigid permanent mounting arrangement should be designed.
- It was discovered on test 3 that the EGR sample and recycle lines could be reversed. After this test, an umbilical line with different quick-disconnect connectors was constructed to eliminate this possibility.
- After test 4, the two redesigned field EGR trains described in Section 4 were constructed, incorporating these and other design upgrades. The two second-generation EGR trains performed well on tests 5 and 6.

Development of CSR Protocol--

At the beginning of the project, the recommended CSR protocol (Farthing 1983) was defined by an abbreviated step-by-step procedure which did not contain all equations to be used. In order to simplify the procedure so that a technician member of a sampling team could make the on-the-spot sampling decisions necessary for CSR, a setup calculation sheet (Table 4-1) was developed before the final test of this series. The table requires only a pocket calculator with typical scientific functions. In the course of the field series, CSR calculations were also performed by using modifications of BASIC programs for Apple II series microcomputers.

Also during the course of the project, further estimates were made of the error to be expected in CSR testing. Rough limits were calculated for several measured and hypothesized aerosol size distributions. The error which may be incurred with CSR depends upon the shape of the size distribution for particles with aerodynamic diameter less than 10 µm. The maximum error possible with CSR sampling an aerosol of 10-µm particles is 20%. However, for real aerosols emitted by sources, the maximum error incurred will be much less than this. These calculations are described by Farthing et al. (1985) and are partially reproduced in Section 3 of this report.

Inertial Sizing Devices--

As discussed in the following subsection, a small but significant difference was observed between PM_{10} measurements using EGR and other techniques (CSR cyclones and cascade impactors) in several of the field tests. These results, while they did not conclusively demonstrate a bias in the EGR technique, did revive concern that the sampling nozzle might perturb the natural cut of the inertial sampler, and the results thus led to an increase in the planned level of effort for the studies described in Section 6.

Comparison of Measurements with Independent Techniques

Several conclusions may be drawn from the field data in summary Table 5-13 as well as the more complete data sets contained in Tables 5-1 through 5-12. First, in every case, the average concentrations measured using different techniques agreed within the combined 95% confidence intervals. Since these intervals for some tests reflect a substantial degree of variation, presumably due mostly to source fluctuations, a more meaningful comparison can be drawn from paired-run analysis of the simultaneous measurements indicated in Table 5-13. Since source fluctuations cancel to first order in the comparisons, the confidence intervals are smaller, and some observed differences are found to be statistically significant. Such comparisons are described in the following paragraphs.

Total Mass Comparisons--

Although the primary purpose of the EGR and CSR techniques is to measure PM_{10} concentrations, both techniques simultaneously provide a measure of total particulate mass as well. Method 17 reference samples were included since in many PM_{10} applications total mass information is also desirable, and since recovery of total mass is an overall indicator of PM_{10} sampler operation. In principle, the EGR sampler should provide total mass measurements identical to Method 17, since both methods use isokinetic sampling and in-stack particulate filters. In fact, at both site 1 and site 4 (tests 1, 5, and 6) the EGR train measured less than Method 17 by a small but significant amount. Mean differences ranging from 5 to 13% were observed, in each case larger than the 95% confidence limits. The reason for this small bias is not clear; however, since it does not exceed 15% at any site tested to date, we do not consider it an extreme difficulty.

Unlike the EGR measurements, CSR total mass measurements at sites 1, 3, and 4 (tests 2, 4, and 6) were not significantly different from the paired total mass measurements from Method 17 or other reference isokinetic sampling trains. Since the CSR technique is expected to be less accurate for total mass, these results are encouraging.

When total mass data using the two techniques are compared, the results are mixed. At site 2, the 9% EGR-CSR difference is marginally significant at the 95% confidence level. At sites 3 and 4 the EGR and CSR data are essentially the same.

PM_{10} Comparisons--

In order to assess the accuracy of EGR and CSR for PM_{10} measurements, single-point, isokinetic particle sizing samplers were used as a reference.

TABLE 5-13. PERCENTAGE DIFFERENCES IN PARTICULATE CONCENTRATIONS MEASURED DURING TEST SERIES*

	Number of Replications	PM_{10}	Total Concentration
EGR Initial Test: Site 1			
EGR Cyclone — Isokinetic Cyclone†	4	-8.3±27%	9.0±29%
EGR — Method 17†	8		-11.5±8.3%
SIM-5 Initial Test: Site 1			
SIM-5 — Method 17†	3		-16±32%
SIM-5 — Isokinetic Impactors†	4	-1.8±22%	-14.0±65%
EGR/SIM-5 Comparison Test: Site 2			
EGR Cyclone — SIM-5 Cyclone†	5	-15.5±6.5%	-9.2±8.5%
EGR — Isokinetic Impactors	5-6‡	-11±31%	1.3±38%
SIM-5 — Isokinetic Impactors	7-6‡	3.8±25%	14±31%
EGR/SIM5 Comparison Test: Site 3			
	Inlet		
EGR — SIM-5†	6	11±9.8%	1.7±21%
EGR — Impactor	6-5‡	27±16%	-9.8±16%
SIM-5 — Impactor	6-5‡	16±16%	-11±14%
	Outlet		
SIM-5 Impactor — Method 17	6-7‡		-7.4±23%
EGR Precision Test: Site 4			
EGR — Method 17†	6		-12.9±4.2%
EGR_1 — EGR_2†	6	-2.4±4.9%	-0.9±4.3%
SIM-5 Precision Test: Site 4			
SIM-5 — Method 17†	9		0.4±6.3%
EGR — Method 17†	7		-4.8±1.7%
EGR — SIM-5†	9	-15.8±7.8	
SIM-5_1 — SIM-5_2†	9	6.6±3.8	1.2±5.4%

*All differences and confidence intervals expressed as percentages of the mean value. Confidence intervals represent 95% significant level.

†These comparisons were analyzed as pairs since the measurements were simultaneous.

‡Where two numbers of replications are given, the first number corresponds to the first listed device and the second to the second device.

This test design assumed that, barring artifacts due to the EGR mixing nozzle, EGR PM_{10} data should have accuracy equivalent to the reference devices. CSR data should by design differ by no more than 20% for worst-case conditions and by less than 10% for the size distributions at the sites tested in this study. In fact, the PM_{10} values measured by the two techniques at every site differ by more than 10% but less than 20%. At sites 2 and 4, the EGR PM_{10} value is about 15% less than the CSR value. At site 3, the EGR value is 11% greater than the CSR value. All three differences are significant at the 95% confidence level.

Comparisons of PM_{10} measurements of both methods with isokinetic impactor trains show differences on the same order of magnitude. In test 2, CSR impactors measured PM_{10} concentrations within 5% of isokinetic impactors, as did CSR cyclones in test 3. In test 3 (site 2) the impactors tended to support the higher CSR PM_{10} concentration over the lower EGR value. These differences, however, are not significant in light of increased confidence limits for the measurements, which were not generally simultaneous. In test 4 (site 3), the inlet impactors were not run isokinetically but according to a modified CSR protocol. In this test, the impactors measured significantly lower PM_{10} than either CSR or EGR. The results of this test reverse what would appear to be a trend at the other three sites for EGR PM_{10} values to be significantly lower by about 5-15% than the CSR values, which are not significantly different from isokinetic impactors. No clear reason for this test-to-test reversal is known.

A significant difference in PM_{10} concentrations may result from at least two causes: a difference in (1) sampling efficiency for sizes less than 10 μm, or (2) in the actual collection characteristics of the inertial sizing device. For sampling trains which give comparable total mass concentrations, sampling efficiency for the smaller size particles in the PM_{10} fraction should also be comparable. On this reasoning, the PM_{10} difference between the paired EGR and CSR runs at sites 2-4 may be taken primarily as a measure of a difference in the D_{50} or nozzle losses of the two samplers. Any such difference is not consistent in sign at the three test sites, and it does not cause average PM_{10} differences to be greater than 16% at any site tested. Likewise, comparisons of PM_{10} between either of the PM_{10} techniques and isokinetic reference trains such as cascade impactors are not generally conclusive because of the effects of source variability on these nonsimultaneous measurements. As with the EGR-CSR comparisons, the direction of any difference in sampler cut is not consistent from site to site, so no systematic difference can be demonstrated from the field data alone.

As mentioned above, the relatively small but significant PM_{10} differences gave impetus to expansion of the planned laboratory characterization of Cyclone I with several sampling nozzles. The results of this study, described in Section 6, show significant D_{50} shifts and misclassified particulate matter in both the EGR and CSR adaptations of Cyclone I. Moreover, these tests indicated that these effects should also occur in other particle sizing samplers such as the impactors used for reference in this study. While no clear reason was found for the reversal of measured PM_{10} concentrations in test 4, these studies indicated the likelihood that all samplers give underestimates of PM_{10} at higher velocity sources. The implications of these data are discussed in Section 6.

Measurement of Precision of EGR and CSR Methods

At site 4, measurements made by collocated pairs of EGR and CSR sampling devices indicated excellent reproducibility between the two trains. In only one instance (CSR PM_{10} concentrations) did the mean difference in the measurements of two nominally identical trains exceed 2.5%. (This bias was found to be due to a systematic difference in cyclone flow rate between the two trains). For both PM_{10} trains, 95% confidence intervals were on the order of ±5%. By this measure, the precision of the PM_{10} trains was the same as that of the paired Method 17 trains operated during these tests.

SECTION 6

LABORATORY CHARACTERIZATION OF CYCLONE I AND NOZZLES

BACKGROUND SUMMARY

Appropriate behavior of the inertial sizing device is obviously a key factor in measurement of PM_{10}. Most characterization of sizing devices for a stack sampling, begun 12 years ago, has been limited to demonstrating basic performance at laboratory conditions and a few flow rates. This has been carried out for various cascade impactors and cyclones. Effects of particle charge and particle bounce on impactors were investigated in the late 1970s; behavior as a function of Reynolds number (varying gas viscosity and density) was investigated in the first half of this decade. In the first half of this decade it was found that to characterize impactor behavior, jet-to-plate spacing had to be taken into account at the low Reynolds numbers (high temperatures) encountered in process streams. The dimensionless size parameter (Stokes number, Stk) of impactor stages was found to vary with Reynolds number (Re). This led to consideration for cyclone behavior in terms of functions of Stk versus Re. Even though no suitable theory exists for cyclones, the simplification achieved with these parameters and the similarity to impactor behavior has produced greater confidence in their use.

In this PM_{10} program, earlier results (Smith et al., 1979) for Cyclone I were extended to include basic performance at flow rates giving 10-μm cut point and characterization under conditions simulating gas velocities encountered in process streams. This investigation of basic performance demonstrates that Cyclone I is a suitable PM_{10} sampler. Laboratory characterization at high gas velocities has revealed that nozzles with small inlets, needed for isokinetic sampling at high velocities, can reduce cyclone cut point to below 10 μm. To eliminate this effect, which probably exists for all existing samplers which are coupled closely to a nozzle inlet, currently available nozzles must be extended away from the cyclone.

EXPERIMENTAL EQUIPMENT AND PROCEDURES

Measurement of Collection Efficiency

Calibrations of Cyclone I have employed the common procedure involving a vibrating orifice aerosol generator (VOAG) similar to that developed by Berglund and Liu (1973) and described in detail by Cushing et al. (1976). The VOAG provides monodisperse dye aerosol of selectable particle size at a rate of about 60,000/s. After lofting and drying with air the aerosol is passed through the sampler with an absolute filter at its exit. After the sampling run, all internal surfaces of the sampler and the filter are carefully washed with a measured volume of solvent. Spectrometry or fluorometry then determines the concentration of dye in the wash solutions and thus the collected aerosol mass for each surface and that passing to the backup filter.

Apparatus--

Calibrations in this investigation were performed in two phases. In the first phase, measuring basic performance, aerosols were passed directly to Cyclone I with minimum drying air. For measurements at elevated temperature, Cyclone I was operated in an oven and heated tubing used to transfer the aerosol to the cyclone.

In the second phase, to simulate sampling from process streams, an apparatus was constructed to establish a flow stream, substantially larger than the nozzles, with a uniform velocity profile at (or near) the nozzle inlet and minimum dilution of the VOAG aerosol. The apparatus is illustrated in Figure 6-1 with the VOAG at the bottom and Cyclone I and filter in the main flow stream near the top. Aerosol leaves the VOAG drying column through a 3/8-in. tube at the center of the main flow stream. This monodisperse aerosol combines with the main flow (makeup air), which is drawn through the air filter and Plexiglass tube (1.5-in. diameter) by the hi-vol blower at upper left. This flow stream with aerosol near the center, along its axis, then passes into the Plexiglass tube with 3.5-in. diameter before encountering the nozzle of Cyclone I.

The blower can be adjusted to establish the desired velocity at the nozzle, which matches the "plug flow" velocity corresponding to the cyclone flow rate and nozzle inlet diameter. The gas velocity is measured at the ports shown, 1.5 in. upstream of the nozzle for this adjustment. Figure 6-2 shows velocity profiles measured at three nozzle "plug flow" velocities studied. The profiles are uniform in the central portion where the nozzle is located and outward to 1/2 in., well beyond the edge of any nozzles tested.

Introduction of the VOAG aerosol at the center of the main flow while limiting the distance over which turbulent mixing occurs reduces dilution of the aerosol. Most of the particles remain near the center of the main flow where it enters the cyclone nozzle. This was verified during construction of the apparatus by passing small, helium-filled bubbles through the VOAG drying column to view the center portion of the flow stream. This feature kept run times necessary to sample sufficient mass of dye particles to about an hour.

Gas not sampled by the Cyclone I passes through an 8- x 10-in. filter and then to the blower. A small portion (1/4 cfm) was drawn off by an optical particle counter, shown at upper right of Figure 6-1, to monitor the aerosol during each run. Plumbing was also available to divert the VOAG aerosol directly to the optical particle counter.

To avoid effects of particle charge which occurs during generation of the aerosol, a charge neutralizer was installed at the top of the VOAG drying column. Because a Krypton 85 source emits beta radiation down along the drying column producing bipolar ions (the radiation level at the VOAG orifice is about 9 millirads), lead shielding was installed around the source to prevents exposure of the operator.

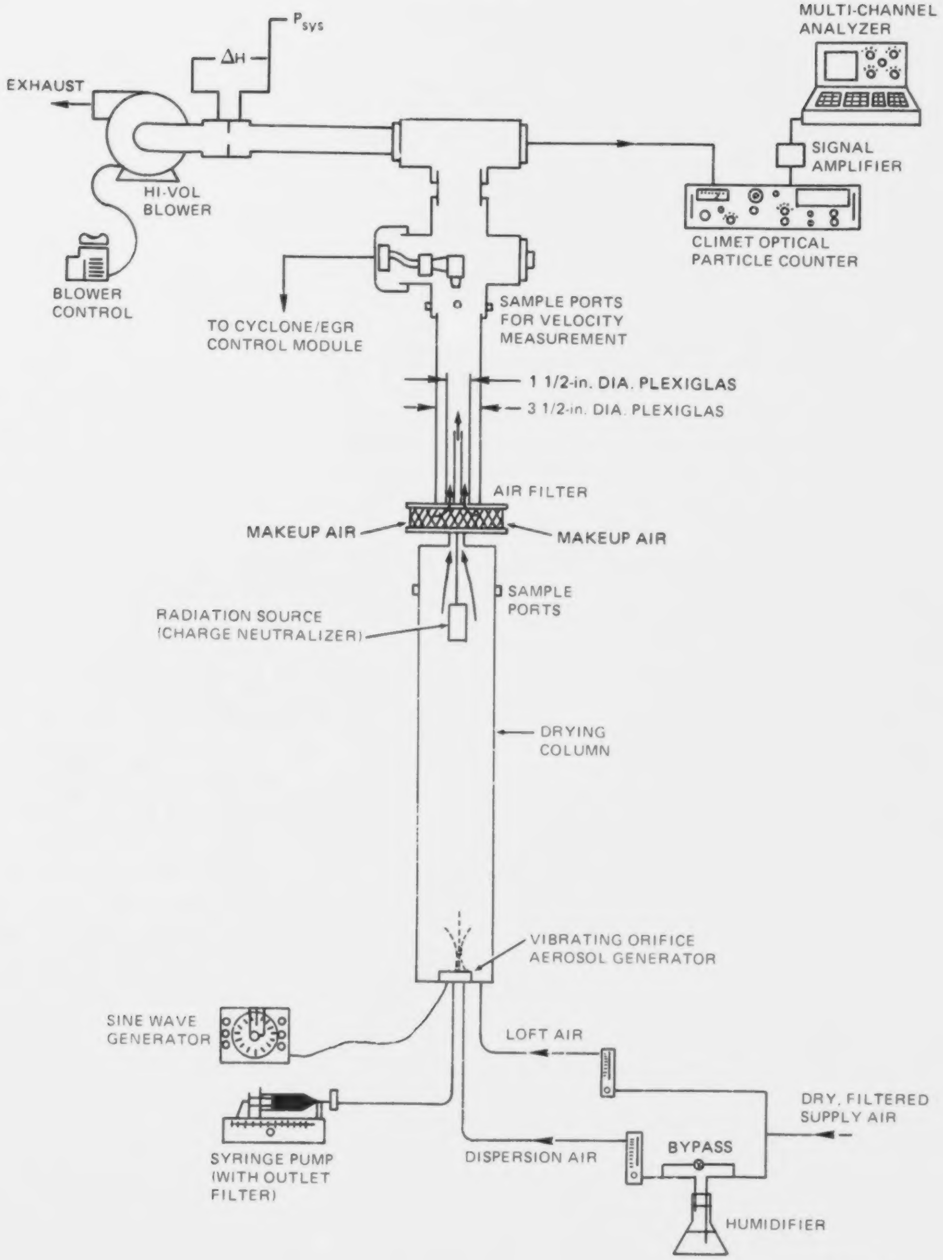
P_sys
ΔH
EXHAUST
HI-VOL BLOWER
BLOWER CONTROL
TO CYCLONE/EGR CONTROL MODULE
SAMPLE PORTS FOR VELOCITY MEASUREMENT
MULTI-CHANNEL ANALYZER
SIGNAL AMPLIFIER
CLIMET OPTICAL PARTICLE COUNTER
1 1/2-in. DIA. PLEXIGLAS
3 1/2-in. DIA. PLEXIGLAS
AIR FILTER
MAKEUP AIR
MAKEUP AIR
SAMPLE PORTS
RADIATION SOURCE (CHARGE NEUTRALIZER)
DRYING COLUMN
VIBRATING ORIFICE AEROSOL GENERATOR
SINE WAVE GENERATOR
LOFT AIR
DRY, FILTERED SUPPLY AIR
SYRINGE PUMP (WITH OUTLET FILTER)
DISPERSION AIR
BYPASS
HUMIDIFIER
5785-18

Figure 6-1. VOAG calibration system with isokinetic velocities at inlet to sampler nozzle.

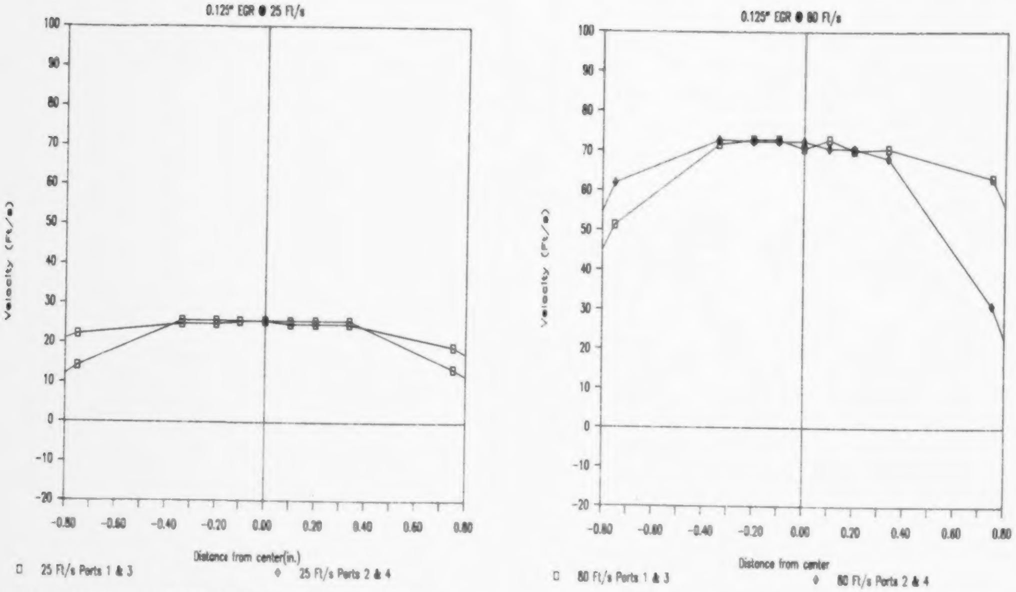

(A) CYCLONE I WITH NOZZLE VELOCITY OF 25 ft/s

(B) CYCLONE I WITH NOZZLE VELOCITY OF 80 ft/s

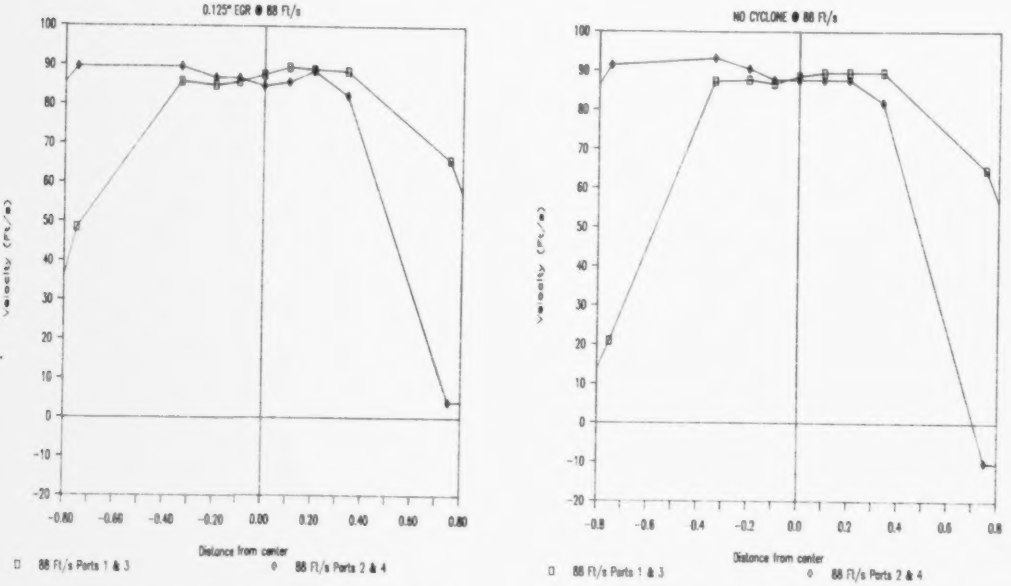

(C) CYCLONE I WITH NOZZLE VELOCITY OF 88 ft/s

(D) SAME AS (C) WITHOUT CYCLONE

5785-24

Figure 6-2. Velocity profiles in flow stream at inlet of Cyclone I nozzles.

Procedure--

In the first phase of this PM_{10} program, extending basic performance data, ammonium fluorescein aerosols with 10-µm aerodynamic diameter were passed directly into Cyclone I, varying the flow rate from run to run. In this manner, flow rates for a 10-µm cut point (50% collection) were determined at 72 and 300 °F. Visual observation of the particles with a microscope indicated that temperatures up to about 350 °F do not affect this dye. Thermogravimetric analysis was also performed on this dye, ramping the temperature to 500 °F with 5 min periods at 200, 300, 400 and 500 °F. This test gave a weight change of only 0.1%.

In the second phase, experiments were performed while holding the flow rate constant and varying the particle size from run-to-run. All runs were performed at a laboratory temperature of 75 to 80 °F and with ammonium fluorescein particles. Flow rates studied were 0.45, 0.35, and 0.27 acfm and most experiments were performed at the highest value, which gives a 10-µm cut point. Prior to starting a run, the cyclone was leak-checked and installed and the sample control box adjusted to the desired flow value(s). Then a calibrated pitot or hot wire anemometer was inserted in front of the nozzle for blower adjustment. The VOAG aerosol was diverted to the optical particle counter during this preparation. After these initial adjustments, the control box was turned off, and the VOAG aerosol was checked for desired size and monodispersity with the optical particle counter and a filter sample, which was observed with a microscope. Immediately after the VOAG output was connected to the main flow stream, the run was begun, gas velocity checked, and the pitot removed. Stability of the blower flow rate was monitored during the run with an orifice, shown in Figure 6-1. After the run checks of the VOAG aerosol were again performed, photomicrographs of particles generated before and after the run were obtained.

For most runs, five different interior surfaces of the sampler were washed separately with 2% ammonium hydroxide solution to characterize behavior. These were the nozzle, the cyclone body and cup, the cap through which the gas exits the cyclone, the exit tube, and the filter and its holder. In some runs nozzles were washed in separate portions to identify how deposits varied along its length. This wash was accomplished by successive dippings of the nozzles into separate test tubes, each dip washing successively more of the nozzle.

A Bausch and Lomb Spectronic 88 spectrometer and a G.K. Turner III fluorometer, both calibrated with current dye samples, were used to measure concentration of wash solutions. The mass collected, percent of the total collected mean, and collection efficiency of each surface were calculated. Total mass collected ranged between 50 and 1000 µg, or 10^6 to 10^7 particles. The collection efficiency of a surface is the ratio of the mass collected by the surface to the mass collected by it and all surfaces downstream of it.

Sampling Nozzles

Figure 6-3 illustrates the geometry of the Cyclone I nozzles for which Cyclone I behavior was characterized. They are classified into four groups: the largest nozzle (denoted 1/2 in.), tapered nozzles (small angle of

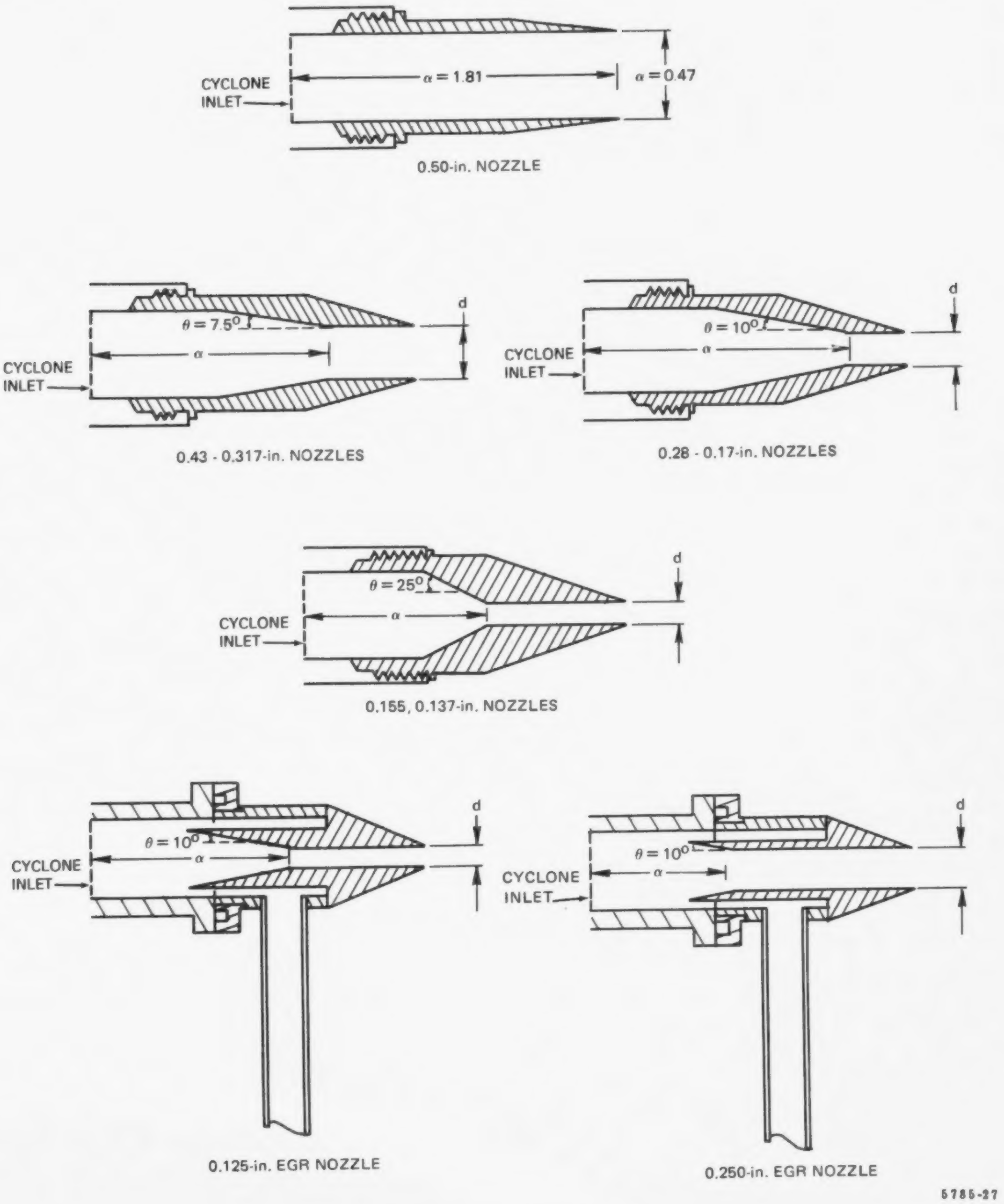
CYCLONE INLET
α = 1.81
α = 0.47
θ = 7.5°
α
d
θ = 10°
θ = 25°
5785-27

0.50-in. NOZZLE

0.43 - 0.317-in. NOZZLES

0.28 - 0.17-in. NOZZLES

0.155, 0.137-in. NOZZLES

0.125-in. EGR NOZZLE

0.250-in. EGR NOZZLE

Figure 6-3. Geometry of Cyclone I nozzles.

expansion), nozzles having a large expansion angle, and the EGR nozzles. In this figure the cyclone inlet (1/2-in. dia.) is also shown to indicate the distance from the nozzle inlet to the nearest inside wall of the cyclone. The inlet diameter (or range of diameters) is also given under each nozzle type.

Table 6-1 gives a more quantitative description of these nozzles. The straight length of the inlet is the distance from the nozzle inlet tip to the point where the diameter begins to flare or expand. The expansion length is the distance from the point when expansion begins to the nearest inside wall of the cyclone.

TABLE 6-1. DIMENSIONS OF CYCLONE I NOZZLES TESTED

Nozzle I.D.	Inlet diameter, inches	Expansion angle, degrees	Expansion length, inches	Straight length at inlet, inches
Standard Cyclone Nozzles:				
1	0.470	0	1.79	1.79
2	0.430	15	0.90	0.89
3	0.395	15	1.03	0.76
4	0.353	15	1.19	0.60
5	0.317	15	1.32	0.47
6	0.276	20	1.27	0.52
7	0.233	20	1.39	0.40
8	0.213	20	1.44	0.35
9	0.193	20	1.50	0.29
10	0.174	20	1.55	0.24
11	0.155	50	1.05	0.74
12	0.137	50	1.07	0.72
EGR Nozzles:				
1	0.117	20	1.22	0.38
2	0.188	20	1.02	0.58
3	0.250	20	0.84	0.76

Measurement of Nozzle Velocity Profiles

Apparatus--

To better understand the effect of the nozzle geometry on the particle sizing performance of Cyclone I, it was desirable to obtain velocity profiles at the cyclone inlet for each of the nozzle geometries. To correlate this data with the collection efficiency data, each velocity profile measurement was performed at conditions which simulated the cyclone calibration conditions. Therefore, the target flow rate through the nozzle and test section for each velocity profile measurement was the PM_{10} flow rate for Cyclone I at ambient conditions, 0.45 acfm. The equipment setup used is shown in Figure 6-4. To include the effects of isokinetic sampling, a blower was used to produce a flow stream at the nozzle inlet such that the velocity of the flow stream matched the nozzle velocity. The velocity of the flow stream delivered by the blower was determined by measuring the velocity pressure at the nozzle inlet with a standard pitot. The blower speed was then adjusted by a Variac until the desired flow stream velocity was achieved.

The test section directly downstream of the nozzle was designed to simulate the geometry of the inlet of Cyclone I as noted previously. To accommodate both nonrecycle nozzles with 3/8-in. straight pipe thread and flange-mounted EGR nozzles, two test sections were fabricated. Each one was a 6-in. length of brass tubing with an internal diameter of 0.50 in. Access ports on a single diameter were located 0.54 in. from the face of the test section, as shown in Figure 6-4. This allows velocity profile measurements at a plane corresponding to the point in Cyclone I where the sample stream leaves the 0.50-in. diameter inlet (see Figure 4-1). Neoprene tubing was used as a septum to prevent leakage through the access ports.

The velocity-sensing device used in the test section was a small pitot made of two 0.03-in. diameter hypodermic needles with beveled openings approximately 0.06 in. in length. A similar device was used by Kamotani and Greber (1972) to determine mean flow direction. For the purpose of traversing the test section in known increments, the pitot was mounted on a horizontal positioner attached to a vernier scale reproducible to 1/0.001 in.

To determine the pitot coefficient, C_p, of the hypodermic, a calibration was performed in a test section identical to that previously described with the exception of a downstream port, which allowed a standard pitot to be positioned in the same plane as the hypodermic pitot. Velocities in the test section ranged from 3.65 ft/s to 55.65 ft/s. Figure 6-5 shows the pitot coefficients, C_p, for the hypodermic as a function of velocity pressure. A curve was fitted to these data, as shown, of the form

$$C_p = 1.035 - a\ (\log \Delta p + 2.398)^2$$

where C_p = the hypodermic pitot coefficient
Δp = the velocity pressure measured by the hypodermic pitot, inches of water
$a = 0.23466$ for $\Delta p \leq 4 \times 10^{-3}$
$a = 0.0304$ for $\Delta p > 4 \times 10^{-3}$.

The remainder of the laboratory setup consisted of a pressure transducer and electronic manometer which transmitted data from the hypodermic pitot to an Apple computer for time averaging. Finally, a Method 5 sample control box was used for nonrecycle nozzles, and an EGR console was used for recycle nozzles to adjust the flow through the nozzle and test section to the desired rate.

Procedures--

Prior to the measurement of a velocity profile, the desired nozzle was attached to the test section and the positioner adjusted to place the face

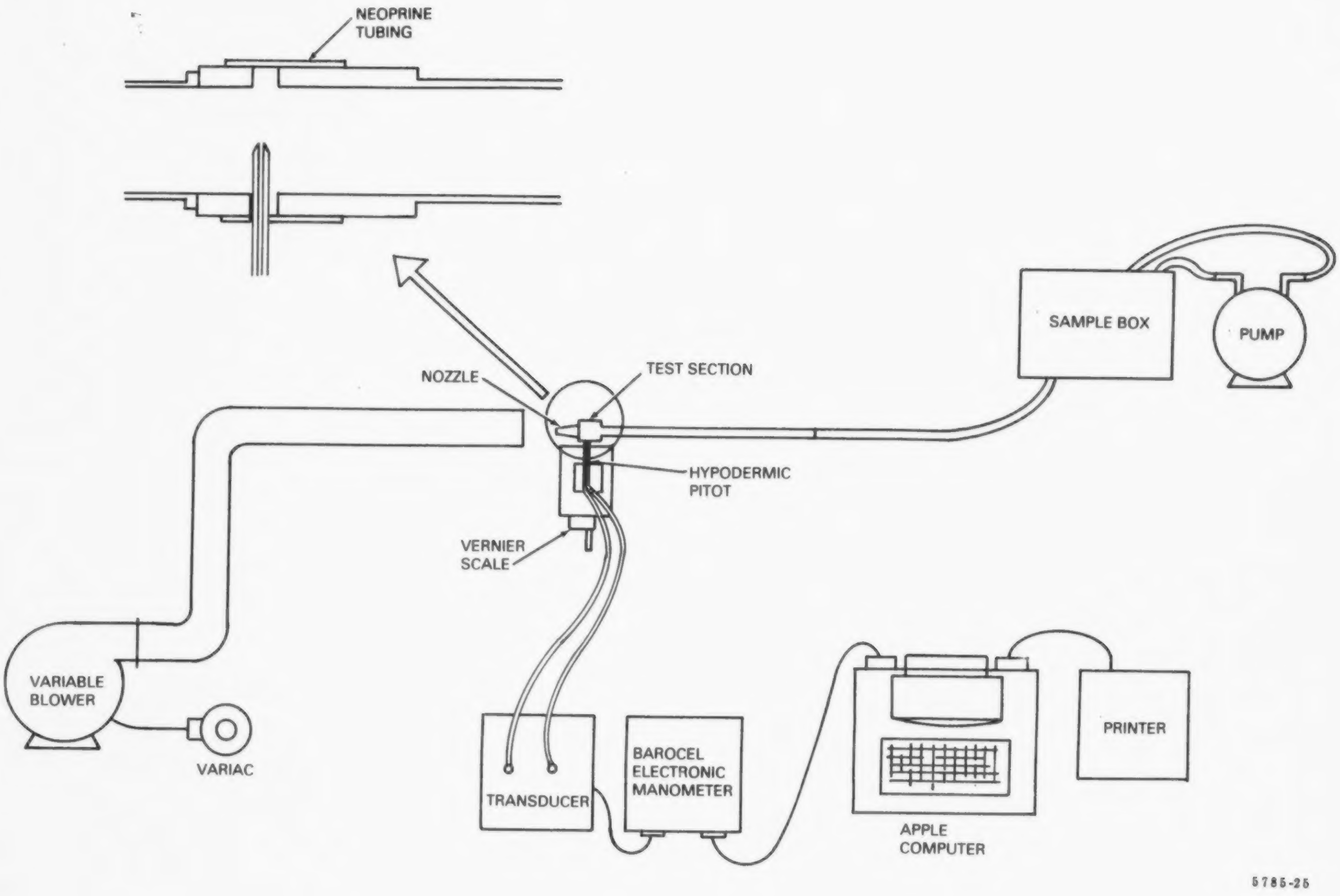
NEOPRINE TUBING
NOZZLE
TEST SECTION
SAMPLE BOX
PUMP
HYPODERMIC PITOT
VERNIER SCALE
VARIABLE BLOWER
VARIAC
TRANSDUCER
BAROCEL ELECTRONIC MANOMETER
APPLE COMPUTER
PRINTER
5785-25

Figure 6-4. Equipment setup for nozzle velocity profile measurements.

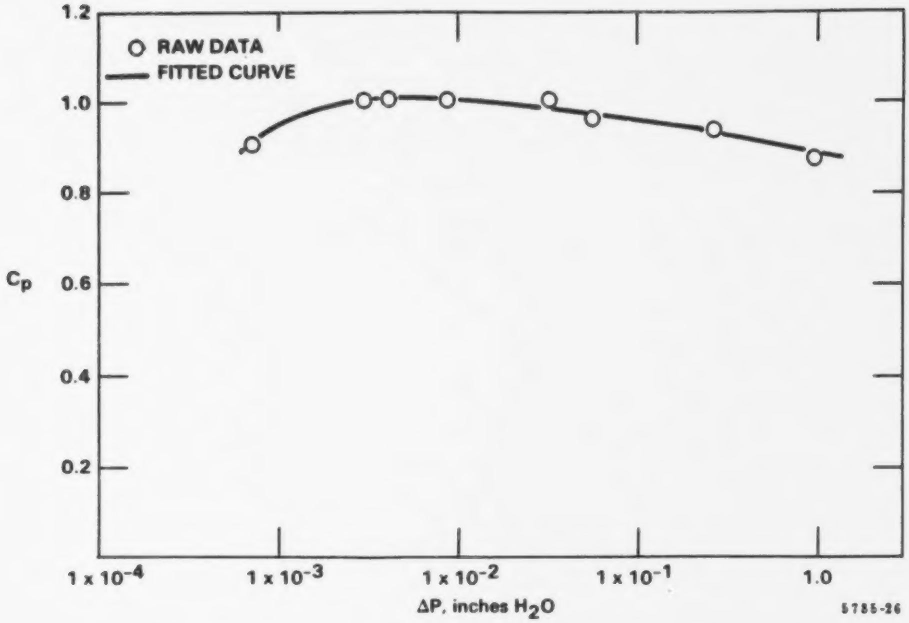

Figure 6-5. Pitot coefficient (C_p) for hypodermic pitot versus pressure drop (Δp), measured with a standard pitot.

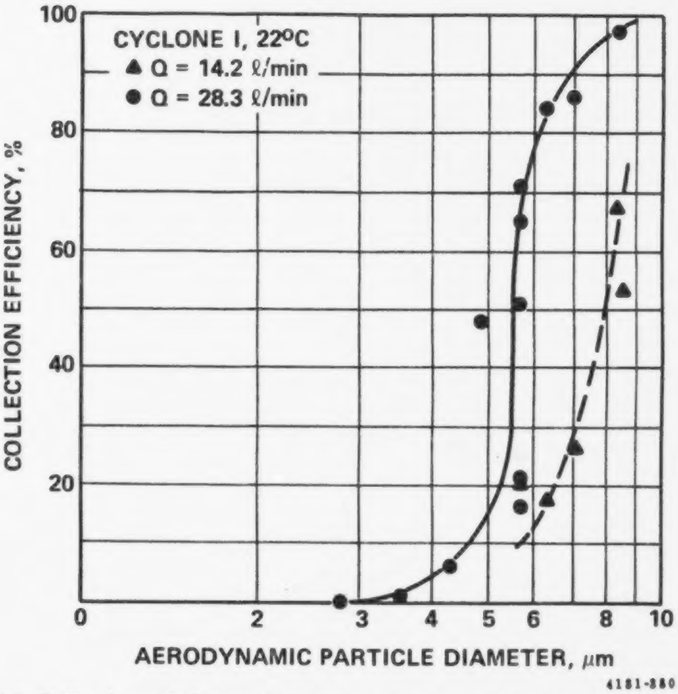

Figure 6-6. Collection efficiency of Cyclone I versus aerodynamic diameter. Diameter of gas stream at cyclone inlet was 1/2 in. (Smith et al. 1981).

of the hypodermic pitot at the wall farthest from the positioner (see Figure 6-4), designated point 1. Next, the zero offset for the electronic manometer was measured. The blower speed was then set to produce the desired flow stream velocity at the nozzle inlet and the valves on the sample box were adjusted to provide the PM_{10} flow rate through the test section. After the system was allowed a short time to stabilize, the velocity profile in the test section was measured. All velocity profiles consisted of 11 traverse points. Clockwise rotation of the vernier scale 0.050 in. backed the pitot out of the test section to the next traverse point, ending with point 11 at the near wall.

The nonrecycle nozzles are symmetrical about the axis of flow, while the EGR nozzle is not. Measurement of velocities of the EGR nozzles was performed with two orientations. In one orientation the tube conveying recycle gas to the nozzle was parallel to the line of the velocity traverse. In the other orientation this tube was perpendicular to this line.

BASIC PERFORMANCE RESULTS

Prior to this program the D_{50} of Cyclone I had been measured at five conditions: three flow rates at ambient conditions and one flow rate at each of two elevated temperatures. Figure 6-6 shows collection efficiency at ambient conditions versus particle size for 1/2 and 1 acfm. The D_{50} for four additional conditions was measured in the PM_{10} program. A 10-μm cut size was obtained at ambient conditions with a flow rate of 0.45 acfm. Figure 6-7 gives the corresponding efficiency curve. The cyclone collection efficiency is 10% at 6 μm and 90% at 15 μm. Figure 6-8 summarizes all of the basic performance data in terms of D_{50} versus flow rate at several temperatures. At ambient conditions the cyclone D_{50} can be fit by an exponential function of flow rate with power of -0.68.

No suitable theory exists for cyclones to assist in extending the available data to other conditions. However, analysis of empirical data indicates that the same two dimensionless parameters which characterize impactor behavior also characterize cyclone behavior. The parameters are Stokes number (Stk) and Reynolds number (Re):

$$\mathrm{Stk} = 4\tau Q/\pi d^3 \text{ and}$$
$$\mathrm{Re} = 4\rho Q/\pi \mu d$$

where τ = particle relaxation time (s) = $D^2/18\mu$,
D = particle diameter (cm),
μ = gas viscosity (micropoise),
Q = gas volume flow rate through the cyclone (cm^3/s),
d = a characteristic cyclone dimension (cm), and
ρ = gas density (g/cm^3).

Beeckmans (1979) found that cyclone collection efficiency correlated with $\sqrt{\mathrm{Stk}}\,\mathrm{Re}^b$, where b was an empirical constant. Investigating the SRI/EPA series cyclone (II through V), Farthing and Williamson (1985) found that when gas density and viscosity were varied over broad ranges with helium, argon, carbon dioxide, and air, the cyclone cut conformed to a function of

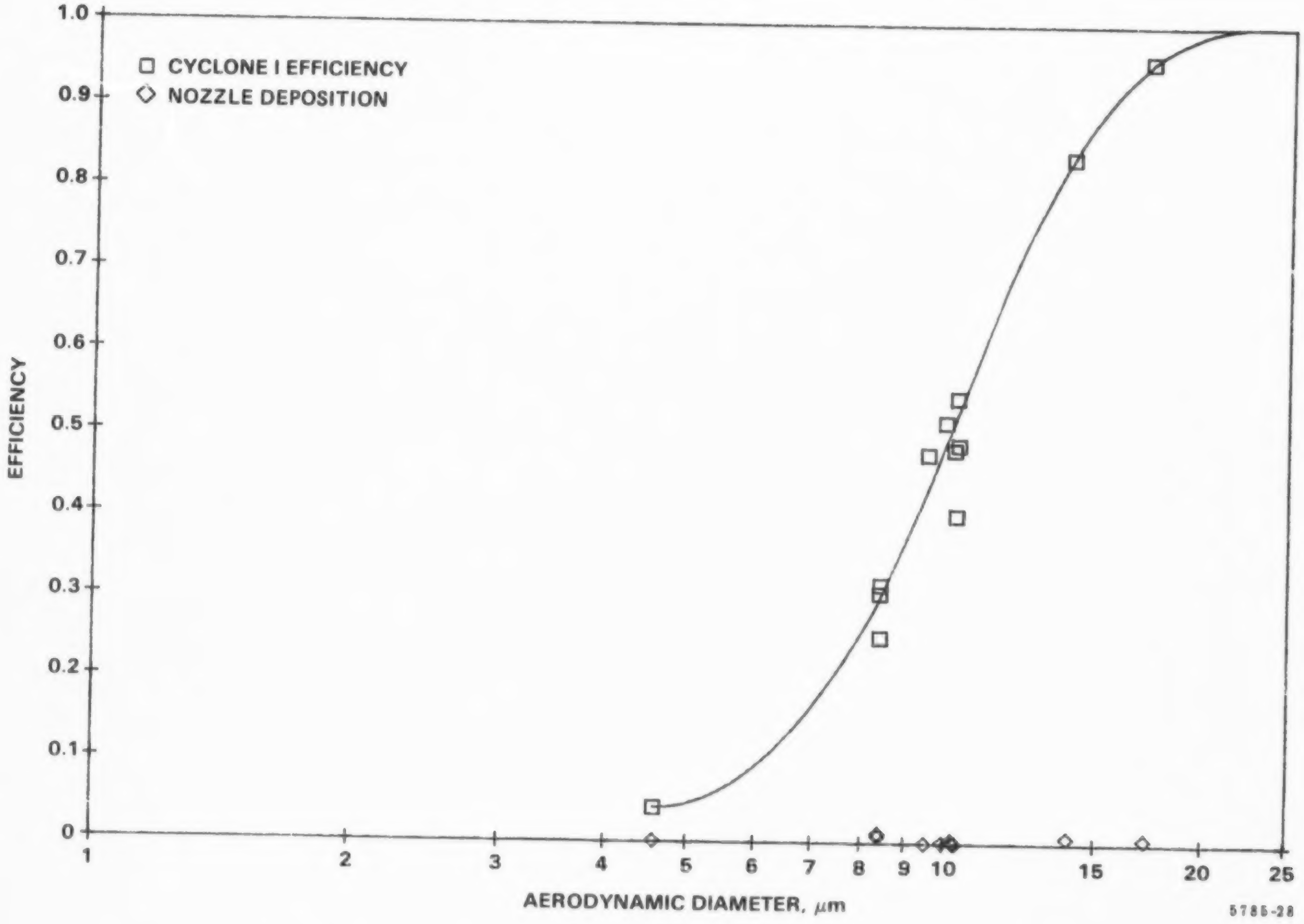

Figure 6-7. Collection efficiency of Cyclone I and 1/2-in. nozzle at 0.45 acfm and 27 °C.

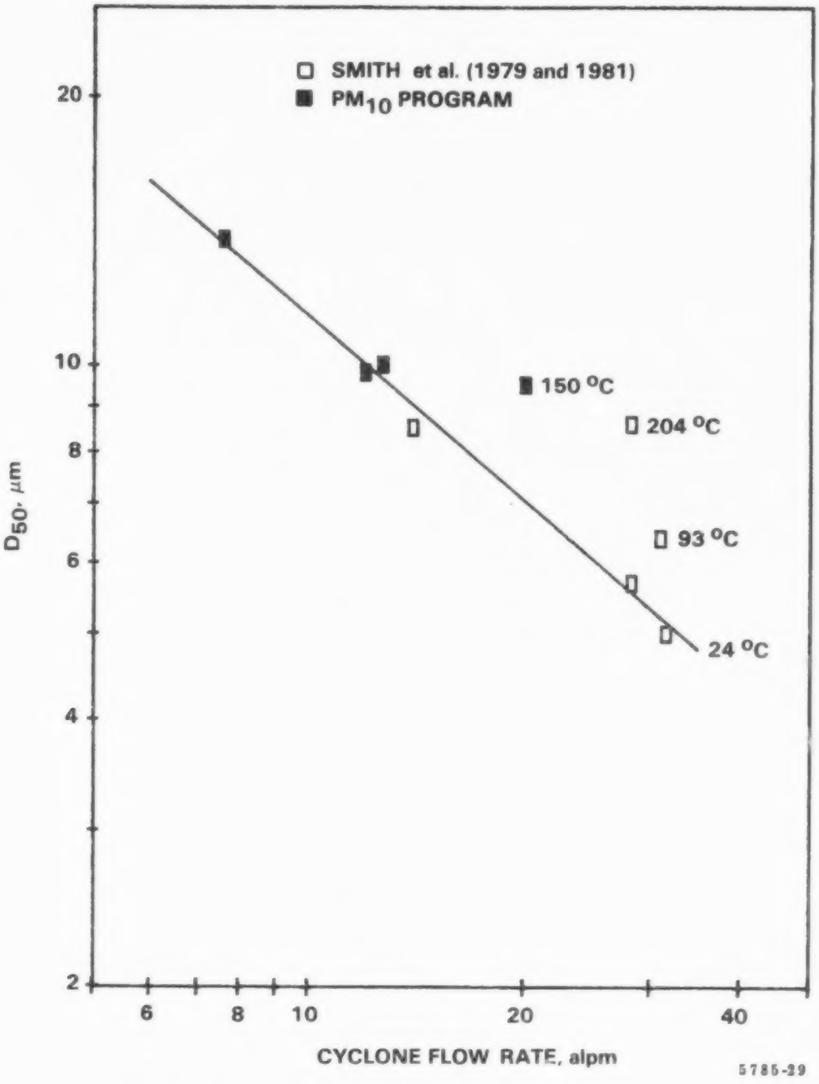

Figure 6-8. Cyclone I D_{50} versus flow rate at several temperatures.

$\sqrt{Stk_{50}}$ versus Re (where $\sqrt{Stk_{50}}$ corresponds to the D_{50}). This is illustrated for Cyclone I in Figure 6-9, where the cyclone D_{50} data of Figure 6-8 are expressed as $\sqrt{Stk_{50}}$ versus Re, and the inlet diameter (0.5 in.) is used for the cyclone dimension. This approach reduces behavior at various temperatures and flow rates to one function. The spread of the data is less than ±8% in $\sqrt{Stk_{50}}$. Cyclones II through V were shown to behave similarly; that is, they have the same $\sqrt{Stk_{50}}$ when operated with different gas densities, viscosities, and flow rates, but the same Re.

It should be noted that the use of the cyclone inlet as the cyclone dimension in evaluating Stk_{50} and Re is not fundamentally relevant to this empirical characterization. Any cyclone dimension would yield a similar function. The degree to which cyclone inlet diameter determines cyclone behavior is not known. The immediate concern is a method to utilize calibration data to predict behavior at the broad range of conditions which may be encountered in process streams. The empirical function in Figure 6-9 appears to be satisfactory, although additional verification may be appropriate.

RESULTS OF VARYING STREAM VELOCITY

All measurements presented in this section were obtained with flow rate at 0.45 acfm at laboratory conditions (27 °C). The cyclone with field sampling nozzles was installed in the apparatus depicted in Figure 6-1. The aerosol flow stream was adjusted so that the nozzle sampled isokinetically.

Existing Sampling Nozzles

As indicated in Figure 6-3 the nozzles used for Cyclone I have been classified into three types, in addition to the largest 1/2-in. nozzle. These results are presented by nozzle type. Three types of data are presented: Cyclone I collection, nozzle efficiency, and velocity profile.

Nonrecycle-Tapered Nozzles--

This nozzle type has a small angle of expansion from the inlet diameter to the cyclone inlet diameter. Measurements were performed for two of this type, those having inlets of 0.233 in. (#7) and 0.195 in. (#9). Figure 6-10 gives cyclone efficiencies. The behavior of Cyclone I appears to be slightly different than with the reference nozzle (the largest, 1/2-in. nozzle) but the cut size is changed by much less than 1 μm. Figure 6-11, giving the nozzle efficiencies corresponding to Figure 6-10, shows significant nozzle losses. The larger nozzle had losses increasing with particle size from 3% (at 1 μm) to about 20% (at 10 μm). With the smaller nozzle, losses decreased only slightly for smaller sizes.

The velocity profiles in Figure 6-12 show what was an unexpected difference between the two nozzles. The one with the larger inlet had higher velocities than the smaller one. The 0.235-in. nozzle has an inlet "plug flow" velocity of 15 ft/s while the 0.195-in. nozzle had "plug flow" velocity of 42 ft/s. The velocity for both nozzles dropped substantially between the inlet and the measurement plane inside the cyclone. However,

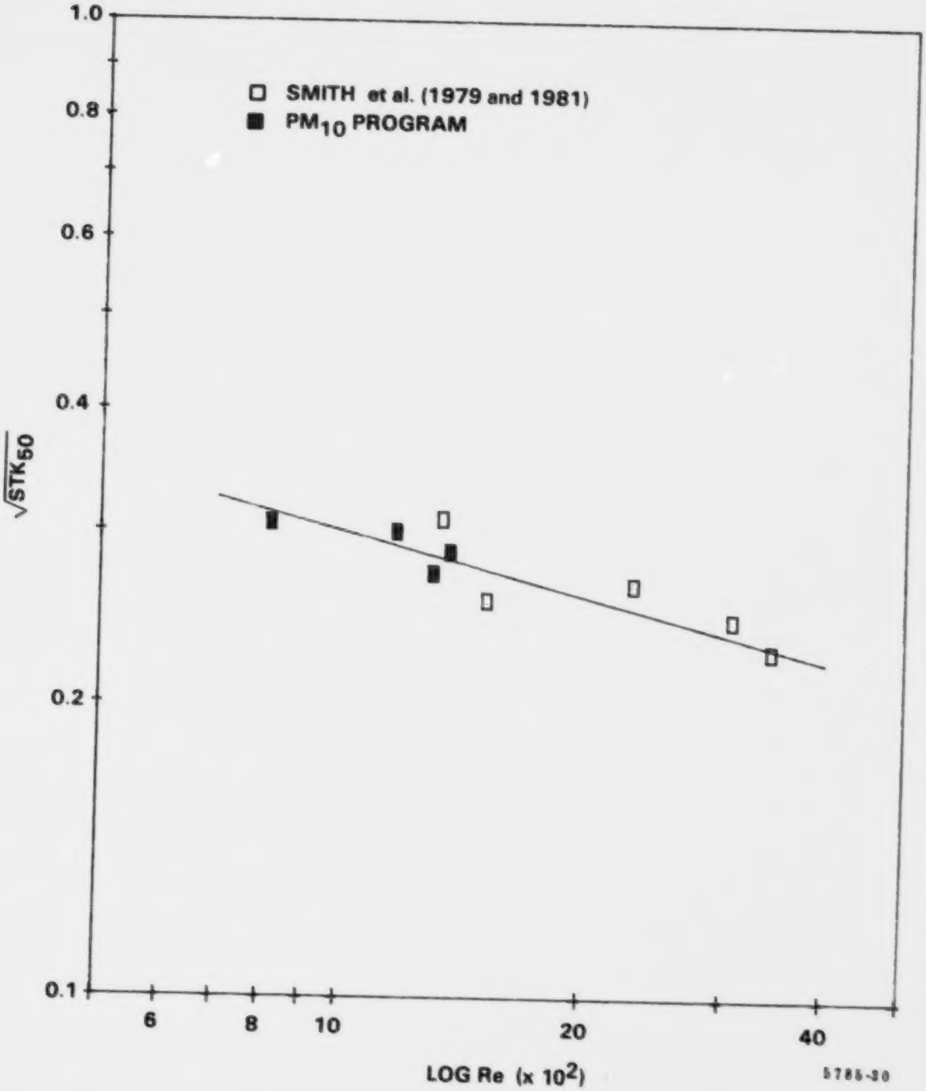

Figure 6-9. Cyclone I $\sqrt{Stk_{50}}$ versus Re.

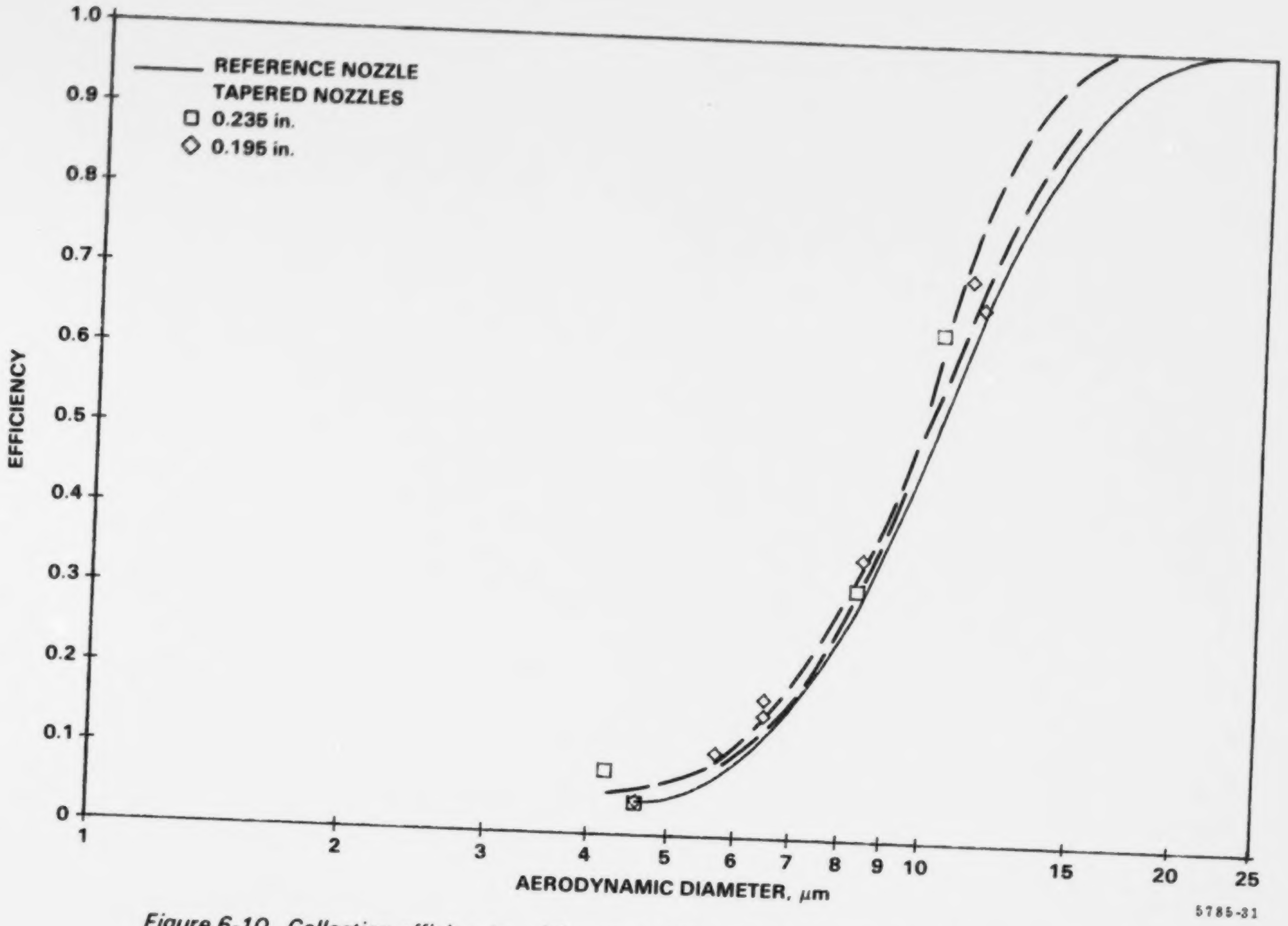

Figure 6-10. *Collection efficiencies of Cyclone I with tapered nonrecycle nozzles and reference nozzle (1/2 in.).*

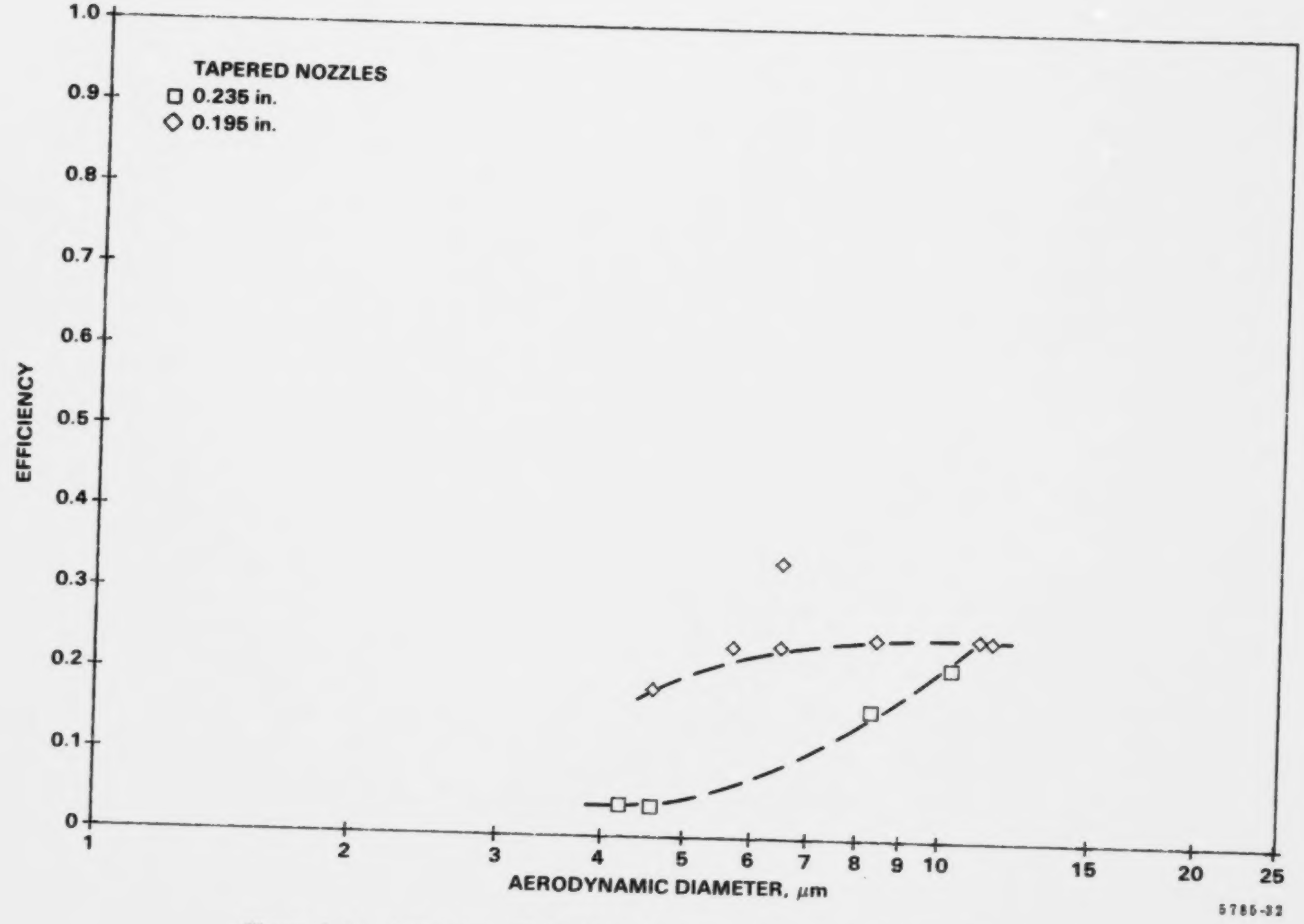

Figure 6-11. Collection efficiencies of tapered nonrecycle nozzles in Cyclone I.

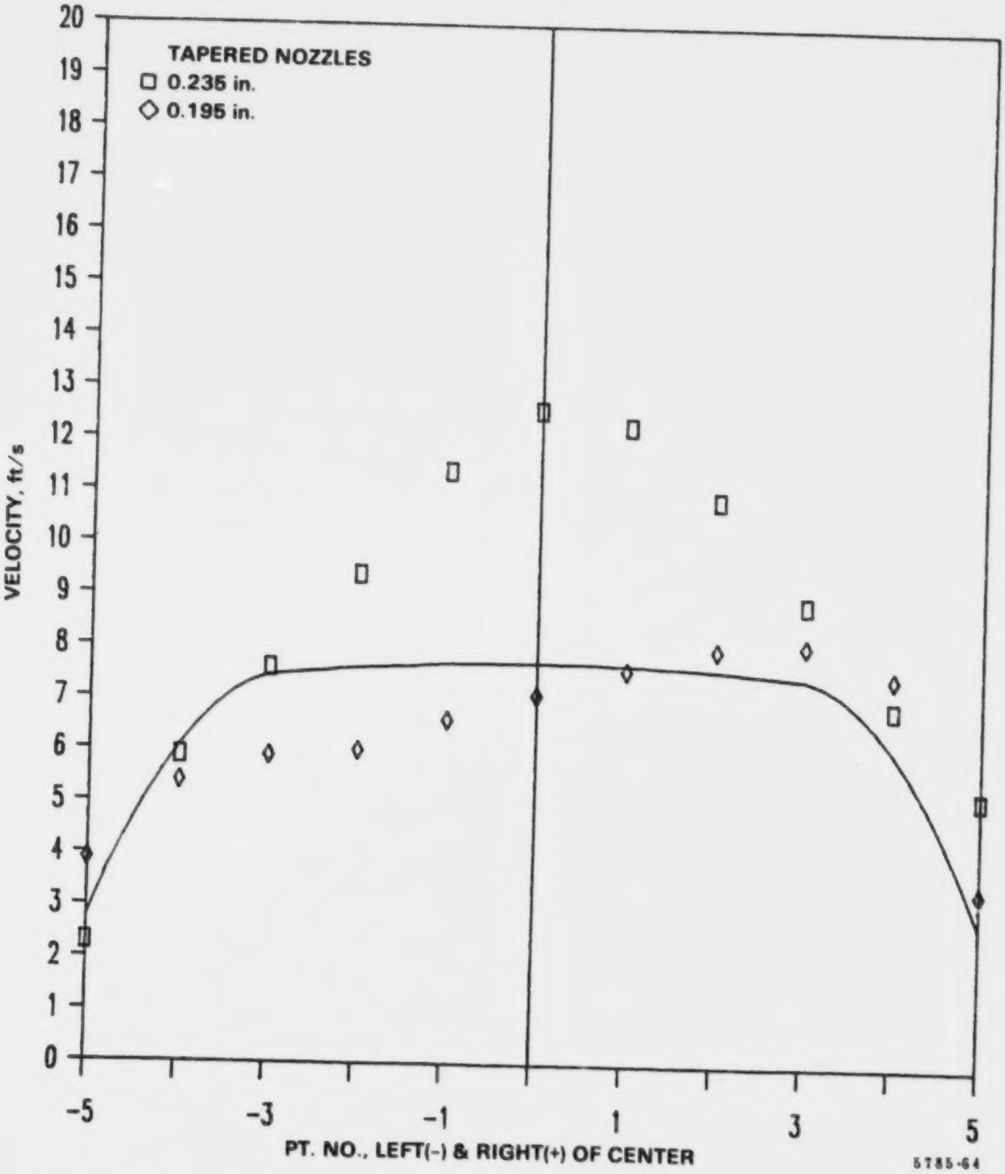

Figure 6-12. Velocity profiles at exit of tapered nonrecycle nozzles and reference nozzle (1/2 in.).

the velocity in the smaller one decreased much more. Geometrical differences in the nozzles were that the larger one has a 0.1-in. longer straight section and a 0.1-in. shorter distance between the start of the taper and the velocity measurement plane. (These distances are given in Table 6-1). The Re of these flows were 3000 for the larger nozzle and 3600 for the smaller one.

It should also be noted that integration of the velocity data in Figure 6-12 gives a significantly higher flow rate than that known to exist in the test section, 40% high for the 0.235-in. nozzle, 10% high for the 0.195-in. nozzle, and 10% high for the 1/2-in. nozzle. The source of this discrepancy is not known; most of the nozzles showed a similar problem with the integration. It is believed that this discrepancy is due mainly to error associated with measuring flow near the wall. The fourth and fifth points form the center represent 50% of the flow. Thus, it is believed that the velocities measured near the center are reliable, while those measured near the walls should not be interpreted quantitatively.

Nonrecycle Nozzles with Large Expansion Angle--

Figure 6-13 gives cyclone collection efficiency with all nozzles with abrupt expansions; that is, large expansion angles, inlet diameters of 0.155 in. (#11) and 0.138 in. (#12). The EGR nozzles with zero recycle air are also included in this group since they also present an abrupt expansion to the flow at the end of the sample tube (see Figure 6-3). Cyclone cut diameter was shifted down to about 6 µm with all of these nozzles. Although more data are needed for confidence, it appears that the 0.138 in. nozzle caused the lowest cut, while the 1/4-in. EGR nozzle gave the largest cut of this group.

Figure 6-14 gives the nozzle efficiency for this group. The highest losses were incurred by the 0.138-in. nozzle, 30% at 4 µm decreasing to 20% at 10 µm. The 0.155-in. nozzle losses were about 10% at 4 µm and 15% at 10 µm. With the 1/8-in. EGR nozzle, the losses around 4 µm (10-20%) appear much higher than at 10 µm (1%). The losses for the two larger EGR nozzles were insignificant. The size dependence of losses for the 0.138-in. nozzle, decreasing with increasing size, may be somewhat surprising because nozzle losses are generally thought to increase with particle size because of increased Stokes number.

Figure 6-15 gives velocity profiles for these nozzles. The velocities for the 0.155-in., 0.138-in., and 3/16-in. EGR nozzles were all close together, about 40 ft/s at the center. The 1/4-in. EGR nozzle had the lowest velocities of this group. This group of nozzles also had reproducible negative velocity measurements near the edge of the expansion type, suggesting flow reversal zones. The plug flow velocities at the inlet to these nozzles were 22, 39, 57, 72, and 88 ft/s, respectively, in order of decreasing size from the 1/4-in. EGR nozzle to the 1/8-in. EGR nozzle. Thus the velocities decreased substantially for all of the smallest three nozzles but relatively more for the 1/8-in. nozzle. This behavior may be associated with the longer expansion distance of this nozzle compared to the others. Unexpectedly, the downstream peak velocities measured for the 1/4- and 3/16-in. EGR nozzles were essentially the same as the respective inlet

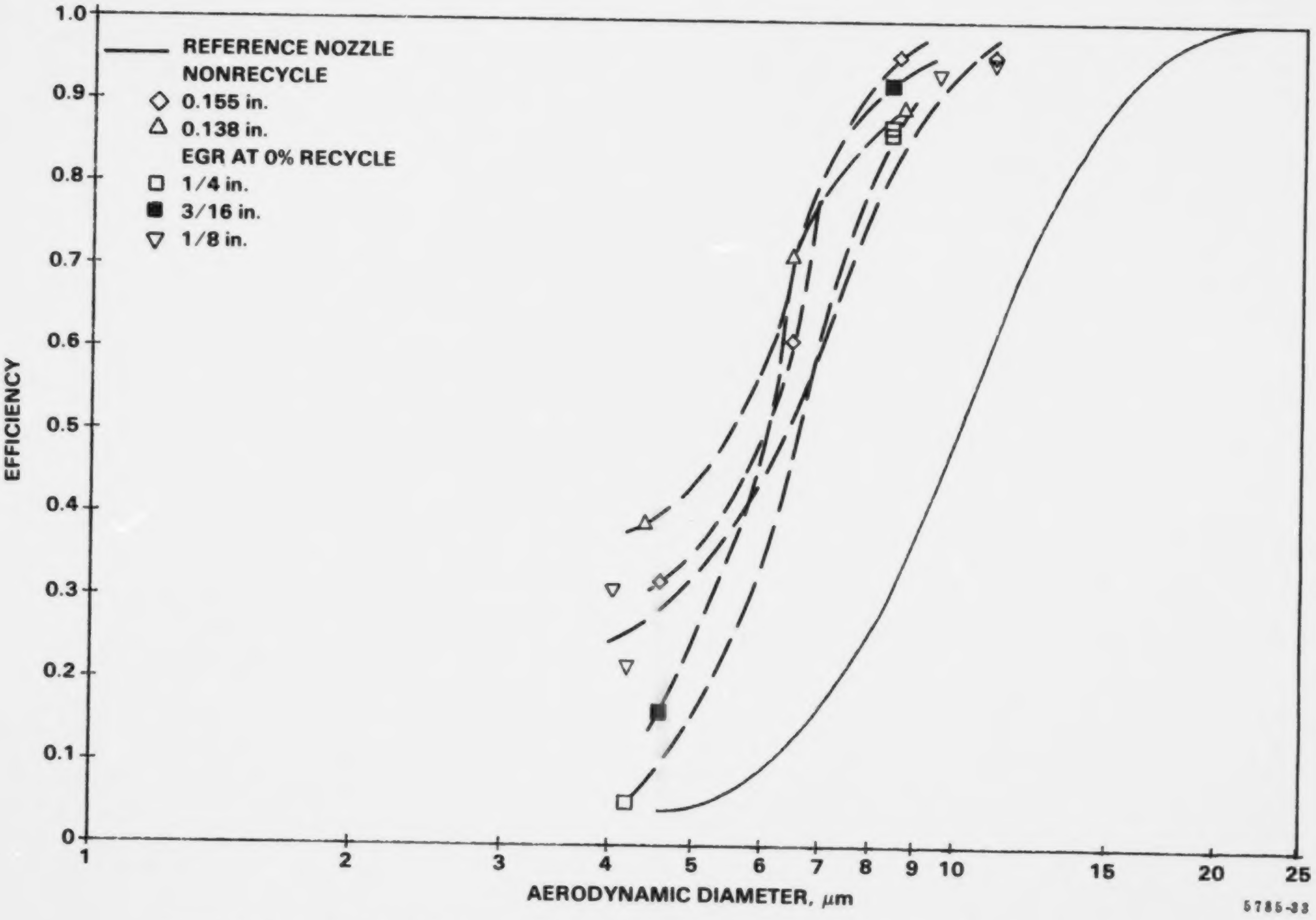

Figure 6-13. Collection efficiencies of Cyclone I with nozzles having large expansion angles and reference nozzle (1/2 in.).

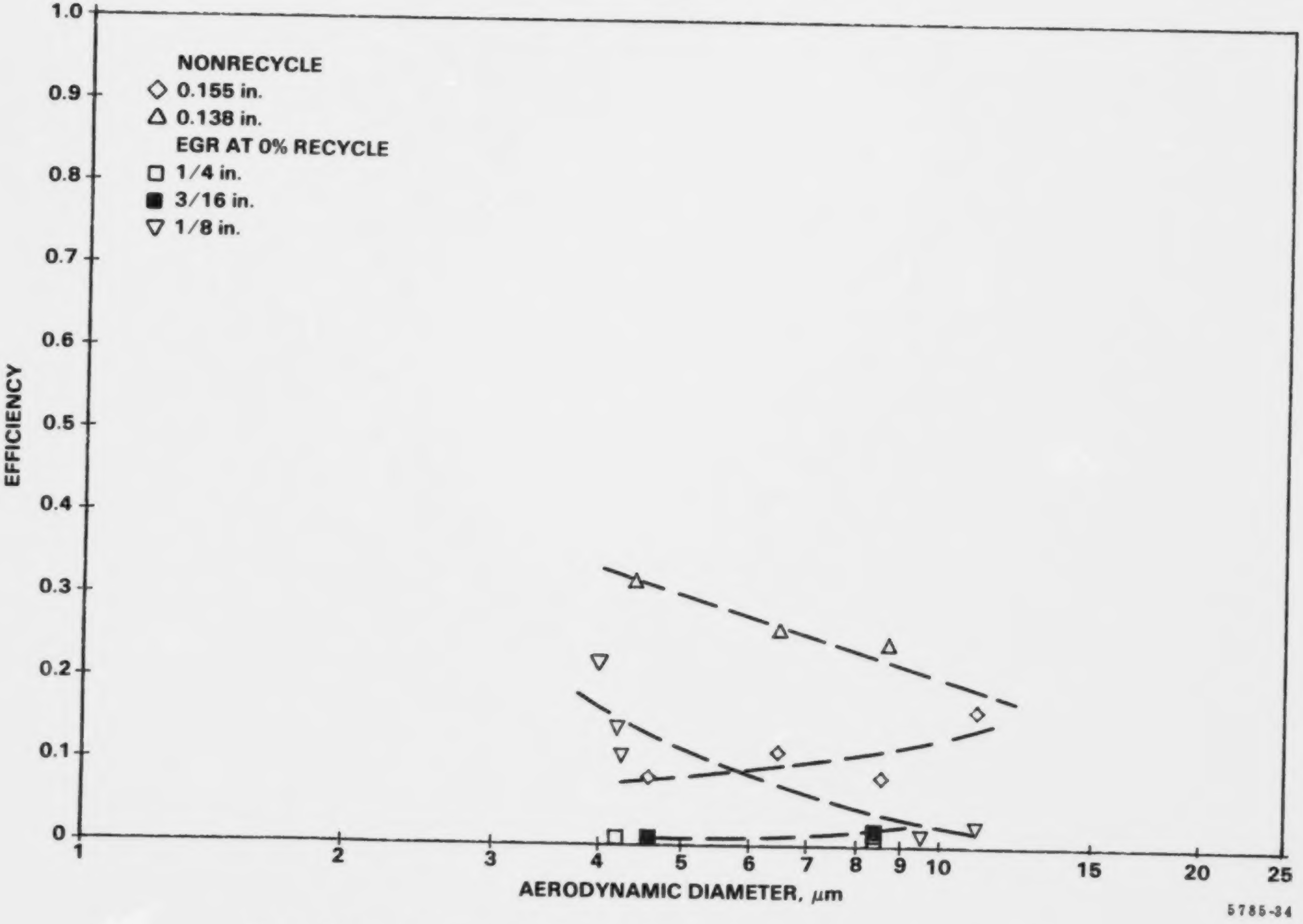

Figure 6-14. Collection efficiencies of nozzles having large expansion angles.

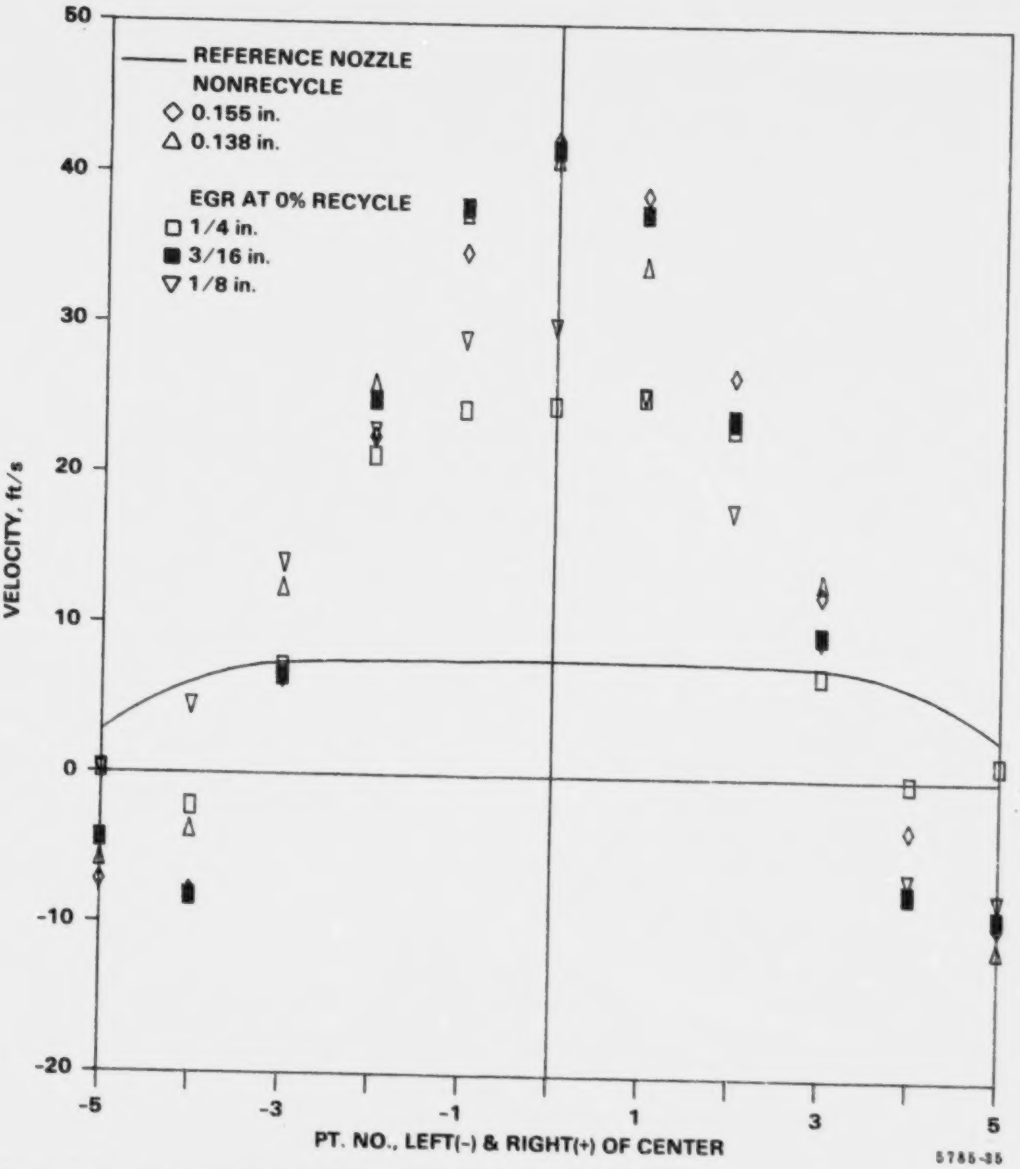

Figure 6-15. Velocity profiles at exit of nozzles having large expansion angles and reference nozzle (1/2 in.).

velocities, suggesting no expansion in these nozzles. Both nozzles also had low or negative velocities at the outer edge, suggesting flow separation. Although more cyclone efficiency data (Figure 6-13) are needed to substantiate the results, it appears that efficiency is correlated with nozzle velocity. The nozzles with higher velocity are associated with a higher cyclone collection.

Recycle (EGR) Nozzles--

Results obtained with the EGR nozzles are given in Figures 6-16 through 6-28. The same data are presented in two sets of figures. First, comparisons are made between different recycle rates for the same EGR nozzle. Then comparisons are made between EGR nozzle sizes at the same recycle rates.

Varying recycle rate--Figures 6-16, 6-18, and 6-20 give measured cyclone collection efficiency for the 1/4-in., 3/16-in., and 1/8-in. EGR nozzles, respectively. Each figure gives efficiencies at three recycle rates. In each instance, efficiency was higher (or cut size smaller) for the lower recycle rate. No significant differences between 0% and 10% recycle rates were observed, while 75% recycle gave a cut size significantly closer to the basic cyclone performance (using the reference 1/2-in. nozzle). Nozzle losses with the 1/4-in. and 1/8-in. EGR nozzles were insignificant (<2%) at all recycle rates studied. Figure 6-21 gives nozzle losses for the 1/8-in. EGR nozzle. These were low (≈3%) at the 75% recycle rate. At 0% and 10% recycle, the losses at 4 μm were about 20% and dropped to a low level at 10 μm.

Figures 6-17, 6-19, and 6-22 give velocity profiles for the EGR nozzles. In each instance the velocity was lower for higher recycle rates. Note also that the profiles for 75% were skewed to the right. This corresponds to the side of the nozzles opposite but downstream from the entrance of the recycle air, the top of the cyclone inlet as viewed in Figure 6-3.

Varying nozzle inlet size--Figures 6-23 and 6-26 present cyclone efficiencies for the EGR nozzles at the 0% and 75% recycle rates, respectively. Each figure gives results for all three recycle nozzles. In each instance all nozzle inlet diameters present about the same cut size, although the 1/8-in. EGR nozzle at 0% recycle appears to have somewhat higher collection efficiency at 4 μm.

Figures 6-24 and 6-27 present EGR nozzle losses at the 0% and 75% recycle rates, respectively. At 0% recycle losses varied with nozzle inlet diameter, but are small for all but the 1/8-in. nozzle. At the 75% recycle rate, losses were small (<5%) for all of the EGR nozzles.

Figures 6-25 and 6-28 present velocity profiles for the EGR nozzles at 0% and 75% recycle rates, respectively. At 0% recycle, velocities vary with nozzle size so that decreasing size from 1/4 in. to 3/16 in. increased the velocity at the cyclone inlet, while decreasing the size further to 1/8 in. decreased velocity at the cyclone inlet. As discussed in an earlier part of this section, this behavior may be due in part to the differences in straight lengths and expansion distances for these nozzles, given in Table 6-1. As noted above, the velocity profiles at the 75% recycle rate were

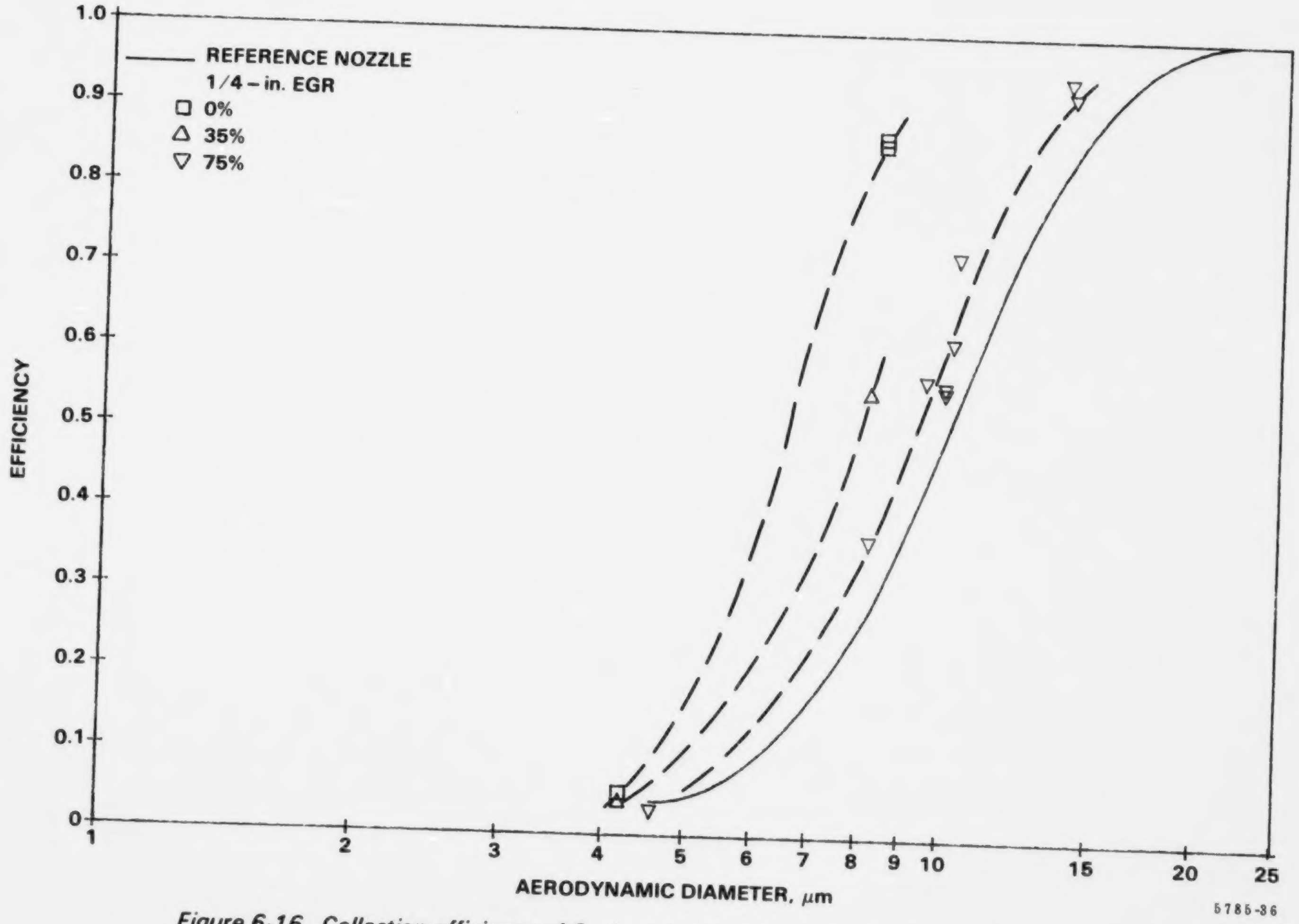

Figure 6-16. *Collection efficiency of Cyclone I with 1/4-in. EGR nozzle at three recycle rates and reference nozzle (1/2 in.).*

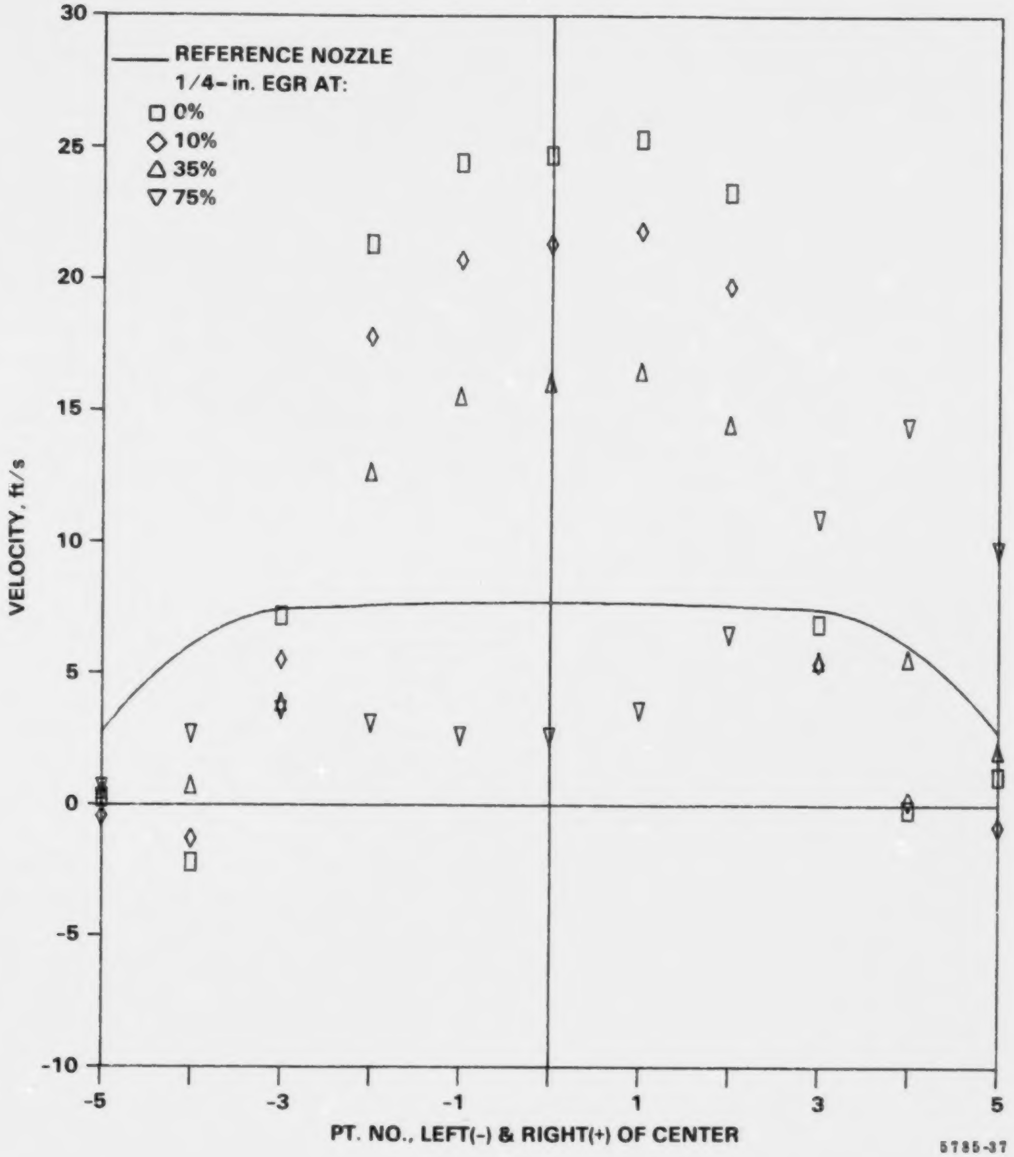

Figure 6-17. Velocity profiles at exit of 1/4-in. EGR nozzles at four recycle rates and reference nozzle (1/2 in.).

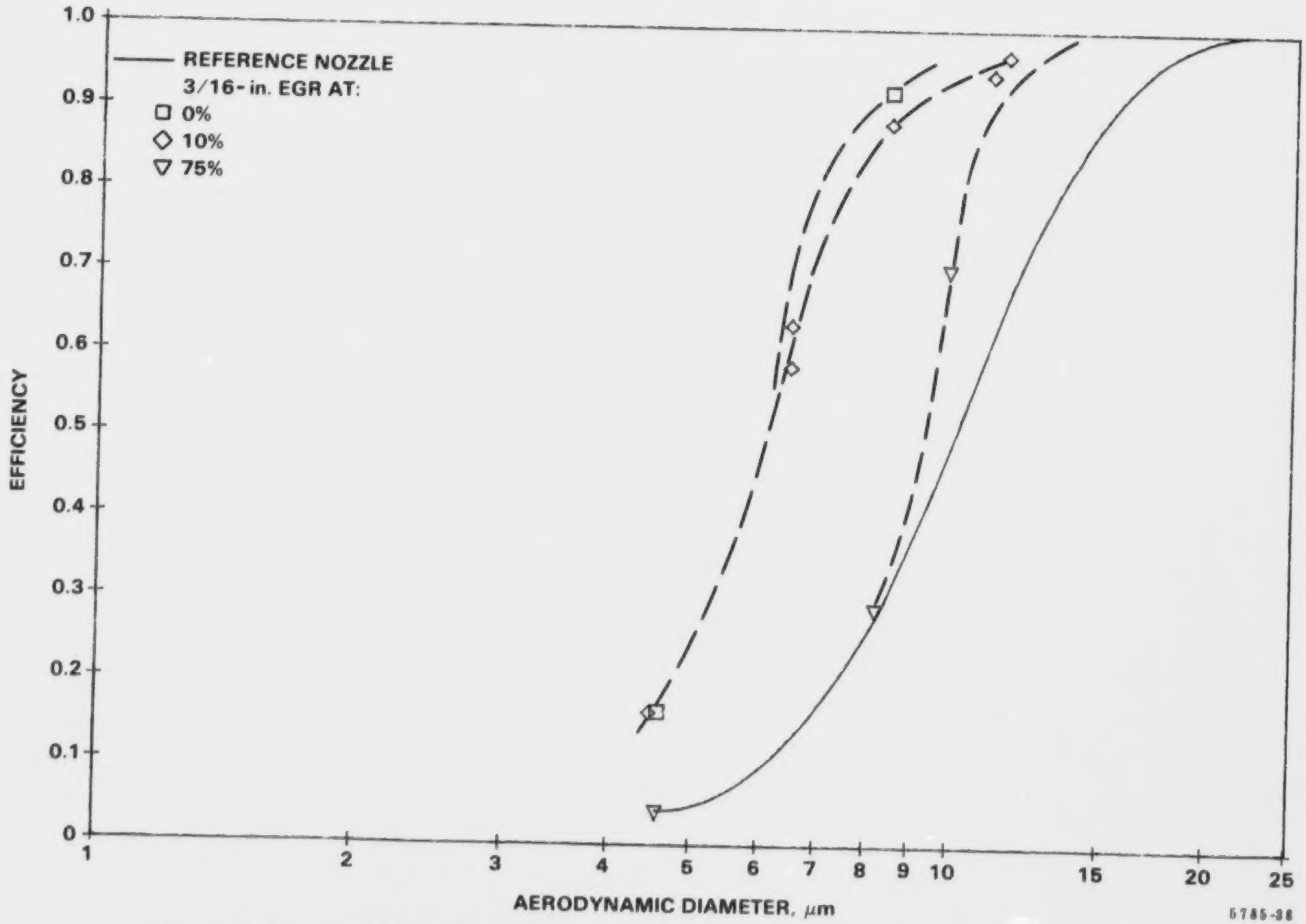

Figure 6-18. Collection efficiencies of Cyclone I with 3/16-in. EGR nozzle at three recycle rates and reference nozzle (1/2 in.).

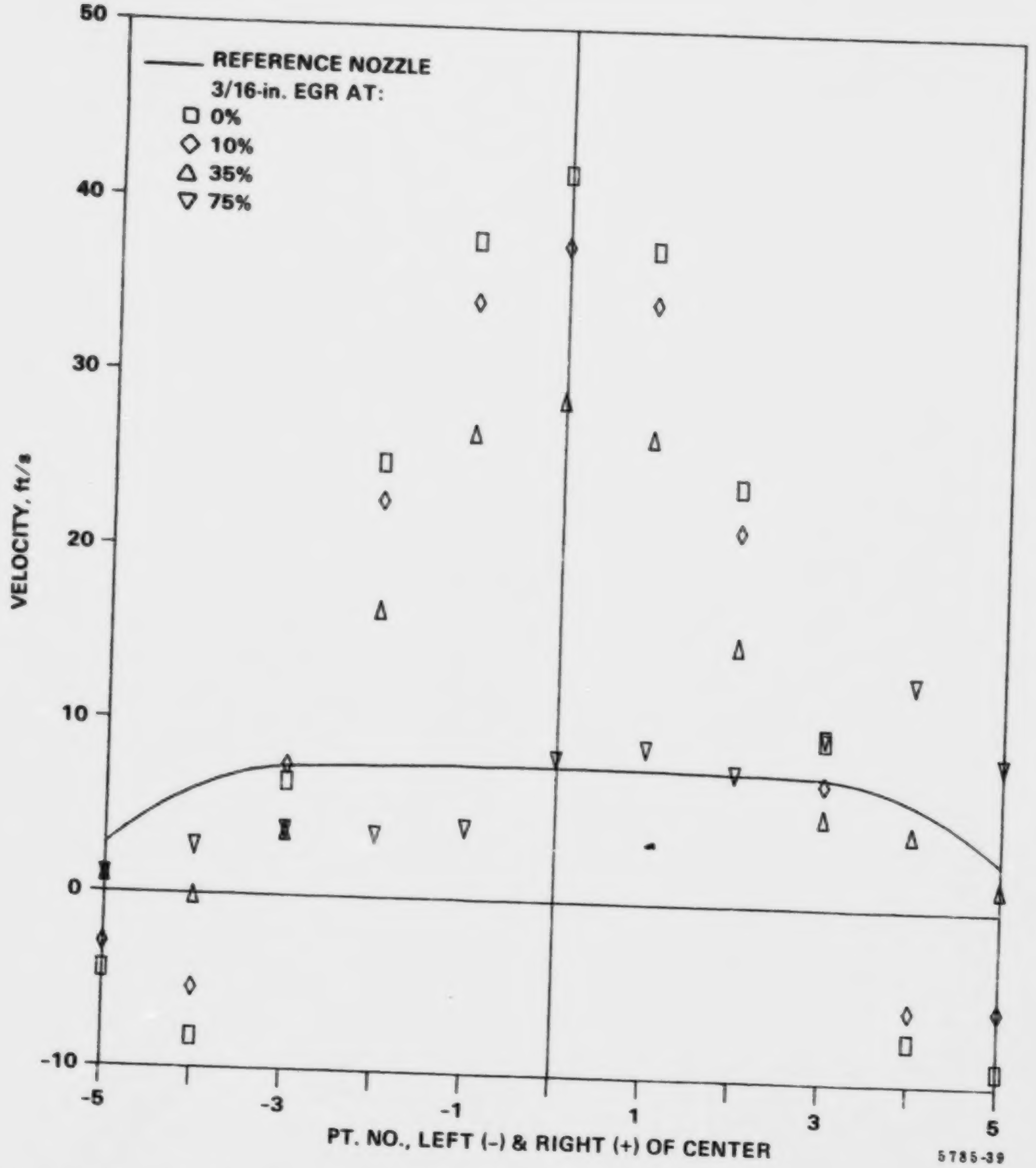

Figure 6-19. Velocity profiles at exit of 3/16-in EGR nozzle at four recycle rates and reference nozzle (1/2 in.).

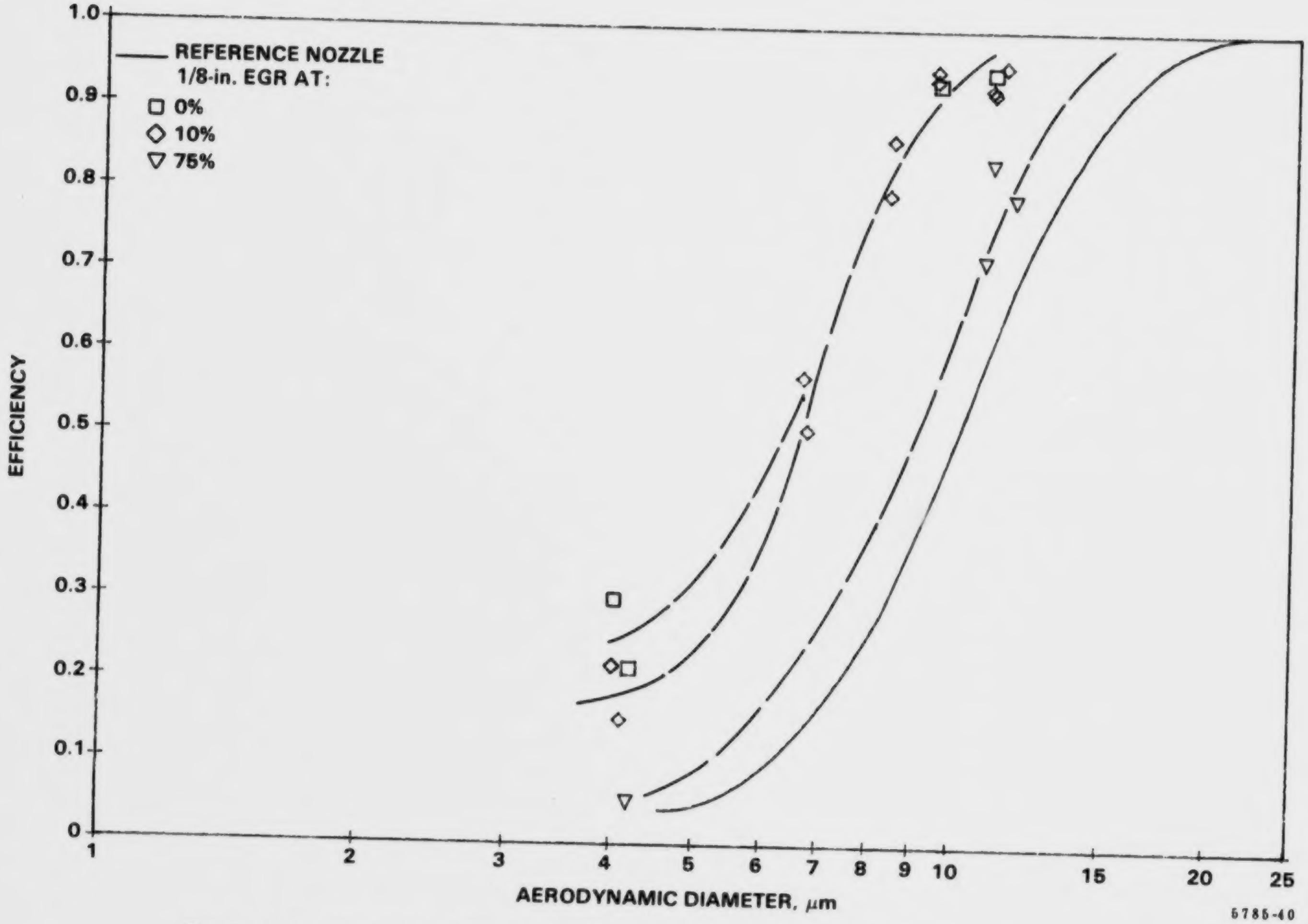

Figure 6-20. Collection efficiencies of Cyclone I with 1/8-in. EGR nozzle at three recycle rates and reference nozzle (1/2 in.).

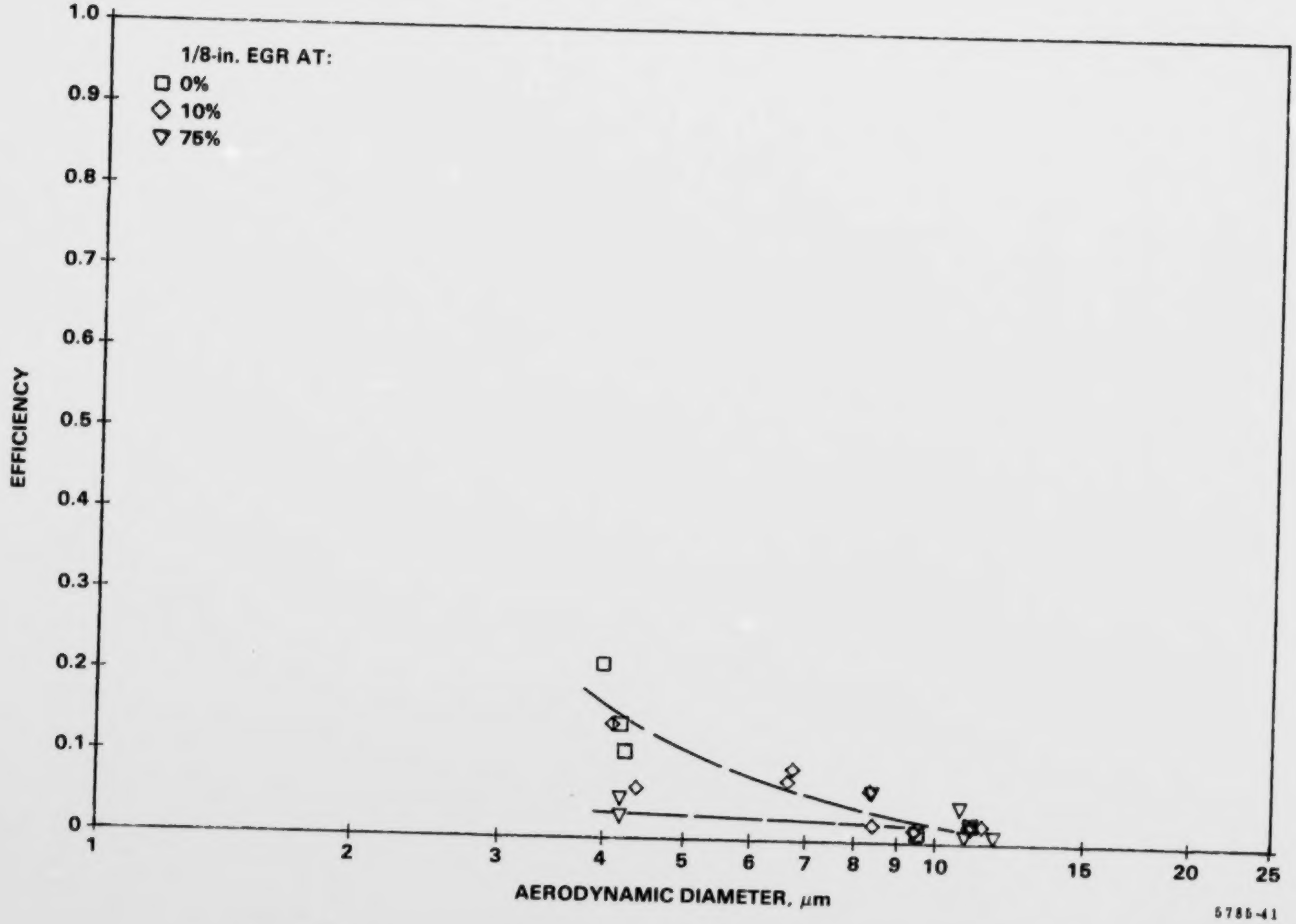

Figure 6-21. Collection efficiencies of 1/8-in. EGR nozzle at three recycle rates.

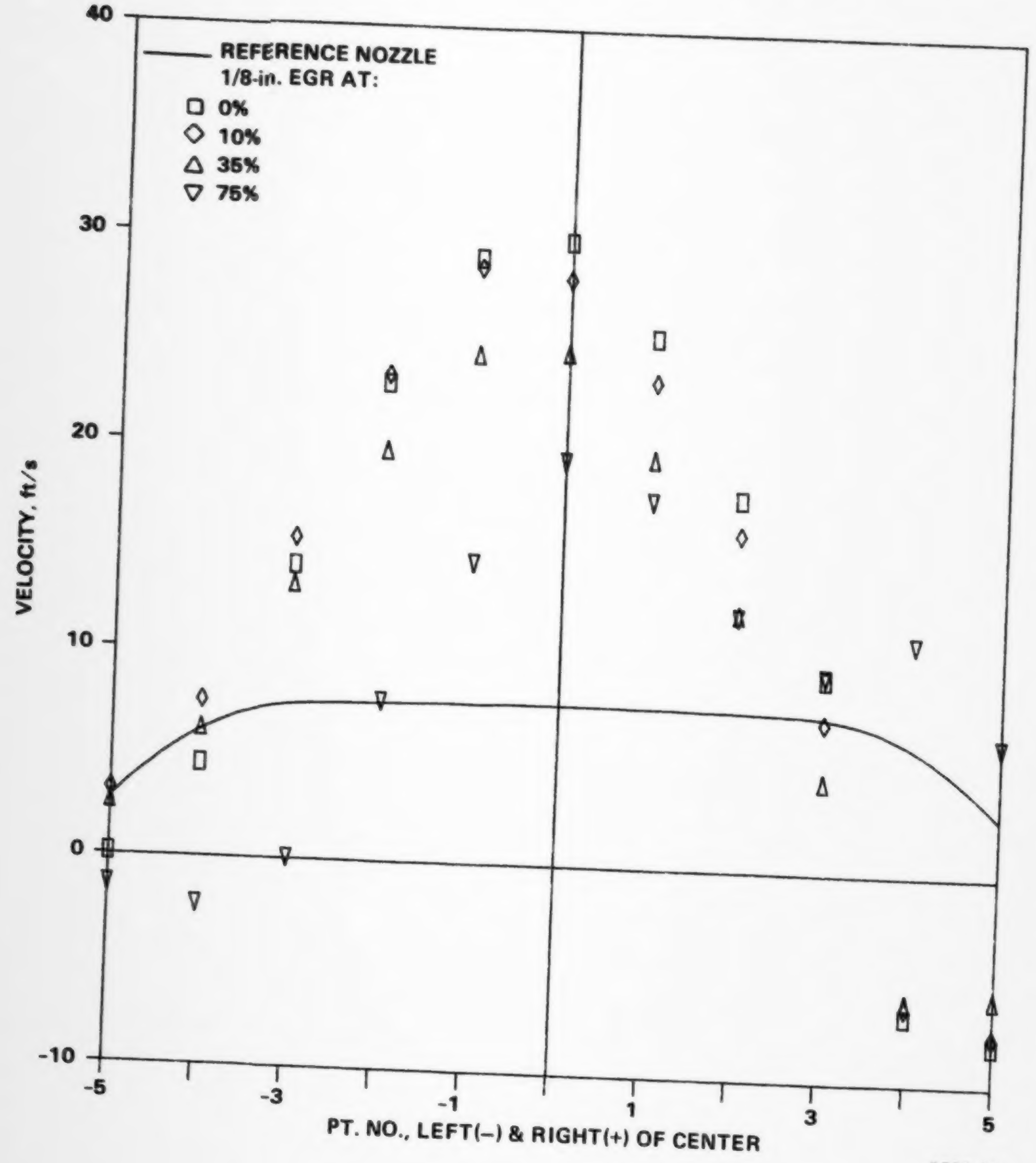

Figure 6-22. Velocity profiles at exit of 1/8-in. EGR nozzle at four recycle rates and reference nozzle (1/2 in.).

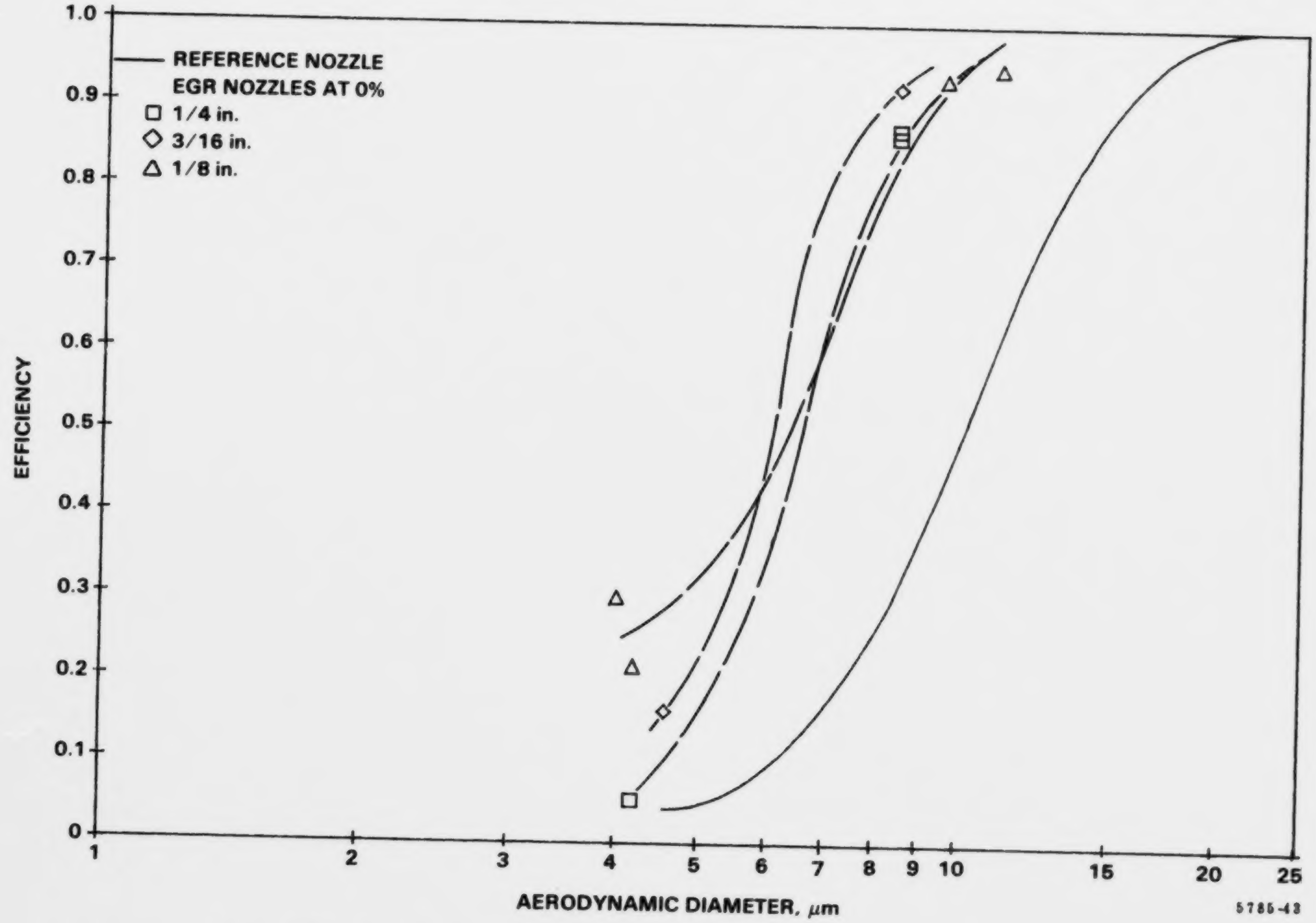

Figure 6-23. Collection efficiencies of Cyclone I with EGR nozzles at 0% recycle rate and reference nozzle (1/2 in.).

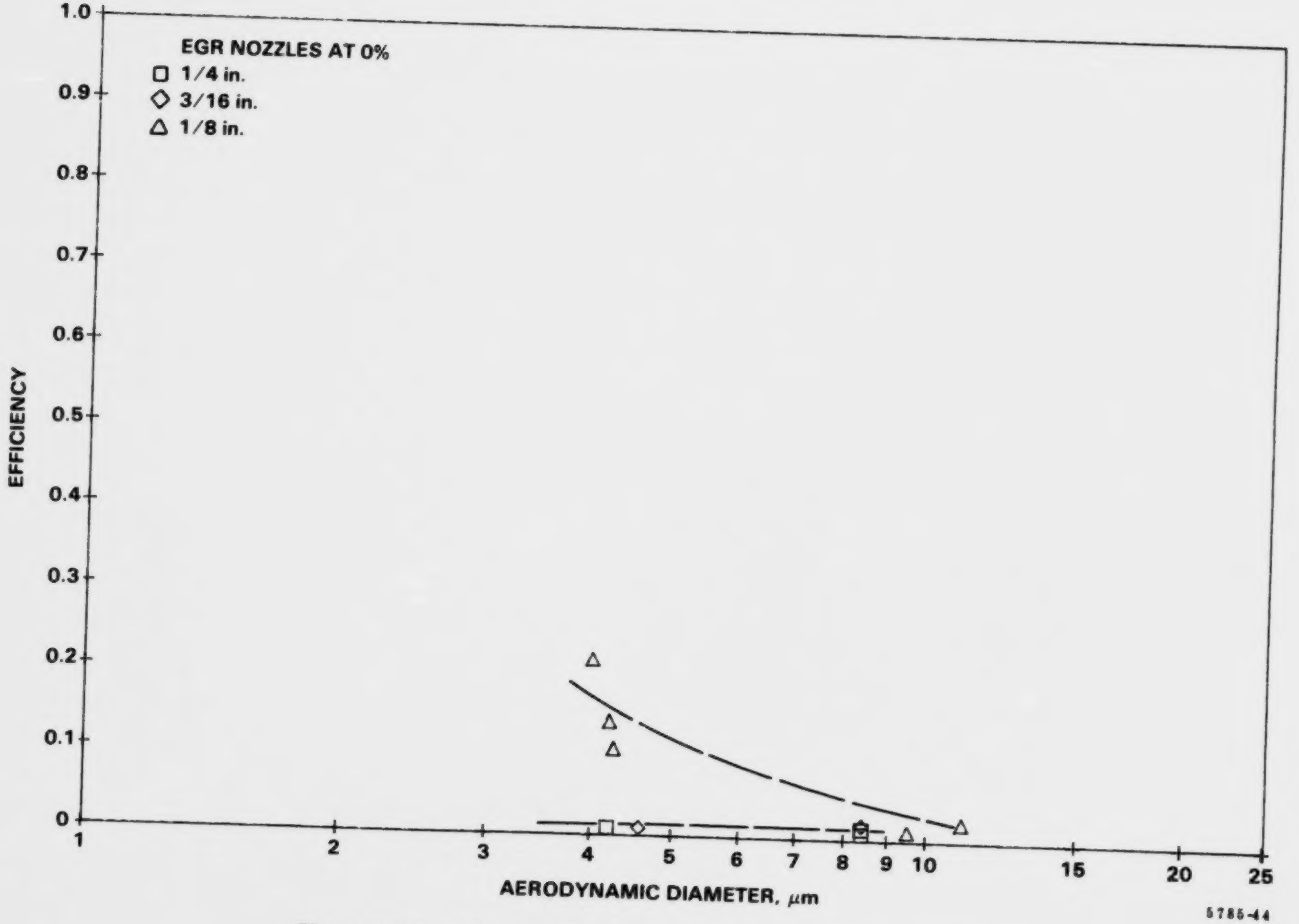

Figure 6-24. Collection efficiencies of EGR nozzles at 0% recycle rate.

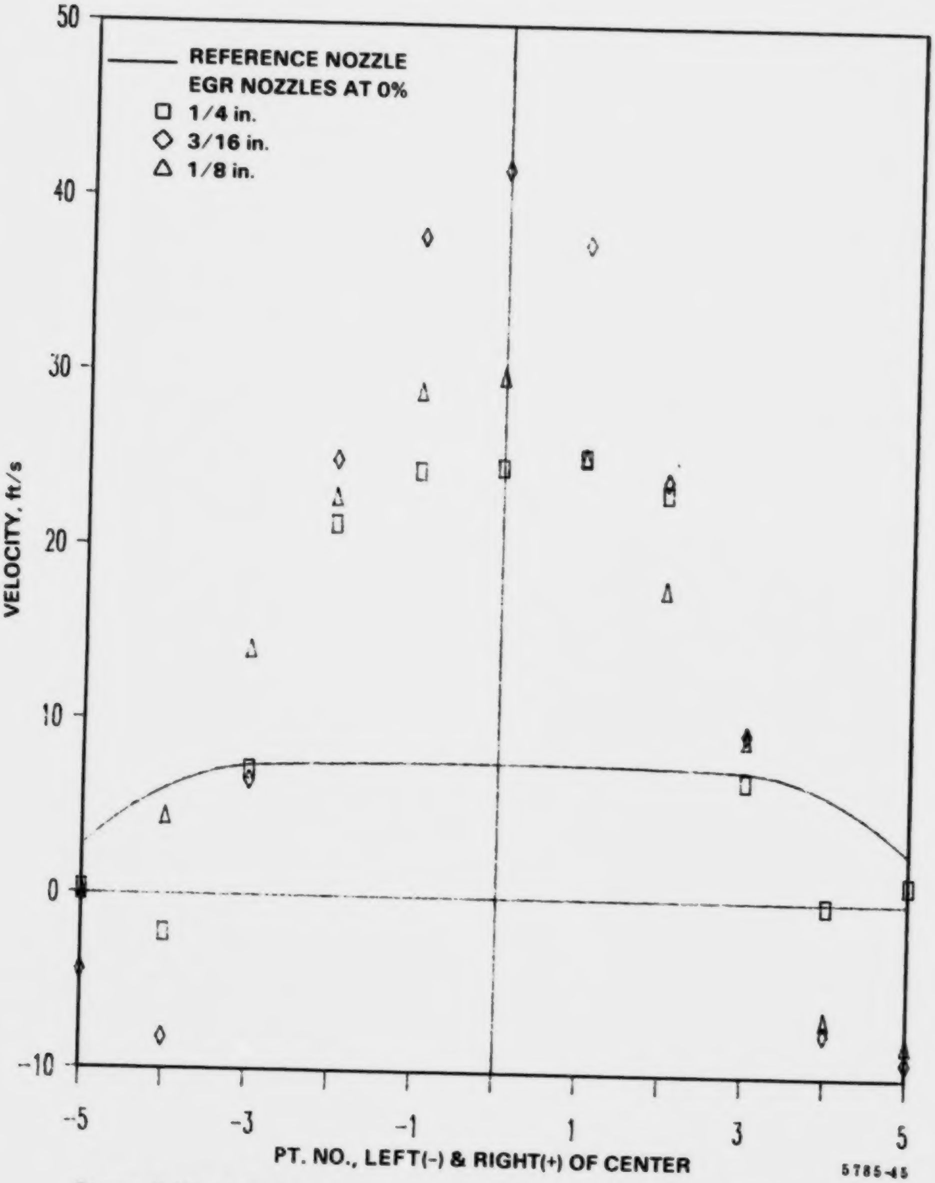

Figure 6-25. Velocity profiles at exit of EGR nozzles at 0% recycle rate and reference nozzle (1/2 in.).

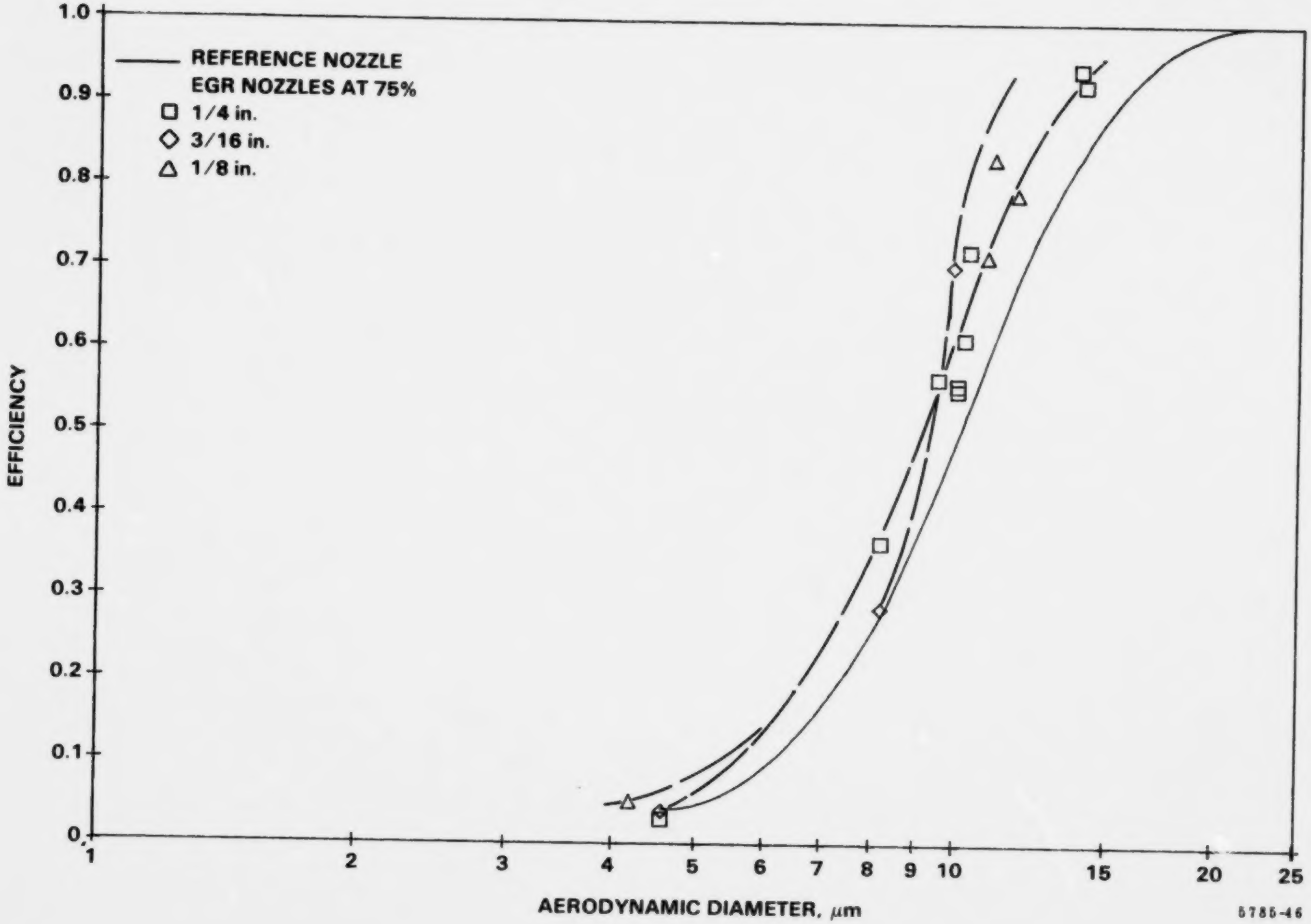

Figure 6-26. Collection efficiencies of Cyclone I with EGR nozzles at 75% recycle rate and reference nozzle (1/2 in.).

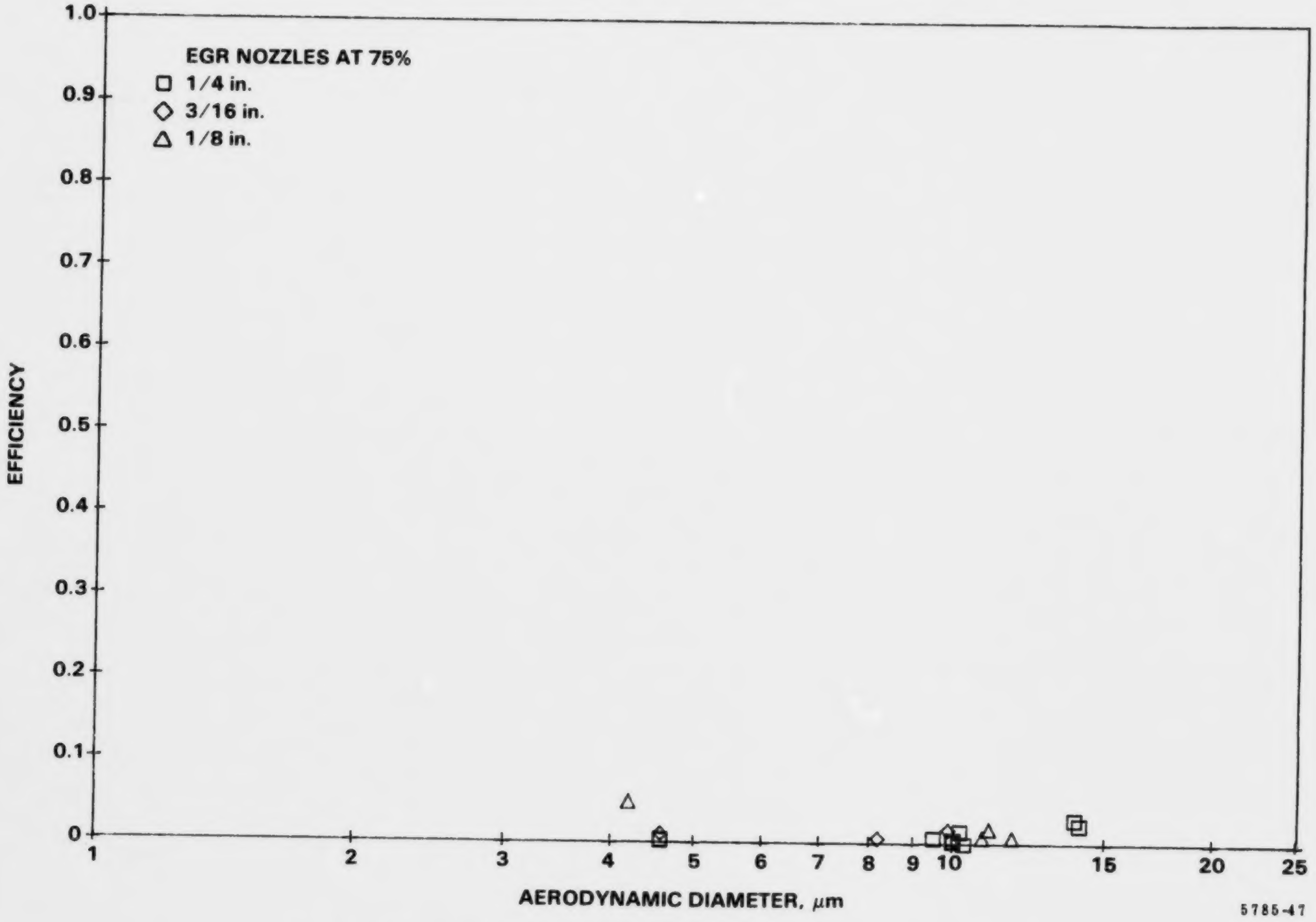

Figure 6-27. Collection efficiencies of EGR nozzles at 75% recycle rate.

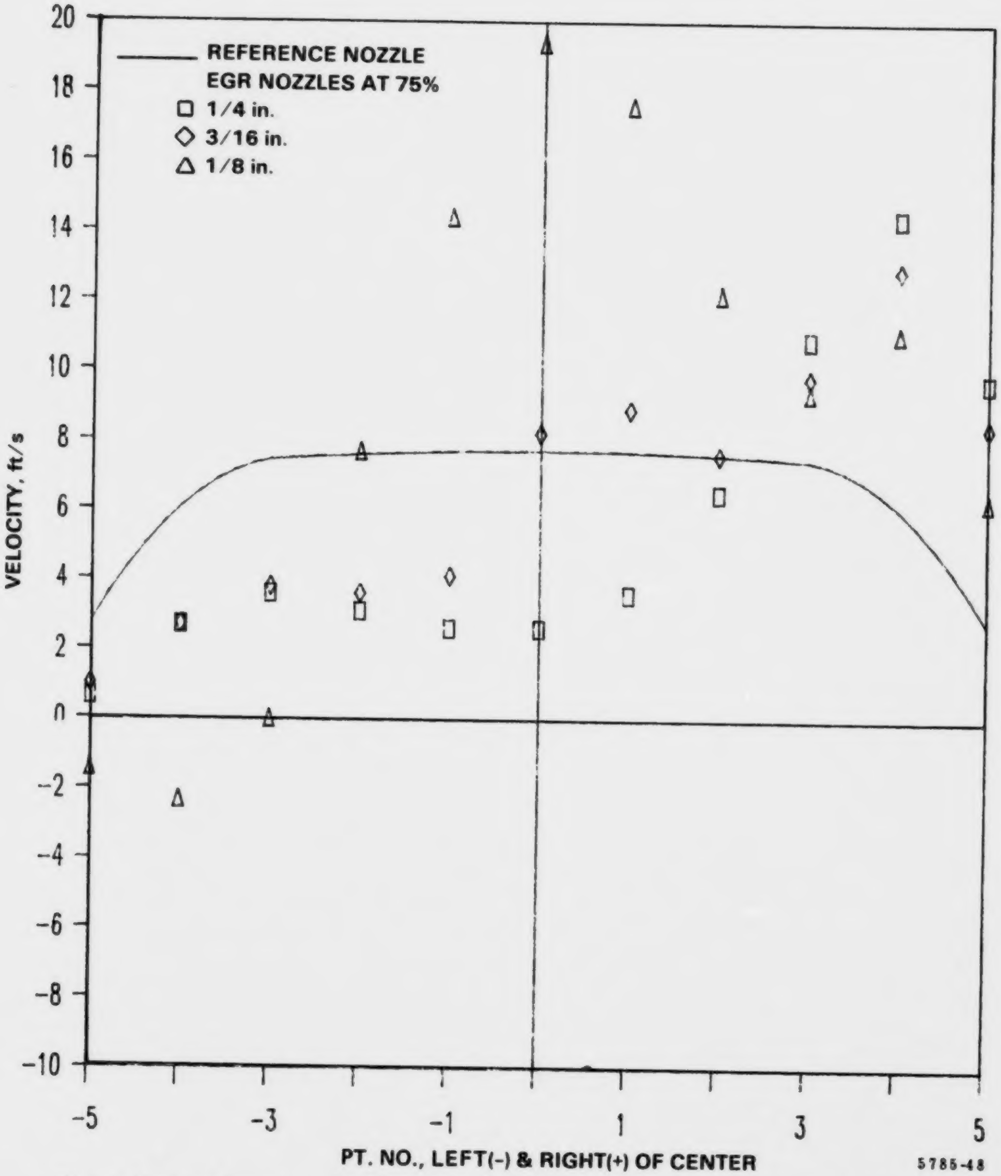

Figure 6-28. Velocity profiles at exit of EGR nozzles at 75% recycle rate and reference nozzle (1/2 in.).

skewed for all of the EGR nozzles, probably because of nonuniform mixing of the recycle gas. This is a clear indication that the design expectations of uniform annular recycle flow are not met. At this recycle rate, peak velocity monotonically increases in the expected manner as the nozzle size decreases.

Modifications of Nozzles

Further measurements were performed to test approaches for eliminating the observed shift in cyclone cut size at the higher nozzle inlet velocities. The results obtained with the original nozzles indicated that the inertia of the higher velocity aerosol streams was not dissipated sufficiently to prevent impaction in the cyclone. Therefore, modifications were tested which appeared likely to reduce the sample gas velocity prior to entering the cyclone.

Two types of nonrecycle nozzles were tested. One group had large expansion angles, while the other group had small expansion angles, 7° and 14°. Figure 6-29 shows geometries of 1/8-in. nozzles with large expansion angles compared to that of the EGR nozzle. One was made initially by installing a cap over the standard 1/2-in. nozzle. Sampling a monodisperse aerosol with it gave a lower collection efficiency for 8-μm particles than with the 1/8-in. EGR nozzle at 0% recycle or with the 0.138-in. nonrecycle nozzle. Thus, the two longer nozzles in Figure 6-29 were also fabricated and tested.

Figure 6-30 shows the geometries of tapered nozzles tested, compared with nozzles having larger expansion angles and the same inlet diameters, 0.16 in. and 1/8 in. The 7° and 14° nozzles were cast with epoxy to reduce cost of fabrication. To ensure that effects of particle charge were not present, conducting paint was applied. An ohmmeter was used to verify that the nozzle tip was at the same potential as the cyclone.

Two types of modifications to EGR nozzles were tested. One was to simply extend them further from the cyclone inlet as indicated in Figure 6-31. The other geometry tested is illustrated in Figure 6-32. This approach was an attempt to use the recycle gas to disrupt the sample gas stream within a short distance. The recycle gas was pumped through a small gap at high velocity. Measurement of velocity profiles for this nozzle indicated that the desired disruption could not be achieved at reasonable pressures for the recycle gas. Thus cyclone sampling with this modified nozzle was not performed. The dimensions of the nozzles in Figures 6-29 to 6-31 are listed in Table 6-2.

Results With Modified Nozzles

Extending Nonrecycle Nozzles With Large Expansion Angles--

Figure 6-33 gives measured cyclone efficiencies with the 1/8-in. nozzles having large expansion angles, shown in Figures 6-29 and 6-31, including the EGR nozzle at 0% recycle rate. The cyclone efficiencies decreased to that with the reference nozzle when the expansion distance was 2.2 in. and greater.

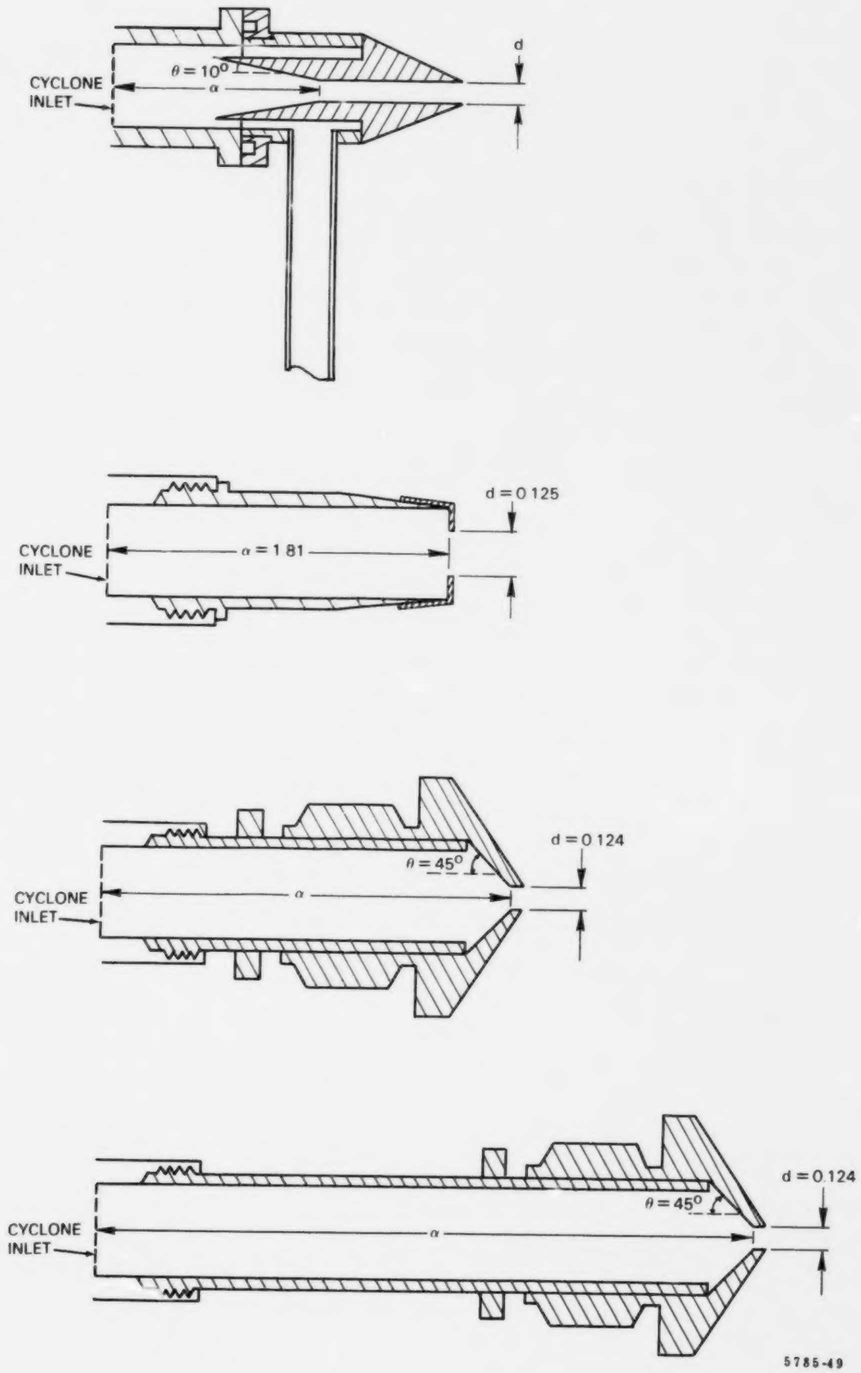
d
CYCLONE INLET
θ = 10°
α
d = 0.125
CYCLONE INLET
α = 1.81
d = 0.124
θ = 45°
CYCLONE INLET
α
d = 0.124
θ = 45°
CYCLONE INLET
α
5785-49

Figure 6-29. Geometries of 1/8-in. nozzles with large expansion angles and varying lengths.

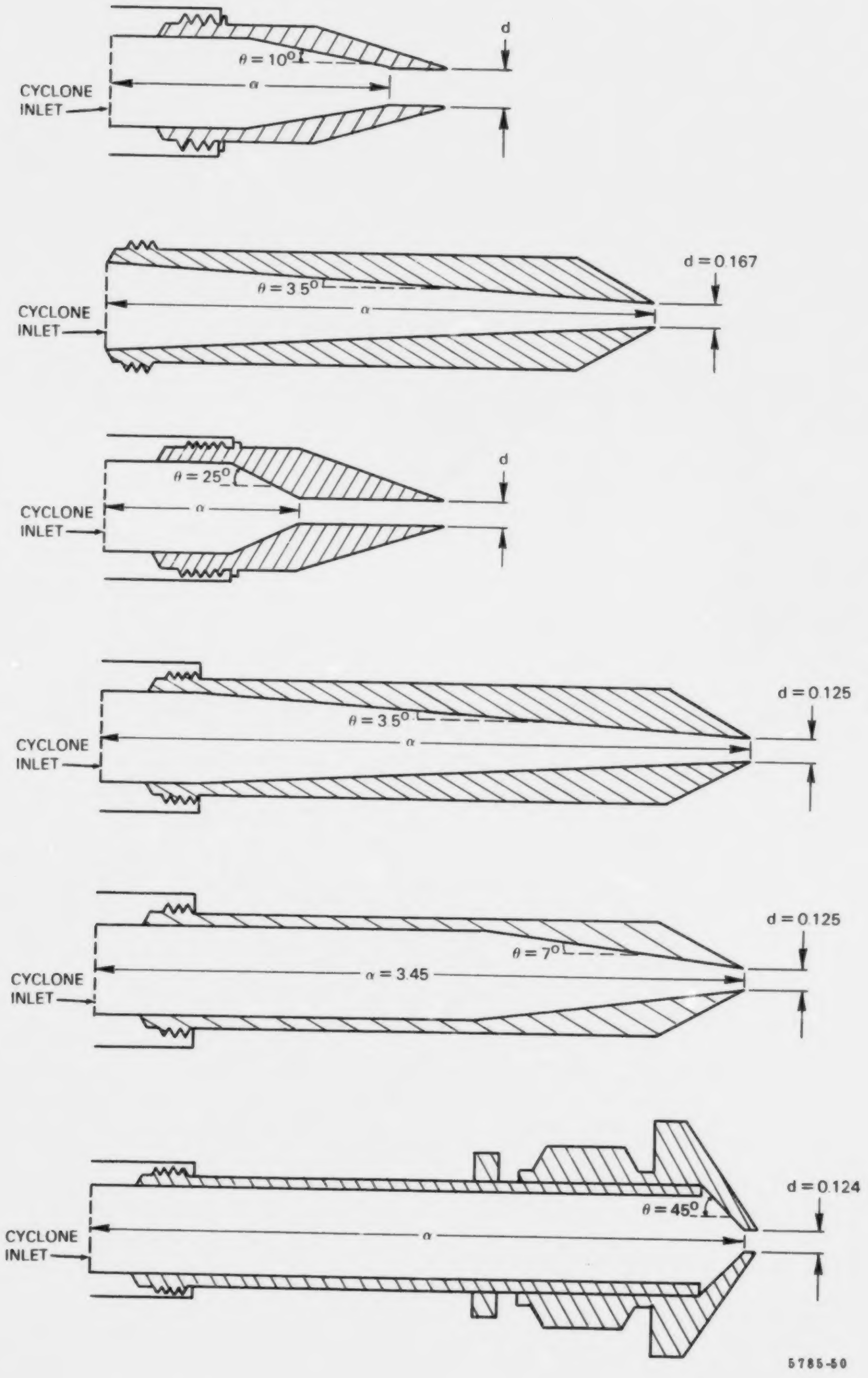
d
θ = 10°
α
CYCLONE INLET
d = 0.167
θ = 3.5°
α
CYCLONE INLET
d
θ = 25°
α
CYCLONE INLET
d = 0.125
θ = 3.5°
α
CYCLONE INLET
d = 0.125
θ = 7°
α = 3.45
CYCLONE INLET
d = 0.124
θ = 45°
α
CYCLONE INLET
5785-50

Figure 6-30. Comparison of geometries of nozzles with small or large expansion angle.

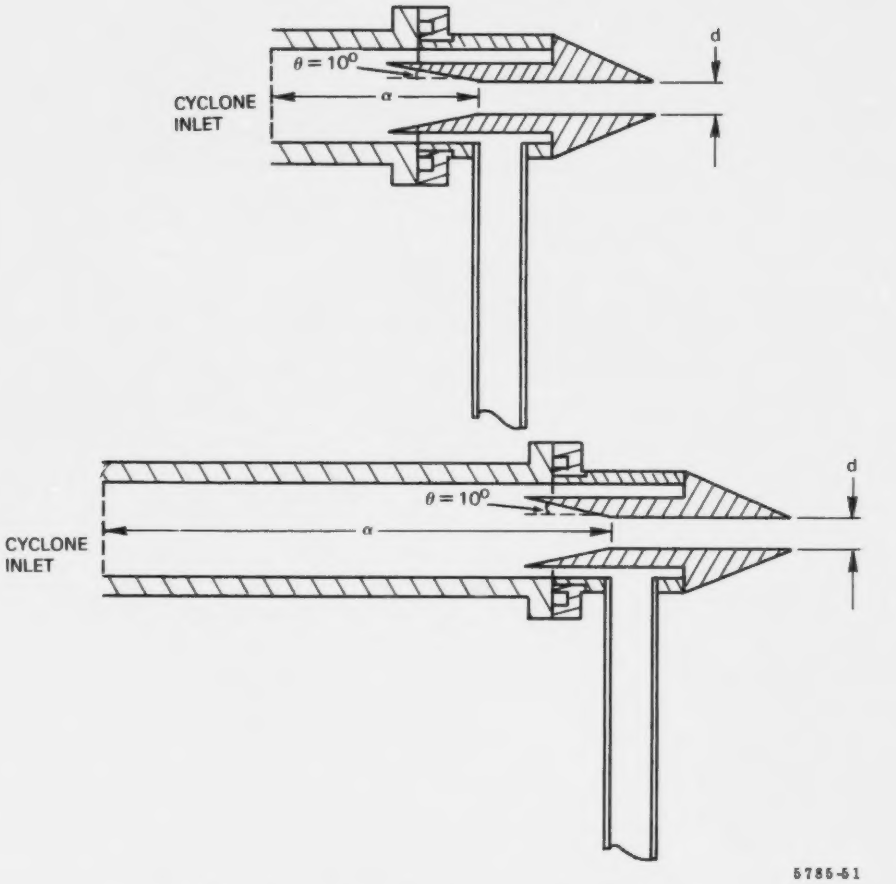
d
θ = 10°
CYCLONE INLET
α
d
θ = 10°
CYCLONE INLET
α
5785-51

Figure 6-31. Geometries of recycle nozzles with and without extensions.

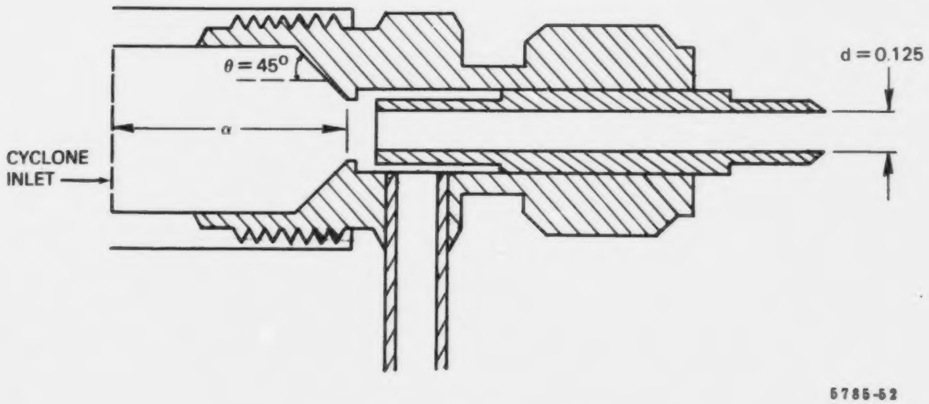
θ = 45°
d = 0.125
α
CYCLONE INLET
5785-52

Figure 6-32. EGR shear nozzle.

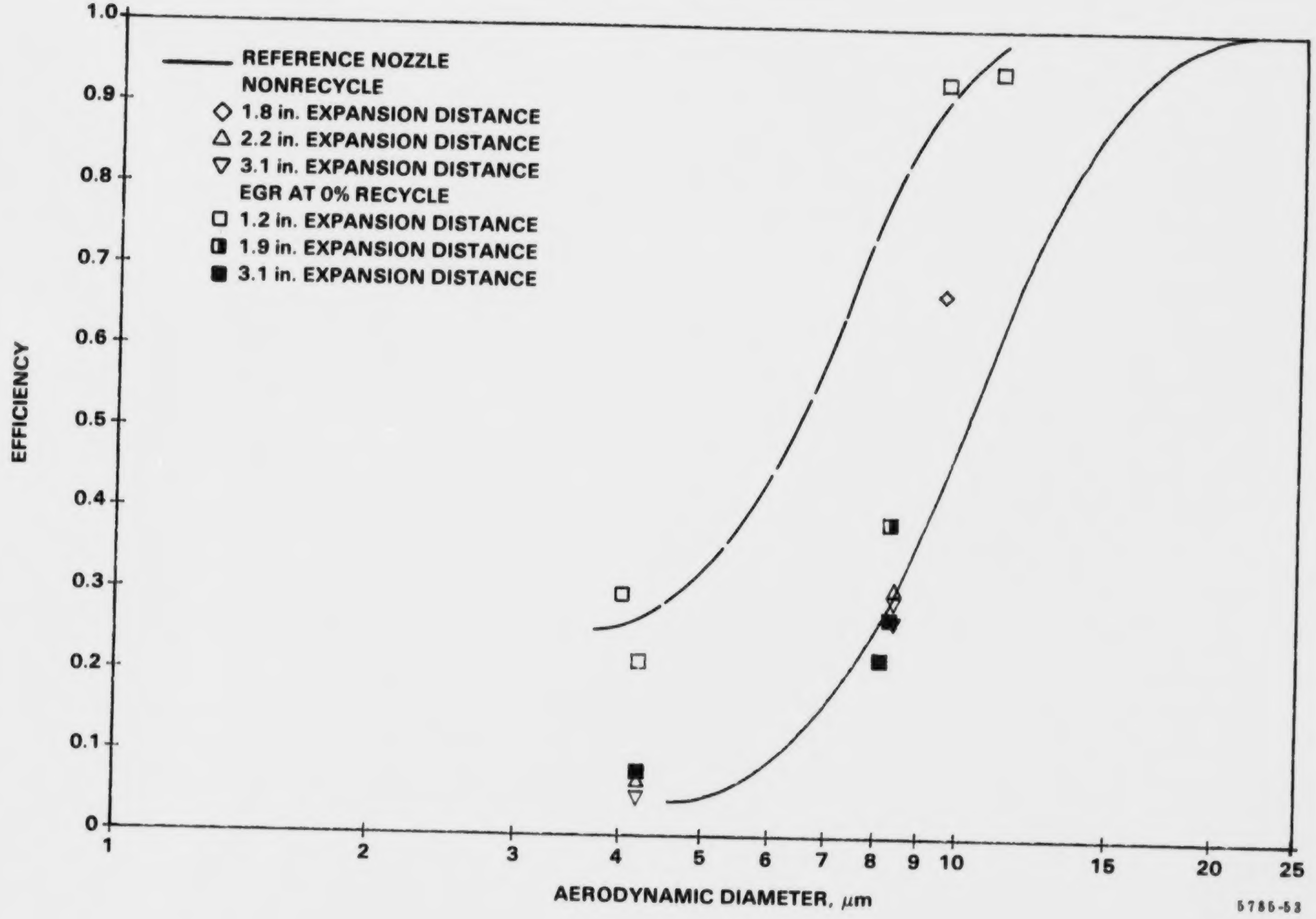

Figure 6-33. Collection efficiencies of Cyclone I with 1/8-in. nozzles having large expansion angles and different lengths and with reference nozzle (1/2 in.). See Figure 6-29 for nozzle geometries.

TABLE 6-2. DIMENSIONS OF MODIFIED NOZZLES TESTED

Nozzle I.D.	Inlet Diameter, Inches	Expansion Angle, Degrees	Expansion Length, Inches	Straight Length at Inlet, Inches
EGR nozzles:				
1-1.60	0.117	20	1.22	0.38
1-2.29	0.117	20	1.91	0.38
1-3.48	0.117	20	3.10	0.38
2-1.60	0.188	20	1.02	0.58
2-2.29	0.188	20	1.71	0.58
2-3.48	0.188	20	2.90	0.58
3-1.60	0.250	20	0.84	0.76
3-2.29	0.250	20	1.53	0.76
3-3.48	0.250	20	2.72	0.76
Cap	0.125	180	1.79	0
Abrupt- 2.23	0.124	90	2.20	0.0313
Abrupt- 3.14	0.124	90	3.11	0.0313
7° - 2.70	0.167	7°	2.70	0
7° - 3.22	0.127	7°	3.22	0
14° - 3.15	0.127	14°	3.15	0

Figure 6-34 presents the nozzle efficiencies corresponding to Figure 6-33. These modified nozzles had substantially higher nozzle losses than the unextended EGR nozzles. Of the nonrecycle nozzles which did not affect cyclone behavior (2.2- and 3.1-in. expansion distance) the shorter one exhibited lower nozzle loss at 8 μm. The extended EGR nozzle with expansion distance of 3.1 (which did not affect cyclone behavior) exhibited nozzle losses of 20% at 4 μm and 35% at 8 μm. Apparently, the initial smaller expansion angle of the EGR nozzle contributed to reduction of nozzle loss.

Figure 6-35 presents the velocity profiles for these nozzles. The differences between the velocity profile of a given nozzle and that for the reference nozzle correlates very closely with the corresponding differences in cyclone efficiency.

Tapered Nozzles--

Figure 6-36 presents measured cyclone efficiency for the tapered nozzles compared to nozzles having large expansion angles and the same inlet diameter. Original nozzles (0.235 in. and 0.195 in.) with small expansion angles are included in this figure with the modified tapered nozzles. Looking first at the 0.16-in. nozzle (with 7° angle) and the 0.154-in. nozzle (with 50° angle), one sees that the effect on cyclone behavior exhibited by the original nozzle is absent with the modified 7° nozzle. Cyclone behavior was not affected by any of the three 1/8-in. nozzles, one

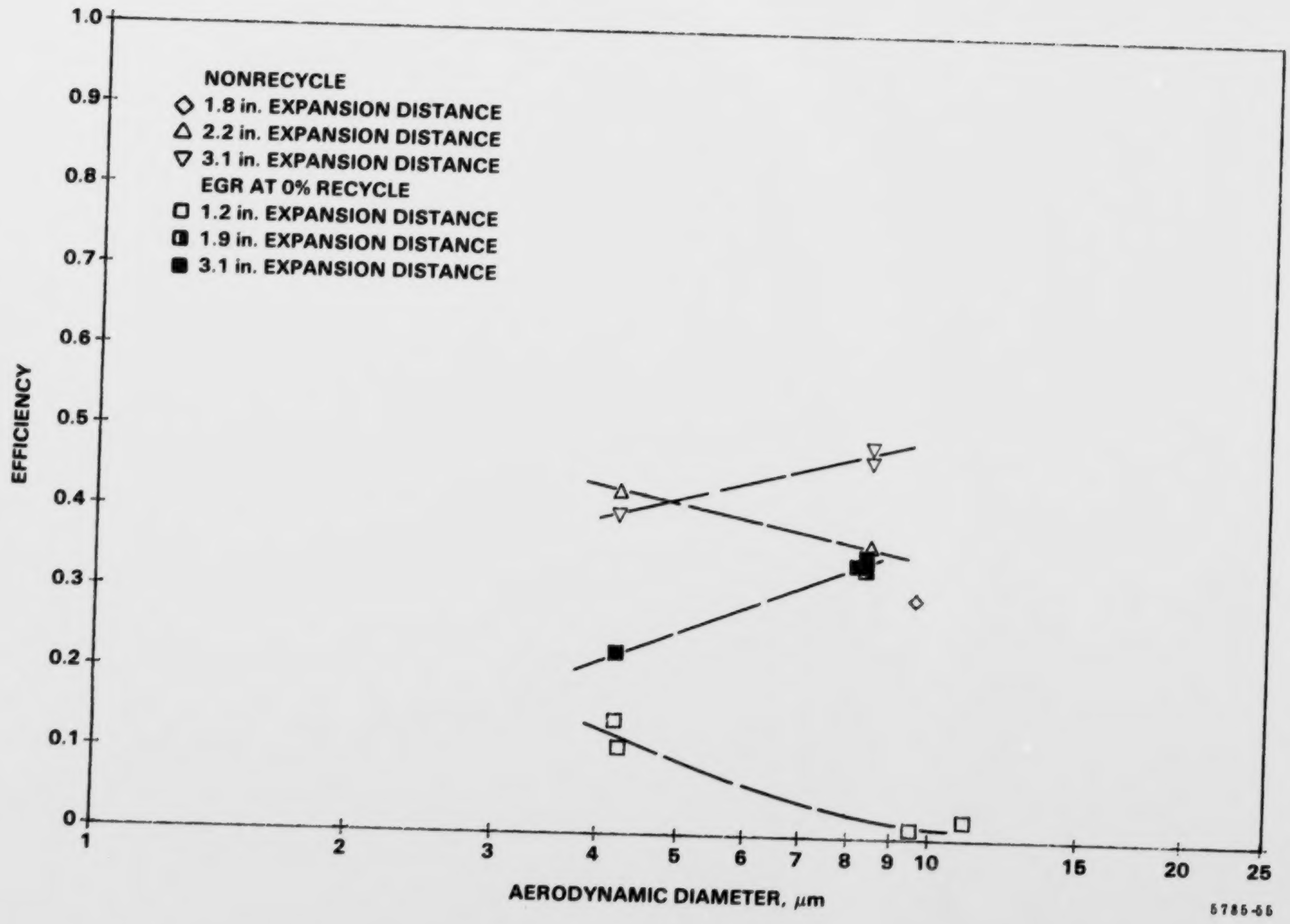

Figure 6-34. *Collection efficiencies of 1/8-in. nozzles having large expansion angles and different lengths. See Figure 6-29 for nozzle geometries.*

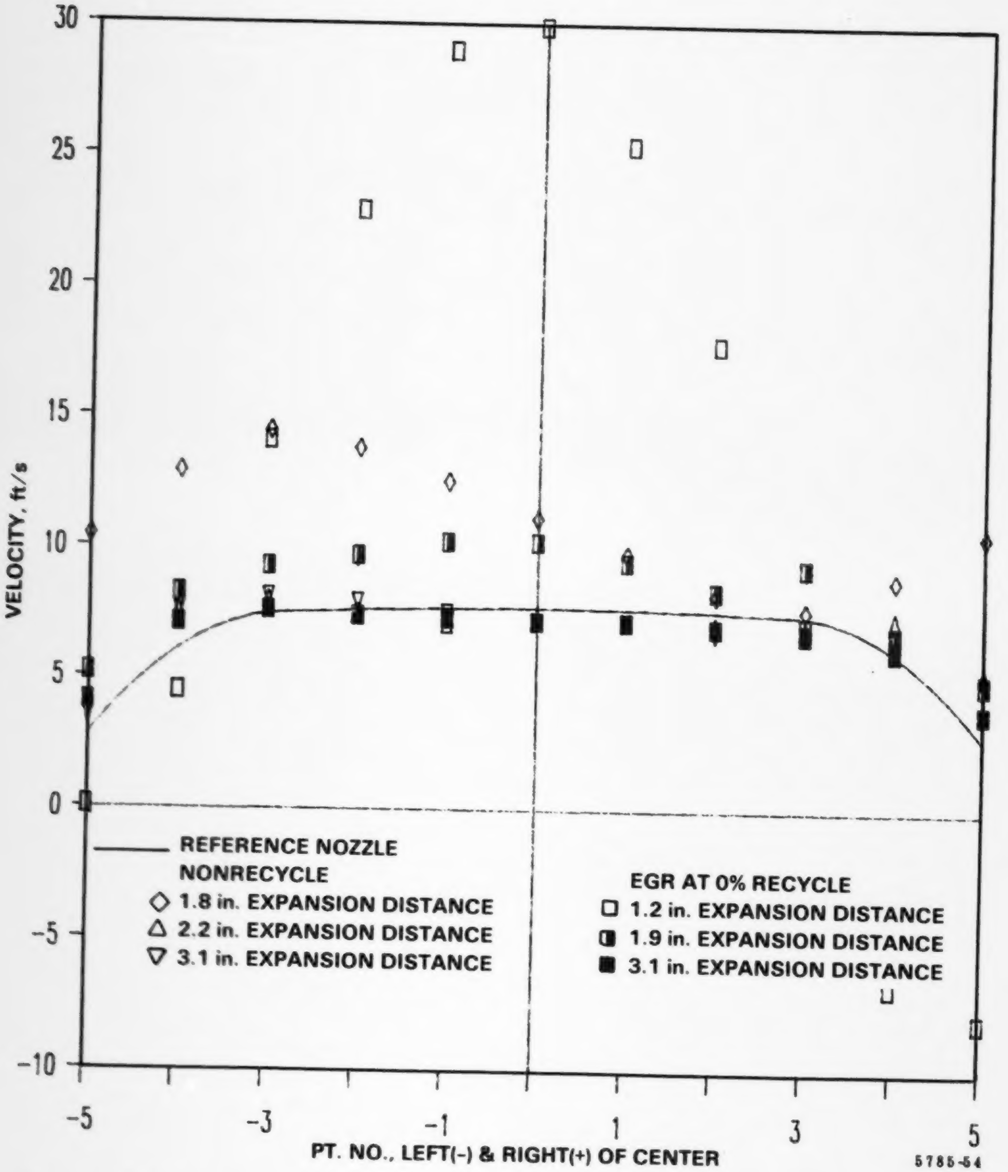

Figure 6-35. Velocity profiles at exit of 1/8-in. nozzles having large expansion angles and different lengths. See Figure 6-29 for nozzle geometries.

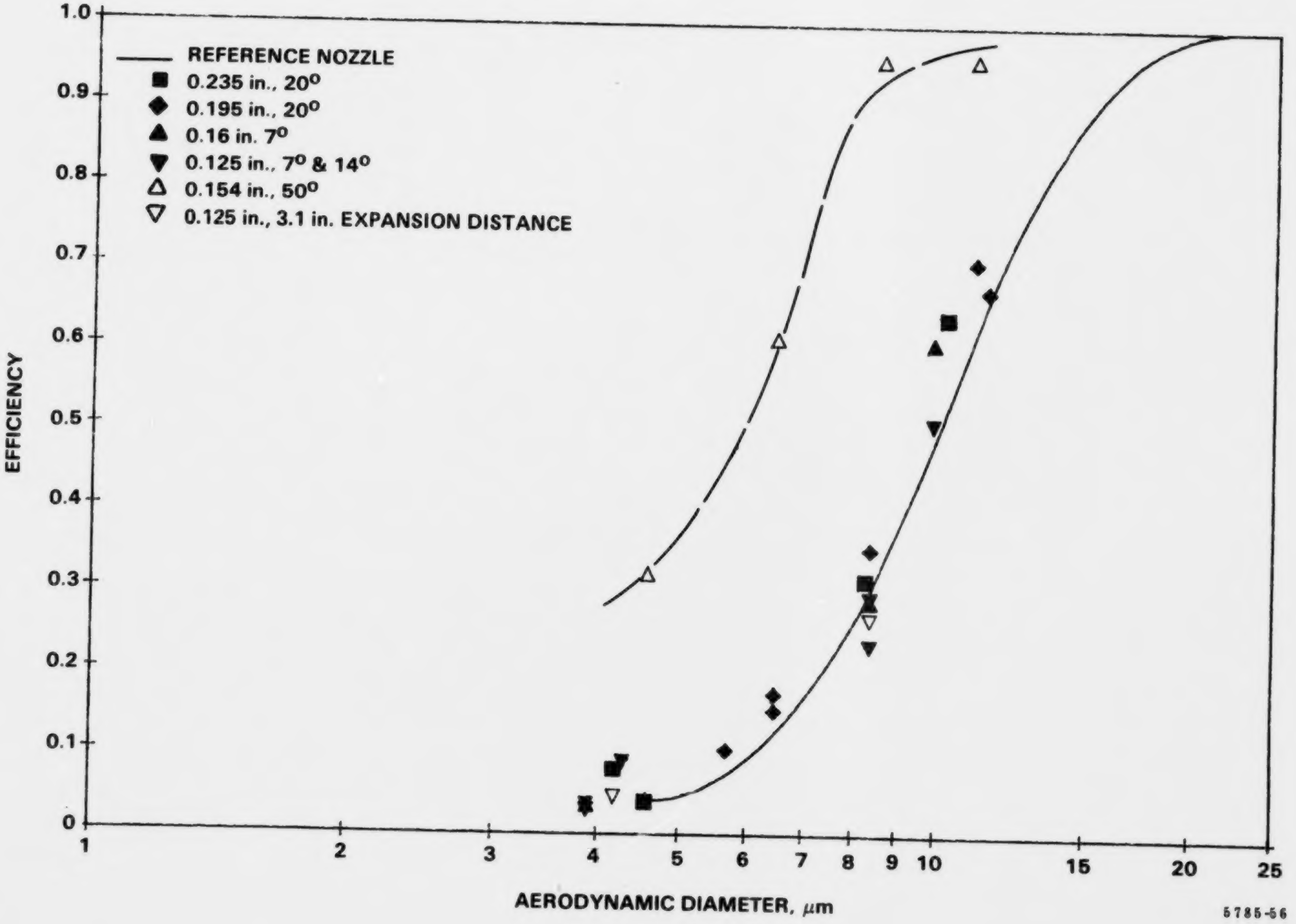

Figure 6-36. Collection efficiencies of Cyclone I with nozzles having large or small expansion angle and reference nozzle (1/2 in.). See Figure 6-30 for nozzle geometries.

with an expansion distance of 3.1 in. and an abrupt expansion and the other two with expansion distance of 3.2 in. and tapered at 7° and 14°, respectively.

Figure 6-37 presents nozzle losses corresponding to cyclone efficiencies in the preceding figure. Looking first at the 0.16-in. and 0.154-in. nozzle, one sees that the tapered nozzle (which does not affect cyclone behavior) exhibited about 5% higher nozzle loss. This 0.16-in. tapered (7°) nozzle had losses about 5% lower than the 0.235-in. nozzle with a 20° expansion angle. Of the three 1/8-in. nozzles (7° and 14° compared to 90° expansion angles), the tapered nozzles had 10% to 15% lower losses (30% compared to 45%).

It should be noted that the data for the tapered 1/8-in. nozzles (with 7° and 14° expansion angles) are presented in combined form for simplicity and because they nearly coincide. A difference which was considered as potentially significant was observed in the nozzle losses for 3.9 µm particles. In Figure 6-37 the higher value of 36% was obtained with the 14° nozzle while the lower value of 24% was obtained with the 7° nozzle. It was concluded that this difference was of little importance because of the observations at 4.3 µm and 8.4 µm particle size. These were 29% with the 14° nozzle (at 4.3 µm) and 34% for both the 7° and 14° nozzles (at 8.4 µm).

Figure 6-38 presents velocity profiles for these nozzles. As one might expect from the preceding data, all of the profiles are near that of the reference nozzle except for the 0.154-in. nozzle, which has a shorter expansion distance (1.05 in.).

Extended Recycle (EGR) Nozzles Varying Recycle Rate--

Figure 6-39 compares cyclone efficiencies for EGR nozzles with and without an extension. The expansion distance without extension was 1.2 in. and 3.1 in. with the extension. For all of these conditions the extension eliminated the effect of the nozzle on the cyclone.

Nozzle losses for these nozzles are given in Figure 6-40. The losses were higher in each instance with the extension. The highest losses were with the 1/8-in. nozzle at 10% recycle rates. These losses correlate closely with sample stream velocity, increasing as stream velocity increased (decreasing recycle rate).

Figure 6-41 presents velocity profiles with these nozzles. As expected from preceding data, all of the profiles with nozzle extensions had profiles close to that of the reference nozzle.

CONCLUSIONS RELATIVE TO LABORATORY DATA

The laboratory data obtained in this PM_{10} program have major importance for PM_{10} methods in two ways. They establish a basis for using Cyclone I as a PM_{10} size separator for a wide range of operating conditions. Also, they establish the existence of, and point to a solution for, a significant effect of existing sampling nozzles upon cyclone behavior, although the

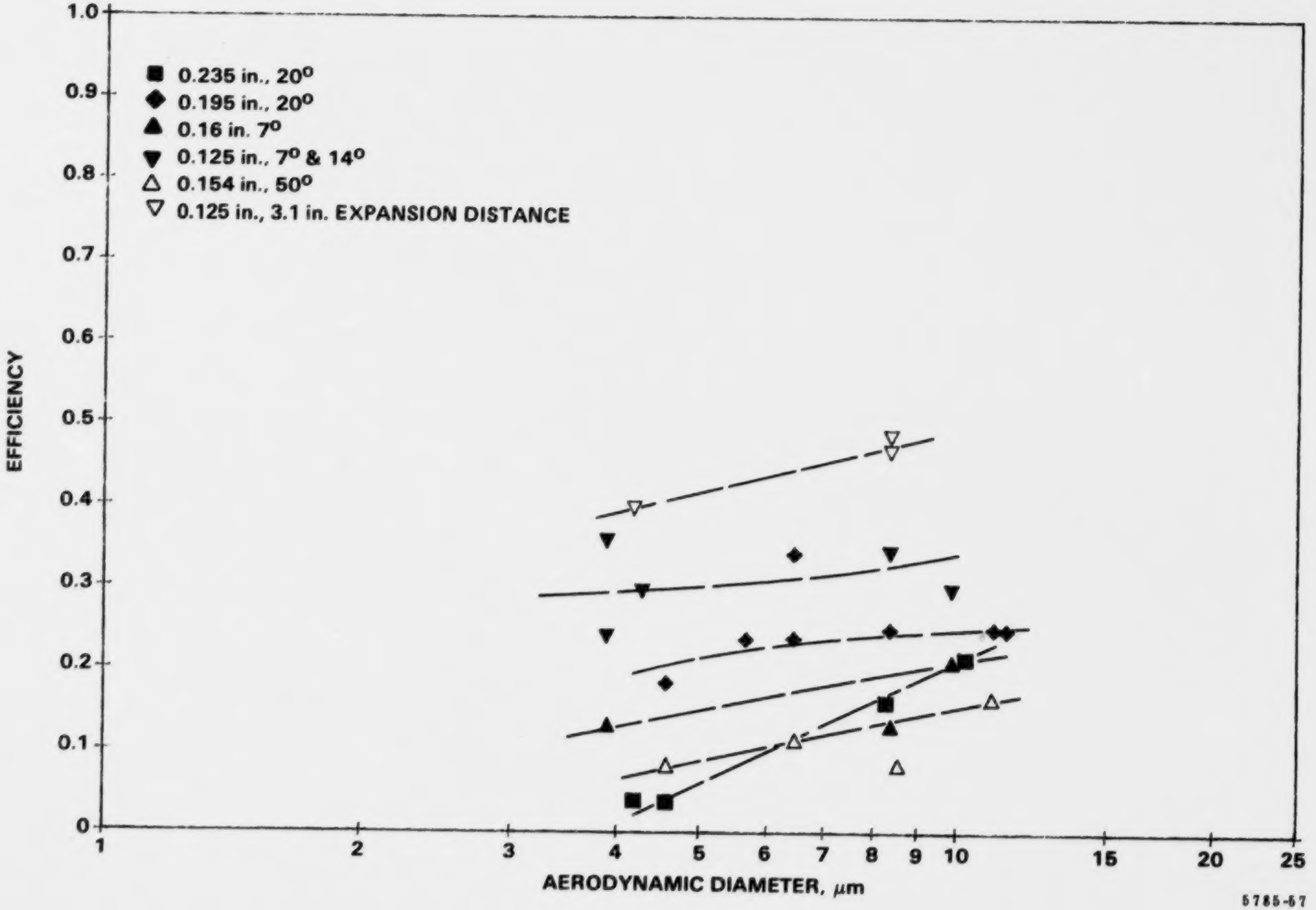

Figure 6-37. Collection efficiencies of nozzles having large or small expansion angle. See Figure 6-30 for nozzle geometries.

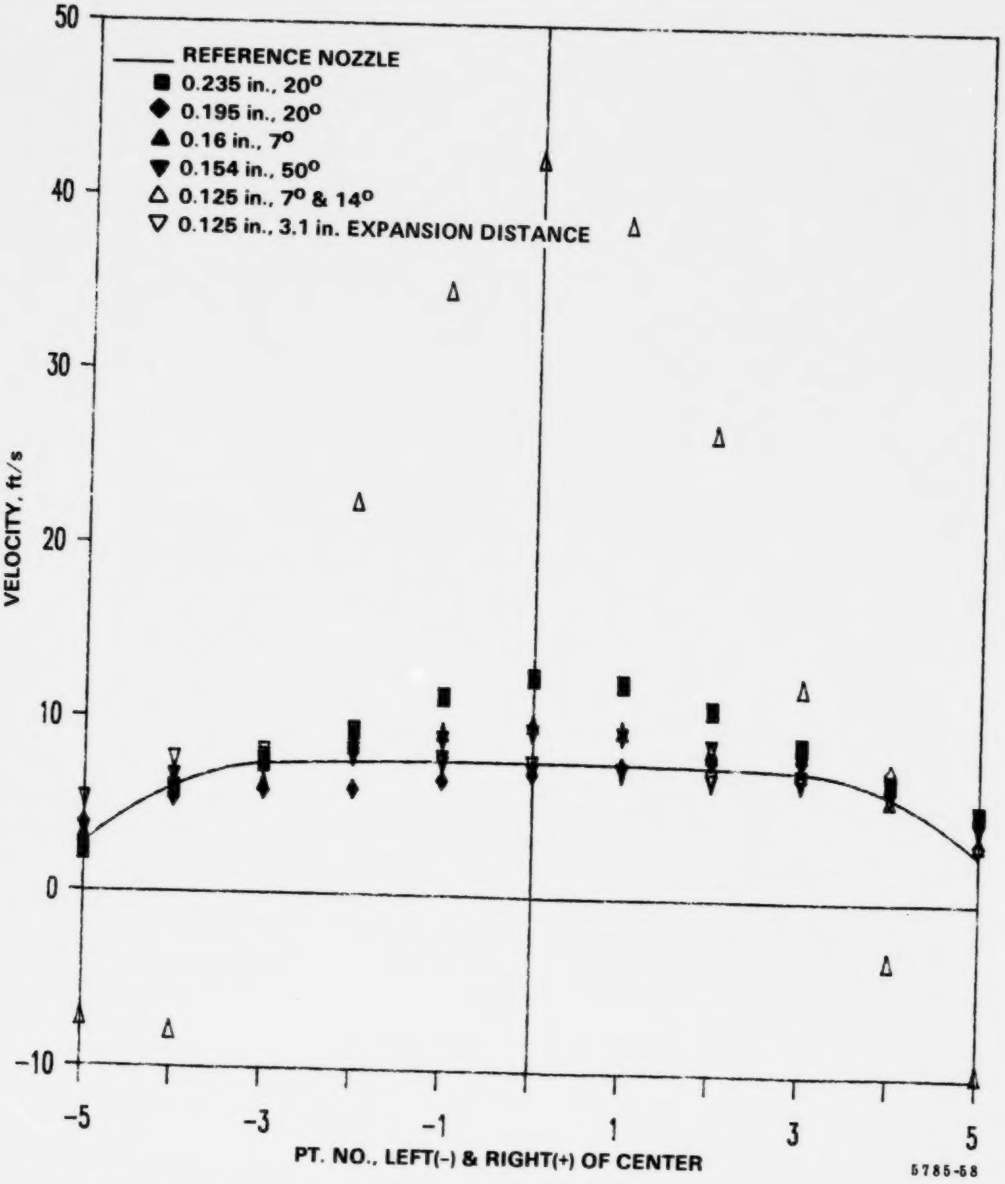

Figure 6-38. Velocity profiles at exit of nozzles having large or small expansion angle and reference nozzle (1/2 in.). See Figure 6-30 for nozzle geometries.

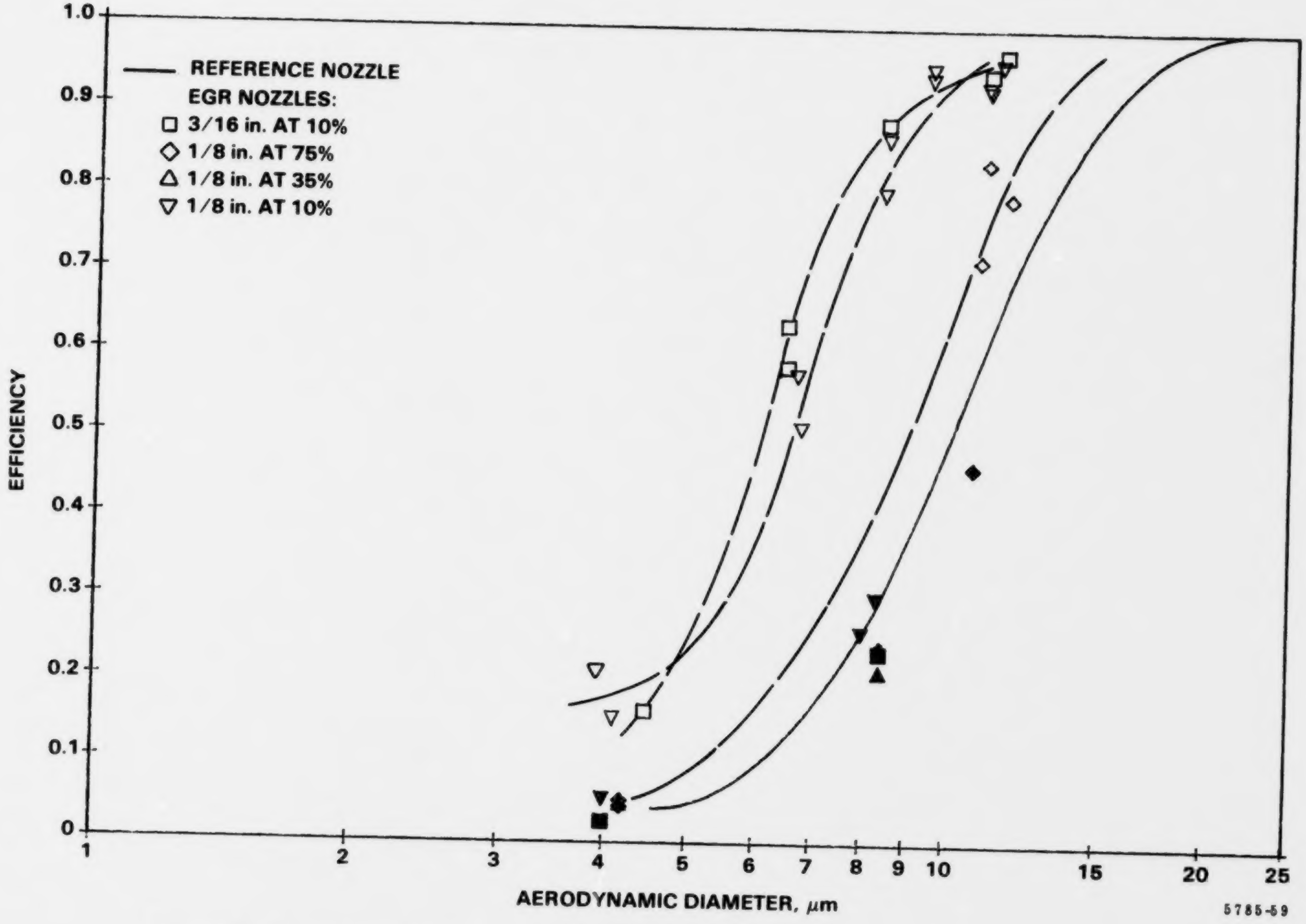

Figure 6-39. *Collection efficiencies of Cyclone I with EGR nozzles of different lengths and reference nozzle (1/2 in.). Solid symbols denote long expansion distance for flow, while open symbols denote short expansion distance.*

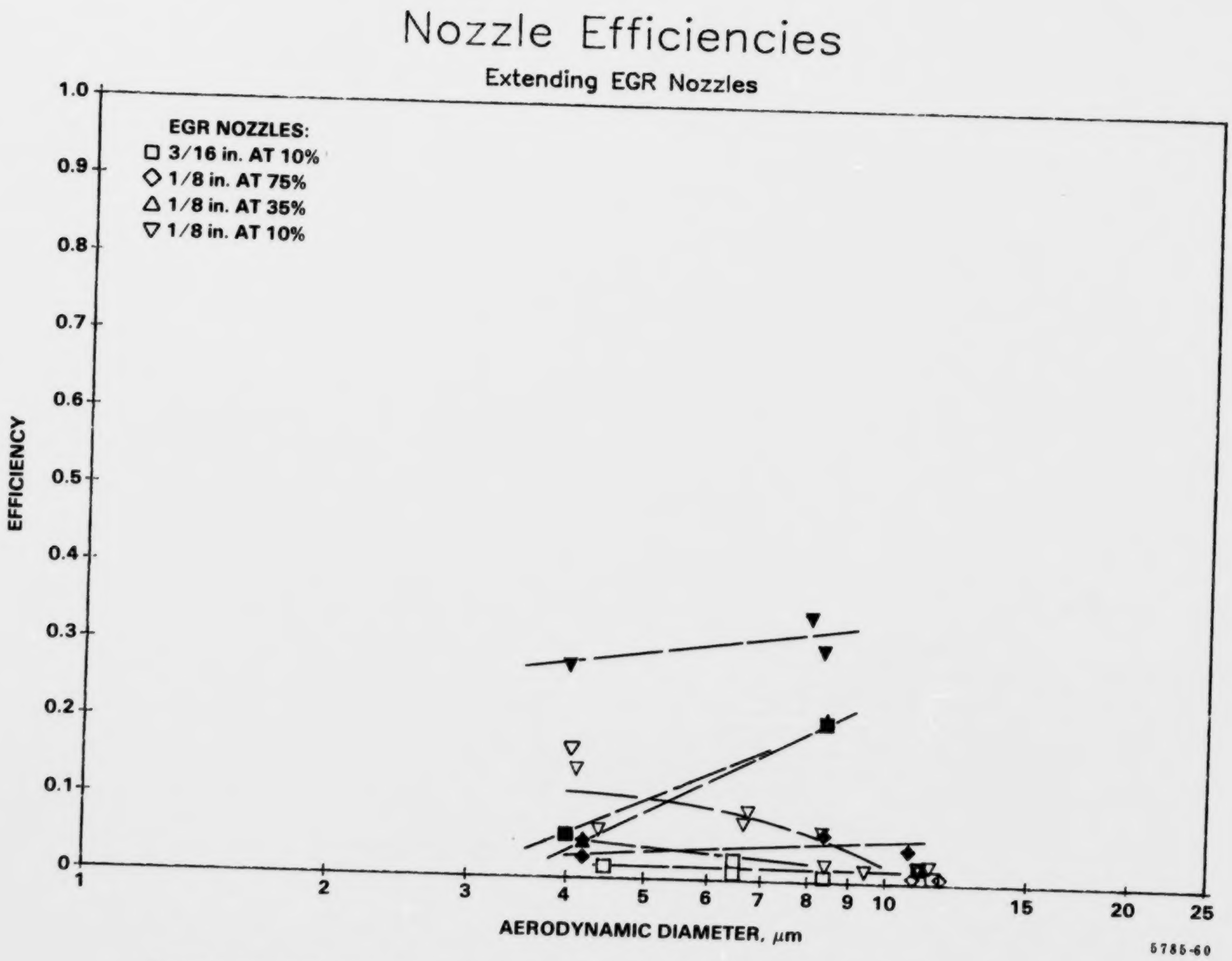

Figure 6-40. *Collection efficiencies of EGR nozzles of different lengths. Solid symbols denote long expansion distance for flow, while open symbols denote short expansion distance.*

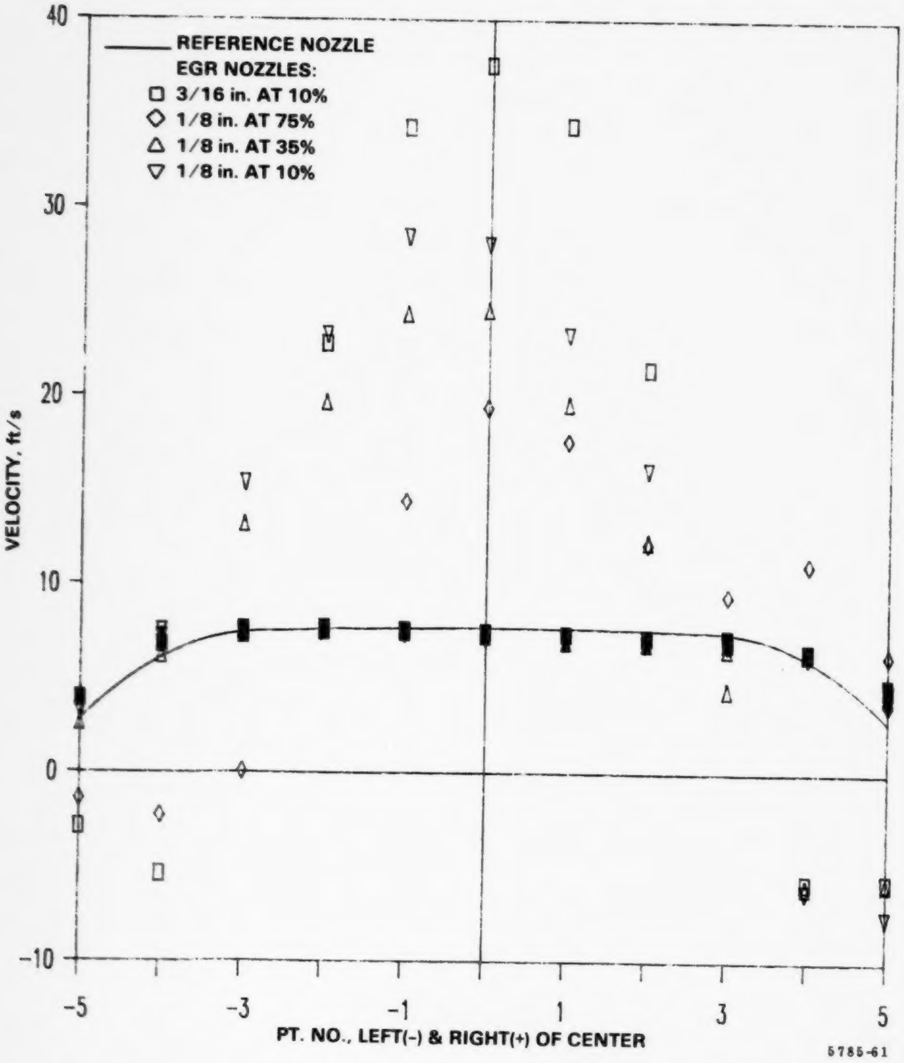

Figure 6-41. Velocity profiles at exit of EGR nozzles of different lengths and reference nozzle (1/2 in.). Solid symbols denote long expansion distance flow, while open symbols denote short expansion distance.

current solution is probably not the optimum one. It is believed that a similar nozzle effect occurs to some degree in all sizing devices used in process streams.

The basis for using Cyclone I as the PM_{10} separator is represented by Figures 6-6, 6-7, and 6-9. The efficiency curve for Cyclone I in Figure 6-7 (D_{50} = 10 μm) has a geometric standard deviation of 1.4. Although this may increase (slope decrease) at elevated temperature (lower Re), it is expected to retain sufficient sharpness of cut to be acceptable. The method of characterizing cyclone behavior depicted by Figure 6-9 is relatively new, but the simplification of cyclone data and similarity to impactor behavior impart significant confidence to it. Only a few additional checks of its validity at elevated temperatures with 10-μm particles would abate any doubts.

The observed effect of small nozzles on behavior was a shift in cut point from 10 μm to as low as 6 μm, the shift generally decreasing as nozzle inlet velocity decreased. This effect would cause measured PM_{10} to be lower than actual concentration to a degree which depends upon the aerosol size distribution. To illustrate the error incurred by this shift, one may consider a lognormal size distribution with geometric standard deviation of 2 and an MMD of 10 μm. At conditions in which the cyclone D_{50} was 6 μm (small nozzles with efficiencies such as shown in Figure 6-13), the cyclone would collect 76% and pass 24% of the particulate mass instead of the true PM_{10} portion, 50%. The resulting error in PM_{10} concentration would then be 52%. The error would be less for a lognormal distribution with smaller MMD or larger σ_g and more for a larger MMD or smaller σ_g.

The cause of the shift in D_{50} associated with some nozzles was found to be high inertia associated with high-velocity gas streams. The shift in D_{50} was found throughout the data to correlate closely with the velocity of the gas entering the nozzle. A comprehensive description of the collection of particles in cyclones is beyond the scope of this study. However, it is obvious from the velocity profiles, such as those in Figure 6-15, that localized values of the impaction parameter, $\sqrt{Stk}$, near the center of the inlet, were a factor of 2 to 3 higher with small nozzles than with the reference nozzle (0.5 in.). Thus impaction in the cyclone was enhanced by the higher gas velocities entering the cyclone.

Obviously, this problem is eliminated by causing the sample gas to decelerate after entering the nozzle. Extending the nozzle inlet farther from the cyclone inlet regained the basic cyclone performance. However, nozzle losses were enhanced in most instances. This is illustrated in Figure 6-42, where averages of observed nozzle losses are plotted versus nozzle inlet velocity for different groups of nozzles. One group is the original nozzles which affected cyclone behavior. These nozzle losses are less than 10% except for the 0.155-in. and 0.138-in. nozzles (shown as open triangles at 58 and 76 ft/s in Figure 6-42), which had abrupt expansion from the inlet diameter to the 0.5-in. exit diameter. The other data in this figure show losses for nozzles of several geometries which did not affect cyclone behavior. The lowest losses occurred for tapered nozzles with

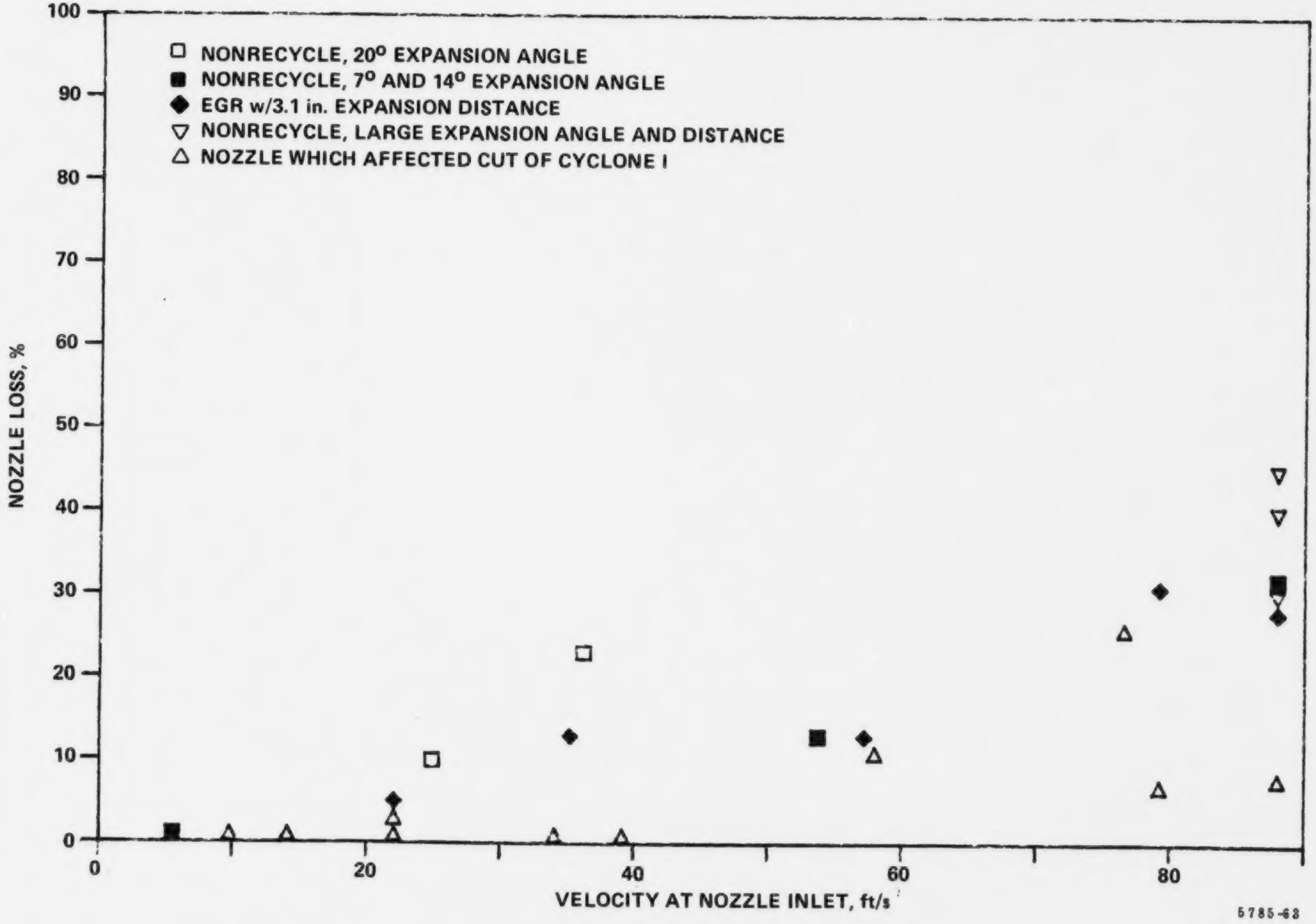

Figure 6-42. Summary of nozzle losses.

expansion angles of 7° or 14°. These differences in losses between nozzle geometries were probably caused by flow separation accompanied by a region of flow recirculation with the larger expansion angles.

These laboratory data clearly show that both nonrecycle and recycle nozzles for Cyclone I should be redesigned with a smooth taper from the nozzle inlet diameter to the 0.5-in. diameter of the cyclone inlet. It appears that modifications of the EGR nozzle should also include enlarging the inside diameter of the annulus, through which recycle gas flows, so that the recycle gas will have a higher average velocity but more uniform velocity profile.

This limited investigation of nozzle modifications used nozzles whose lengths at high stream velocities would require ports larger than 4 in. The data obtained for geometries tested thus far indicate that nozzle losses will be significant for small nozzles or high stream velocities. Average losses for particle diameters within the range studied here (4 to 10 μm) would increase from about 1% at 5 ft/s, to 13% between 30 and 60 ft/s, to 30% at 88 ft/s (see Figure 6-42, closed symbols). Note that these velocities relate to this laboratory study in which the PM_{10} flow rate (for Cyclone I) was 0.45 acfm. The PM_{10} flow rate, and the corresponding nozzle velocities, is typically 20 to 30% higher in field measurements. These losses may not be avoidable. However, sufficient information for that conclusion is not currently available. With the commercial version of Cyclone I, the available distance between the nozzle inlet and the cyclone inlet is 1.67 in., leaving 1/4 in. tolerance between the nozzle tip and the wall of a 4-in. port. With an 1/8-in. nozzle, this distance would permit a maximum expansion angle of 12.8°. The original (SRI/EPA) version of Cyclone I permitted a distance of 1.94 in. between the nozzle inlet and the cyclone inlet. This distance would permit an expansion angle of 11.0°. It is not clear from the laboratory data obtained thus far whether or not 12.8° or 11.0° would be sufficiently small to preserve basic cyclone performance. The geometry of the 14° nozzle tested was not optimum (not short enough to fit through a 4-in. port).

REFERENCES

Beeckmans, J. M. 1979. "Analysis of the Cyclone As A Size Selective Aerosol Sampler." In: Aerosol Measurement, D. A. Lundgren, et al., eds. University Presses of Florida, Gainesville, FL. pp. 56-69.

Belyaev, S. P. and L. M. Levin. 1974. "Techniques for Collection of Representative Aerosol Samples." J. Aerosol Sci. 5(4):325.

Berglund, R. N., and R. Y. H. Liu. 1973. "Generation of Monodisperse Aerosol Standards." Environ. Sci. Technol., 7(2):147-153.

Blake, D. E. 1978. Source Assessment Sampling System: Design and Development. EPA-600/7-78-018, U.S. Environmental Protection Agency, Research Triangle Park, NC.

Cushing, K. M., G. E. Lacey, J. D. McCain, and W. B. Smith. 1976. "Particulate Sizing Techniques for Control Device Evaluation: Cascade Impactor Calibrations." EPA-600/2-76-280, U.S. Environmental Protection Agency, Research Triangle Park, NC.

Dixon, W. J. 1953. "Processing Data for Outliers." Biometrics 9(1):74-89.

Durham, M. D. 1978. "Isokinetic Sampling of Aerosols from Tangential Flow Streams." Ph.D. Thesis, University of Florida, Gainesville. 140 pp.

Farthing, W. E. 1983. "Evaluation and Recommendations of Protocols for PM_{10} in Process Streams: Recommended Methods; Volume I." SoRI-EAS-83-1038. Southern Research Institute, Birmingham, AL. 72 pp.

Farthing, W. E., and A. D. Williamson. 1985. "A Unified View of Inertial Impactors and Cyclones." Paper #7 presented at 1985 Annual Meeting of AAAR, Albuquerque, NM.

Farthing, W. E., A. D. Williamson, J. D. McCain, and T. E. Ward. 1985. "Evaluation of Protocols for Size-Specific Emission Measurements." Paper 85-14.3, 78th Annual Meeting, Air Pollution Control Association, Detroit, MI.

Farthing, W. E., R. S. Martin, S. S. Dawes, and A. D. Williamson. 1988. PM_{10} Source Measurement Methodology: Field Studies. EPA-600/3-88-055, Southern Research Institute, Birmingham, AL.

Farthing, W. E., A. D. Williamson, S. S. Dawes, R. S. Martin, and J. W. Ragland. 1986. Investigation of Source Emission PM_{10} Particulate Matter Field Studies of Candidate Methods. EPA 600/4-86-042. U.S. Environmental Protection Agency, Research Triangle Park, NC, 137 pp.

Farthing, W. E. and S. S. Dawes. 1988. Application Guide for Source PM_{10} Measurement with Constant Sampling Rate. EPA-600/3-88-057, U. S. Environmental Protection Agency, Research Triangle Park, NC. 75 pp.

Grubbs, F. E., and G. Beck. 1972. Extension of Samples, Sizes and Percentage Points for Significance Tests of Outlying Observations. Technometrics 14(4):847-854, November 1972.

Hanson, H. A., R. J. Davini, J. K. Morgan, and A. A. Iverson. 1976. Particulate Sampling Strategies for Large Power Plants Including Nonuniform Flow. EPA-600/2-76-170. U.S. Environmental Protection Agency, Research Triangle Park, NC.

Harris, D. B., and L. Beddingfield. 1981. "Isokinetic Sampling With Fixed Flow Rate Devices Using Exhaust Gas Recirculation." Presented at the Third EPA Symposium on Advances in Particulate Sampling and Measurement, Daytona Beach, FL.

Iinoya, K. 1979. "Research on Dust Sampling and Measurements." In: Proceedings: Advances in Particle Sampling and Measurement. Asheville, NC, May 1978, EPA-600/7-79-065, U.S. Environmental Protection Agency, Research Triangle Park, NC.

Johnson, J. W., G. I. Clinard, L. G. Felix, and J. D. McCain. 1978. A Computer-Based Cascade Impactor Data Reduction System. EPA-600/7-78-042 (NTIS PB285433), U.S. Environmental Protection Agency, Research Triangle Park, NC. 601 pp.

Kamotani, Y., I. Greber. 1972. "Experiments on a Turbulent Jet in a Cross Flow." AIAA J., 10(11):1425-1429.

Martin, R. S., S. S. Dawes, A. D. Williamson, and W. E. Farthing. 1988. Application Guide for the Source PM_{10} Exhaust Gas Recycle Sampling System. EPA-600/3-88-058, U. S. Environmental Protection Agency, Research Triangle Park, NC. 95 pp.

Shigehara, R. T. 1982. Proposed Revisions to Reduce Number of Traverse Points in Method 1 - Background Information Document. EPA-450/3-82-016a, U.S. Environmental Protection Agency, Research Triangle Park, NC.

Smith, W. B., D. B. Harris and R. R. Wilson, Jr. 1979. "A Five-Stage Cyclone System for In Situ Sampling." Environ. Sci. Technol. 13(11):1387-1392.

Smith, W. B., C. T. Parsons, and R. R. Wilson, Jr. May 1981. "A Five-Stage Cyclone System for Measuring Particle Size and Concentration in Process Streams." J. Aerosol Sci. 13(3).

Smith, W. B., K. M. Cushing, J. W. Johnson, C. T. Parsons, A. D. Williamson, and R. R. Wilson, Jr. 1982a. Sampling and Data Handling Methods for Inhalable Particulate. EPA-600/7-82-036. U.S. Environmental Protection Agency, Research Triangle Park, NC.

Smith, W. B., K. M. Cushing, R. R. Wilson, Jr., and D. B. Harris. 1982b. "Cyclone Samplers for Measuring the Concentration of Inhalable Particles in Process Streams." J. Aerosol Sci. 13(3):259.

Spencer, H. W., III. 1976. Rapping Reentrainment in a Nearly Full-Scale Pilot Electrostatic Precipitator. EPA-600/2-76-140. U.S. Environmental Protection Agency, Research Triangle Park, NC.

Ward, T. E., M. R. Midgett, T. J. Logan, A. D. Williamson, W. E. Farthing, R. S. Martin, and J. W. Ragland. 1985. "Measurement of PM_{10} Emissions from Stationary Sources." Paper 85-14.1, 78th Annual Meeting, Air Pollution Control Association, Detroit, MI.

Williamson, A. D., D. L. Iozia, P. V. Bush, W. E. Farthing, J. D. McCain, W. B. Smith. 1983. "Development, Application, and Support of Particulate Sampling Procedures - Third Annual Report." SoRI-EAS-83-348, Southern Research Institute, Birmingham, AL.

Williamson, A. D., R. S. Martin, D. B. Harris, T. E. Ward. 1984. "Design and Characterization of an Isokinetic Sampling Train for Particle Size Measurements using Exhaust Recirculation." Paper 84-56.5, 77th Annual Meeting, Air Pollution Control Association, San Francisco, CA.

Williamson, A. D., R. S. Martin, and T. E. Ward. 1985. "Development of a Source PM_{10} Sampling Train using Emission Gas Recycle (EGR)." Paper 85-14.2, 78th Annual Meeting, Air Pollution Control Association, Detroit, MI.

Williamson, A. D., W. E. Farthing, and T. E. Ward. 1986. "Development and Validation of Source PM_{10} Measurement Methods." Paper presented at the EPA/APCA Symposium on Air Toxics, Raleigh, NC.

APPENDIX A

Determination of Emissions From Stationary Sources (Using A Single-Stage PM_{10} Cyclone, Constant Sample Rate, and In-Stack Filtration)

In this appendix the preliminary procedure of the method is named Simulated Method 5 (SIM-5). A more detailed document which describes this procedure completely is published under separate cover where it is now named Constant Sampling Rate (Farthing and Dawes, 1988).

INTRODUCTION

The technical difficulties in size-specific (i.e., PM_{10}) particulate sampling are greater than, but similar to, those of total particulate sampling by EPA Reference Methods 5 or 17. Potential sampling biases exist because of variations in the spatial distribution of particulate concentrations across the sampling plane defined by the duct cross section. Likewise, temporal variations in particulate concentrations due to process variations can cause inaccurate or unrepresentative emissions measurements. EPA reference methods for particulate sampling (Methods 5 and 17) deal with these problems by specifications on the sampling location to minimize stratification (Method 1) and by spatial and temporal averaging using a traversing protocol which collects a weighted average of the particulate emissions at an array of points spanning the sample plane. Method 5 specifications also require at least three separate measurements, allowing further temporal averaging. A second potential error in particulate measurements is duct/nozzle sampling bias. Unless the gas velocity entering the sampling nozzle equals the local duct velocity (isokinetic sampling) particulate matter will be selectively depleted or enriched in the sample gas stream because of inertial separation at the nozzle entrance.

Separation of particulate matter according to aerodynamic diameter can be accomplished by sampling through inertial size separators, impactors, or cyclones. In these devices, gas flow is such that large particles are deposited and retained on suitable collection surfaces, while small particles continue with the gas flow to subsequent separation stages or a filter. Flow rate, gas density, and viscosity determine the size cut. Thus the flow rate in the size separator must be held constant throughout the sampling run. In principle, single or multiple-stage impactors or cyclones could be used. However, procedures for these different types of instruments differ substantially. Flow rate is selectable with multiple-stage size separators, whereas for a single-stage size separator it is uniquely determined by gas density and viscosity when a size cut of 10 μm is desired. PM_{10} sample recovery involves several collection surfaces when a multiple-stage configuration is used but only a filter when a single-stage configuration is used. Data reduction may involve interpolation or extrapolation for the multiple-stage configuration, while it is essentially the same as in Methods 5 and 17 for a single-stage configuration. Impactors require additional procedures associated with their special collection substrates so as to limit particle bounce, reentrainment, and anomalous weight changes by the substrates. Therefore, for the sake of simplicity this method describes PM_{10} measurements using a single-stage cyclone only.

The requirement of a constant flow rate through inertial size separators dictates other procedural differences between PM_{10} measurement methods and methods for total particulate emissions. Methods 5 and 17 specify an array of points spanning the sample plane (via Method 1) to limit the sampling error due to spatial variation of emission rates. With these methods, flow rate is adjusted from point to point to match stream and sampling nozzle velocities, thus obtaining a velocity-weighted sample and minimizing anisokinetic sampling error, i.e., depletion or enrichment of particles in the sample gas due to inertial separation at the nozzle caused by an isokinetic velocity ratio different from unity. Such point-to-point adjustment of sample (or nozzle) flow rate while maintaining constant flow rate through the inertial size separator can be accomplished only through the addition of makeup gas to the sample gas before entering the size separator. The hardware for that approach, called the Emission Gas Recycle (EGR) Method for PM_{10}, has extensive differences from a Method 5 or 17 sample train. The method described here, Simulated Method 5 (SIM-5) uses Method 5 or 17 hardware with minor differences. The sample gas flow rate is held constant during a run to provide a fixed size cut (at 10 µm), dwell time for sampling at each point is proportional to the velocity at each point to provide a velocity-weighted sample, and anisokinetic sampling error is kept within acceptable limits by specifying a range of process stream velocities (in terms of pitot readings) for each nozzle. Often only one nozzle is required, but the use of more than one nozzle per traverse may be necessary.

1. Principle and Applicability

1.1 Principle: Particulate matter is withdrawn from the source with limited isokinetic variation and inertially segregated into two size fractions: those with an aerodynamic diameter greater than 10 µm and those with an aerodynamic diameter less than or equal to 10 µm. The particulate mass collected in the size range less than or equal to 10 µm, and in the larger size range if desired, is determined gravimetrically.

1.2 Applicability: This method applies to the determination of particulate emissions from stationary sources for determining compliance with new source performance standards only when specifically provided for in an applicable subpart of the standards. This method has not been tested in stacks that contain liquid droplets or are saturated with water vapor.

2. Apparatus

2.1 Sampling Train. A schematic of the sampling train used in this method is shown in Figure A-1. With the exception of the collection device, this train is exactly the same as a standard Method 17 train. Construction details for many, but not all, of the train components are given in APTD-0581 (Citation 1 in Section 7); for changes from the APTD-0581 document and for allowable modifications to Figure A-1, consult with the Administrator.

The operating and maintenance procedures for many of the sampling train components are described in APTD-0576 (Citation 2 in Section 7). Since correct

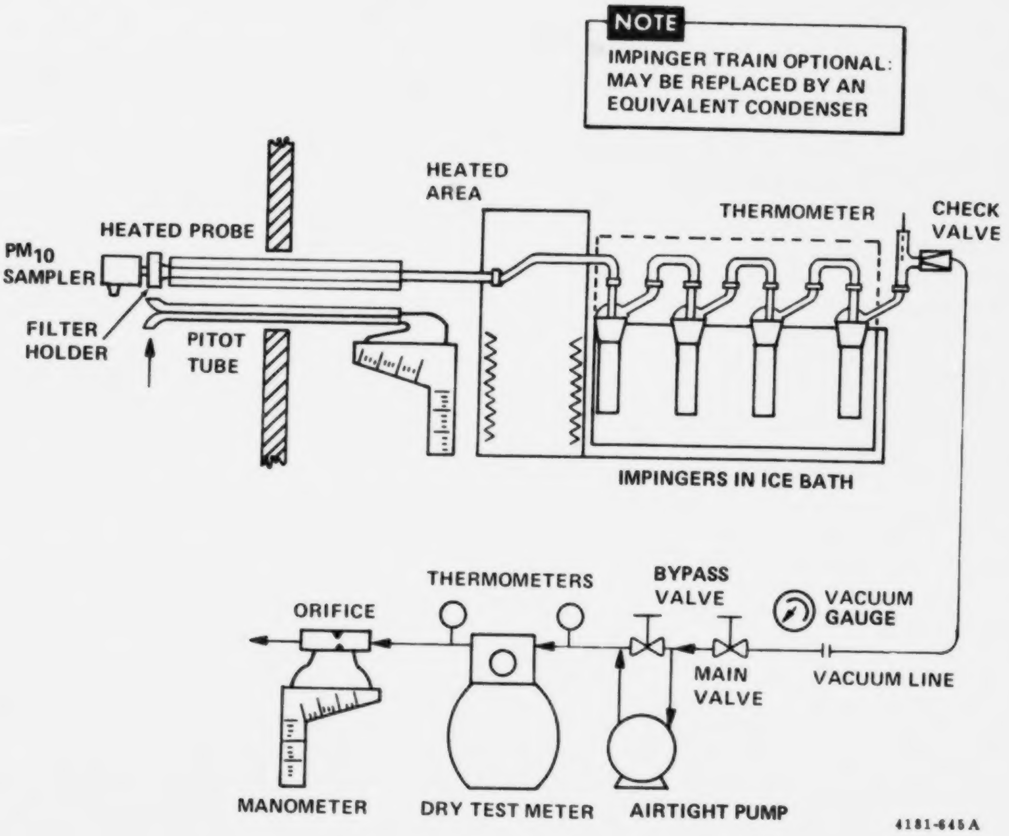
NOTE
IMPINGER TRAIN OPTIONAL: MAY BE REPLACED BY AN EQUIVALENT CONDENSER
HEATED AREA
THERMOMETER
CHECK VALVE
HEATED PROBE
PM10 SAMPLER
FILTER HOLDER
PITOT TUBE
IMPINGERS IN ICE BATH
THERMOMETERS
BYPASS VALVE
VACUUM GAUGE
ORIFICE
MAIN VALVE
VACUUM LINE
MANOMETER
DRY TEST METER
AIRTIGHT PUMP
4181-645A

Figure A-1. PM $_{10}$ particulate sampling train for particulate matter (Modified EPA Method 17 train).

use is important in obtaining valid results, all users should read the APTD-0576 document and adopt the operating and maintenance procedures outlined in it, unless otherwise specified herein. The sampling train consists of the following components:

2.1.1 Inertial Sampler Nozzle. Stainless steel (316), with sharp, tapered leading edge. The taper shall be on the outside to preserve a constant internal diameter. Other materials of construction may be used subject to the approval of the Administrator.

A range of sizes suitable for isokinetic sampling should be available, that is, 0.32 to 1.27 cm (1/8 to 1/2 in.) or larger if higher volume sampling trains are used--inside diameter (ID) nozzles in increments of 0.16 cm (1/16 in.). Each nozzle shall be calibrated according to the procedures outlined in Section 5.1.

Because of severe inertial deposition of particles in the PM_{10} size range in bends, only straight sampling nozzles should be used. "Gooseneck" or other nozzles designed to turn the sampled gas flow 90°, as in Methods 5 and 17, will not be acceptable.

2.1.2 PM_{10} Cyclone

The cyclone chosen here as the PM_{10} sizing device is the commercially available version of Cyclone I, the first stage of the SoRI/EPA five-stage series cyclone (see citation 3 of Section 7). Laboratory calibration (refer to Section 6.11) has shown Cyclone I produces a 10-μm fractionation at approximately 0.5 cfm, depending on local stack conditions. With the approval of the Administrator, other inertial sizing devices (i.e., cascade impactors, other cyclones) may be used as the PM_{10} classifier if performance equivalent to the designated PM_{10} cyclone is demonstrated. However, the differences in the calibrated behavior of an alternate classifier would require changes in the equations for target ΔH pressure differential (Section 4.1.2.3) and actual classifier D_{50} (Section 6.11).

2.1.3 Filter Holder. The in-stack filter holder shall be constructed of stainless steel; if a gasket is used, it shall be made of silicone rubber, Teflon, or Viton A. Other holder and gasket materials may be used subject to the approval of the Administrator. The filter holder shall be designed to provide a positive seal against leakage from the outside or around the filter.

2.1.4 Probe Extension. Any suitable rigid probe extension may be used after the filter holder.

2.1.5 Pitot Tube. Type S, as described in Section 2.1 of Method 2, or other device approved by the Administrator; the pitot tube shall be attached to the probe extension to allow constant monitoring of the stack gas velocity (see Figure A-1). The impact (high pressure) opening plane of the pitot tube shall be even with or above the nozzle entry plane during sampling (see Method 2, Figure 2-6b). It is recommended: (1) that the pitot tube have a known baseline coefficient, determined as outlined in Section 4 of Method 2; and (2) that this known coefficient be preserved by placing the pitot tube in an interference-free arrangement with respect to the sampling nozzle, inertial sampler, filter holder, and temperature sensor (see Figure A-1).

Source-sampling assemblies that do not meet the minimum spacing requirements of Figure 2-7 of Method 2 may be used; however, the pitot tube coefficients of such assemblies shall be determined by calibration, using methods subject to the approval of the Administrator.

NOTE: Experience has indicated that the criteria stated in Method 2, Section 4.1.1 for pitot positioning relative to sampling nozzles may not be sufficient to prevent flow perturbations. Continued investigation of this problem is planned with more definitive guidelines expected as a result. At present, the only means of eliminating this type of error with confidence is to calibrate pitots in the expected sampling configuration in a flow field significantly larger than the inertial sizing device.

2.1.6 Differential Pressure Gauge. Inclined manometer or equivalent device (two), as described in Section 2.2 of Method 2. One manometer shall be used for velocity head (Δp) readings, and the other for orifice differential pressure readings.

2.1.7 Condenser. It is recommended that the impinger system described in Method 5 be used to determine the moisture content of the stack gas. Alternatively, any system that allows measurement of both the water condensed and the moisture leaving the condenser, each to within 1 mL or 1 g may be used. The moisture leaving the condenser can be measured either by (1) monitoring the temperature and pressure at the exit of the condenser and using Dalton's law of partial pressures or (2) passing the sample gas stream through a silica gel trap with exit gases kept below 20 °C (68 °F) and determining the weight gain.

Flexible tubing may be used between the probe extension and condenser. If means other than silica gel are used to determine the amount of moisture leaving the condenser, it is recommended that silica gel still be used between the condenser system and pump to prevent moisture condensation in the pump and metering devices and to avoid the need to make corrections for moisture in the metered volume.

2.1.8 Metering System. Vacuum gauge, leak-free pump, thermometers capable of measuring temperature to within 3 °C (5.4 °F), dry gas meter capable of measuring volume to within 2%, and related equipment, as shown in Figure A-1. Other metering systems capable of maintaining sampling rates within the 5% of a target value and of determining sample volumes to within 2% may be used. In conjunction with a pitot tube, the system shall enable checks of isokinetic rates.

2.1.9 Barometer. Barometric pressure should be determined in the same way as described in Section 2.1.9 of Method 5.

2.1.10 Gas Density Determination Equipment. Temperature sensor and pressure gauge, as described in Sections 2.3 and 2.4 of Method 2, and gas analyzer, if necessary, as described in Method 3.

The temperature sensor shall be attached to either the pitot tube or to the probe extension, in a fixed configuration. If the temperature sensor is attached in the field, the sensor shall be placed in an interference-free arrangement with respect to the Type S pitot tube openings (as shown in Figure 2-7 of Method 2). Alternatively, the temperature sensor need not be attached to either the probe extension or pitot tube during sampling, provided that a difference of not more than 1% in the average velocity measurement is introduced. This alternative is subject to the approval of the Administrator.

2.2 Sample Recovery. The following items are needed:

2.2.1 Brushes. Nylon bristle brushes with stainless steel wire handles. The brushes should be of the proper size and shape for brushing out the nozzle and the PM_{10} cyclone.

2.2.2 Wash Bottles. Two glass wash bottles are recommended; polyethylene wash bottles may be used at the option of the tester. It is recommended that acetone not be stored in polyethylene bottles for longer than a month.

2.2.3 Glass Sample Storage Containers. Chemically resistant, borosilicate glass bottles, for acetone washes, 500 mL or 1000 mL. Screw cap liners shall either be rubber-backed Teflon or shall be constructed so as to be leak-free and resistant to chemical attack by acetone. (Narrow mouth glass bottles have been found to be less prone to leakage.) Alternatively, polyethylene bottles may be used.

2.2.4 Petri Dishes. For particulate catches and filter samples; glass or polyethylene, unless otherwise specified by the Administrator.

2.2.5 Graduated Cylinder and/or Balance. To measure condensed water to within 1 mL or 1 g. Graduated cylinders shall have subdivisions no greater than 2 mL. Most laboratory balances are capable of weighing to the nearest 0.5 g or less. Any of these balances is suitable for use here and in Section 2.3.4.

2.2.6 Plastic Storage Containers. Airtight containers to store silica gel.

2.2.7 Funnel and Rubber Policeman. To aid in transfer of silica gel to container; not necessary if silica gel is weighed in the field.

2.2.8 Funnel. Glass or polyethylene, to aid in sample recovery.

2.3 Analysis. For analysis, the following equipment is needed.

2.3.1 Glass Weighing Dishes.

2.3.2 Desiccator.

2.3.3 Analytical Balance. To measure to within 0.1 mg.

2.3.4 Balance. To measure to within 0.5 g.

2.3.5 Beakers. 250 mL.

2.3.6 Hygrometer. To measure the relative humidity of the laboratory environment.

2.3.7 Temperature Gauge. To measure the temperature of the laboratory environment.

3. Reagents.

3.1 Sampling. The reagents used in sampling are as follows:

3.1.1 Filters. The in-stack filters shall be glass mats without organic binders, and shall exhibit at least 99.95% efficiency (<0.05% penetration) on 0.3-µm dioctyl phthalate smoke particles. The filter efficiency tests shall be conducted in accordance with ASTM Standard Method D2986-71 (Reapproved 1978; incorporated by reference--see §60.17). Test data from the supplier's quality control Program are sufficient for this purpose. In sources containing SO_2 or SO_3, the filter material must be of a type that is unreactive to SO_2 or SO_3. Citation 4 in Section 7 may be used to select the appropriate filter.

3.1.2 Silica Gel. Indicating type, 6 to 16 mesh. If previously used, dry at 175 °C (350 °F) for 2 h. New silica gel may be used as received. Alternatively, other types of desiccants (equivalent or better) may be used, subject to the approval of the Administrator.

3.1.3 Crushed Ice.

3.1.4 Stopcock Grease. Acetone-insoluble, heat-stable silicone grease. This is not necessary if screw-on connectors with Teflon sleeves, or similar, are used. Alternatively, other types of stopcock grease may be used, subject to the approval of the Administrator.

3.2 Sample Recovery. Acetone, reagent grade, ≤0.001% residue, in glass bottles. Acetone from metal containers generally has a high residue blank and should not be used. Sometimes, suppliers transfer acetone to glass bottles from metal containers. Thus, acetone blanks shall be run prior to field use, and only acetone with low blank values (0.001%) shall be used. In no case shall a blank value of greater than 0.001% of the weight of acetone used be subtracted from the sample weight.

3.3 Analysis.

3.3.1 Acetone. Same as 3.2

3.3.2 Desiccant. Anhydrous calcium sulfate, indicating type. Alternatively, other types of desiccants may be used, subject to the approval of the Administrator.

4. Procedure

4.1 Sampling. The complexity of this method is such that, in order to obtain reliable results, testers should be trained and experienced with the test procedures.

4.1.1 Pretest Preparation. All components shall be maintained and calibrated according to the procedure described in APTD-0576 (Citation 2 in Section 7), unless otherwise specified herein.

Weigh several 200- to 300-g portions of silica gel in airtight containers to the nearest 0.5 g. Record the total weight of the silica gel plus container, on each container. As an alternative, the silica gel need not be preweighed, but may be weighed directly in its impinger or sampling holder just prior to train assembly.

Check filters visually against light for irregularities and flaws or pinhole leaks. Label filters of the proper size on the back side near the edge using numbering machine ink. As an alternative, label the shipping containers (glass or plastic Petri dishes), and keep the filters in these containers at all times except during sampling and weighing.

Small envelopes should be cut from aluminum foil to hold the PM_{10} cyclone catch. Each envelope should be marked with a unique identification number and placed in a glass or plastic Petri dish.

Desiccate the filters and foil envelopes at 20±5.6 °C (68±10 °F) and ambient pressure for at least 24 h, and weigh at intervals of at least 6 h to a constant weight, i.e., 0.5 mg change from previous weighing; record results to the nearest 0.1 mg. During each weighing the filter must not be exposed to the laboratory atmosphere for a period greater than 2 min or a relative humidity above 50%. Alternatively (unless otherwise specified by the Administrator), the filters may be oven dried at 105 °C (220 °F) for 2 or 3 h, desiccated for 2 h, and weighed. Procedures other than those described which account for relative humidity effects may be used, subject to the approval of the Administrator.

4.1.2 Preliminary Determinations.

4.1.2.1 General. Select the sampling site. Make a projected-area model of the probe extension-PM_{10} sampling assembly, with the pitot tube face openings positioned along the centerline of the stack, similar to Figure 17-2 of Method 17. Calculate the estimated cross-section blockage. If the blockage exceeds 5% of the duct cross-sectional area, consult with the Administrator. Determine the stack pressure and temperature. Determine the moisture content using Approximation Method 4 or its alternatives.

The stack gas dry molecular weight, as described in Method 2, Section 3.6, is calculated by the following equation:

$$M_d = 44\ f_{CO_2} + 32\ f_{O_2} + 28(1 - f_{CO_2} - f_{O_2}) \qquad \text{Equation 1}$$

NOTE: The equation above does not consider argon in air (about 0.9%, molecular weight of 37.7). A negative error of approximately 0.4% is introduced. The tester may wish to include argon in the analysis using procedures subject to approval of the Administrator.

The wet molecular weight of the stack gases is calculated (refer to Method 2, Section 5.1) as follows:

$$M_s = M_d\ (1-B_{ws}) + 18.0\ B_{ws} \qquad \text{Equation 2}$$

If integrated Method 3 sampling is used for molecular weight determination, the integrated bag sample shall be taken simultaneously with, and for the same total length of time as, the particulate sample run.

4.1.2.2 Velocity Profile. Determine the number of traverse points required by using Figure A-2. For rectangular stacks, the equivalent duct diameter should be calculated as in Method 1. Once the number of traverse points has been determined, these should be located within the duct as described in Method 1. Select a probe extension length such that all traverse points can be sampled. For large stacks, consider sampling from opposite sides of the stack to reduce the length of probes.

At each traverse point record the stack gas temperature and the velocity pressure. A leak check of the pitot lines is recommended (see Method 2, Section 3.1).

4.1.2.3 Target ΔH to Obtain Aerodynamic Size Cut. Given the results of stack gas constituent analysis from Method 3 and average stack gas temperature, determine the stack gas viscosity. A rigorous algorithm for the calculation of the viscosity of a gas mixture in terms of its components is given by Wilke (Citation 5 in Section 7). A simplified equation for combustion gasses was derived by Williamson et al. (Citation 6 in Section 7) from Wilke's method:

$$\mu_s = C_1 + C_2 T_s + C_3 T_s^{2} + C_4\ f_{O_2} - C_5\ B_{ws} \qquad \text{Equation 3}$$

Given the calibration of the PM_{10} sampler and the above viscosity, the flow rate required to obtain the desired 10-μm cut is calculated using Equation 6 below.

$$Q_{cyc} = \alpha_5 \left(\frac{P_s M_s}{T_s}\right)^{-0.2949} \mu_s \qquad \text{Equation 4}$$

The orifice pressure drop, ΔH, corresponding to this sample flow rate may then be calculated using the following equation:

$$\Delta H = \left(\frac{Q_{cyc}\ (1-B_{ws})\ P_s}{T_s}\right)^2 T_m\ M_d \left(\frac{1.083\ \Delta H@}{P_{bar}}\right) \qquad \text{Equation 5}$$

4.1.2.4 Pitot Δp Limits. For a series of nozzles, calculate the nozzle velocity corresponding to the above-mentioned sample flow rate by using the following equation:

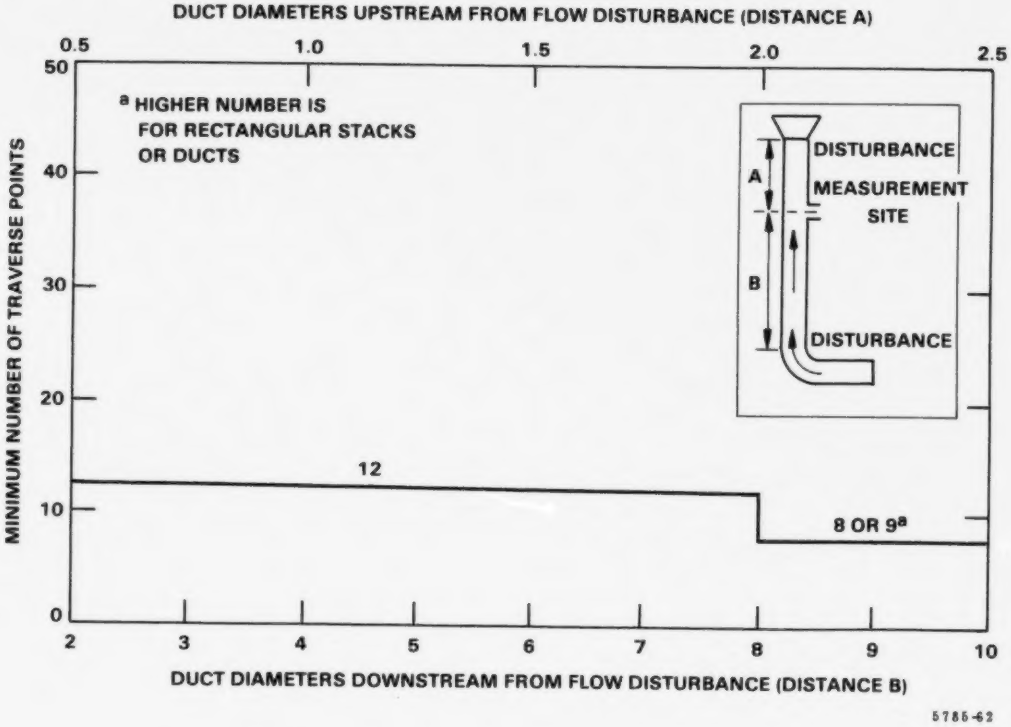

Figure A-2. Minimum number of traverse points for SIM-5 traverse.

$$u = \frac{3.056\ Q_{cyc}}{d^2} \qquad \text{Equation 6}$$

Use the SIM-5 nomograph, shown in Figure A-3, to determine the upper and lower limits of stream velocity for whichever nozzle is usable. Calculate the quantity $\mu_s \sqrt{Q_{cyc}}$ in units of micropoise $\sqrt{(alpm)}$. Overlay the R = v/u curve so that its center falls on the line R = 1 at v = u. Convert the above stream velocities to pitot Δp limits for each nozzle. Figure A-4, SIM-5 setup form, may be used for this purpose.

$$\Delta p = 1.3686 \times 10^{-4} \frac{P_s M_s}{T_s} \left(\frac{v_s}{c_p}\right)^2 \qquad \text{Equation 7}$$

4.1.2.5 Selection of Nozzles and Regions. List the pitot Δp's measured during the velocity traverse. Note that if the velocity pitot coefficient differs from the SIM-5 pitot coefficient, conversion to equivalent values for the pitot on the SIM-5 probe is advisable. The conversion factor is $(c_p/c_p')^2$, where c_p' is the coefficient for the velocity pitot. Choose the nozzle for which the limiting Δp values bracket those measured. If more than one nozzle is acceptable, choose the one giving the greatest symmetry. Note that if the expected pitot Δp for one or more points is near a limit for the chosen nozzle, it may be outside the limits at the time of the run.

The SIM-5 nomograph (Figure 3) has limits broad enough that multiple nozzles for a single traverse will seldom be necessary. However, the temporal and/or spatial variation of stream velocity is sufficient, at some sources to require more than one nozzle.

4.1.2.6 Dwell Time at First Point. The dwell time at each point of a run should be proportional to the velocity at the point. The dwell time for the first sample point is calculated prior to starting the run as the average dwell time per point multiplied by the ratio of $(\sqrt{\Delta p_1})/(\sqrt{\Delta p})_{avg}$ using Δp's from the velocit traverse. Each succeeding dwell time is then calculated during the run using Δp's from the same run. It is recommended that the number of minutes sampled at each point be rounded to the nearest 1/4 min.

Select an average per point dwell time such that the total sampling time is greater than or equal to the minimum total sampling time specified in the test procedures for the specific industry. Further, it is required that (1) the sampling time per point is not less than 2 min (or some greater time interval if specified by the Administrator), and (2) the sample volume taken (corrected to standard conditions) will exceed the required minimum total gas sample volume. The latter is based on an approximate average sampling rate.

In some circumstances (e.g., batch cycles), it may be necessary to sample for shorter times at the traverse points and to obtain smaller gas sample volumes. In these cases, the Administrator's approval must first be obtained.

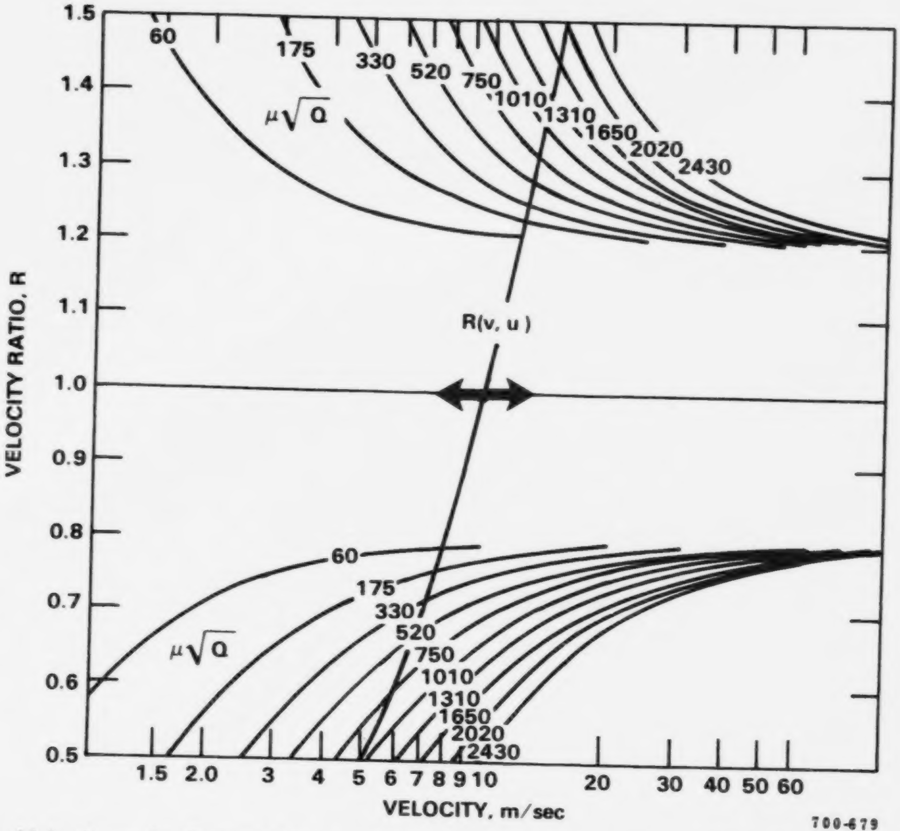

Figure A-3. Velocity ratio, R, versus duct velocity to give aspiration coefficient of 1.2 (upper curves) and 0.8 (lower curves) for 10-μm particles.

(5785-6)

CSR SETUP WITH CYCLONE I (PM_{10} SIZE CUT)

1. $Q = 3.35\text{x}10^{-6}\ \mu^{2.228} = 3.35\text{x}10^{-6}\ (\underline{\qquad})^{2.228} = \boxed{\qquad\qquad}$ (acfm) with μ in micropoise

2. $\mu\sqrt{Q} = (\underline{\qquad})\ \sqrt{(\qquad)\text{x}28.32} = \underline{\qquad}$, Round UP to the nearest value in CSR Nomograph, _____

Nozzle velocity, $u = 3.056\ Q/d^2 = 3.056\ (\qquad)/d^2 = \boxed{\qquad /d^2}$ (ft/s) with d in inches

Nozzle ID = __________ __________ __________

d = __________ __________ __________ (inches)

u = __________ __________ __________ (ft/s)

Minimum Velocity, $V_{\ell\ell}$ = __________ __________ __________ (ft/s)

Maximum Velocity, $V_{u\ell}$ = __________ __________ __________ (ft/s)

3. Pitot $\Delta P = 1.368\text{x}10^{-4}\ \frac{P_{stk}}{T_{stk}}\ M_w \frac{1}{C_P^2}\ v^2 = 1.368\text{x}10^{-4}\ \frac{(\qquad)(\qquad)}{(\qquad)(\qquad)^2}\ v^2 = \underline{\qquad\qquad}\ v^2\ (H_2O'')$
with v in ft/sec

$\Delta P_{\ell\ell}$ = __________ __________ __________ (H_2O'')

$\Delta P_{u\ell}$ = __________ __________ __________ (H_2O'')

4. Choose Nozzle(s) from $\Delta P_{\ell\ell}$ and $\Delta P_{u\ell}$ and Expected Pitot ΔP's (From Last Traverse)

	Port ___		Port ___		Port ___		Port ___	
Point #	ΔP	Noz. ID	ΔP	Noz. ID	ΔP	Noz. ID	ΔP	Noz. ID
1								
2								
3								
4								

Note: During a traverse, if ΔP of a point is found to be out of range for the current nozzle, skip it and come back with an appropriate nozzle.

5. $\Delta H = Q^2\ \frac{T_{dgm}}{T_{stk}^2}\ \frac{P_{stk}^2}{P_o}\ (1\text{-}f_{H_2O})^2\ M_d\ K_{cal} = (\qquad)^2\ \frac{T_{dgm}}{(\qquad)^2}\ \frac{(\qquad)^2}{(\qquad)}\ (1\text{-}0.\underline{\qquad})^2\ (\underline{\qquad})\ K_{cal}$

$= \underline{\qquad\qquad}\ T_{dgm}\ K_{cal} = \underline{\qquad\qquad}\ (\underline{\qquad})\ (\underline{\qquad}) = \boxed{\qquad\qquad}\ H_2O''$

DWELL TIMES

6. $t_1 = \frac{\sqrt{\Delta P_1}}{\sqrt{\overline{\Delta P}}}\ \frac{\text{Total run time}}{\text{No. points}} = \frac{(\qquad)}{(\qquad)}\ (\qquad) = \underline{\qquad}$; $t_n = \frac{t_1}{\sqrt{\Delta P_1}}\ \sqrt{\Delta P_n} = \frac{(\qquad)}{\sqrt{(\qquad)}}\sqrt{\Delta P_n} = \underline{\qquad}\ \sqrt{\Delta P_n}$

DWELL TIMES AND ΔP

	Port ___		Port ___		Port ___		Port ___	
Point #	ΔP	t	ΔP	t	ΔP	t	ΔP	t
1								
2								
3								
4								

Traverse # ____________________ Setup by ____________________ Operator ____________________

5785-6

Figure A-4. SIM-5 setup with Cyclone I (PM_{10} size cut).

4.1.3 Preparation of Collection Train. During preparation and assembly of the sampling train, keep all openings where contamination can occur covered until just prior to assembly or until sampling is about to begin.

If impingers are used to condense stack gas moisture, prepare them as follows: place 100 mL of water in each of the first two impingers, leave the third impinger empty, and transfer approximately 200 to 300 g of preweighed silica gel from its container to the fourth impinger. More silica gel may be used, but care should be taken to ensure that it is not entrained and carried out from the impinger during sampling. Place the container in a clean place for later use in the sample recovery. Alternatively, the weight of the silica gel plus impinger may be determined to the nearest 0.5 g and recorded. If some means other than impingers is used to condense moisture, prepare the condenser (and, if appropriate, silica gel for condenser outlet) for use.

With tweezers or clean disposable surgical gloves, place a labeled (identified) and weighed filter in the filter holder. Be sure that the filter is properly centered and the gasket properly placed so as not to allow the sample gas stream to circumvent the filter. Check filter for tears after assembly is completed. Mark the probe extension with heat resistant tape or by some other method to denote the proper distance into the stack or duct for each sampling point.

Assemble the train as in Figure 1, using a very light coat of silicone grease on all ground glass joints and greasing only the outer portion (see Citation 2 in Section 7) to avoid possibility of contamination by the silicone grease. Place crushed ice around the impingers.

4.1.4 Leak Check Procedures

4.1.4.1 Pretest Leak Check. A pretest leak check is recommended, but not required. If the tester opts to conduct the pretest leak check, the following procedure shall be used.

Assemble the entire sample train, including the collection device. Plug the inlet of the PM_{10} cyclone with a material that will be able to withstand the stack temperature. Insert the probe into the stack and wait approximately 15 min (or longer, if necessary) to allow the system to come to thermal equilibrium with the stack gas stream. Turn on the pump and draw a vacuum in the system. If the system is being checked without the PM_{10} cyclone and nozzle in place, a vacuum of 253 mm Hg (10 in. Hg) should be used. If the system includes the PM_{10} sampler, a vacuum of 127 mm Hg (5 in. Hg) is acceptable, as long as the system downstream of the sizing device satisfies the leak criteria at the greater vacuum. Note that a lower vacuum may be used, provided that it is not exceeded during the test. Determine the leakage rate. A leakage rate in excess of 4% of the average sampling rate or 0.00057 m^3/min (0.02 cfm), whichever is less, is unacceptable.

The following leak check instructions for the sampling train described in APTD-0576 and APTD-0581 (Citation 1 and 2 in Section 7) may be helpful. Start the pump with bypass valve fully open and coarse-adjust valve completely closed. Partially open the coarse-adjust valve, and slowly close the bypass valve until the desired vacuum is reached. Do not reverse direction of bypass valve. If the desired vacuum is exceeded, either leak check at this higher vacuum or end the leak check as shown below and start over.

When the leak check is completed, first slowly remove the plug from the inlet to the sample nozzle and immediately turn off the vacuum pump. This prevents water from being forced backward and keeps silica gel from being entrained backward.

NOTE: The positive pressure leak test described in Section 5.5 is not required for each sampling run but must be performed upon initial setup of the sampling train at each test site.

4.1.4.2 Leak Checks During Sample Run. If, during the sampling run, a component change other than the nozzle (e.g., filter assembly or impinger) becomes necessary, a leak check shall be conducted immediately before the change is made. The leak check shall be done according to the procedure outlined in Section 4.1.4.1 above, except that it shall be done at a vacuum equal to or greater than the maximum value recorded up to that point in the test. If the leakage rate is found to be no greater than 0.00057 m^3/min. (0.02 cfm) or 4% of the average sampling rate (whichever is less), the results are acceptable, and no correction will need to be applied to the total volume of dry gas metered. If, however, a higher leakage rate is obtained, the tester shall either record the leakage rate and plan to correct the sample volume as shown in Section 6.3 of this method, or shall void the sampling run.

Immediately after component changes, leak checks are optional; if such leak checks are done, the procedure outlined in Section 4.1.4.1 above shall be used.

4.1.4.3 Posttest Leak Check. A leak check is mandatory at the conclusion of each sampling run. The leak check shall be done in accordance with the procedures outlined in Section 4.1.4.1, except that it shall be conducted at a vacuum equal to or greater than the maximum value reached during the sampling run. If the leakage rate is found to be no greater than 0.00057 m^3/min. (0.02 cfm) or 4% of the average sampling rate (whichever is less), the results are acceptable, and no correction need be applied to the total volume of dry gas metered. If, however, a higher leakage rate is obtained, the tester shall either record the leakage rate and correct the sample volume as shown in Section 6.3 of this method, or shall void the sampling run.

4.1.5 Sampling Train Operation

For each run, record the data required on the example data sheet shown in Figure 5-2 of Method 5 and the example setup sheet shown in Figure A-4. Be sure to record the initial dry gas meter reading. Record the dry gas meter readings at the beginning and end of each port traverse, and after each leak check, and when sampling is halted. Take other readings required by Figure 5-2 and Figure A-4 at least once at each sample point during each time increment. Level and zero the manometer. Because the manometer level and zero may drift because of vibrations and temperature changes, make periodic checks during the traverse.

Clean the portholes prior to the test run to minimize the chance of sampling the deposited material. To begin sampling, remove the nozzle cap and verify that the pitot tube and probe extension are properly positioned. Position the nozzle at the first traverse point with the tip pointing directly into the gas stream.

When the stack is under significant negative pressure (water gauge differential greater than the height of impinger stem), take care to close the coarse-adjust valve before inserting the probe extension assembly into the stack to prevent water from being forced backward. If necessary, the pump may be turned on with the coarse-adjust valve closed. When the probe is in position, block off the openings around the probe and porthole to prevent unrepresentative dilution of the gas stream.

Start the pump and adjust the flow to the target orifice pressure drop, ΔH, calculated in Section 4.1.2.3 and recorded on the setup sheet shown in Figure A-4. Sample at the first traverse point for the dwell time calculated as described in Section 4.1.2.6 (Figure A-4).

The dwell times at subsequent traverse points are calculated during the run by using the following formula:

$$t_n = t_1 \frac{\sqrt{\Delta p_n}}{\sqrt{\Delta p_1}} \qquad \text{Equation 8}$$

In cases where the expected pitot Δp for one or more points is near a limit for the chosen nozzle, then it may be outside the limits at the time of the run. In such instances, make a note on the run sheet and sample the point as previously planned.

When traversing the stack cross section, care should be taken not to bump the probe nozzle into the stack walls when sampling near the walls or when removing or inserting the probe extension through the portholes, to minimize the chance of extracting deposited material. The pump should remain on while traversing the points in a single port but should be shut off when moving the probe from one port to another.

During the test run, take appropriate steps (e.g., adding crushed ice to the impinger ice bath) to maintain a temperature of less than 20 °C (68 °F) at the condenser outlet; this will prevent excessive moisture loses. Also, periodically check the level and zero of the manometer.

If the pressure drop across the filter becomes too high, making the target ΔH difficult to maintain, the filter may be replaced in the midst of a sample run. It is recommended that another complete filter holder assembly be used rather than attempting to change the filter itself. Before a new filter holder is installed, conduct a leak check as outlined in Section 4.1.4.2. The total particulate weight shall include the summation of all filter assembly catches.

At the end of the sample run, turn off the coarse-adjust valve, remove the probe extension assembly from the stack, turn off the pump, record the final dry gas meter reading, and perform a leak check, as outlined in Section 4.1.4.3. Also, leak check the pitot lines as described in Section 3.1 of Method 2; the lines must pass this leak check in order to validate the velocity head data.

4.1.6 Calculation of Aerodynamic Size Cut and Percent Isokinetic.

By using the equation for the actual flow rate through the PM_{10} sampler and the calibration equation of the cyclone, the actual size cut of the cyclone should be determined (see Section 6.11). Calculate percent isokinetic (see Section 6.13) for the test run. If either value calculated above falls outside the acceptance criterion listed in section 6.14, the test should be run again.

4.2 Sample Recovery. Proper cleanup procedure begins as soon as the probe extension assembly is removed from the stack at the end of the sampling period. Allow the assembly to cool.

When the assembly can be safely handled, wipe off all external particulate matter near the tip of the nozzle and place a cap over it to prevent losing or gaining particulate matter. Do not cap off the probe tip tightly while the sampling train is cooling down, as this would create a vacuum in the filter holder, forcing condenser water backward if impingers are used.

Before moving the sample train to the cleanup site, disconnect the filter holder-cyclone assembly from the probe extension; cap the open inlet of the probe extension. Be careful not to lose any condensate, if present. Remove the umbilical cord from the condenser outlet and cap the outlet. If a flexible line is used between the first impinger (or condenser) and the probe extension, disconnect the line at the probe extension and let any condensed water or liquid drain into the impingers or condenser. Disconnect the probe extension from the condenser; cap the probe extension outlet. After wiping off the silicone grease, cap off the condenser inlet. Ground glass stoppers, plastic caps, or serum caps (whichever are appropriate) may be used to close these openings.

Transfer both the filter holder-cyclone assembly and the condenser to the cleanup area. This area should be clean and protected from the wind so that the chance of contaminating or losing the sample will be minimized.

Save a portion of the acetone used for cleanup as a blank. Take 200 mL of this acetone directly from the wash bottle being used and place it in a glass sample container labeled "acetone blank".

Inspect the train prior to and during disassembly and note any abnormal conditions. Treat the samples as follows:

Container 1. Carefully remove the sampling nozzle from the cyclone and brush particulate matter into a preweighed foil envelope with a nylon bristle or camel's hair brush. Any particulate matter adhering to the outside of the nozzle or the nozzle threads should not be included. Brush into this same foil envelope the particulate catch of the cyclone, being careful to exclude the particulate matter in the "turnaround" cup and interior of the exit tube.

Container 2. Carefully remove the filter from the filter holder and place it in its identified Petri dish container. Use a pair of tweezers and/or clean disposable surgical gloves to handle the filter. Carefully transfer to the surface of the filter any particulate matter and/or filter fibers which adhere to the inside of the cyclone exit tube and the filter holder gasket. To avoid cross-contamination, the brush used for the cyclone body should not be used for this. If it is necessary to fold the filter, do so such that the particulate cake is inside the fold. Alternatively, a preweighed foil envelope could be used to hold the filter.

Container 3. Carefully clean all surfaces assigned to container 1 with acetone from a wash bottle. A funnel (glass or polyethylene) may be used to aid in transferring liquid washes to the container. Rinse the brush with acetone and collect these washings as well. Between sampling runs, keep brushes clean and protected from contamination.

Container 4. Perform acetone wash as described above on all surfaces assigned to container 2. Multiple washings should be performed on the connective tubing between the cyclone exit and the filter holder inlet. Rinse the brush and the filter holder gasket.

After all acetone washings and particulate matter are collected in the sample container, tighten the lid on the sample container so that acetone will not leak out when it is shipped to the laboratory. Mark the height of the fluid level to determine whether or not leakage occurred during transport. Label the container to clearly identify its content.

Container 5. If silica gel is used in the condenser system for moisture content determination, note the color of the silica gel to determine if it has been completely spent; make a notation of its condition. Transfer the silica gel back to its original container and seal. A funnel may make it easier to pour the silica gel without spilling, and a rubber policeman may be used as an aid in removing the silica gel. It is not necessary to remove the small amount of dust particles that may adhere to the walls and are difficult to remove. Since the gain in weight is to be used for moisture calculations, do not use water or other liquids to transfer the silica gel. If a balance is available in the field, follow the procedure for container 5 under "Analysis."

Condenser Water. Treat the condenser or impinger water as follows: make a notation of any color or film in the liquid catch. Measure the liquid volume to within ±1 mL by using a graduated cylinder, or, if a balance is available, determine the liquid weight to within ±0.5 g. Record the total volume or weight of liquid present. This information is required to calculate the moisture content of the effluent gas. Discard the liquid after measuring and recording the volume or weight.

NOTE: Actual data regarding particles of diameter greater than 10 µm (cyclone and nozzle catch) may not be required. In these cases, recovery of the cyclone catch is not necessary. The cyclone and sample nozzle should be rinsed thoroughly with acetone for use in the next test run.

4.3 Analysis. Record the data required on the example sheet shown in Figure 5-2 of Method 5 and in Figure A-4.

Handle each sample container as follows:

Containers 1 and 2. Leave the contents in the Petri dish or transfer to a tared glass weighing dish. Desiccate for 24 h in a desiccator containing anhydrous calcium sulfate or similar desiccant. Weigh to a constant weight and report the results to the nearest 0.1 mg. The term "constant weight," as used above, means a difference of no more than 0.5 mg or 1% of total weight less tare weight, whichever is greater, between two consecutive weighings, with no less than 6 h of desiccation time between weighings.

Alternatively, the samples may be oven dried at the average stack temperature or 105 °C (220 °F), whichever is less, for 2 to 3 h, cooled in the desiccator, and weighed to a constant weight, unless otherwise specified by the Administrator. The tester may also opt to oven dry the sample at the average stack temperature or 105 °C (220 °F), whichever is less, for 2 to 3 h, weigh the sample, and use this weight as a final weight.

Whichever weighing method is used, completed weights of all cyclone and filter samples should be obtained on site, prior to shipping.

Containers 3 and 4. Note the level of liquid in the container and confirm on the analysis sheet whether or not leakage occurred. If a noticeable amount of leakage has occurred, either void the sample or use methods, subject to the approval of the Administrator, to correct the final results. Measure the liquid in this container either volumetrically to ±1 mL or gravimetrically to ±0.5 g. Transfer the contents to a tared 250 mL beaker or suitable container and evaporate to dryness at ambient temperature and pressure. Desiccate for 24 h and weigh to a constant weight. Report the results to the nearest 0.1 mg.

Container 5. This step may be conducted in the field. Weigh the spent silica gel (or silica gel plus impinger) to the nearest 0.5 g using a balance.

"Acetone Blank" Container. Measure acetone in this container either volumetrically or gravimetrically. Transfer the acetone to a tared 250-mL beaker or suitable container and evaporate to dryness at ambient temperature and pressure. Desiccate for 24 h and weigh to a constant weight. Report the results to the nearest 0.1 mg.

NOTE: At the option of the tester, the contents of containers 3 and 4, as well as the acetone blank container, may be evaporated at temperatures higher than ambient. If evaporation is done at an elevated temperature, the temperature must be below the boiling point of the solvent; also, to prevent "bumping," the evaporation process must be closely supervised, and the contents of the beaker must be swirled occasionally to maintain an even temperature. Use extreme care, as acetone is highly flammable and has a low flash point.

5. Calibration. Maintain a laboratory log of all calibrations.

5.1 Inertial Sampler Nozzle. Nozzles shall be calibrated before their initial use in the field. With a micrometer, measure the inside diameter of the nozzle to the nearest 0.025 mm (0.001 in.). Make three separate measurements by using different diameters each time, and obtain the average of the measurements. The difference between the high and low numbers shall not exceed 0.1 mm (0.004 in.). When nozzles become nicked, dented, or corroded, they shall be reshaped, sharpened, and recalibrated before use. Each nozzle shall be permanently and uniquely identified.

5.2 Pitot Tube. If the pitot tube is placed in an interference-free arrangement with respect to the other probe assembly components, its baseline (isolated tube) coefficient shall be determined as outlined in Section 4 of Method 2. If the probe assembly is not interference-free, the pitot tube assembly coefficient shall be determined by calibration, using methods subject to the approval of the Administrator.

5.3 Metering System. Before its initial use in the field, the metering system shall be calibrated according to the procedure outlined in APTD-0576 (Citation 2 in Section 7). Instead of physically adjusting the dry gas meter dial readings to correspond to the wet test meter readings, calibration factors may be used to mathematically correct the gas meter dial readings to the proper values.

Before calibrating the metering system, it is suggested that a leak check be conducted. For metering systems having diaphragm pumps, the normal leak check procedure will not detect leakages within the pump. For these cases the following leak check procedure, as outlined in Method 5, Section 5.3, is suggested: make a 10-min calibration run at 0.00057 m^3/min. (0.02 cfm); at the end of the run, take the difference of the measured wet test meter and dry gas meter volumes, and divide the difference by 10 to get the leak rate. The leak rate should not exceed 0.00057 m^3/min (0.02 cfm).

NOTE: If differential pressure gauges other than inclined manometers are used (e.g., Magnehelic® gauges), their calibration must be checked after each test series. To check the calibration of a differential pressure gauge, compare the readings of the gauge with those of a gauge-oil manometer at a minimum of three points, approximately representing the range of expected values. If, at each point, the values as read by the differential pressure gauge and gauge-oil manometer agree to within 5%, the differential pressure gauge shall be considered to be in proper calibration. Otherwise, either the test series shall be voided, or procedures to adjust the measured values and final results shall be used, subject to the approval of the Administrator.

After each field use, the calibration of the metering system shall be checked by performing three calibration runs at a single, intermediate orifice setting (based on the previous field test), with the vacuum set at the maximum value reached during the test series. To adjust the vacuum, insert a valve between the wet test meter and the inlet of the metering system. Calculate the average value of the calibration factor. If the calibration has changed by more than 5%, recalibrate the meter over the full range of orifice settings, as outlined in APTD-0576 (Citation 2 in Section 7).

Alternative procedures, e.g. (using the orifice meter coefficients) may be used, subject to the approval of the Administrator.

NOTE: If the dry gas meter coefficient values obtained before and after a test series differ by more than 5%, either the test series shall be voided, or calculations for the test series shall be performed using whichever meter coefficient value (i.e., before or after) gives the lower value of total sample volume.

5.4 Temperature Gauges. Use the procedure in Section 4.3 of Method 2 to calibrate in-stack temperature gauges. Dial thermometers, such as are used for the dry gas meter and condenser outlet, shall be calibrated against mercury-in-glass thermometers.

5.5 Leak Check of Metering System Shown in Figure A-1. That portion of the sampling train from the pump to the orifice meter should be leak checked prior to initial use and after each shipment. Leakage after the pump will result in less volume being recorded than is actually sampled. The following procedure is suggested (see Figure 5-4 of Method 5). Close the coarse-adjust valve on the meter box. Insert a one-hole rubber stopper with rubber tubing attached into the orifice exhaust pipe. Disconnect and vent the low side of the orifice manometer. Close off the low side orifice tap. Pressurize the system to 13 to 18 cm (5 to 7 in.) water column by blowing into the rubber tubing. Pinch off the tubing and observe the manometer for 1 min. A loss of pressure on the manometer indicates a leak in the meter box; leaks, if present, must be corrected.

5.6 Barometer. Calibrate against a mercury barometer.

6. Calculations. Carry out calculations, retaining at least one extra decimal figure beyond that of the acquired data. Round off figures after the final calculation. Other forms of the equations may be used as long as they give equivalent results.

6.1 Nomenclature.

A_n = Cross-sectional area of nozzle, m^2 (ft^2).
B_{ws} = Water vapor fraction in the gas stream, by volume, dimensionless.
C_1 = Viscosity constant, 51.12 micropoise for K (51.05 micropoise for °R).
C_2 = Viscosity constant, 0.372 micropoise/K (0.207 micropoise/°R).
C_3 = Viscosity constant, 1.0483×10^{-4} micropoise/$°K^2$ (3.24×10^{-5} micropoise/$°R^2$).
C_4 = Viscosity constant, 53.147 micropoise/fraction O_2.
C_5 = Viscosity constant, 74.143 micropoise/fraction H_2O.
C_a = Acetone blank residue concentration, mg/g.
C_p = SIM-5 pitot coefficient, dimensionless.
C_p' = Coefficient of the pitot used to obtain the velocity traverse information (Section 4.1.2.5), dimensionless.
c_s = Concentration of particulate matter in stack gas, dry basis, corrected to standard conditions, g/dscm (g/dscf).

f_{CO_2} = Stack gas fraction CO_2, by volume (dry basis).
f_{O_2} = Stack gas fraction O_2, by volume (dry basis).
I_j = Percent of isokinetic sampling, as determined for nozzle j. The subscript is used only when multiple nozzles are required, percent.
$\overline{I}$ = Average percent isokinetic when two or more separate nozzles are used to synthesize a single traverse, percent.
K_1 = 0.3858 K/mm Hg (17.647 °R/in. Hg).
K_2 = 0.001333 m^3/mL (0.04707 ft^3/mL).
K_3 = 0.003454 mm Hg-m^3/mL-K (0.002669 in. Hg-ft^3/mL-°R).
K_4 = 4.320 for metric units (0.09450 for English units).
L_a = Maximum acceptable leakage rate for either a pretest leak check or for a leak check following a component change; equal to 0.00057 m^3/min. (0.02 cfm) or 4% of the average sampling rate, whichever is less.
L_i = Individual leakage rate observed during the leak check conducted prior to the "i th" component change (i=1, 2, 3 ..n), m^3/min. (cfm).
L_p = Leakage rate observed during the posttest leak check, m^3/min. (cfm).
M_d = Dry molecular weight of stack gas, g/g-mole (lb/lb-mole).
M_s = Wet molecular weight of stack gas, g/g-mole (lb/lb-mole).
M_w = Molecular weight of water, 18.0 g/g-mole (18.0 lb/lb-mole).
m_a = Mass of residue of acetone after evaporation, mg.
m_n = Total amount of particulate matter collect, mg.
P_{bar} = Barometric pressure at the sampling site, mm Hg (in. Hg).
P_s = Absolute stack gas pressure, mm Hg (in. Hg)
P_{std} = Standard absolute pressure, 760 mm Hg (29.92 in. Hg).
Q_{cyc} = Cyclone flow rate at wet stack conditions, m^3/min (acfm).
R = Ideal gas constant, 0.06236mm Hg-m^3/K-g-mole (21.85 in.Hg-ft^3/°R-lb-mole).
T_m = Absolute average dry gas meter temperature (see Figure 5-2 of Method 5), K (°R).
T_s = Absolute average stack gas temperature (see Figure 5-2 of Method 5), K (°R).
T_{std} = Standard absolute temperature, 293 K (528°R).
t_1 = Dwell time at traverse point 1, min.
t_n = Dwell time at traverse point n, min.
u = Nozzle velocity required for a aerodynamic size cut of 10 μm at stack conditions when a nozzle of diameter d is used with Cyclone I, m/s (ft/s).
V_a = Volume of acetone blank, mL. V_{aw} = Volume of acetone used in wash, mL.
V_{lc} = Total volume of liquid collected in impingers and silica gel (see Figure 5-3 of Method 5), mL.
V_m = Volume of gas sample as measured by dry gas meter, dcm (dcf).
$V_{m(std)}$ = Volume of gas sample measured by the dry gas meter, dscm (dscf).
$V_{w(std)}$ = Volume of water vapor in gas sample (standard conditions), scm(scf).
$\overline{v}_j$ = Average weighted stack gas velocity, for points traversed with nozzle j, m/s (ft/s).
$\overline{v}$ = Average of $\overline{v}_j$ for all nozzles used, m/s (ft/s).
W_a = Weight of residue in acetone wash, mg.
α_5 = 2.48 x 10^{-4} for metric units (2.84 x 10^{-3} for English units).

β_1 = 0.027754 for metric units (0.15625 for English units).
γ = Dry gas meter calibration coefficient, dimensionless.
ΔH = Average pressure differential across the orifice meter (see Figure 5-2 of Method 5), mm H_2O (in. H_2O).
$\Delta H@$ = Orifice pressure differential required for a flow rate of 0.75 cfm at standard conditions, mm H_2O (in. H_2O).
Δp = Local velocity head of stack gas, mm H_2O (in. H_2O).
Δp_1 = Local velocity head of stack gas at the first traverse point, mm H_2O (in. H_2O).
Δp_n = Local velocity head of stack gas at traverse point n, mm H_2O (in. H_2O).
$(\sqrt{\Delta p})_{avg}$ = Average of the square roots of the velocity heads for each point in the traverse, $\sqrt{mm\ H_2O}$ ($\sqrt{in.H_2O}$).
μ_s = Wet stack gas viscosity, micropoise.
ρ_a = Density of acetone, mg/mL (see label on bottle).
ρ_w = Density of water, 0.9982 g/mL (0.002201 lb/mL).
θ = Total sampling time, min.
θ_1 = Sampling time interval, from the beginning of a run until the first component change, min.
θ_j = Sampling time interval, between two successive component changes, beginning with the interval between the first and second changes, min.
θ_n = Sampling time interval, from the final (nth) component change until the end of the sampling run, min.
13.6 = Specific gravity of mercury.
60 = S/min.
100 = Conversion to percent.

6.2 Average Dry Gas Meter Temperature and Average Orifice Pressure Drop. See data sheet (Figure 5-2 of Method 5). In order to calculate the resultant values from a test run, the average values of the recorded temperatures and pressure drops (see Figure 5-2 of Method 5) must be calculated. The pressure drop across the pitot tube, however, requires special attention. The stack velocity is a function of the square root of the pitot Δp; therefore, a straight average of the Δp's over a given run would not result in the true average velocity. Because of this, the value used for calculating the average velocity must be the square of the average square root of the velocity heads. This will result in a Δp value which will allow calculation of the true average velocity.

6.3 Dry Gas Volume. Correct the sample volume measured by the dry gas meter to standard conditions (20 °C, 760 mm Hg or 68 °F, 29.92 in. Hg) by using equation:

$$V_{m(std)} = V_m\gamma \left[\frac{T_{std}}{T_m}\right] \left[\frac{P_{bar} + \frac{\Delta H}{13.6}}{P_{std}}\right] \qquad \text{(Equation 9)}$$

$$= K_1 V_m \gamma \left[\frac{P_{bar} + (\Delta H/13.6)}{T_m}\right]$$

NOTE: Equation 9 can be used as written unless the leakage rate observed during any of the mandatory leak checks (i.e., the posttest leak check or leak check conducted prior to component changes) exceeds L_a. If L_p exceeds L_a, Equation 9 must be modified as follows:

(a) Case I. No component changes made during sampling run. In this case replace V_m in Equation 9 with the expression:

$$V_m + \left(V_m - (L_p - L_a)\theta\right) \qquad \text{Equation 10}$$

(b) Case II. One or more component changes made during the sampling run. In this case, the procedures in Section 6.3 of Method 5 should be followed.

6.4 Volume of Water Vapor.

$$V_{w(std)} = V_{lc}\left[\frac{\rho_w}{M_w}\right]\left[\frac{R\ T_{std}}{P_{std}}\right] = K_2V_{lc} \qquad \text{Equation 11}$$

6.5 Moisture Content of Stack Gas.

$$B_{ws} = \frac{V_{w(std)}}{V_{m(std)}+V_{w(std)}} \qquad \text{Equation 12}$$

6.6 Acetone Blank Concentration.

$$C_a = \frac{m_a}{V_a - \rho_a} \qquad \text{Equation 13}$$

6.7 Acetone Wash Blank.

$$W_a = C_aV_{aw}\,\rho_a \qquad \text{Equation 14}$$

6.8 Total Particulate Weight.

6.8.1 Particles 10 μm and Greater. Determine the total particulate catch in this size range from the sum of the weights obtained from containers 1 and 3 less the acetone blank.

6.8.2 Particles Less than 10 μm. Determine the total particulate catch in the PM_{10} range from the sum of the weights obtained from containers 2 and 4 less the acetone blank.

6.9 Particulate Concentration.

$$C_s = (0.001\ \text{g/mg})(m_n/V_{m(std)}) \qquad \text{Equation 15}$$

6.10 Weighted Averages. If two or more separate nozzles are used to synthesize a single traverse, each sample should be analyzed separately and then averaged to obtain data representative of the entire sampling plane. These weighted averages should be calculated by using the following equation:

$$C_s = \frac{\sum \theta_i\ C_i}{\theta} \qquad \text{Equation 16}$$

6.11 Aerodynamic Size Cut. The actual size cut obtained with the cyclone should be calculated from the actual sample flow rate and sample conditions. The sample flow rate can be determined from the following equation:

$$Q_{cyc} = T_s \left[K_3 V_{lc} + T_s (\gamma V_m / T_m)(P_{bar} + \frac{\Delta H}{13.6}) \right] / (\theta P_s) \qquad \text{Equation 17}$$

Given the above sample flow rate, the actual cyclone cut size can be determined from Equation 18 below:

$$D_{50} = \beta_1 \left(\frac{M_s P_s}{T_s} \right)^{-0.2091} Q_{cyc}^{-0.7091} \mu_s^{0.7091} \qquad \text{Equation 18}$$

6.12 Conversion Factors.

From	To	Multiply by
ft^3	m^3	0.02832
g/ft^3	gr/ft^3	15.43
g/ft^3	lb/ft^3	2.205×10^{-3}
g/ft^3	g/m^3	35.31

6.13 Isokinetic Variation.

6.13.1 Calculation of Average Weighted Stack Velocity for Nozzle j.

$$\bar{v}_j = \frac{1}{\theta_j} \sum_i v_{j,i} t_{j,i} \qquad \text{Equation 19}$$

6.13.2 Calculation of Isokinetic Variation, Single Nozzle Case, Raw Data.

$$I = \frac{100 \; T_s \left[K_3 V_{lc} + (\gamma V_m / T_m)(P_{bar} + \Delta H/13.6) \right]}{60 \; \theta \; \bar{v} \; P_s A_n} \qquad \text{Equation 20}$$

6.13.3 Calculation from Intermediate Values.

$$I = K_4 \left[\frac{T_s V_{m(std)}}{P_s \bar{v} A_n \theta \; (1 - B_{ws})} \right] \qquad \text{Equation 21}$$

If more than one nozzle is used, then the following variables are subscripted for each nozzle j: I_j, θ_j, $\bar{v}_j$, $V_{m(std)j}$, A_{nj}, and T_{sj}.

6.13.4 Average Percent Isokinetic for the Case Where Two or More Nozzles Are Used.

$$\bar{I} = \frac{1}{\theta} \sum_j \theta_j I_j \qquad \text{Equation 22}$$

6.14 Ratio Limits. As described in Section 4.1.2.4 (see Figures A-3 and A-4) the use of different nozzles will result in different limits for the velocity ratio ($u_j/ \bar{v}_j$). Determine a max R and min R by using $\bar{v}_j$, d_j, and viscosity (μ) for the actual run for each of the nozzles. Where $\bar{R}_{max}$ and $\bar{R}_{min}$ are the respective averages, calculate

$$A = 100/ \bar{R}_{max} \qquad \text{Equation 23}$$

$$B = 100/ \bar{R}_{min} \qquad \text{Equation 24}$$

6.15 Acceptable Results. To be acceptable, data must meet two acceptance criteria.

1) If $A < I < B$, the results are acceptable. If the results are low in comparison to the standard and "I" is beyond the acceptable range, or, if "I" is less than "B" percent, the Administrator may opt to accept the results. Otherwise, reject the results and repeat the test.

2) If the PM_{10} cyclone cut point is between 9 and 11 μm, the results are acceptable. If the cut point is greater than 11 μm, acceptance of the test is at the Administrator's discretion. If the cut point is less than 9 μm, the test is not acceptable and should be repeated unless the sum of the concentrations of particles "less than 10 microns" and "10 micron and greater" is low in comparison to the standard for PM_{10} only. In this case, acceptance of the test is at the Administrator's discretion.

7. Bibliography.

1. Martin, R.M., Construction Details of Isokinetic Source-Sampling Equipment. U.S. Environmental Protection Agency. Research Triangle Park, NC. APTD-0581. April 1971.

2. Rom, J.J., Maintenance, Calibration, and Operation of Isokinetic Source-Sampling Equipment. U.S. Enviromental Protection Agency. Research Triangle Park, NC. APTD-0576. March 1972.

3. Smith, W.B., D.B. Harris, and R.R. Wilson, Jr. A Five-Stage Cyclone System for In Situ Sampling. Environ. Sci. Technol., 13(11): 1387-1392, 1979.

4. Felix, L.G., G.I. Clinard, G.E. Lacey, and J.D. McCain. Inertial Cascade Impactor Substrate Media for Flue Gas Sampling. U.S. Environmental Protection Agency. Research Triangle Park, NC. EPA-600/7-77-060. June 1977. 83 pp.

5. Wilke, C.R., A Viscosity Equation for Gas Mixtures. J. Chem. Phys. 8:517, 1950.

6. Williamson, A.D., D.L. Iozia, P.V. Bush, W.E. Farthing, J.D. McCain, W.B. Smith. Development Application, and Support of Particulate Sampling Procedures: Third Annual. Southern Research Institute, Birmingham, AL. SoRI-EAS-83-348. 1983. 119 pp.

APPENDIX B

Determination of Source Emission PM_{10} Particulate Matter Using Emission Gas Recycle (EGR) Sampling Procedures and A Single Stage PM_{10} Cyclone

In this appendix the preliminary procedure of the method is named Emission Gas Recycle. A more detailed document which describes this procedure completely is published under separate cover where it is now named Exhaust Gas Recycle (Martin et al. 1988).

INTRODUCTION

The technical difficulties in size-specific (i.e., PM_{10}) particulate sampling are greater than, but similar to, those of total particulate sampling by EPA Reference Methods 5 or 17. Potential sampling biases exist due to variations in the spatial distribution of particulate concentrations across the sampling plane defined by the duct cross section. Likewise, temporal variations in particulate concentrations due to process variations can cause inaccurate or unrepresentative emissions measurements. EPA reference methods for particulate sampling (Methods 5 and 17) deal with these problems by specifications on the sampling location to minimize stratification (Method 1) and by spatial and temporal averaging using a traversing protocol which collects a weighted average of the particulate emissions at an array of points spanning the sample plane. Method 5 specifications also require at least three separate measurements, allowing further temporal averaging. A second potential error in particulate measurements is duct/nozzle sampling bias. Unless the gas velocity entering the sampling nozzle equals the local duct velocity (isokinetic sampling), particulate matter will be selectively depleted or enriched in the sample gas stream due to inertial separation at the nozzle entrance.

These potential problems are enhanced in PM_{10} sampling by the fact that inertial size segregation must be performed. Any inaccuracies in the inertial cutoff diameter, which is determined by sample flow rate, will lead to errors in the PM_{10} measurement by misclassification of particulate matter in the size range near 10 μm. Misclassification of particles larger than 10 μm can also occur due to bounce or reentrainment, causing these particles to be counted in the PM_{10} fraction. Likewise, if extensive deposition of particles smaller than 10 μm occurs upstream of the inertial sizing device, then the PM_{10} fraction will be depleted even if the nozzle deposits are reentrained as agglomerates and pass into the sizing stage. All these potential problems must be faced in a PM_{10} sampling strategy.

The most obvious potential inaccuracy in PM_{10} sampling is due to a "built in" anisokinetic sampling bias. Inertial sizing devices (impactors and cyclones) are available which have a sufficiently sharp collection efficiency cut at 10 μm, but only for specified flow rates which are dependent on gas temperature and composition. Without a sampling nozzle of continuously variable cross-sectional area, this fixed flow rate requirement makes isokinetic sampling in the manner of Method 5 impossible. Since anisokinetic sampling bias can be significant for particles near 10 μm, this effect cannot be ignored.

This method describes an in-stack sampling system which allows isokinetic sampling while maintaining a constant flow rate through an inertial particle sizing device. The sampling train uses the principle of emission gas recycle (EGR). Its design allows a variable fraction of conditioned and filtered exhausted emission gas to be added to the sample between the sampling nozzle and the inertial sampler. This allows a preselected constant flow rate to be maintained through the inertial sampler while the gas flow rate into the sampling nozzle is adjusted to remain isokinetic with the local duct velocity.

1. Principle and Applicability.

1.1 Principle. Particulate matter is withdrawn isokinetically from the source and inertially segregated into two size fractions: those with an aerodynamic diameter greater than 10 μm, and those with an aerodynamic diameter less than or equal to 10 μm. The particulate mass collected in the size range less than or equal to 10 μm, and the larger size range if desired, is determined gravimetrically.

1.2 Applicability. This method applies to the determination of particulate emissions from stationary sources for determining compliance with new source performance standards, only when specifically provided for in an applicable subpart of the standards. This method is not applicable to stacks that contain liquid droplets or are saturated with water vapor.

2. Apparatus

2.1 Sampling Train. A schematic of the sampling train used in this method is shown in Figure B-1 (see Citation 1 in Section 7). Several of the components in this train are identical in construction and function to a Method 5 sampling train. Construction details for many, but not all, of these components are given in APTD-0581 (Citation 2 in Section 7); for changes from the APTD-0581 document and for allowable modifications to Figure B-1, consult with the Administrator. Construction details for the EGR specific components are given in Citation 1 of Section 7.

The operating and maintenance procedures for many of the sampling train components are described in APTD-0576 (Citation 3 in Section 7). Since correct usage is important in obtaining valid results, all users should read the APTD-0576 document and adopt the operating and maintenance procedures outlined in it, unless otherwise specified herein. Operation and maintenance of EGR specific components is more completely described in Citation 1. The sampling train consists of the following components:

2.1.1 Emission Gas Recycle (EGR) Nozzle. Stainless steel (316) with sharp, tapered leading edge. The angle of taper shall be less than or equal to 30°, and the taper shall be on the outside to preserve a constant internal diameter. As shown in Figure B-2, the recycled emission gas enters the nozzle through a side entry tube and fills an annulus around the sample tube.

A range of sizes suitable for isokinetic sampling at varying recycle rates should be available, e.g., 0.32 to 0.64 cm (1/8 to 1/4 in.) inside diameter (ID) nozzles in increments of 0.16 cm (1/16 in.). Each nozzle shall be calibrated according to the procedures outlined in Section 5.1.

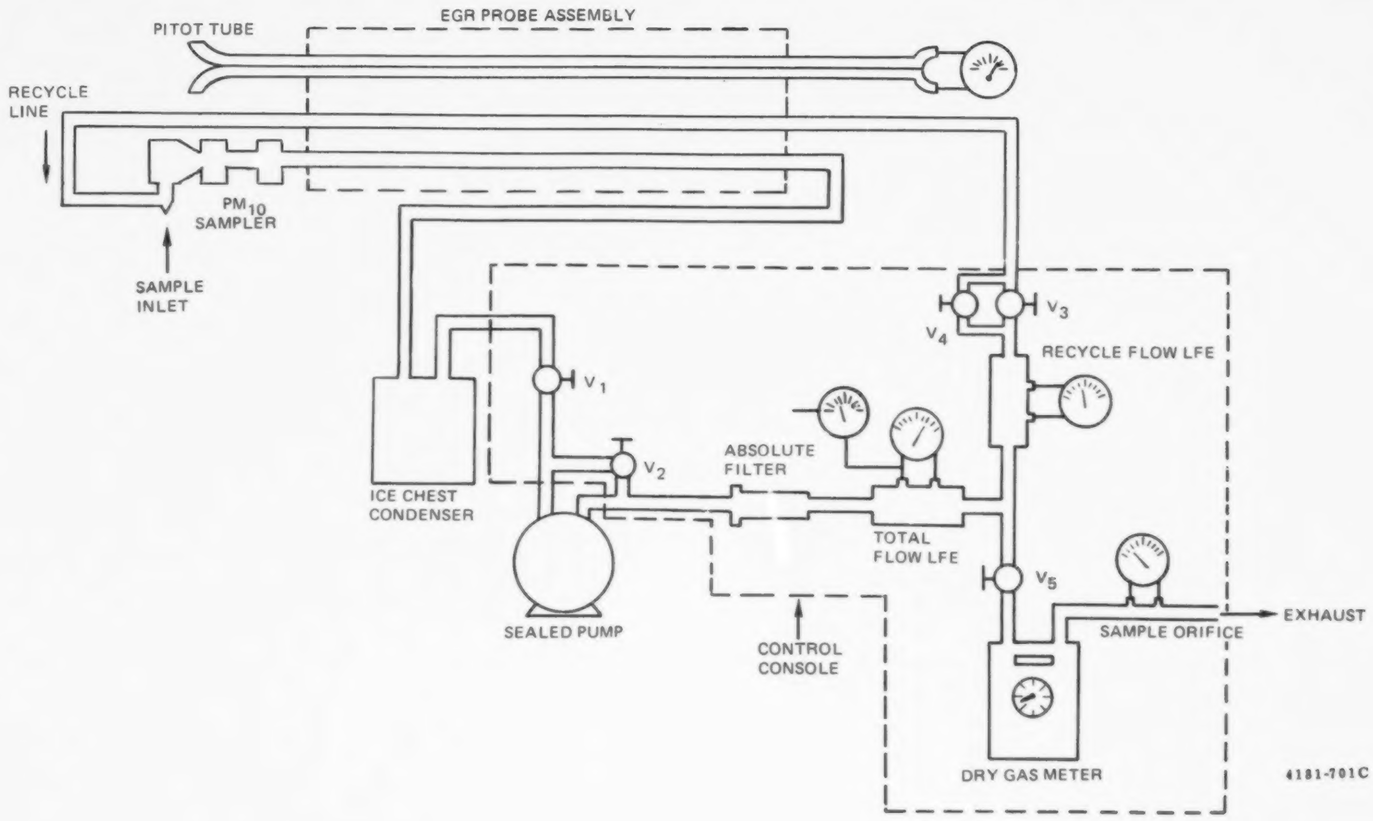
EGR PROBE ASSEMBLY
PITOT TUBE
RECYCLE LINE
PM10 SAMPLER
SAMPLE INLET
ICE CHEST CONDENSER
V1
V2
SEALED PUMP
ABSOLUTE FILTER
TOTAL FLOW LFE
CONTROL CONSOLE
V4
V3
RECYCLE FLOW LFE
V5
SAMPLE ORIFICE
EXHAUST
DRY GAS METER
4181-701C

Figure B-1. Schematic of the emission gas recycle train (Williamson, et al., 1984).

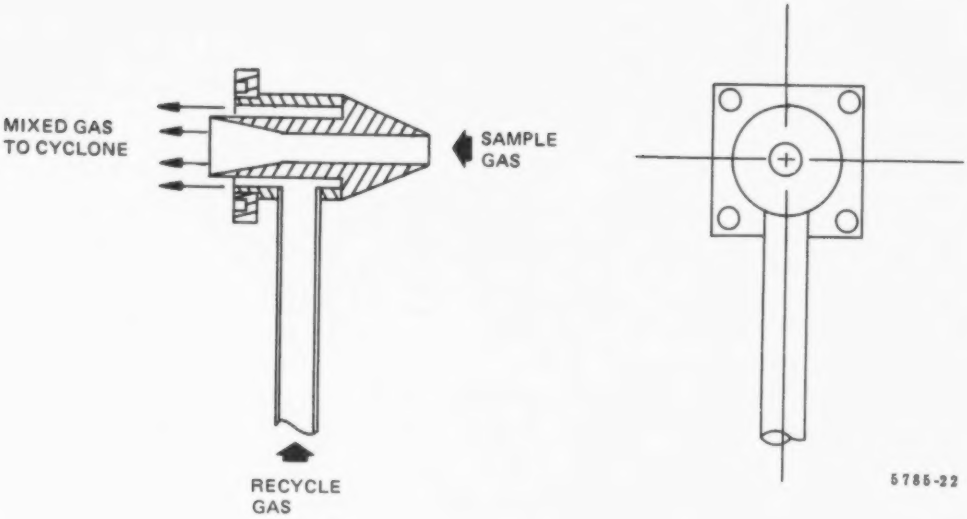
MIXED GAS
TO CYCLONE
SAMPLE
GAS
RECYCLE
GAS
5785-22

Figure B-2. EGR concept nozzle assembly.

Because of inertial deposition of particles in the PM_{10} size range in bends, only straight sampling nozzles should be used. "Gooseneck" or other nozzle extensions designed to turn the sampled gas flow 90°, as in Methods 5 and 17, will not be acceptable.

2.1.2. PM_{10} Cyclone. The cyclone chosen here as the PM_{10} sizing device is the commercially available version of Cyclone I, the first stage of the SoRI/EPA Five-Stage Series Cyclone (see Citation 4 of Section 7). Laboratory calibration (refer to Section 6.11) has shown Cyclone I produces a 10 μm fractionation at approximately 0.5 cfm, depending on local stack conditions. With the approval of the Administrator, other initial sizing devices (i.e., cascade impactors, other cyclones) may be used as the PM_{10} classifier if performance equivalent to the designated PM_{10} cyclone is demonstrated. However, the differences in the calibrated behavior of an alternate classifier would require changes in the equations involving nozzle selection (Section 4.1.2.2), target total LFE pressure differential (Section 4.1.2.4), and actual classifier D_{50} (Section 6.11).

2.1.3. Filter Holder. The in-stack filter holder shall be constructed of stainless steel; if a gasket is used, it shall be made of silicone rubber, Teflon, or Viton A. Other holder and gasket materials may be used subject to the approval of the Administrator. The filter holder shall be designed to provide a positive seal against leakage from the outside or around the filter.

2.1.4 Pitot Tube. Type S, as described in Section 2.1 of Method 2, or other device approved by the Administrator; the pitot tube shall be attached to the probe extension to allow constant monitoring of the stack gas velocity. The impact (high pressure) opening plane of the pitot tube shall be even with or above the nozzle entry plane during sampling (see Method 2, Figure 2-6b). It is recommended (1) that the pitot tube have a known baseline coefficient, determined as outlined in Section 4 of Method 2, and (2) that this known coefficient be preserved by placing the pitot tube in an interference-free arrangement with respect to the sampling nozzle, inertial sampler, filter holder, and temperature sensor.

Source-sampling assemblies that do not meet the minimum spacing requirements of Figure 2-7 of Method 2 may be used; however, the pitot tube coefficients of such assemblies shall be determined by calibration, using methods subject to the approval of the Administrator.

NOTE: Experience has indicated that the criteria stated in Method 2, Section 4.1.1, for pitot positioning relative to sampling nozzles may not be sufficient to prevent flow perturbations. Continued investigation of this problem is planned with more definitive guidelines expected as a result. At present, the only means of eliminating this type of error with confidence is to calibrate pitots in the expected sampling configuration in a flow field significantly larger than the inertial sizing device.

2.1.5 Differential Pressure Gauge. Inclined manometers, Magnehelic® gauges, and/or equivalent devices are used, as described in Section 2.2 of Method 2. The EGR system requires the monitoring of five pressure differentials: duct velocity head, sample orifice differential pressure, total system flow laminar flow element (LFE) differential pressure, differential pressure (with respect to ambient) at the inlet of the total flow LFE, and recycle gas flow LFE differential pressure.

2.1.6 EGR Probe. The EGR probe should be constructed of suitably rigid tubing or pipe with an inside diameter large enough to hold the recycle gas line, sample gas line, and pitot lines. Each of these separate, smaller lines should also be constructed of suitably rigid tubing. A heating system capable of raising the recycle gas temperature to the duct temperature prior to entering the sample nozzle is required. Power to the heater should be regulated by a proportional temperature controller using a thermocouple reference sensor attached to the surface of the recycle line, located securely under the heating tape or mantle.

2.1.7 Condenser. It is recommended that the impinger system described in Method 5 be used to determine the moisture content of the stack gas. Alternatively, any system that allows measurement of both the water condensed and the moisture leaving the condenser, each to within 1 mL or 1 g may be used. The moisture leaving the condenser can be measured either by (1) monitoring the temperature and pressure at the exit of the condenser and using Dalton's law of partial pressures; or (2) passing the sample gas stream through a silica gel trap with exit gases kept below 20 °C (68 °F) and determining the weight gain.

Flexible tubing may be used between the probe extension and condenser. If means other than silica gel are used to determine the amount of moisture leaving the condenser, it is recommended that silica gel still be used between the condenser system and pump to prevent moisture condensation in the pump and metering devices and to avoid the need to make corrections for moisture in the metered volume.

2.1.8 EGR Metering System. The EGR sample train requires monitoring of three flow rates. The total flow through the system should be measured using a calibrated laminar flow element (LFE). The recycle flow rate should be monitored in the same way. The sample flow rate is determined from the conventional Method 5 dry gas meter - calibrated orifice system. The dry gas meter should be capable of measuring volume to within 2 percent. Related equipment such as vacuum gauges, leak-free pumps, and thermometers capable of measuring temperature to within 3 °C (5.4 °F) should also be used as shown in Figure B-1. Other metering systems capable of maintaining sampling rates within 10 percent of isokinetic and of determining sample volumes to within 2 percent may be used. In conjunction with a pitot tube, the system shall enable checks of isokinetic rates.

2.1.9 Barometer. Barometric pressure should be determined in the same way as described in Section 2.1.9 of Method 5.

2.1.10 Gas Density Determination Equipment. Temperature sensor and pressure gauge, as described in Sections 2.3 and 2.4 of Method 2, and gas analyzer, if necessary, as described in Method 3.

The temperature sensor shall be attached to either the pitot tube or to the probe extension, in a fixed configuration. If the temperature sensor is attached in the field, the sensor shall be placed in an interference-free arrangement with respect to the Type S pitot tube openings (as shown in Figure 2-7 of Method 2). Alternatively, the temperature sensor need not be attached to either the probe extension or pitot tube during sampling, provided that a difference of not more than 1 percent in the average velocity measurement is introduced. This alternative is subject to the approval of the Administrator.

2.2 Sample Recovery. The following items are needed.

2.2.1 Brushes. Nylon bristle or camel's hair brushes with stainless steel wire handle. The brushes should be of the proper size and shape for brushing out the sample nozzle and the PM_{10} cyclone.

2.2.2 Wash Bottles. Two glass wash bottles are recommended; polyethylene or Teflon wash bottles may be used at the option of the tester. It is recommended that acetone not be stored in polyethylene bottles for longer than a month.

2.2.3 Glass Sample Storage Containers. Chemically resistant, borosilicate glass bottles, for acetone washes, 500 mL or 1000 mL. Screw cap liners shall either be rubber backed Teflon or shall be constructed so as to be leak-free and resistant to chemical attack by acetone. (Narrow mouth glass bottles have been found to be less prone to leakage.) Alternatively, polyethylene bottles may be used.

2.2.4 Petri Dishes. For particulate catches and filter samples; glass or polyethylene, unless otherwise specified by the Administrator.

2.2.5 Graduated Cylinder and/or Balance. To measure condensed water to within 1 mL or 1 g. Graduated cylinders shall have subdivisions no greater than 2 mL. Most laboratory balances are capable of weighing to the nearest 0.5 g or less. Any of these balances is suitable for use here and in Section 2.3.4.

2.2.6 Plastic Storage Containers. Airtight containers to store silica gel.

2.2.7 Funnel and Rubber Policeman. To aid in transfer of silica gel to container; not necessary if silica gel is weighed in the field.

2.2.8 Funnel. Glass or polyethylene, to aid in sample recovery.

2.3 Analysis. The following equipment is needed for analysis.

2.3.1 Glass Weighing Dishes.

2.3.2 Desiccator.

2.3.3 Analytical Balance. To measure to within 0.1 mg.

2.3.4 Balance. To measure to within 0.5 g.

2.3.5 Beakers. 250 mL.

2.3.6 Hygrometer. To measure the relative humidity of the laboratory environment.

2.3.7 Temperature Gauge. To measure the temperature of the laboratory environment.

3. Reagents. The reagents used in sampling are as follows.

3.1 Sampling.

3.1.1 Filters. The in-stack filters shall be glass mats without organic binders, and shall exhibit at least 99.95% efficiency (<0.05% penetration) on 0.3 μm dioctyl phthalate smoke particles. The filter efficiency tests shall be conducted in accordance with ASTM Standard Method D2986-71 (Reapproved 1978; incorporated by reference--see §60.17). Test data from the supplier's quality control program are sufficient for this purpose.

3.1.2 Silica Gel. Indicating type, 6 to 16 mesh. If previously used, dry at 175 °C (350 °F) for 2 h. New silica gel may be used as received. Alternatively, other types of desiccants (equivalent or better) may be used, subject to the approval of the Administrator.

3.1.3 Crushed Ice.

3.1.4 Stopcock Grease. Acetone-insoluble, heat-stable silicone grease. This is not necessary if screw-on connectors with Teflon sleeves, or similar, are used. Alternatively, other types of stopcock grease may be used, subject to the approval of the Administrator.

3.2 Sample Recovery. Acetone, reagent grade, <0.001% residue, in glass bottles. Acetone from metal containers generally has a high residue blank and should not be used. Sometimes, suppliers transfer acetone to glass bottles from metal containers. Thus, acetone blanks shall be run prior to field use and only acetone with low blank values (0.001%) shall be used. In no case shall a blank value of greater than 0.001% of the weight on acetone used be subtracted from the sample weight.

3.3 Analysis.

3.3.1 Acetone. Same as 3.2

3.3.2 Desiccant. Anhydrous calcium sulfate, indicating type. Alternatively, other types of desiccants may be used, subject to the approval of the Administrator.

4. Procedure.

4.1 Sampling. The complexity of this method is such that, in order to obtain reliable results, testers should be trained and experienced with the test procedures.

4.1.1 Pretest Preparation. All components shall be maintained and calibrated according to the procedure described in APTD-0576 (see Citation 3 in Section 7), unless otherwise specified herein.

Weigh several 200- to 300-g portions of silica gel in airtight containers to the nearest 0.5 g. Record the total weight of the silica gel plus container, on each container. As an alternative, the silica gel need not be preweighed, but may be weighed directly in its impinger or sampling holder just prior to train assembly.

Check filters visually against light for irregularities and flaws or pinhole leaks. Label filters of the proper size on the back side near the edge using numbering machine ink. As an alternative, label the shipping containers (glass or plastic Petri dishes) and keep the filters in these containers at all times except during sampling and weighing.

Small envelopes should be cut from aluminum foil to hold the PM_{10} cyclone catch. Each envelope should be marked with a unique identification number and placed in a glass or plastic Petri dish.

Desiccate the filters and foil envelopes at 20 ± 5.6 °C (68 ± 10 °F) and ambient pressure for at least 24 h and weigh at intervals of at least 6 h to a constant weight, i.e., 0.5 mg change from previous weighing; record results to the nearest 0.1 mg. During each weighing the filter must not be exposed to the laboratory atmosphere for a period greater than 2 min and a relative humidity above 50%. Alternatively (unless otherwise specified by the Administrator), the filters may be oven dried at 105 °C (220 °F) for 2 to 3 h, desiccated for 2 h, and weighed. Procedures other than those described, which account for relative humidity effects, may be used, subject to the approval of the Administrator.

4.1.2 Preliminary Determinations.

4.1.2.1 General. Select the sampling site and the minimum number of sampling points according to Method 1 or as specified by the Administrator. Make a projected-area model of the probe extension/PM_{10} sampler assembly, with the sample nozzle face opening positioned along the centerline of the stack. Calculate the estimated cross-section blockage, as shown in Figure B-3. If the blockage exceeds 5% of the duct cross-sectional area, consult with the Administrator (see also Citation 5 in Section 7).

Determine the stack pressure, temperature, and the range of velocity heads using Method 2; it is recommended that a leak-check of the pitot lines (see Method 2, Section 3.1) be performed. Determine the moisture content using Approximation Method 4 or its alternatives for the purpose of making isokinetic sampling rate settings.

The stack gas dry molecular weight, as described in Method 2, Section 3.6, is calculated by the following equation:

$$M_d = 44\ f_{CO_2} + 32\ f_{O_2} + 28(1 - f_{CO_2} - f_{O_2}) \qquad \text{Equation 1}$$

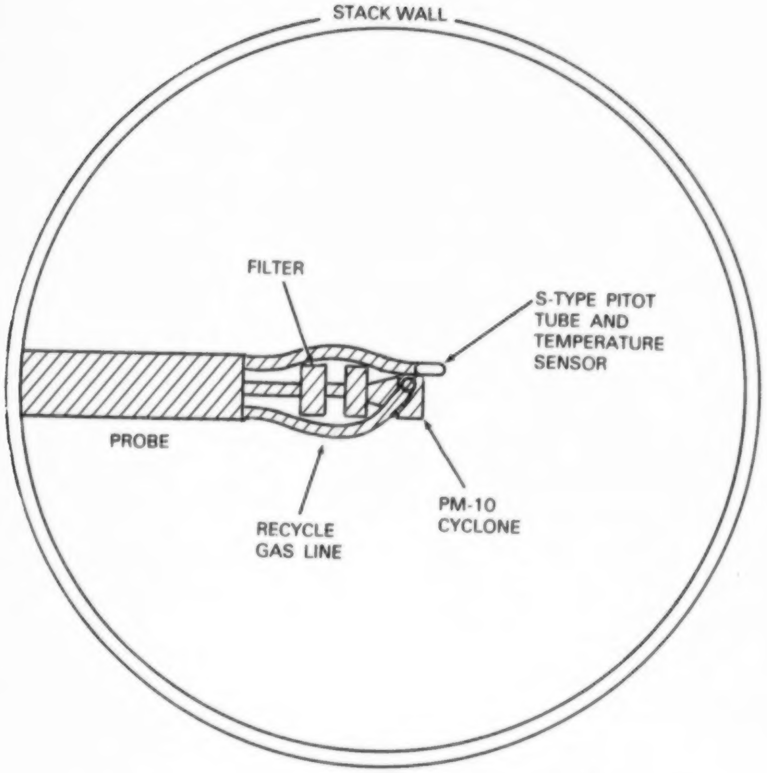
STACK WALL
FILTER
S-TYPE PITOT
TUBE AND
TEMPERATURE
SENSOR
PROBE
RECYCLE
GAS LINE
PM-10
CYCLONE

$$\text{ESTIMATED BLOCKAGE, \%} = \left[\frac{\text{SHADED AREA}}{\text{DUCT AREA}}\right] \times 100$$

5785-23

Figure B-3. Projected area model of cross-section blocks.

NOTE: The equation above does not consider argon in air (about 0.9%, molecular weight of 37.7). A negative error of approximately 0.4% is introduced. The tester may wish to include argon in the analysis using procedures subject to approval of the Administrator.

The wet molecular weight of the stack gases is calculated (refer to Method 2, Section 5.1) as follows:

$$M_s = M_d\ (1-B_{ws}) + 18.0\ B_{ws} \qquad \text{Equation 2}$$

Similarly, the wet and dry viscosity of the stack gas must be determined. An algorithm for the calculation of the viscosity of a gas mixture in terms of its components is given by Wilke (see Citation 6 in Section 7). An approximate equation for viscosity determination of combustion gases was derived by Williamson et al. (see Citation 7 in Section 7) from Wilke's method. The dry stack gas viscosity in micropoise is determined by the following:

$$\mu_d = C_1 + C_2 T_s + C_3 T_s^{\,2} + C_4 f_{O_2} \qquad \text{Equation 3}$$

The stack gas viscosity, on a wet basis, is calculated by:

$$\mu_s = \mu_d - C_5 B_{ws} \qquad \text{Equation 4}$$

4.1.2.2 EGR Nozzle Selection. A nozzle which is small enough to provide a sampling (nozzle) flow rate less than or equal to 90% of the total, cyclone flow rate required for the desired size cut over the entire range of expected velocities should be used. Additionally, the chosen nozzle should not be operated at a flow rate below 20% of the total flow rate (80% recycle) as it becomes increasingly difficult to maintain stable flow conditions as the recycle percentages increases. Therefore, the largest diameter nozzle which satisfies the criterion, based on the currently available PM_{10} cyclone calibration data, shown in either Equation 5 or Equation 6 should be used.

$$D_n < \alpha_1 \left(\frac{M_s P_s}{T_s}\right)^{-0.1475} (\mu_s / v_{max})^{0.5} \qquad \text{Equation 5}$$

Equivalently,

$$D_n < \alpha_2 \left(\frac{M_s P_s}{T_s}\right)^{0.1025} \left[\frac{\mu_s}{C_p \sqrt{\Delta P_{max}}}\right]^{0.5} \qquad \text{Equation 6}$$

4.1.2.3 Target ΔH for Isokinetic Sampling. For each sample point, the target orifice pressure differential, ΔH, may be found as shown below:

$$\Delta H = \left[\alpha_3 (\Delta H@)(D_n^{\,4} C_p^{\,2})\left(\frac{P_s T_m}{T_s P_{bar}}\right)(1-B_{ws})^2\right](\Delta P) \qquad \text{Equation 7}$$

4.1.2.4 Target ΔP_T for the Total (PM_{10} Cyclone) Flow Rate. The calibration of the PM_{10} cyclone has shown the desired flow rate for a specific size cut is a function of the viscosity and density of the gas through the sampler (refer to

Section 6.11). When the cyclone is used in conjunction with the EGR system, the flow rate through the cyclone is the sum of the wet sample flow withdrawn from the process stream and the dry recycle flow introduced at the EGR nozzle. The addition of dry recycle gas to the sample stream changes the moisture content of the total flow in proportion to the percent of recycle gas added in respect to the total cyclone flow rate. While the exact moisture content of the total flow rate would have to be calculated by an iterative process, this mixed gas water fraction, B_{cyc}, is approximated by multiplying the stack gas moisture, B_{ws}, by the ratio of the wet, isokinetic sample flow rate and the PM_{10} flow rate calculated using dry stack gas molecular weight and viscosity. The sample flow rate can be found as follows:

$$Q_s = \left[\alpha_4 \; D_n^2 \; C_p \; \left(\frac{T_s}{P_s M_s}\right)^{1/2} \right] \sqrt{\Delta P} \qquad \text{Equation 8}$$

The PM_{10} flow rate, at dry stack conditions is determined (as outlined in Section 6.11) from Equation 9.

$$Q_d = \alpha_5 \; \left(\frac{M_d P_s}{T_s}\right)^{-0.2949} \mu_d \qquad \text{Equation 9}$$

The moisture content of the gas entering the cyclone is then approximated as shown below:

$$B_{cyc} = \frac{Q_s}{Q_d} \; (B_{ws}) \qquad \text{Equation 10}$$

The target PM_{10} flow rate through the cyclone is found using the relationship shown in Equation 11.

$$Q_{cyc} = \alpha_5 \; \left(\frac{P_s}{T_s}\right)^{-0.2949} \left[M_d - (M_d - 18) B_{cyc} \right]^{-0.2949} (\mu_d - C_5 B_{cyc}) \qquad \text{Equation 11}$$

Finally, the target pressure differential across the total flow LFE, ΔP_T, is found as follows:

$$\Delta P_T = \frac{\mu_{LFE}}{X_T \; \mu_{std}} \left(\frac{Q_{cyc} \; P_s \; T_{LFE} \; (1 - B_{cyc})}{T_s \; P_{LFE}} - Y_T \right) \qquad \text{Equation 12}$$

4.1.2.5 Target ΔP_R for Recycle Flow Rate. Although not required for any specific data reduction, the recycle flow rate serves as an internal check against the sample and total flow rate. By definition, the sum of the recycle and sample flows (at stack conditions) must equal the total, PM_{10} flow rate. The recycle flow (at stack conditions), Q_R, can be determined as shown:

$$Q_R = Q_{cyc} - Q_s \qquad \text{Equation 13}$$

Subsequently, the target pressure differential across the recycle LFE, ΔP_R, can be found as shown in Equation 14.

$$\Delta P_R = \frac{\mu_{LFE}}{X_R \, \mu_{std}} \left(\frac{Q_R \, P_s \, T_{LFE}}{T_s \, P_{LFE}} - Y_R \right) \qquad \text{Equation 14}$$

4.1.2.6 Dwell Time. After determining the overall sampling duration (based on estimated or previously determined duct loading) and the number of sampling points across the traverse (Method 1), the dwell time at each sampling point can be determined simply by dividing the overall duration by the number of points. Each traverse point will be sampled for the same amount of time.

It is recommended that the number of minutes at each sample point be no less than two minutes. Furthermore, the number of minutes sampled at each point should be an integer or an integer plus one-half minute, in order to avoid timekeeping errors. It should be noted that when sampling the effluents from variable or cyclical processes, the dwell time at each sampling point should extend through a complete process cycle to insure that a representative sample is obtained.

4.1.3 Preparation of Collection Train. During preparation and assembly of the sampling train, keep all openings where contamination can occur covered until just prior to assembly or until sampling is about to begin.

If impingers are used to condense stack gas moisture, prepare them as follows: place 100 mL of water in each of the first two impingers, leave the third impinger empty, and transfer approximately 200 to 300 g of preweighed silica gel from its container to the fourth impinger. More silica gel may be used, but care should be taken to ensure that it is not entrained and carried out from the impinger during sampling. Place the container in a clean place for later use in the sample recovery. Alternatively, the weight of the silica gel plus impinger may be determined to the nearest 0.5 g and recorded. If some means other than impingers is used to condense moisture, prepare the condenser (and, if appropriate, silica gel for condenser outlet) for use.

Using tweezers or clean disposable surgical gloves, place a labeled (identified) and weighed filter in the filter holder. Be sure that the filter is properly centered and the gasket properly placed so as not to allow the sample gas stream to circumvent the filter. Mark the probe extension with heat resistant tape or by some other method to denote the proper distance into the stack or duct for each sampling point.

4.1.4 Leak-Check Procedures.

4.1.4.1 Pretest Leak-Check. A pretest leak-check is recommended, but not required. If the tester opts to conduct the pretest leak-check, the following procedure shall be used.

Assemble the entire sample train, including the collection device. Plug the inlet of the PM_{10} cyclone with a material that will be able to withstand the stack temperature. Completely close both the coarse and fine adjust recycle valves. Insert the probe into the stack and wait approximately 15 min (or longer, if necessary) to allow the system to come to thermal equilibrium with the stack gas stream; remove sampler from stack. Turn on the pump and draw a vacuum in the system If the system is being checked without the PM_{10} cyclone and nozzle in place, a vacuum of at least 253 mm Hg (10 in. Hg) should be used. If the system includes the PM_{10} sampler, a vacuum of 127 mm Hg (5 in. Hg) is acceptable as long as the system downstream of the sizing device satisfies the leak criteria at the greater vacuum. Note that a lower vacuum may be used, provided that it is not exceeded during the test. Determine the leakage rate by noting the gas meter deflection for a period of one minute. A leakage rate in excess of 4 percent of the average sampling rate or 0.00057/min. (0.02 cfm), whichever is less, is unacceptable.

The following leak-check instructions for the sampling train may be helpful. Start the pump with bypass (total flow fine adjust) and coarse-adjust valve completely closed. Partially open the coarse adjust valve and slowly close the bypass valve until the desired vacuum is reached. Do not reverse direction of bypass valve. If the desired vacuum is exceeded, either leak-check at this higher vacuum or end the leak-check as shown below and start over.

When the leak-check is completed, first slowly remove the plug from the inlet to the sample nozzle and immediately turn off the vacuum pump. This prevents water from being forced backward and keeps silica gel from being entrained backward.

The positive pressure portion of the EGR control system should be leak checked prior to initial use and after each shipment. The leak-check requires use of a second leak-free Method 5-type sampling system. Close the coarse and fine total flow valves, as well as the sample back-pressure valve. Completely open both the coarse and fine recycle valves. Attach a length of thick wall latex or similar tubing from the recycle outlet port to the sample inlet port on the additional Method 5 control box. Turn the spare system's pump on and adjust the system vacuum to at least 254 mm Hg (10 in. Hg). Determine the leakage rate by noting the gas meter deflection of the spare system for a period of one minute. A leakage rate in excess of 4% of the average total flow rate or 0.00057 m^3/min (0.02 cfm), whichever is less, is unacceptable.

4.1.4.2 Leak-Checks During Sample Run. If, during the sampling run, a component change (e.g., filter assembly or impinger) becomes necessary, a leak-check shall be conducted immediately before the change is made. The leak-check shall be done according to the procedure outlined in Section 4.1.4.1 above, except that it shall be done at a vacuum equal to or greater than the maximum value recorded up to that point in the test. If the leakage rate is found to be no greater than 0.00057 m^3/min (0.02 cfm) or 4% of the average sampling rate (whichever is less), the results are acceptable (no correction will need to be applied to the total volume of the dry gas meter; if, however, a higher leakage rate is obtained, the tester shall either record the leakage rate and plan to correct the sample volume with methods as approved by the Administrator, or shall void the sampling run).

4.1.4.3 Post-Test Leak Check. A leak-check is mandatory at the conclusion of each sampling run. The leak-check shall be done in accordance with the procedures outlined in Section 4.1.4.1, except that it shall be conducted at a vacuum equal to or greater than the maximum value reached during the sampling run. If the leakage rate is found to be no greater than 0.00057 m^3/min (0.02 cfm) or 4% of the average sampling rate (whichever is less), the results are acceptable, and no correction need be applied to the total volume of dry gas metered. If, however, a higher leakage rate is obtained, the tester shall either record the leakage rate and correct the sample volume as shown in Section 6.3 of this method, or shall void the sampling run.

4.1.5 Sampling Train Operation.

4.1.5.1 General. For each run, record the data required on a sample data sheet as shown in Figure A-4. Be sure to record the initial dry gas meter reading. Record the dry gas meter readings at the beginning and end of each port traverse, and after each leak-check, and when sampling is halted. Take other readings as required by Figure A-4 at least once at each sample point. Level and zero the manometer.

Clean the portholes prior to the test run to minimize the chance of sampling the deposited material. To begin sampling, remove the nozzle cap and verify that the pitot tube and probe extension are properly positioned. Position the nozzle at the first traverse point with the tip pointing directly into the gas stream.

When the stack is under significant negative pressure (water gauge differential greater than the height of impinger stem), take care to close the coarse adjust valve before inserting the probe extension assembly into the stack to prevent water from being forced backward. If necessary, the pump may be turned on with the coarse adjust valve closed. When the probe is in position, block off the openings around the probe and porthole to prevent unrepresentative dilution of the gas stream.

When traversing the stack cross section, care should be taken not to bump the probe nozzle into the stack walls when sampling near the walls or when removing or inserting the probe extension through the portholes, to minimize the chance of extracting deposited material. The pump should remain on while traversing the points in a single port but should be shut off when moving the probe from one port to another.

During the test run, take appropriate steps (e.g., adding crushed ice to the impinger ice bath) to maintain a temperature of less than 20 °C (68 °F) at the condenser outlet; this will prevent excessive moisture losses. Also, periodically check the level and zero of the manometer.

At the end of the sample run close off the total flow and recycle lines; turn off the pump, remove the probe extension assembly from the stack, and record the final dry gas meter reading, as well as the total sample time. Perform a leak-check, as outlined in Section 4.1.4.3. Also, leak-check the pitot lines as described in Section 3.1 of Method 2; the lines must pass this leak-check in order to validate the velocity head data.

Run Code	Date	Stack Temperature (°F)	Gas Composition %CO_2 %O_2 %CO
Sampler ID	Start Time	Differential Stack Pressure (in. H_2O)	Moisture Content
Filter ID	End Time	Ambient Temperature (°F)	
Sampler Orientation	Sampling Duration (min)	Ambient Pressure (in. Hg)	
Sampling Location	DGM (initial)	Gas Velocity	Pitot Leak Check (Pos) (Neg)
Nozzle Diameter-ID (in)	DGM (final)	System Leak Check	Notes
Operator(s)	Sample Volume (ft³)		
Dual Manometer Leveled and Zeroed?			
Magnehelics Zeroed?			

Run Time	Port No / Trav.Pt.	ΔP Pitot	ΔH Sample	DGM Volume	ΔP Total	P Inlet	ΔP Recycle	T_1 Stack	T_2 Recycle	T_3 Probe	T_4 LFE	T_5 DGM

Figure B-4. Suggested EGR runsheet.

4.1.5.2 Resetting Total Flow ΔP_T to Maintain Constant Flow Through PM_{10} Cyclone. Temporal variations within the duct and varying recycle rates through the sampler may make it necessary to make slight adjustments to the total flow LFE to maintain a constant cut point through the PM_{10} cyclone. The total flow ΔP_T should be adjusted for a given set of conditions using values as calculated in Section 4.1.2.4. The total flow valves (coarse and/or fine, as needed) are adjusted until the desired ΔP_T is achieved.

4.1.5.3 ΔH Adjustments to Maintain Isokinetic Sampling. At each traverse point, after resetting the total flow ΔP_T, adjust the orifice pressure drop, ΔH, using the recycle coarse and/or fine-adjust valves. In certain cases, particularly at higher recycle rates, it may also be necessary to make slight adjustments with the sample back-pressure valve. The values for ΔH must be previously determined (Section 4.1.2.3) as a function of local duct velocity and temperature. The adjustment of ΔH may slightly interact with the previously set total flow rate. In such a case, a slight iteration between the total flow and recycle valves may be necessary. When the target ΔH and ΔP_T values have been obtained, ΔP_R should approximate the value calculated in Section 4.1.2.5.

4.1.6 Calculation of Aerodynamic Size Cut and Percent Isokinetic. Calculate PM_{10} cyclone aerodynamic size cut using the actual total cyclone flow rate (see Section 6.10 and 6.11). The percent isokinetic for the run can be calculated using the sample flow rate as determined by the sample dry gas meter (see Section 6.13). If either value calculated falls outside the acceptance criterion listed in Section 6.14, the test should be run again.

4.2 Sample Recovery. Proper cleanup procedure begins as soon as the probe extension assembly is removed from the stack at the end of the sampling period. Allow the assembly to cool.

When the assembly can be safely handled, wipe off all external particulate matter near the tip of the nozzle and place a cap over it to prevent losing or gaining particulate matter. Do not cap off the probe tip tightly while the sampling train is cooling down as this would create a vacuum in the sample lines, forcing impinger water backward, if impingers are used.

Before moving the sample train to the cleanup site, disconnect the filter holder/cyclone assembly from the probe extension; cap the open inlet of the probe extension and recycle line. Be careful not to lose any condensate, if present within the sample line. Remove the umbilical cord from the condenser outlet and cap the outlet. If a flexible line is used between the first impinger (or condenser) and the probe extension, disconnect the line at the probe extension and let any condensed water or liquid drain into the impingers or condenser. Disconnect the probe extension from the condenser; cap the probe extension outlet. After wiping off any silicone grease present, cap off the condenser inlet. Ground glass stoppers, plastic caps, or serum caps (whichever are appropriate) may be used to close these openings.

Transfer both the filter holder/cyclone assembly and the condenser to the cleanup area. This area should be clean and protected from the wind so that the chances of contaminating or losing the sample will be minimized.

Save a portion of the acetone used for cleanup as a blank. Take 200 mL of this acetone directly from the wash bottle being used and place it in a glass sample container labeled "acetone blank."

Inspect the train prior to and during disassembly and note any abnormal conditions. Treat the samples as follows:

Container 1. Carefully remove the EGR sampling nozzle from the cyclone and brush particulate matter into a preweighed foil envelope with a nylon bristle or camel's hair brush. Any particulate matter adhering to the outside of the nozzle or the nozzle attachment should not be included. Brush into this same foil envelope the particulate catch of the cyclone being careful to exclude the particulate matter in the "turn-around" cup and the interior of the exit tube.

Container 2. Carefully remove the filter from the filter holder and place it in its identified Petri dish container. Use a pair of tweezers and/or clean disposable surgical gloves to handle the filter. Carefully transfer to the surface of the filter any particulate matter and/or filter fibers which adhere to the inside of the cyclone exit tube "turn-around" cap and the filter holder gasket. To avoid cross-contamination, the brush used for the cyclone body should not be used for this. If it is necessary to fold the filter, do so such that the particulate cake is inside the fold. Alternatively, a preweighed foil envelope could be used to hold the filter.

Container 3. Carefully clean all surfaces assigned to container 1 with acetone from a wash bottle. A funnel (glass or polyethylene) may be used to aid in transferring liquid washes to the container. Rinse the brush with acetone and collect these washings as well. Between sampling runs, keep brushes clean and protected from contamination.

Container 4. Perform acetone wash as described above on all surfaces assigned to container 2. Multiple washings should be performed on the connective tubing between the cyclone exit and the filter holder inlet. Rinse the brush and the filter holder gasket.

After all acetone washings and particulate matter are collected in the the appropriate sample containers, tighten the lid on the sample containers so that acetone will not leak out when it is shipped to the laboratory. Mark the height of the fluid level to determine whether or not leakage occurred during transport. Label the container to clearly identify its contents.

Container 5. If silica gel is used in the condenser system for moisture content determination, note the color of the gel to determine if it has been completely spent; make a notation of its condition. Transfer the silica gel back to its original container and seal. A funnel may make it easier to pour the silica gel without spilling, and a rubber policeman may be used as an aid in removing the silica gel. It is not necessary to remove the small amount of dust particles that may adhere to the walls and are difficult to remove. Since the gain in weight is to be used for moisture calculations, do not use water or other liquids to transfer the silica gel. If a balance is available in the field, follow the procedure for Container 5 under "Analysis."

Condenser Water. Treat the condenser or impinger water as follows: make a notation of any color or film in the liquid catch. Measure the liquid volume to within ±1 mL by using a graduated cylinder or, if a balance is available, determine the liquid weight to within ±0.5 g. Record the total volume or weight of liquid present. This information is required to calculate the moisture content of the effluent gas. Discard the liquid after measuring and recording the volume or weight.

NOTE: Actual data regarding particles of diameter greater than 10 μm (cyclone and nozzle catch) may not be required. In these cases, recovery of the cyclone catch is not necessary. The cyclone and sample nozzle should be rinsed thoroughly with acetone for use in the next test run.

4.3 Analysis. Record the data required in the field test log book or on an appropriate data sheet. Handle each sample container as follows:

Containers 1 and 2. Leave the contents in the Petri dish or transfer to a tared glass weighing dish. Desiccate for 24 hours in a desiccator containing anhydrous calcium sulfate or similar desiccant. Weigh to a constant weight and report the results to the nearest 0.1 mg. The term "constant weight," as used above, means a difference of no more than 0.5 mg or 1% of total weight less tare weight, whichever is greater, between two consecutive weighings, with no less than 6 h of desiccation time between weighings.

Alternatively, the samples may be oven dried at the average stack temperature or 105 °C (220 °F), whichever is less, for 2 to 3 h, cooled in the desiccator, and weighed to a constant weight, unless otherwise specified by the Administrator. The tester may also opt to oven dry the sample at the average temperature or 105 °C (220 °F), whichever is less, for 2 to 3 h, weigh the sample, and use this weight as a final weight. Whichever weighing method is used, completed weights of all cyclone and filter samples should be obtained on site, prior to shipping.

Containers 3 and 4. Note the level of liquid in the container and confirm on the analysis sheet whether or not leakage occurred. If a noticeable amount of leakage has occurred, either void the sample or use methods, subject to the approval of the Administrator, to correct the final results. Measure the liquid in this container either volumetrically to ±1 mL or gravimetrically to ±0.5 g. Transfer the contents to a tared 250-mL beaker or suitable container and evaporate to dryness at ambient temperature and pressure. Desiccate for 24 h and weigh to a constant weight. Report the results to the nearest 0.1 mg.

Container 5. This step may be conducted in the field. Weigh the spent silica gel (or silica gel plus impinger) to the nearest 0.5 g using a balance.

"Acetone Blank" Container. Measure acetone in this container either volumetrically or gravimetrically. Transfer the acetone to a tared 250-mL beaker or suitable container, and evaporate to dryness at ambient temperature and pressure. Desiccate for 24 h and weigh to a constant weight. Report the results to the nearest 0.1 mg.

NOTE: At the option of the tester, the contents of containers 3 and 4, as well as the acetone blank container, may be evaporated at temperatures higher than ambient. If evaporation is done at an elevated temperature, the temperature must be below the boiling point of the solvent; also, to prevent "bumping," the evaporation process must be closely supervised, and the contents of the beaker must be swirled occasionally to maintain an even temperature. Use extreme care, as acetone is highly flammable and has a low flash point.

5. Calibration. Maintain a laboratory log of all calibrations.

5.1 EGR Nozzles. Nozzles shall be calibrated before their initial use in the field. Using a micrometer, measure the inside diameter of the nozzle to the nearest 0.025 mm (0.001 in.). Make three separate measurements using different diameters each time, and obtain the average of the measurements. The difference between high and low numbers shall not exceed 0.1 mm (0.004 in.). When nozzles become nicked, dented, or corroded, they shall be reshaped, sharpened, and recalibrated before use. Each nozzle shall be permanently and uniquely identified.

5.2 Pitot Tube. If the pitot tube is placed in an interference-free arrangement with respect to the other probe assembly components, its baseline (isolated tube) coefficient shall be determined as outlined in Section 4 of Method 2. If the probe assembly is not interference-free, the pitot tube assembly coefficient shall be determined by calibration, using methods subject to the approval of the Administrator.

5.3 Metering System. Before its initial use in the field, the metering system shall be calibrated according to the procedure outlined in APTD-0576 (see Citation 3 in Section 7). Instead of physically adjusting the dry gas meter dial readings to correspond to the wet test meter readings, calibration factors may be used to mathematically correct the gas meter dial readings to the proper values.

Before calibrating the metering system, it is suggested that a leak-check be conducted. For metering systems having diaphragm pumps, the normal leak-check procedure will not detect leakages within the pump. For these cases the following leak-check procedure as outlined in Method 5, Section 5.3 is suggested: make a 10-min calibration run at 0.00057 m^3/min (0.02 cfm); at the end of the run, take the difference of the measured wet test meter and dry gas meter volumes; divide the difference by 10 to get the leak rate. The leak rate should not exceed 0.00057 m^3/min (0.02 cfm).

NOTE: If differential pressure gauges other than inclined manometers are used (e.g., Magnehelic® gauges), their calibration must be checked after each test series. To check the calibration of a differential pressure gauge, compare ΔP readings of the gauge with those of a gauge-oil manometer at a minimum of three points, approximately representing the range of expected ΔP values. If, at each point, the values of ΔP as read by the differential pressure gauge and gauge-oil manometer agree to within 5%, the differential pressure gauge shall be considered to be in proper calibration. Otherwise, the test series shall either be voided, or procedures to adjust the measured ΔP values and final results shall be used, subject to the approval of the Administrator.

After each field use, the calibration of the metering system shall be checked by performing three calibration runs at a single, intermediate orifice setting (based on the previous field test), with the vacuum set at the maximum value reached during the test series. To adjust the vacuum, insert a valve between the wet test meter and the inlet of the metering system. Calculate the average value of the calibration factor. If the calibration has changed by more than 5 percent, recalibrate the meter over the full range of orifice settings, as outlined in APTD-0576 (see Citation 3 in Section 7).

This same flow rate should be used to check the calibration of the total and recycle laminar flow elements. Before each calibration run of the dry gas meter, completely close the recycle valve. Record the total flow laminar flow element pressure drop during the calibration. At the end of each run, shut off the pump and record the final dry gas meter reading. Without adjusting any valves, restart the pump, open the recycle valve, and close the flow restricting valve (sample backpressure) at the inlet of the dry gas meter. This configuration corresponds to 100% recycle. Record the recycle pressure drop. Compare the two laminar flow element pressure drops with those obtained from the calibration equation of each device at the wet test meter flow rate. If the calibration check pressure drops vary from the calculated valves by more than 10%, the laminar flow elements should be recalibrated.

Alternative procedures, e.g., using the orifice meter coefficients, may be used, subject to the approval of the Administrator.

NOTE: If the dry gas meter coefficient and total flow LFE calibration values obtained before and after a test series differ by more than 5 or 10%, respectively, the test series shall either be voided, or calculations for the test series shall be performed using the meter coefficient (i.e., before or after) that gives the lower value of sample volume, and the calibration that gives the higher cyclone flow rates.

5.4 Temperature Systems.

5.4.1 Temperature Gauges. Use the procedure in Section 4.3 of Method 2 to calibrate in-stack temperature gauges. Dial thermometers, such as are used for the dry gas meter and condenser outlet, shall be calibrated against mercury-in-glass thermometers.

5.4.2 Temperature Controllers. The proportional temperature controllers used to maintain the probe at stack temperatures should be checked for calibration before field use. Set the temperature selection dial to the desired temperature, turn the controller on, and allow the probe to warm up. By monitoring the temperature at the controlling thermocouple, it can be determined if the controller is appropriately calibrated. If the calibration is not correct, refer to the particular manufacturer's procedures for calibration of the given controller.

5.5 Leak Check of Metering System. That portion of the sampling train consisting of the dry gas meter and orifice meter should be leak checked prior to initial use and after each shipment. Leakage here will result in less volume being recorded than is actually sampled. The following procedure is suggested. Close the sample back-pressure valve on the meter box. Insert a one-hole rubber stopper with rubber tubing attached into the orifice exhaust pipe. Disconnect and vent the low side of the orifice manometer. Close off the low side orifice tap. Pressurize the system to 13 to 18 cm (5 to 7 in.) water column by blowing into the rubber tubing. Pinch off the tubing and observe the manometer for one minute. A loss of pressure on the manometer indicates a leak in the meter box; leaks, if present, must be corrected.

The negative pressure side of the system may be leak checked by plugging the sample inlet and closing the recycle valve. Start the pump to induce a vacuum across the system. A leak in the system will be indicated by changes in the dry gas meter reading (refer to Section 4.1.4.1).

The positive pressure side of the system may be similarly leak checked by closing the coarse and fine flow valves and the sample-back pressure valve and opening the coarse and fine recycle valves. Use an external Method 5-type control box, attached to the recycle gas outlet, to create a vacuum within the EGR system. A leak in the system will be indicated by the gas meter of the external system (refer to Section 4.1.4.1).

5.6 Barometer. Calibrate against a mercury barometer.

6. Calculations. Carry out calculations, retaining at least one extra decimal figure beyond that of the acquired data. Round off figures after the final calculation. Other forms of the equations may be used as long as they give equivalent results.

6.1 Nomenclature.

A_n = Cross-sectional area of EGR nozzle, m^2 (ft^2).
B_{cyc} = Moisture fraction of mixed cyclone gas, by volume, dimensionless.
B_{ws} = Water vapor fraction in sample gas stream, by volume, dimensionless.
C_1 = Viscosity constant, 51.12 micropoise for K (51.05 micropoise for °R).
C_2 = Viscosity constant, 0.372 micropoise/K (0.207 micropoise/°R).
C_3 = Viscosity constant, 1.0483×10^{-4} micropoise/K^2 (3.24×10^{-5} micropoise/°R^2).
C_4 = Viscosity constant, 53.147 micropoise/fraction O_2.
C_5 = Viscosity constant, 74.143 micropoise/fraction H_2O.
C_a = Acetone blank residue concentration, mg/g.
C_p = Pitot tube coefficient, dimensionless.
C_s = Concentration of particulate matter in stack gas, dry basis, corrected to standard conditions, g/dscm (g/dscf).
D_{50} = Diameter of particles having a 50 percent probability of penetration, microns (μm).
D_n = EGR nozzle sample inlet diameter, cm (inches).
f_{CO_2} = Stack gas fraction CO_2, by volume (dry basis).
f_{O_2} = Stack gas fraction O_2, by volume (dry basis).
I = Percent of isokinetic sampling.
K_1 = 0.3858 K/mm Hg (17.647 °R/in. Hg).
K_2 = 0.001000 m^3/mL (0.04707 ft^3/mL).

K_3 = 0.003454 mm Hg-m^3/ml-K (0.002669 in Hg-ft^3/ml-°R).
K_4 = 4.320 for metric units (0.09450 for English units).
L_a = Maximum acceptable leakage rate for a pretest leak check; equal to 0.00057 m^3/min (0.02 cfm) or 4 percent of the average total cyclone flow rate, whichever is less.
L_p = Leakage rate observed during post-test leak check, m^3/min (cfm).
M_{cyc} = Wet molecular weight of mixed gas through the PM_{10} cyclone, g/g-mole (lb/lb-mole).
M_d = Dry molecular weight of stack gas, g/g-mole (lb/lb-mole).
M_s = Wet molecular weight of stack gas, g/g-mole (lb/lb-mole).
M_w = Molecular weight of water 18.0 g/g-mole (18.0 lb/lb-mole).
m_a = Mass of residue of acetone after evaporation, mg.
m_n = Total amount of particulate matter collected for a given stage, mg.
P_{bar} = Barometric pressure at sampling site, mm Hg (in. Hg).
P_{inl} = Gauge pressure at inlet to total LFE, mm H_2O (in. H_2O).
P_{LFE} = Absolute pressure at inlet to LFE, mm Hg (in. Hg).
= P_{bar} + 0.588 for setup calculations.
= P_{bar} + P_{inl} /13.6 for total LFE flow reduction.
= P_{bar} + (P_{inl} - ΔP_T)/13.6 for recycle LFE flow reduction.
P_s = Absolute stack pressure, mm Hg (in. Hg).
P_{std} = Standard absolute pressure, 760 mm Hg (29.92 in. Hg).
Q_{cyc} = Total cyclone flow rate at wet cyclone conditions, m^3/min (acfm).
$Q_{cyc(std)}$ = Total cyclone flow rate at standard conditions, dsm^3/min (dscfm).
Q_d = Total cyclone flow rate at dry cyclone conditions, m^3/min (acfm).
Q_R = Recycle flow rate at dry cyclone conditions, m^3/min (acfm).
Q_s = Isokinetic sample flow rate at stack conditions, m^3/min (acfm).
R = Ideal gas constant, 0.06236 mm Hg-m^3/K-g-mole, (21.85 in. Hg-ft^3/°R-lb-mole).
T_{LFE} = Absolute average temperature of LFE, K (°R).
T_m = Absolute average temperature of dry gas meter, K (°R).
T_s = Absolute average stack gas temperature, K (°R).
T_{std} = Standard absolute temperature, 293 K (528 °R).
V_a = Volume of acetone blank, mL.
V_{aw} = Volume of acetone used in wash, mL.
V_{lc} = Total volume of liquid collected in impingers (or condenser) and silica gel, mL.
V_m = Volume of gas measured by dry gas meter, m^3 (ft^3).
$V_{m(std)}$ = Volume of gas sample measured by dry gas meter, corrected to standard conditions, dscm (dscf).
$V_{w(std)}$ = Volume of water vapor in gas sample (standard conditions), scm(scf).
v_{max} = Maximum expected stack gas velocity, m/s (ft/s).
v_s = Calculated stack gas velocity, refer to Method 2, m/s (ft/s).
W_a = Weight of residue in acetone wash, mg.
X_R = Recycle LFE linear calibration constant, m^3/min-mm H_2O (acfm/in. H_2O).

X_T = Total LFE linear calibration constant, m^3/min-mm H_2O (acfm/in. H_2O).
Y_R = Recycle LFE linear calibration constant, m^3/min (acfm).
Y_T = Total LFE linear calibration constant, m^3/min (acfm).
α_1 = 0.2154 for metric units (17.647 for English units).
α_2 = 0.03699 for metric units (0.009598 for English units).
α_3 = 0.78576 for metric units (830.73 for English units).
α_4 = 0.1632 for metric units (27.713 for English units).
α_5 = 2.48×10^{-4} for metric units (2.84×10^{-3} for English units).
β_1 = 0.027754 for metric units (0.15625 for English units).
γ = Dry gas meter calibration coefficient, dimensionless.
ΔH = Pressure differential across orifice meter, mm H_2O (in. H_2O).
$\Delta H@$ = Orifice pressure differential required for a flow rate of 0.75 cfm at standard conditions, mm H_2O (in. H_2O).
ΔP = Local velocity head of stack gas, mm H_2O (in. H_2O).
ΔP_{max} = Maximum expected velocity head of stack gas, mm H_2O (in. H_2O).
ΔP_R = Pressure differential across recycle LFE, mm H_2O (in. H_2O).
ΔP_T = Pressure differential across total LFE, mm H_2O (in. H_2O).
θ = Total sampling time, min.
μ_{cyc} = Viscosity of mixed cyclone gas, micropoise.
μ_d = Dry stack gas viscosity, micropoise.
μ_{LFE} = Viscosity of gas at laminar flow elements, micropoise.
= $C_1 + C_2 T_{LFE} + C_3 T_{LFE}^2 + C_4 f_{O_2}$.
μ_s = Wet stack gas viscosity, micropoise.
μ_{std} = Viscosity of standard air, 180.1 micropoise.
ρ_a = Density of acetone, mg/mL (see label on bottle).
ρ_w = Density of water, 0.9982 gm/mL (0.002201 lb/mL).
13.6 = Specific gravity of mercury.
18.0 = Molecular weight of water, g/g-mole (lb/lb-mole).
28 = Molecular weight of N or CO, g/g-mole (lb/lb-mole).
32 = Molecular weight of O, g/g-mole (lb/lb-mole).
44 = Molecular weight of CO, g/g-mole (lb/lb-mole).
60 = S/min.
100 = Conversion to percent.

6.2 Average System Temperatures and Pressure Drops. In order to calculate the resultant values from a test run the average values of the recorded temperatures and pressure drops (see Figure 4) must be calculated. The pressure drop across the pitot tube, however, requires special attention. The stack velocity is a function of the square root of the pitot ΔP; therefore, a straight average of the ΔP's over a given run would not result in the true average velocity. Because of this, the value used for calculating the average velocity must be the square of the average square root of the velocity heads. This will result in a ΔP value which will allow calculation of the true average velocity.

6.3 Dry Gas Volume. Correct the sample volume measured by the dry gas meter to standard conditions (20 °C, 760 mm Hg or 68 °F, 29.92 in. Hg) by using Equation 15.

$$V_{m(std)} = V_m \gamma \left[\frac{T_{std}}{T_m}\right] \left[\frac{P_{bar} + \frac{\Delta H}{13.6}}{P_{std}}\right] \qquad \text{Equation 15}$$

$$= K_1 V_m \gamma \left[\frac{P_{bar} + \frac{\Delta H}{13.6}}{T_m} \right]$$

NOTE: Equation 15 can be used as written unless the leakage rate observed during the post-test leak check exceeds L_a. If L_p exceeds L_a Equation 15 must be modified by replacing V_m with the expression:

$$[V_m - (L_p - L_a)\theta]$$

6.4 Volume of Water Vapor.

$$V_{w(std)} = V_{lc} \left[\frac{\rho_w}{M_w} \right] \left[\frac{R \ T_{std}}{P_{std}} \right] = K_2 V_{lc} \qquad \text{Equation 16}$$

6.5 Moisture Content of Stack Gas.

$$B_{ws} = \frac{V_{w(std)}}{V_{m(std)} + V_{w(std)}} \qquad \text{Equation 17}$$

6.6 Acetone Blank Concentration.

$$C_a = \frac{m_a}{V_a - \rho_a} \qquad \text{Equation 18}$$

6.7 Acetone Wash Blank.

$$W_a = C_a V_{aw} \rho_a \qquad \text{Equation 19}$$

6.8 Total Particulate Weight.

6.8.1 10 Microns and Greater. Determine the total particulate catch in this size range from the sum of the weights obtained from containers 1 and 3 less the acetone blank.

6.8.2 Less than 10 Microns. Determine the total particulate catch in the PM_{10} range from the sum of the weights obtained from containers 2 and 4 less the acetone blank.

6.9 Particulate Concentration.

$$c_s = (0.001 \text{ g/mg})(m_n / V_{m(std)}) \qquad \text{Equation 20}$$

6.10 Total Cyclone Flow Rate. The average total flow rate, at standard conditions, is determined from the average pressure drop across the total flow LFE and is found using Equation 21.

$$Q_{cyc(std)} = K_1 \left[X_T \left(\Delta P_T \frac{\mu_{std}}{\mu_{LFE}} \right) + Y_T \right] \left[\frac{P_{bar} + \frac{P_{inl}}{13.6}}{T_m} \right] \qquad \text{Equation 21}$$

The PM_{10} flow rate, at actual cyclone conditions, is calculated as follows:

$$Q_{cyc} = \frac{1}{K_1}\left[Q_{cyc(std)} + \frac{V_{w(std)}}{\theta}\right]\left[\frac{T_s}{P_s}\right] \qquad \text{Equation 22}$$

6.11 Aerodynamic Size Cut. Calibration data for SoRI/EPA Cyclone I is reported in Citations 4 and 8 of Section 7. From the currently available data, the fractionation behavior of the PM_{10} cyclone can be described as a function of the cyclone flow rate, the mixed stream density, and the mixed stream viscosity. The cyclone flow rate calculation (at stack conditions) is described in Section 6.10. The water fraction of the mixed gas through the cyclone can be found by the following equation:

$$B_{cyc} = \frac{V_{w(std)}}{(Q_{cyc(std)}\ \theta) + V_{w(std)}} \qquad \text{Equation 23}$$

This value is used to calculate the cyclone gas viscosity:

$$\mu_{cyc} = C_1 + C_2 T_s + C_3 T_s^2 + C_4 f_{O_2} - C_5 B_{cyc} \qquad \text{Equation 24}$$

The molecular weight, on a wet basis, of the mixed cyclone gas is likewise calculated:

$$M_{cyc} = M_d(1-B_{cyc}) + 18.0(B_{cyc}) \qquad \text{Equation 25}$$

The actual D_{50} of cyclone for the given conditions may then be determined using the equation shown below:

$$D_{50} = \beta_1 \left(\frac{M_{cyc} P_s}{T_s}\right)^{-0.2091} Q_{cyc}^{-0.7091}\ \mu_{cyc}^{0.7091} \qquad \text{Equation 26}$$

6.12 Conversion Factors.

From	To	Multiply by
ft^3	m^3	0.02832
g/ft^3	gr/ft^3	15.43
g/ft^3	lb/ft^3	2.205×10^{-3}
g/ft^3	g/m^3	35.31

6.13 Isokinetic Variation.

6.13.1 Calculation from Raw Data.

$$I = \frac{100\ T_s\left[K_3 V_{1c} + (V_m Y/T_m)\ (P_{bar} + \frac{\Delta H}{13.6})\right]}{60\ \theta v_s P_s A_n} \qquad \text{Equation 27}$$

6.13.2 Calculation from Intermediate Values.

$$I = \frac{T_s \; V_{m(std)} P_{std} \; 100}{T_{std} \; v_s \; \theta \; A_n P_s \; 60 \; (1-B_{ws})}$$

$$= K_4 \left[\frac{T_s V_{m(std)}}{P_s v_s A_n \; \theta \; (1-B_{ws})} \right] \qquad \text{Equation 28}$$

6.14 Acceptable Results. To be acceptable, data must meet two acceptance criteria:

1) If $90\% < I < 110$ percent, the results are acceptable. If the results are low in comparison to the standard and I is beyond the acceptable range, or if I is less than 90 percent, the Administrator may opt to accept the results. Otherwise, reject the results and repeat the test.

2) If the PM_{10} cyclone cut point is greater than 11 microns, acceptance of the test is at the Administrator's discretion. If the cut point is less than 9 µm, the test is not acceptable and should be repeated unless the sum of the concentrations of particulate "less than 10 microns" and "10 microns and greater" is low in comparison to the standard for PM_{10} only. In this case, acceptance of the test is at the Administrator's discretion.

7. Bibliography.

1. Addendum to Specifications for Incinerator Testing at Federal Facilities. PHS, NCAPC. December 6, 1967.

2. Martin, Robert M. Construction Details of Isokinetic Source-Sampling Equipment. Environmental Protection Agency. Research Triangle Park, N.C. APTD-0581. April, 1971.

3. Rom, Jerome J. Maintenance, Calibration, and Operation of Isokinetic Source-Sampling Equipment. Environmental Protection Agency. Research Triangle Park, N.C. APTD-0576. March, 1972.

4. Smith, W. S., R. T. Shigehara and W. F. Todd. A Method of Interpreting Stack Sampling Data. Paper Presented at the 63rd Annual Meeting of the Air Pollution Control Association, St. Louis, MO. June 14-19, 1970.

5. Smith, W. S., et. al. Stack Gas Sampling Improved and Simplified with New Equipment. APCA Paper No. 67-119. 1967.

6. Specifications for Incinerator Testing at Federal Facilities. PHS, NCAPC. 1967.

7. Shigehara, R. T. Adjustments in the EPA Nomograph for Different Pitot Tube Coefficients and Dry Molecular Weights. Stack Sampling News 2:4-11. October, 1974.

8. Vollaro, R. F. A Survey of Commercially Available Instrumentation for the Measurement of Low-Range Gas Velocities. U.S. Environmental Protection Agency, Emission Measurement Branch. Research Triangle Park, N.C. November, 1976 (unpublished paper).

9. Annual Book of ASTM Standards. Part 26. Gaseous Fuels; Coal and Coke; Atmospheric Analysis. American Society for Testing and Materials, Philadelphia, PA. 1974. pp. 617-622.

10. Vollaro, R. F. Recommended Procedure for Sample Traverses in Ducts Smaller than 12 inches in Diameter. U.S. Environmental Protection Agency, Emission Measurement Branch. Research Triangle Park, N.C. November, 1976.